

**QUALITY ANALYSIS MODELLING FOR DEVELOPMENT OF A PROCESS
CONTROLLER IN RESISTANCE SPOT WELDING USING NEURAL NETWORK
TECHNIQUES**

By

Pius Nwachukwu Oba

Supervised by

Professor HD. Chandler and Dr. S. Oerder

QUALITY ANALYSIS MODELLING FOR DEVELOPMENT OF A PROCESS
CONTROLLER IN RESISTANCE SPOT WELDING USING NEURAL NETWORK
TECHNIQUES

Pius Nwachukwu Oba

A thesis submitted to the Faculty of Engineering and the Built Environment, University
of the Witwatersrand, Johannesburg, in fulfilment of the requirements for the degree of
Doctor of Philosophy.

Johannesburg
January, 2006

DECLARATION

I declare that this thesis is my own, unaided work. It is being submitted for the degree of Doctor of Philosophy at the University of the Witwatersrand, Johannesburg. It has not been submitted before for any degree or examination in any other University.

Experiments for generation of resistance spot welding data were carried out in collaboration with the Technical University (TU) Berlin and the Federal Institute of Materials Research (BAM) Berlin, Germany.

PN Oba

13th day of January 2006

ABSTRACT

Methods are presented for obtaining models used for predicting welded sample resistance and effective weld current (RMS) for desired weld diameter (weld quality) in the resistance spot welding process. These models were used to design predictive controllers for the welding process. A suitable process model forms an important step in the development and design of process controllers for achieving good weld quality with good reproducibility.

Effective current, dynamic resistance and applied electrode force are identified as important input parameters necessary to predict the output weld diameter. These input parameters are used for the process model and design of a predictive controller.

A three parameter empirical model with dependent and independent variables was used for curve fitting the nonlinear halfwave dynamic resistance. The estimates of the parameters were used to develop charts for determining overall resistance of samples for any desired weld diameter. Estimating resistance for samples welded in the machines from which dataset obtained were used to plot the chart yielded accurate results. However using these charts to estimate sample resistance for new and unknown machines yielded high estimation error. To improve the prediction accuracy the same set of data generated from the model were used to train four different neural network types. These were the Generalised Feed Forward (GFF) neural network, Multilayer Perceptron (MLP) network, Radial Basis Function (RBF) and Recurrent neural network (RNN).

Of the four network types trained, the MLP had the least mean square error for training and cross validation of 0.00037 and 0.00039 respectively with linear correlation coefficient in testing of 0.999 and maximum estimation error range from 0.1% to 3%. A prediction accuracy of about 97% to 99.9%. This model was selected for the design and implementation of the controller for predicting overall sample resistance. Using this predicted overall sample resistance, and applied electrode force, a second model was developed for predicting required effective weld current for any desired weld diameter. The prediction accuracy of this model was in the range of 94% to 99%.

The neural network predictive controller was designed using the MLP neural network models. The controller outputs effective current for any desired weld diameter and is observed to track the desired output accurately with same prediction accuracy of the model used which was about 94% to 99%. The controller works by utilizing the neural network output embedded in Microsoft Excel as a digital link library and is able to generate outputs for given inputs on activating the process by the push of a command button.

To the cherished memory of my mother, who passed away
Mrs Ruth Nkeoyem Oba

ACKNOWLEDGEMENTS

I wish to express my appreciation to the following:

- My dear wife and daughters, Joy, Gracia and Naomi for their support and encouragement.
- Special thanks to Dr. K. Battle, who was the initial supervisor of this project. For her consistent encouragement and support. We both stormed through the initial difficulties.
- Prof. Kin-inchi Matsuyama for getting me to sit with him and learn at the Massachusetts Institute of Technology (MIT), USA and for giving me useful contacts that made this work possible.
- Prof. Dr.-Ind. Dr. h.c.L. Dorn, and Dr. Kevin Momeni for arranging all the facilities used at the Federal Institute of Materials Research (BAN) Berlin, Germany for this research.
- Professor D. Chandler and Dr. S. Oerder for their supervision, commitment and encouragement during the period of this research. Special gratitude for the advice given on dynamic resistance modelling by Professor D. Chandler.
- Prof. T. Marwala, Mr. Brain Leke, and Dr. H. Campbell of Wits University and Gareth Shaw support at Optinum Solutions for their noteworthy answers to my numerous questions and technical advice.
- Afrox Pty and United Thermal Spray for their financial assistance.
- Finally, I wish to thank the Almighty God for life and strength to be able to carry out this work.

CONTENTS

	Page
DECLARATION	ii
ABSTRACT	iii
ACKNOWLEDGEMENTS	vi
CONTENTS	vii
APPENDICES	xii
LIST OF FIGURES	xvii
LIST OF TABLES	xxii
LIST OF SYMBOLS	xxii
CHAPTER 1 INTRODUCTION	1
1.1 Background	1
1.2 Research Hypothesis	4
1.3 Research Contribution	4
1.4 Thesis Outline	7
CHAPTER 2 BACKGROUND AND HISTORICAL DEVELOPMENT OF RESISTANCE SPOT WELDING PROCESS	
MODELLING	8
2.1 Introduction	8
2.2 Resistance Spot Welding	8
2.2.1 Electrode	11
2.2.1.1 Electrode Force	11
2.2.1.2 Electrode Diameter	11
2.2.1.3 Effect of Electrode Degradation	12
2.2.2 Squeeze Time	13
2.2.3 Weld Time	13
2.2.4 Forge Time (Cooling Time)	14
2.2.5 Weld Current	14
2.3 Development of Resistance Spot Welding Process Models and Control	15

	Page	
2.4	Effect of Machine Mechanical Characteristics on Weld Quality	18
2.5	Concluding Remarks	20
 <i>CHAPTER 3 NEURAL NETWORKS</i>		 21
3.1	Introduction	21
3.2	Background	21
	3.2.1 How Neural Networks Work	23
	3.2.2 Benefits and Applications of Neural Networks	27
	3.2.3 Neural Networks Limitations	29
3.3	Neural Networks versus Other Methods	30
3.4	Classification of Neural Networks	32
	3.4.1 Neural Network Architectures	35
	3.4.1.1 Multi-layer Perceptron (MLP)	35
	3.4.1.2 Radial Basis Function Networks	39
	3.4.1.3 Self-Organizing Maps (SOM)	40
	3.4.1.4 Recurrent Neural Networks	42
	3.4.2 Neural network Training and Learning methods	44
	3.4.2.1 Inverse Neural Network	47
	3.4.2.2 Brute Force Method	49
	3.4.2.3 Bounded Minimisation Technique (Fminbnd)	49
	3.4.2.4 Descent Optimisation Methods	52
	3.4.2.5 Quasi-Newton Method	53
	3.4.2.6 Learning Rates	54
	3.4.2.7 Learning Algorithms	54
3.5	Neural Network Design Formulation	57
	3.5.1 Input Data Processing	58
3.6	Noise and Generalization	60
3.7	Overfitting	61

	Page	
3.8	Reconditioning of the Neural Networks	62
3.9	The Application of Neural Networks in RSW	63
3.10	Neural Network Process Controller Model Design	65
	3.10.1 Model based controller (Predictive Control)	66
	3.10.2 Direct Inverse Control	68
	3.10.3 Neural Adaptive Control	70
	3.10.4 Back-Propagation Through Time (BPTT)	70
	3.10.5 Adaptive Critic Methods (ACM)	71
3.11	Pole Assignment (Placement) in Control Systems	72
3.12	Design Steps for the Neural Network	
	Predictive Controller	73
3.13	Sensitivity Analysis	74
3.14	Concluding Remarks	75
CHAPTER 4 TEST CONDITION		76
4.1	Introduction	76
4.2	Materials Selection	76
4.3	Welding of Plate Samples	77
4.4	Concluding Remarks	85
CHAPTER 5 RESULTS: DATA GENERATED		86
5.1	Introduction	86
5.2	Dynamic Voltage and Dynamic Current Data	86
5.3	Dynamic Resistance Data	88
5.4	Effective Weld Current and Weld Diameter Dataset	90
5.5	Concluding Remarks	95
CHAPTER 6 MODELLING THE PROCESS PARAMETERS		97
6.1	Introduction	97

	Page	
6.2	Empirical Model for the Dynamic Resistance Parameter	98
6.2.1	First Stage	99
6.2.2	Second Stage	100
6.2.3	Third Stage	101
6.2.4	Total Resistance	103
6.3	Applying the Empirical Model	109
6.4	Improving the Empirical Model using ANN	118
6.4.1	Training using Generalized Feed Forward Network	119
6.4.2	Training using Multilayer Perceptron Network	123
6.4.3	Training with Radial Basis Function Neural Network	127
6.4.4	Training with Recurrent Network	131
6.5	Improving Prediction Accuracy using MLP Architecture	136
6.6	Sensitivity analysis of the Result	140
6.7	Modelling the Overall Welding Process	143
6.7.1	Neural Network Model for the Overall Welding Process	143
6.7.2	Relationship Analysis of the Process Parameters	148
6.7.2.1	Effect of Dynamic Resistance on Weld Quality	149
6.7.2.2	Effect of Applied Electrode Force on Weld Quality	157
6.7.2.3	Effect of Weld Current on Weld Diameter	158
6.8	Concluding Remarks	159
 CHAPTER 7 DESIGN AND IMPLEMENTATION OF THE PREDICTIVE CONTROLLER		 161
7.1	Introduction	161

	Page
7.2 Design and Development of the Inverse MLP Neural Network Model	161
7.3 Design Implementation of the Predictive Process Controller	166
7.6 Concluding Remarks	171
 CHAPTER 8 CONCLUSION	 161
8.1 Introduction	161
8.2 Conclusion on Findings	173
8.3 Future Work	177
REFERENCES	179
BIBLIOGRAPHY	188
APPENDICES	191

APPENDIX A	DYNAMIC VOLTAGE AND DYNAMIC CURRENT DATA SET	191
Table A1	Step-1 (HW 1-20): Halfwave Voltage Values for C-Zange Machine at Applied Force of 2.2kN	191
Table A2	Step-2 (HW 1-20): Halfwave Voltage Values for C-Zange Machine at Applied Force of 2.2kN	192
Table A3	Step-3 (HW 1-20): Halfwave Voltage Values for C-Zange Machine at Applied Force of 2.2kN	194
Table A4	Step-4 (HW 1-20): Halfwave Voltage Values for C-Zange Machine at Applied Force of 2.2kN	195
Table A5	Step-5 (HW 1-20): Halfwave Voltage Values for C-Zange Machine at Applied Force of 2.2kN	197
Table A6	Step-6 (HW 1-20): Halfwave Voltage Values for C-Zange Machine at Applied Force of 2.2kN	198
Table A7	Step-1 (HW 1-20): Halfwave Current Values for C-Zange Machine at Applied Force of 2.2kN	200
Table A8	Step-2 (HW 1-20): Halfwave Current Values for C-Zange Machine at Applied Force of 2.2kN	201
Table A9	Step-3 (HW 1-20): Halfwave Current Values for C-Zange Machine at Applied Force of 2.2kN	203
Table A10	Step-4 (HW 1-20): Halfwave Current Values for C-Zange Machine at Applied Force of 2.2kN	204
Table A11	Step-5 (HW 1-20): Halfwave Current Values for C-Zange Machine at Applied Force of 2.2kN	206
Table A12	Step-6 (HW 1-20): Halfwave Current Values for C-Zange Machine at Applied Force of 2.2kN	207

	Page
APPENDIX B CALCULATED SAMPLE DYNAMIC RESISTANCE	
PLOT	209
Figure B1: C-Zange (2.6 kN) steps 1-6, Dynamic Resistance plot	210
Figure B2: C-Zange (3.0 kN) steps 1-6, Dynamic Resistance plot	211
Figure B3: PMS (2.2 kN) steps 1-6, Dynamic Resistance plot	212
Figure B4: PMS (2.6 kN) steps 1-6, Dynamic Resistance plot	213
Figure B5: PMS (3.0 kN) steps 1-6, Dynamic Resistance plot	214
Figure B6: Dalex-25 (1.76 kN) steps 1-6, Dynamic Resistance plot	215
Figure B7: Dalex-25 (2.16 kN) steps 1-6, Dynamic Resistance plot	216
Figure B8: Dalex-25 (2.2 kN) steps 1-6, Dynamic Resistance plot	217
Figure B9: Dalex-25 (2.46 kN) steps 1-6, Dynamic Resistance plot	218
Figure B10: Dalex-25 (2.6 kN) steps 1-6, Dynamic Resistance plot	219
Figure B11: Dalex-25 (3.0 kN) steps 1-6, Dynamic Resistance plot	220
Figure B12: DZ-35 (2.2 kN) steps 1-6, Dynamic Resistance plot	221
Figure B13: DZ-35 (2.6 kN) steps 1-6, Dynamic Resistance plot	222
Figure B14: DZ-35 (3.0 kN) steps 1-6, Dynamic Resistance plot	222

	Page
APPENDIX C	223
FITTED DYNAMIC RESISTANCE CURVES	
Figure C1	223
Fitted Dynamic Resistance Curve: C-Gun Machine at 2.2 kN Force	
Figure C2	224
Fitted Dynamic Resistance Curve: PMS Machine at 2.2 kN Force	
Figure C3	224
Fitted Dynamic Resistance Curve: PMS Machine at 2.6 kN Force	
Figure C4	225
Fitted Dynamic Resistance Curve: Dalex-35 Machine at 2.2 kN Force	
Figure C5	225
Fitted Dynamic Resistance Curve: Dalex-25 Machine at 3.0 kN Force	
Figure C6	226
Fitted Dynamic Resistance Curve: Dalex-35 Machine at 3.0 kN Force	
Figure C7	226
Fitted Dynamic Resistance Curve: Dalex-25 Machine at 2.16 kN Force	
Figure C8	227
Fitted Dynamic Resistance Curve C-Gun Machine at 3.0 kN Force	
Figure C9	228
Fitted Dynamic Resistance Curve: Dalex-25 Machine at 2.6 kN Force	
APPENDIX D	229
Code for Running the Embedded Neural Network Model Controller for Predicting Sample Resistance	
APPENDIX E	232
Code for Running the Embedded Neural Network Model Controller for Predicting Overall Process Controller	
APPENDIX F	235
Prediction of Effective Current for Desired Weld Diameter using the Controller Form	
Figures F1:	235
Effective Current Predicted for C-Zange Machine 3.0kN Applied Force	
Figures F2:	236
Effective Current Predicted for C-Zange Machine 2.6kN Applied Force	

	Page
Figures F3: Effective Current Predicted for C-Zange Machine 2.2kN Applied Force	236
Figures F4: Effective Current Predicted for Dalex Machine 1.76kN Applied Force	237
Figures F5: Effective Current Predicted for Dalex Machine 2.46kN Applied Force	237
Figures F6: Effective Current Predicted for PMS Machine 3.0kN Applied Force	238
Figures F7: Effective Current Predicted for PMS Machine 2.2kN Applied Force	238
Figures F8: Effective Current Predicted for PMS Machine 2.6kN Applied Force	239
Figures F9: Effective Current Predicted for PMS Machine 3.0kN Applied Force	239
Figures F10: Effective Current Predicted for DZ Machine 3.0kN Applied Force	240
Figures F11: Effective Current Predicted for DZ Machine 2.2kN Applied Force	240
Figures F12: Effective Current Predicted for DZ Machine 2.2kN Applied Force	241
 APPENDIX G PAPER SUBMISSION 1	 242
 APPENDIX H PAPER SUBMISSION 2	 243
 APPENDIX I PAPER 3 DEVELOPED FOR SUBMISSION	 244
 APPENDIX J PAPER 4 DEVELOPED FOR SUBMISSION	 246

LIST OF FIGURES		Page
Figure 2.1	Resistance Spot Welding Cycle	9
Figure 3.1	A Neural Network Architecture	24
Figure 3.2	Neural Network Adaptive process	24
Figure 3.3	Single Layer Neural Network Structure	25
Figure 3.4	The Simple Neuron Model	26
Figure 3.5	A Simple Feedforward Neural Network Diagram	33
Figure 3.6	Simple Feedback Network Diagram	34
Figure 3.7	Architecture of a Multi-layer Perceptron Network	36
Figure 3.8	Radial Basis Function (RBF) Network	39
Figure 3.9	Dimensional Reduction of Data by Self-organising map	41
Figure 3.10	Self-Organising Map Architecture	42
Figure 3.11	Fully recurrent neural networks	43
Figure 3.12	Neural Network Inverse Controller	69
Figure 3.13	Inverse Model Optimal Controller	69
Figure 3.14	Inverse controller with disturbance correction	70
Figure 3.15	Data Generation and Training of Neural Network	73
Figure 4.1	Shape and Size of the Sample Plates welded	77
Figure 4.2	PMS-Stationary Resistance Spot Welding Machine	79
Figure 4.3	Dalex-25 Mobile Resistance Spot Welding Machine	80
Figure 4.4	Plug Failure	83
Figure 4.5	Shear Failure	83
Figure 4.6	Instron Torsion Machine	84
Figure 4.7	Double Plates with Welded Spot	84
Figure 4.8	Microstructure of a Spot Weld Nugget	85
Figure 5.1	Dynamic Voltage Steps 1-6 for Dalex – Gun 25 Applied Force 2.2kN	87

	Page	
Figure 5.2	Dynamic Current Steps 1-6 for Dalex – Gun 25 Applied Force 2.2kN	88
Figure 5.3	C-Gun (2.2kN) Steps 1-6 Dynamic Resistance Plot	89
Figure 5.4	C-Gun (2.2kN) Steps 1 and 6, Effective Current	92
Figure 5.5	C-Gun (2.2kN) Steps 1 and 6, Weld Diameter	92
Figure 5.6	Metallography of weld spot nuggets of step 1, welded sample, Dalex PMS	93
Figure 5.7	Metallography of weld spot nuggets of step 6, welded sample, Dalex PMS	93
Figure 6.1	Trend Patterns of Early Stages of Resistance Spot Welding with Peak Point	98
Figure 6.2	Influence of Parameter M on Resistance	100
Figure 6.3	Dynamic resistance trends from the peak point Downwards	101
Figure 6.4	Influence of Parameter K on Resistance	103
Figure 6.5	Curve fitted Model at $n = 0.5$	105
Figure 6.6	Fitted Dynamic Resistance Curve: DZ Machine at 3.0 kN Force	109
Figure 6.7	Machine C-Zange – Parameters M and K and Applied electrode force 2.2KN	112
Figure 6.8	Parameters K and M Generated	114
Figure 6.9	Parameters Ro Generated	115
Figure 6.10	Predicted Resistance to Actual in Dalex Machine	116
Figure 6.11	Generated generalized feedforward network architecture design	120
Figure 6.12	Training performance of the generalized feedforward network	120
Figure 6.13	Testing performance of the generalized feedforward network	121

	Page	
Figure 6.14	Validation performances of the generalized feedforward network	123
Figure 6.15	Generated multilayer perceptrons (MLP) network architecture design	124
Figure 6.16	Training performance of the multilayer perceptrons (MLP) network	124
Figure 6.17	Testing performance of the multilayer perceptrons (MLP) network	125
Figure 6.18	Validation performance of the multilayer perceptrons (MLP) network	127
Figure 6.19	Generated Radial basis function (RBF) network architecture design	128
Figure 6.20	Training performance of the Radial basis function (RBF) network	128
Figure 6.21	Testing performance of the Radial basis function network	129
Figure 6.22	Validation performance of the Radial basis function (RBF) network	131
Figure 6.23	Generated Recurrent Network architecture design	132
Figure 6.24	Training performance of the Recurrent Neural Network	132
Figure 6.25	Testing performance of the Recurrent Neural Network	133
Figure 6.26	Validation performance of the Recurrent Network	135
Figure 6.27	Generated Multilayer Perceptron Network Architecture Design with more input parameters	136
Figure 6.28	Training performance of the Multilayer Perceptron Network with more input parameters	137
Figure 6.29	Testing performance of the Multilayer Perceptron Network with more input parameters	138

	Page
Figure 6.30 Validation performance of the Multilayer perceptron Neural Network using Production Data	140
Figure 6.31 Sensitivity Analysis of the Input Parameters to the Output	142
Figure 6.32 Generated Multilayer Perceptron (MLP) Network Architecture Design	145
Figure 6.33 Training Performance of the Multilayer Perceptron (MLP) Network Design	145
Figure 6.34 Testing Performance of the Multilayer Perceptron Network	146
Figure 6.35 Validation Performance of the Multilayer Perceptron Network	147
Figure 6.36 Sensitivity of the selected Inputs Parameters to the Output	149
Figure 6.37 Sensitivity Result of the Varied Input Resistance to Weld Diameter	150
Figure 6.38 Calculated Sample Resistance welded with C-Zange Machine	151
Figure 6.39 Calculated Sample Resistance welded with DZ Machine	152
Figure 6.40 Calculated Sample Resistance welded with Dalex Machine	153
Figure 6.41 Calculated Sample Resistance welded with PMS Machine	154
Figure 6.42 Calculated Sample Resistance in all four Machines at 2.2kN Force	155
Figure 6.43 Calculated Sample Resistance in all four Machines at 2.6kN Force	155
Figure 6.44 Calculated Sample Resistance in all four Machines at 3.0kN Force	156

	Page	
Figure 6.45	Result of the Varied Input Force to Weld Diameter	157
Figure 6.46	Result of the Varied Input Current to Weld Diameter	158
Figure 7.1	Generated multilayer perceptron (MLP) Inverse Network Architecture Design	162
Figure 7.2	Testing performance of the multilayer perceptron (MLP) network design	163
Figure 7.3	Testing Performance of the Multilayer Perceptron Network	163
Figure 7.4	Validation Performance of the Multilayer Perceptron Network	164
Figure 7.5	Neural Network Controller Design for Predicting Effective Current	166
Figure 7.6	Controller Model form for Predicting Sample Resistance	167
Figure 7.7	Controller form for generating network output	168
Figure 7.8	Effective Current Predicted for C-Zange Machine 3.0 kN Applied Force	168
Figure 7.9	Embedded Controller for Predicting Effective Weld Current	169

LIST OF TABLES

	Page	
Table 2.1	Definition of the wear classes	12
Table 3.1	Different Types of Activation Functions	36
Table 4.1	Chemical Composition of the coated plain Carbon Steel	76
Table 4.2:	Mechanical properties Supplied by Manufacturer	77
Table 5.1	Observed Maximum Values: weld diameter, effective current and observed expulsion weld diameter	94
Table 6.1	Estimation Sample Resistance (R)	110
Table 6.2	Correlations Matrix	117
Table 6.3	Multiple Correlations Matrix	117
Table 6.4	Predicted Resistance to Actual Resistance using Generalized Feedforward Neural Network type	122
Table 6.5	Predicted Resistance to Actual Resistance using Multilayer Perceptron Neural Network type	126
Table 6.6	Predicted Resistance to Actual Resistance using Radial basis function neural network type	130
Table 6.7	Predicted Resistance to Actual Resistance using Recurrent neural network type	134
Table 6.8	Comparism of Performance Results of the Four Neural network types Used	135
Table 6.9	Predicted Resistance to Actual Resistance using Multilayer perceptron neural network with More input parameters	139
Table 6.10	Comparism of performance results of four neural network types	144
Table 6.11	Predicted Weld Diameter to Actual using Multilayer Perceptron Neural Network	147

	Page	
Table 7.1	Predicted Effective Weld Current to Actual Effective Weld Current using Multilayer Perceptron (MPL) network	165
Table 7.2:	Prediction of Effective Weld Current for Different Machines and Applied Electrode Force	170

CHAPTER 1

INTRODUCTION

1.1 Background

There are two main approaches to quality analysis in a manufacturing environment; they are reactive and proactive quality analysis ⁽¹⁾. Strategies for reactive quality analysis include individual inspection of all products according to specifications, sampling plans, and lot acceptance determination. Proactive strategy includes physical cause-effect knowledge, risk analysis, process control, statistical quality control (including statistical process control and control charts), monitoring and diagnosis ⁽¹⁾. Proactive strategy is considered important in continuous manufacturing processes because of the savings of cost in time loss that would have been caused by interruption in the process during quality check.

In resistance spot welding there is the need to either control the changing variables that affect weld quality during the welding process or to model the parameters that affect the process so that the products of the process will be of the desired quality. From 1912 when E.G.Budd ⁽²⁾ made spot welds on the first automobile body in Philadelphia, Pennsylvania, USA, using resistance spot welding process, research work has been ongoing in trying to guarantee quality of resistance spot welds.

Specifically, resistance spot welding is one of the most widely used materials joining processes in the automotive industry. Thousands of welds are made on vehicle bodies and other material components. The quality of the spot welds are of paramount importance in the automotive assembly process. More than 30% redundant (excess) spot welds are often required by design specifications ⁽³⁾ in resistance spot welded structures because of the uncertainty and difficulty in making and reproducing good quality spot welds. This measure is aimed at reducing the chance of failure of the spot welded structure.

Eliminating this waste (excess weld) by correctly predicting parameters that will give good spot welds with possibility for reproducibility of the good weld quality will help reduce production cost in this area.

Currently on the traditional shop floor ⁽³⁾, destructive techniques for assessing weld quality, though considered inappropriate, expensive and time consuming, are still conducted periodically in assembly plants, because current monitoring and control systems in use have failed to adequately meet the challenge of determining (predicting) weld quality ⁽³⁾.

Studies carried out over the last fifty years ^(3, 4) on modelling and controlling the resistance spot welding process have proved that the physical laws governing the resistance spot welding process are highly complex and non linear. This makes control of the process a difficult task, particularly with the increased usage of corrosion resistant galvanized steel sheets ⁽⁴⁾ compared to the use of bare steel sheets. The difficulty arises because of unpredictable quality variation in the spot weld due to changes in current density resulting from the changes in the diameter of the electrode tip during the welding process ⁽⁴⁾. This change in diameter is caused by the rapid wear of the electrode tip surface in contact with the galvanised steel sheet during the spot welding process ⁽⁴⁾.

Feng et al ⁽³⁾ suggest that to consistently achieve good resistance spot welds, two conditions must be met. First, an optimum set of welding parameters must be defined to produce the properties desired of the weld. Secondly, control must be implemented to maintain the process variables within necessary ranges so that optimized welds can be made with good reproducibility.

Matsuyama ⁽⁵⁾ in his review of previous research work done in the mid sixties cited the work by Waller et al ⁽⁶⁾, in which the researchers formulated regression equations (obtained by regression analysis) for quality monitoring of resistance spot welding. The equation was determined using many preliminary experimental data. Similarly, other researchers in the seventies tried different monitoring systems like using thermo sensors to measure surface temperature of weld or monitoring the resistance between the

electrode tips by monitoring voltage between electrode tips and welding current⁽⁵⁾. In the eighties there were attempts to use simulation techniques built and run on computers⁽⁵⁾, to model the actual resistance spot welding process. Research has continued to be active in this field. Presently, neural network models are being explored in this area because of their suitability for nonlinear problems as well as ease in adjustment of pre-set parameters and adaptability to learning⁽⁶⁾.

The Literature suggest that to be able to develop and design a process control application, a proper model of the physical process has to be established^(3, 5). This means that the critical parameters that affect quality in the process has to be identified, then modelled using an appropriate framework and finally used to develop a controller that can predict the quality of output for any combination of input variables for the process.

The resistance spot welding machine and the welding process are made up of mechanical and electrical characteristics^(3, 7). In the literature review the views and findings of researchers on these characteristics as sources of variations to resistance spot weld quality are discussed. The specific features of the parameters that influence the characteristics covered in this thesis are dynamic resistance, effective current, machine friction, stiffness and weight of the welding machine cylinder head^(7, 8, 9). Applied electrode force which is used during the welding process is also discussed. The benefits of using neural networks and the approach for designing a neural network controller are outlined.

Other forms of variations in the resistance spot welding process exist. Wei et al⁽¹⁰⁾ mentioned abnormal conditions which include welding plate misalignment and parts not fitting correctly during the welding process as an example of such variation. Such process abnormalities affect the relationships between the weld size (weld quality) and the input process variables and thus cause the weld quality to vary. The variations however, can be easily managed by good engineering practice and are therefore not considered in this research.

Further discussed in this thesis is the design methodology for the development of a predictive controller. The methodology involves relationship analysis of the resistance

spot welding input parameters and identification of signals used as inputs and outputs in the neural network architecture. An empirical model was developed for curve fitting the nonlinear dynamic resistance parameter (one of the required neural network input signal) necessary for predicting overall resistance of each welded sample. Neural network types were analysed and the most appropriate neural network type and architecture based on least prediction error criteria was employed for the development and design of the predictive controller.

A neural network predictive controller model was used in this application because other design methodology which embodies a conventional continuous frequency domain controller design and neural network adaptive control architectures are considered inappropriate for the design of a predictive process controller^(11, 12). Similarly fuzzy logic is considered inappropriate for developing the process controller because of the problem with designing membership functions which Kumar et al⁽¹³⁾ give as type and number of member functions, their shape and range and the difficulty with choosing appropriate fuzzy rules⁽¹³⁾.

1.2 Research Hypothesis

Is it possible to empirically model dynamic resistance variable and predict with accuracy of about 100%, the required effective weld current for a desired weld diameter (weld quality) with good chance of reproducibility in the resistance spot welding process?

1.3 Research Contribution

Reproducing desired weld quality in the resistance spot welding process has remained a challenge. Addressing the research hypothesis will give rise to the possibility of reproducing desired quality of spot welds using specified combinations of the welding parameters. The aim of this research therefore is to model the parameters that affect the

final product and thus ensure a desired quality output with possibility for exact reproducibility. Based on this need this research work aims to:

- Carry out further research to determine the contributory effects of electrical parameters on the resistance spot welding process, and to demonstrate that the data generated from the electrical characteristic sources alone are sufficient and appropriate to build a process model. The process model will be used to predict the optimum welding parameters that give a good weld quality output with possibility for good reproducibility. For the sake of error minimisation the same material composition and thickness are used for all the samples investigated.
- Investigate different neural network types and select the most appropriate (ability to predict accurately) that can be used to model and optimise the resistance spot welding process, based on the identified input parameters from the welding process data.
- Investigate the possibility of deploying the identified neural network model for the development and design of controller with capability of predicting effective weld current for any desired weld diameter, given applied electrode force and predicted (estimated) resistance.
- Confirm the most important parameter(s) that would be used to set boundary ranges for which these controllers can work and predict outcomes accurately.

Included in this work is an empirical model for curve fitting the dynamic resistance curve in order to obtain the parameters that can be used to estimate each sample resistance with good accuracy. The predicted sample resistance, applied electrode force and effective current will be used as input variables to train the neural network with the weld diameter as the output variable. The weld diameter is normally taken as the production criterion of weld quality. However, because effective current is what can be controlled in the welding process and is presently in the industry determined by trial and error. A unique contribution of this research is to overcome this trial and error method by using neural

network to learn the pattern of the data so that effective current can be accurately predicted for any desired weld diameter.

An important contribution of this work was the use of only electrical characteristics and applied electrode force data to model the resistance spot welding process. The data were generated from four different resistance spot welding machines and were used to train and validate the selected neural network types. The trained neural networks were used to predict (generalise) weld quality for situations it has not experienced or seen before using real data from the welding machines.

The neural network model which gave the least error prediction was used in the development and design of the predictive controllers. This was used for predicting effective current required to achieve desired weld diameter in any resistance spot welding machine with materials type, electrode type and thickness specified as the boundary conditions.

In summary the contributions of this work to the pool of knowledge are as follows:

- The application of an approximate empirical mathematical function to model the dynamic resistance curve and to use the generated parameters to train the neural network for predicting sample resistance.
- Use of feedforward multi layer perceptron algorithm for developing resistance spot welding process model and inverting the initial feedforward network architecture, such that effective current can be predicted and controlled in the welding process for desired weld quality (weld diameter). The selection of the neural network type is based on least error minimization and other criteria.
- Use of this model to optimize welding parameters for best quality of weld in any resistance spot welding machine.
- The development and design of a controller, such that for a desired weld diameter, required effective current will be predicted.
- Present an appropriate controller for use in this application based on prediction accuracy.

- Accurately predict the current that will be used to achieve a desired weld diameter without identifying the welding machine in the model.
- Show that electrical characteristics and applied electrode force data alone are enough to predict weld quality. This will help resolve the debate on the real importance of electrical characteristics data to mechanical characteristics data in the resistance spot welding process and weld quality determination.
- Based on findings to present electrical characteristics data alone as sufficient data to use in modelling and developing controller for predicting weld quality output.
- Show that it is possible to use data generated from the welding machines to train the neural network and then validate its ability to generalise using any of the spot welding machines to accurately predict output.

1.4 Thesis Outline

To address the research hypothesis, two approaches are used. First approach deals with the qualitative theory and development of the resistance welding process, dynamic resistance theory, neural network types and applications and the numerical techniques required for applying the theory to practical applications. The second part deals with quantitative development and design process, from the analysis of the problem specification, to the choice of appropriate neural network type for the process model, and finally to the actual neural network controller design using the models.

The dynamic resistance concept, mechanical characteristics, historical development of real time control methodology discussed in Chapter 2 forms a crucial part of the modelling methodology. Chapter 3 deals with the literature review on neural network types and design steps for the process controller. Chapter 4 discusses the experimental procedure for process data generation. Chapter 5 presents the Results and Discussions of the data generated. Chapter 6 discusses the modelling of the welding process parameters. Controller design implementation is presented in Chapter 7. Chapter 8 presents the final conclusions relating to this study.

CHAPTER 2

BACKGROUND AND HISTORICAL DEVELOPMENT OF RESISTANCE SPOT WELDING PROCESS MODELLING

2.1 Introduction

This section consists of a review of the analysis of resistance spot welding process parameters. A proper theoretical understanding of the resistance spot welding techniques and process parameters is very crucial for the development of process model and predictive controller. The work of researchers who developed mathematical models and simulation of the resistance spot welding process are explored so as to identify the parameters that critically affect weld quality and their relationships to one another. The section begins with the primary definition of the welding process, progressing to more detailed description of the concepts and theories around the process. This review will also include discussion on electrode degradation and the views of researchers on the effect of mechanical characteristics on weld quality.

2.2 Resistance Spot Welding

Work by Gupta et al ⁽¹⁴⁾ as cited by Aravinthan et al ⁽¹⁵⁾ mentioned that the resistance welding process was invented in 1877 by Elihu Thomson, but only put to use in manufacturing by E.G.Budd ⁽²⁾. This process has since then been used as a joining process in the manufacturing industries, particularly in the automobile and aircraft industry ⁽¹⁵⁾. Some of the advantages of resistance spot welding over other joining techniques are the ease of automating the process, high energy efficiency, and high speed ⁽¹⁶⁾.

Spot welding is a joining process in which coalescence of sheet metals is produced between the surfaces of two or more metal parts by the application of heat and pressure in a localized area ⁽¹⁶⁾. Figure 2.1, shows the sequence of a typical resistance spot welding process cycle. It consists of squeeze stage, weld stage and forge stage. At the beginning of the welding process, the workpiece (metal sheet) to be joined are placed in-between the two copper electrodes shown. The electrodes are subsequently closed onto the workpiece and optimum pressure is applied such that the electrodes exert some compressive stress on the workpiece. The applied pressure causes an increase in the electrical contact of the surfaces in contact. The copper electrodes also provide support and pass current to the work piece, when the current is applied.

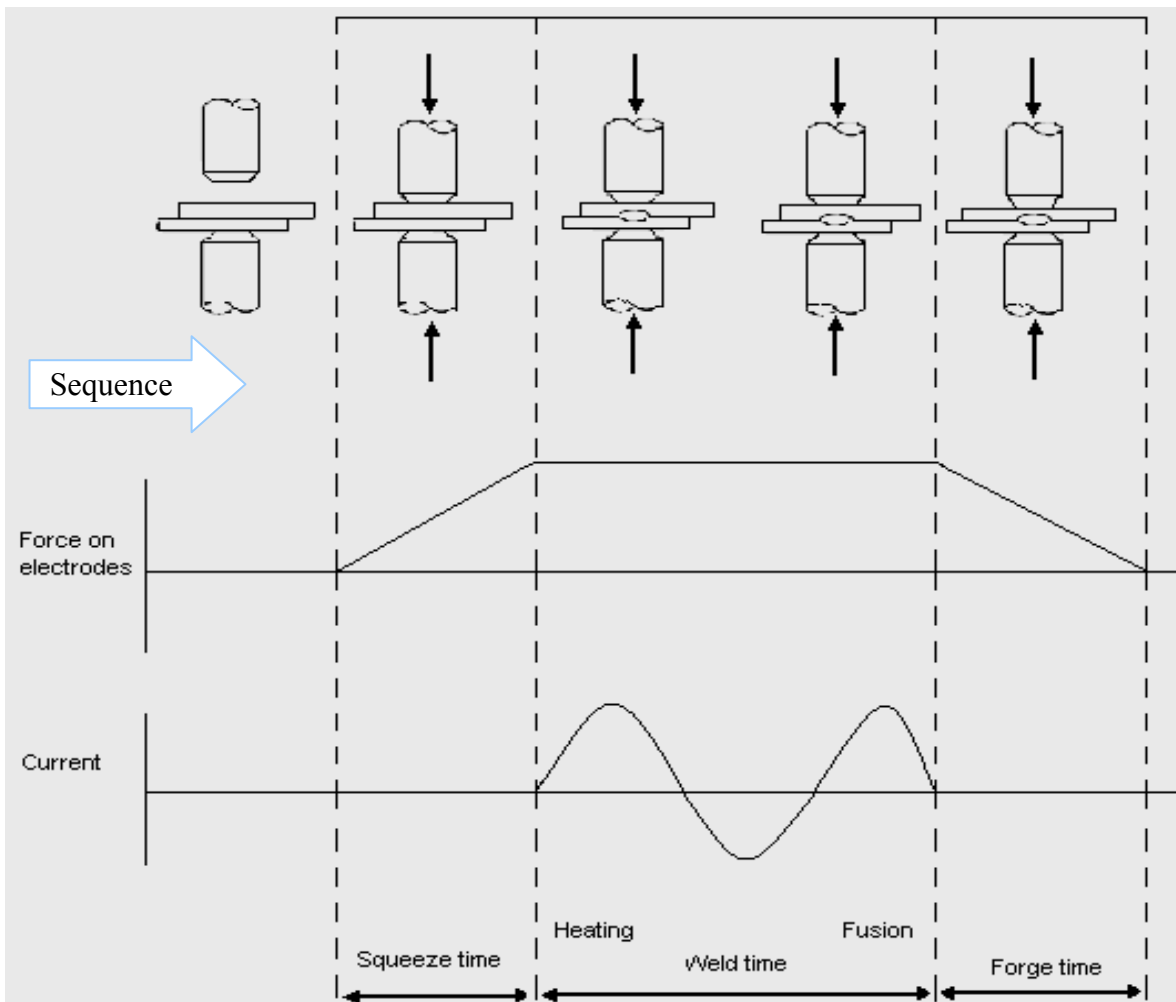


Figure 2.1: Resistance spot welding cycle ⁽¹⁷⁾

With electrical contact achieved by the effect of the electrode force, current is passed through the sheet metals for a set time period. Heat is generated between the surfaces of the sheet metals by the resistance offered to the flow of current. During this time a nugget is formed in-between the plate samples ⁽¹⁶⁾ and grows further to become the spot weld as heat generated by the resistance effect is sustained. After the weld is formed the applied pressure is maintained to enhance solidification of the weld and to prevent expulsion. The pressure is subsequently released and the electrodes are lifted away from the work piece ⁽¹⁷⁾.

During the welding process, once the specified cycle time which marks the process completion is reached, the current supply is switched off and the weld (nugget) is allowed to solidify by slow cooling under pressure ⁽¹⁶⁾. The applied electrode force and the surrounding solid metal help to contain the molten pool ⁽¹⁶⁾. The effect of the applied electrode pressure under plastic deformation on the heated metal sealing creates a ring on the surface of the metal. This effect can lead to corona (part with the ring impression) bonding ⁽¹⁶⁾. Expulsion occurs when this sealed ring ruptures suddenly during the welding process such that some of the molten nugget metal is spewed out from between the sheets ⁽¹⁶⁾.

Expulsion is accelerated when welding close to an edge due to bad fit or lack of mechanical supports or low applied electrode force ⁽¹⁶⁾. Expulsion can also occur at the electrode work interface if the generation of heat is too quick and excessive ⁽¹⁶⁾. This can happen when scales which build up high resistance are present on the surfaces of the sheets to be welded or when low resistivity metals are used ⁽¹⁶⁾.

The parameters which are considered in the spot welding process are electrode force, diameter of the electrode contact surface, squeeze time, weld time, hold time and weld current ⁽¹⁸⁾. These parameters will each be briefly discussed.

2.2.1 Electrode

The copper electrodes used during the resistance spot welding process plays a very important role. The specific roles played by the electrode in the welding process are as follows:

2.2.1.1 Electrode Force

The electrode force is obtained by the compressive effect of the two electrodes applied to the sheet metals thereby squeezing the metal sheets to be joined together⁽¹⁸⁾. Adequate electrode force is necessary to achieve good weld. The applied electrode force has some inverse relationship with heat energy⁽¹⁸⁾. Too low an applied force is inadequate for achieving good weld quality. Excessively increasing the applied electrode force can lead to expulsion⁽¹⁸⁾. Optimum value of applied electrode force has to be determined for best output.

2.2.1.2 Electrode Diameter

Diameter of the electrode contact surface is used to determine the weld diameter. Weld diameter is a measure of weld quality. As the welding progresses the diameter of the electrode will change due to effect of wear. Weld diameter (nugget diameter) is determined based on the number of spot welds that has been made with the electrode. Generally the nugget diameter is slightly less than the contact electrodes diameter⁽¹⁸⁾.

A general recommendation⁽¹⁸⁾ is that the weld should have a nugget diameter of greater than $4\sqrt{t}$, ($5\sqrt{t}$ is recommended as appropriate), “t” being the thickness of the steel sheet. However, the work done by Weber et al⁽¹⁹⁾ gave further wear classes of electrodes based on the number of weld spots made with the electrode. Such that the nugget diameter should be based on wear state of the electrode. The wear classes, the number of corresponding spot welds and the nugget diameter that the weld should have as given by

Weber et al ⁽¹⁹⁾ findings are presented in Table 2.1. Transition state 1 presented in the Table 2.1 indicates the state of mild wear while transition state 2 is the state of rapid wear of the welding electrode. In this research the electrode to be used is the one that has made more than 900 number of spot welds but less than 1700 (Wear class V1). So an achieved weld diameter of $4\sqrt{t} \leq d < 5\sqrt{t}$ will be considered satisfactory. Optimisation of the resistance spot welding process however is to maximise the size of the weld diameter for a given set of input parameters.

Table 2.1: Definition of the wear classes ⁽¹⁹⁾

Wear class	Number of spot welds	Quality	Remark
V0 – non-wear state	≤ 900	$d \geq 5\sqrt{t}$	Spot weld is “good”.
V1 – transition state 1	900 ... 1700	$4\sqrt{t} \leq d < 5\sqrt{t}$	Spot weld is “satisfactory”.
V2 – transition state 2	1700 ... 2000	$3\sqrt{t} \leq d < 4\sqrt{t}$	Spot weld is “adequate”.
V3 – worn state	≥ 2000	$d < 3\sqrt{t}$	Spot weld is “inadequate”.

2.2.1.3 Effect of Electrode Degradation

Many research and studies have been carried out on the degradation of electrodes during resistance spot welding ⁽²⁰⁾. Particularly because of the rapid wear of these electrodes with the increased usage of Zinc coated steels in manufacturing ^(20, 21). This has raised production cost in the areas of frequent electrode change over time, cost of replacing electrodes and high possibility for poor weld joint quality ⁽²¹⁾. Zinc coated steel protects the steel sheet from corrosion ⁽²⁰⁾.

Dupuy et al ⁽²⁰⁾ reported a study on degradation of electrodes when spot welding zinc coated steels. The main findings of the study were that degradation of electrodes was characterized by an enlargement of the electrode tip ⁽²⁰⁾. This enlarged electrode tip causes current density passing through the electrode to drop and can get to a point where the weld current is not sufficient to achieve a weld ⁽²⁰⁾.

Dupuy et al ⁽²⁰⁾ and De et al ⁽²¹⁾ in their respective studies mentioned that the actual cause of electrode enlargement is still not very clear however, a number of phenomena are given as the likely causes of the enlargement of the electrode tip. This ranges from possibility of diffusion of zinc into copper, possibility of pitting erosion, cracking of electrode tip, mushrooming and other reasons ⁽²⁰⁾.

The importance of this electrode wear to this study is the fact that changes in the tip size and topography of the electrode governs the nugget size and shape formation during the welding process ⁽²⁰⁾. Also, zinc coated metal sheet which is known to wear the copper electrodes away so quickly are used for the experiment in this research. Electrode condition is therefore an important quality consideration in the development of the process model.

2.2.2 Squeeze time

Squeeze time as shown in Figure 2.1, is the time at which the required level of the pressure is set and no current flowing through the circuit ⁽¹⁸⁾. This is done to achieve good electrical contact between the electrodes and the work piece, and between the two surfaces of the work piece ^(17, 18).

2.2.3 Weld time

Weld time is the duration in which the welding current is applied to the sheet plates after the squeeze time is completed as shown in Figure 2.1. Weld time is giving in weld cycles with peaks and troughs such that one peak and a trough give a complete wave length. In a

50 Hz power system one cycle is given as 1/50 of a second ⁽¹⁸⁾. The welding time is represented as half wave cycle time in the welding process. Two half wave cycles gives one cycle time ⁽¹⁸⁾, a number of halfwave cycle time are required to successively make a spot weld. The total welding process time (program) to make a number of spot welds are further divided into a number of small time steps ⁽¹⁸⁾. Typically the time steps are planned (arranged) in such a way that they fall within the entire welding current window range that will be used to spot weld a number of samples.

2.2.4 Forge time (cooling-time)

Hold time is the period from when the weld time is completed, the current switched off, and the electrodes still applied to the welded metal sheet for cooling. This period helps the weld to chill ⁽¹⁸⁾ as the nugget solidifies as shown in Figure 2.1. Optimum hold time is necessary to prevent the electrode in contact with the hot spot weld heating up, or the weld spot cooling too fast as it can alter the metallurgical property of the metal ⁽¹⁸⁾.

2.2.5 Weld current

The weld current is made available in the welding circuit during spot welding by setting the transformer tap switch to a level that allows a maximum amount of current to be made available ⁽¹⁸⁾. The effective current used during the welding cycle is based on the percentage of current set (current window) for making the weld. Most spot welding machine current tap switch are set so that between seventy and ninety percent current are utilized ⁽¹⁸⁾. Determining actual current to use, is usually by trial and error, the guide is that weld current should be kept as low as possible to reduce excessive heat input into the sheet metal, but has to be sufficiently high enough to achieve good weld ⁽¹⁸⁾ (should achieve good weld diameter size as is practically possible).

When determining the current to be used, the current is gradually increased until weld expulsion (splatter) occurs between the metal sheets ⁽¹⁸⁾. This indicates that the correct weld current has been exceeded. The lower boundary is the current that will be enough to

exceed the stick limit ⁽¹⁸⁾. Stick limit is the threshold weld diameter that is sufficient to form a welded joint. This trial and error approach introduces much variability in the spot weld quality and presents difficulty with reproducibility of the desired quality.

Having established the welding sequence in the resistance spot welding process, it is important to investigate the previous techniques and methods that have been used for modelling the process parameters.

2.3 Development of Resistance Spot Welding Process Control Models

This section presents the modelling and control approach used by previous researchers in this area of study. Several techniques and procedures have been suggested for welding process modelling, monitoring and control, involving routine or continuous monitoring of the process variables.

Investigations on the development of real time control methodology by Tsai et al ⁽²²⁾, found that the initial approach to resistance spot welding modelling in the fifties was based on observing the electrodes movement during the welding process. Electrode displacements were assumed to relate to the achieved weld size. Monitoring and control equipment developed then was based on thermal expansion rate or maximum expansion displacement ⁽²²⁾. Other researchers continued to try improving on this model ⁽²²⁾. This lead to a number of monitoring and control equipment produced in this area but with little or no success ^(22, 23, 24).

Progressing from the fifties to the sixties Tsai et al ⁽²²⁾ reported J.A. Greenwood as having developed a model that correlates the surface temperatures of spot welds to maximum temperature at the nugget centre during the welding process ⁽²²⁾. In order to determine temperature of the weld nugget using infrared emission from the metal surface, thermocouples were mounted on either the workpiece or the electrodes ⁽²²⁾. This approach was reported as unsuccessful because the welding operation had to be interrupted to attach the thermocouples with an additional problem of spurious feedback signals and

erroneous temperature reading from the thermocouple due to variations in infrared emissivity⁽²²⁾.

Tsai et al⁽²²⁾ mentioned that to improve the monitoring and control process an automatic load adjusting system was developed in the seventies by Johnson and Needham. This system was based on the observation that by combining electrode force, weld current and welding duration it will be possible to determine weld quality, provided a critical value of applied electrode force was used. This system was able to restrict weld expansion during welding⁽²²⁾. A linear relationship was said to exist between the subsized nugget and the expulsion limit⁽²²⁾. Electrode force was at that stage presented as the most important control parameter necessary to achieve good weld quality⁽²²⁾. The drawback as reported⁽²²⁾ was that while trying to use the thermal expansion curve to adjust weld current, weld time and electrode force, the electrode displacement in a number of cases were insensitive and sometimes had no response to the expansion signal in the initial expansion rate based control system⁽²²⁾.

Further and more advanced techniques like ultrasonic signals and acoustic emission techniques were employed to detect weld size⁽²²⁾. However, cost and complexity made these systems unsuitable for use in most applications⁽²²⁾.

Feng et al⁽³⁾ gave a different perspective to the modelling and performance development of the resistance spot welding process. He proposed an “integrated interdisciplinary modelling approach to simulate the performance properties of resistance spot weld joints”. The approach used basic physical phenomena such as the physics, mechanics and metallurgy of the process, which occur during the welding process and in service under loading conditions. However, this optimisation procedure was limited and could not be effectively applied to high-strength steels because weldment properties depend on microstructure⁽³⁾.

Further work in resistance spot welding process was in using numerical simulation techniques to predict pattern and size of nugget during the welding cycle⁽²³⁾. In most of the earlier investigations temperature and pattern of formation of nuggets were calculated

without accounting for varying contact diameters at the electrode-workpiece surface and the faying (surface of member that is in contact with another member to which it is joined) surface between the sheet metals ⁽²³⁾.

Matsuyama ⁽²³⁾ reviewed the research work done in the mid eighties by Nishiguchi in which the study produced a numerical simulation of nugget formation for estimating contact diameters at the electrode-sheet interface. The review concluded that it was possible to predict with some accuracy the nugget formation process without including the electrical contact resistance at the faying surfaces ⁽²³⁾.

In 2000, Matsuyama ⁽²⁴⁾ developed a numerical simulation procedure to predict the nugget formation process using varying contact diameter concept and observed interface contact resistance on the nugget formation process. The study applied varying contact diameter model without incorporating contact resistance model and concluded that the interface contact resistance can be ignored in normal resistance spot welding as it is not very important. The research work presented varying contact diameter alone as adequate for estimating the nugget formation process ⁽²⁴⁾.

An improvement to an earlier method that used a heat conduction differential equation was the recent work in 2002, by Matsuyama et al ⁽²⁵⁾. In this new approach an algorithm based on an integral form of an energy balance model for monitoring and control of the resistance spot welding process was developed. The simulation was set to calculate the average temperature of a weld during the welding cycle by using measured parameters which are welding voltage, welding current and total plate thickness. This was used to predict both weld diameter and expulsion occurrence ⁽²⁵⁾. Current and voltage measurements made across the electrodes were processed according to equation 2.1, to provide dynamic resistance, given as ⁽²⁵⁾:

$$R = V / I \quad 2.1$$

Where R is the dynamic resistance (ohms), V is voltage (Volts) and I is current (Ampere).

Only peak values of voltage and current were used in order to avoid the effect of inductance (effect due to voltage drop in the circuit) on the value of these parameters ⁽²⁵⁾.

Tsai et al ⁽²²⁾ mentioned that the use of electrical parameters for monitoring and control of the resistance spot welding process are considered the most successful of all in-process quality control systems. However, there are a number of limitations ⁽²²⁾, which are;

1. The method is mostly suitable for uncoated mild steels, compared to other metal alloys and coated mild steels because of electrode wear during the welding process, which makes reproducibility of same weld quality with the same machine setting difficult ⁽²²⁾. This can though be accounted for in a model, by using the wear state of the electrodes to set boundary conditions.
2. The voltage clip position on the electrode to capture data during the welding process gets on the way ⁽²²⁾.

In these techniques, trial and error and experience still dominates its effective use ⁽²²⁾ particularly in the determination and setting of the welding machine for achieving desired spot weld quality. Use of artificial intelligence applications like the artificial neural networks are been used to model the resistance spot welding process ⁽⁶⁾. This application technique is further explored in this research for overcoming weld quality prediction uncertainty. Work by previous researchers in developing neural network application in resistance spot welding are presented and extensively discussed in Chapter 3.

2.4 Effect of Machine Mechanical Characteristics on Weld Quality

Many researchers agree that welding machine mechanical characteristics does affect weld quality with explanations on how. However, the extent has not been quantified in terms of what quantity (value) of mechanical characteristics affects weld diameter ⁽⁸⁾. Tang et al ⁽⁸⁾ stated that the resistance spot welding machine is made up primarily of electrical and mechanical subsystems which are believed to affect weld quality in some ways ⁽⁸⁾. Lipa ⁽⁹⁾ mentioned that the resistance spot welding machine had always been viewed as a

transformer and its importance as far as influence on weld quality is concerned has been the object of debates by many authors ⁽⁹⁾.

A recent work in 2003 by Tang et al ⁽⁸⁾ was carried out by experimental investigation on welding machines using modified mechanical characteristics, which were welding force, electrode displacement, and other process characteristics, such as electrode alignment. The identified characteristics were then linked to weld quality through process signature analysis ⁽⁸⁾. Emphasis was placed on the signals during welding stage when electric weld current is applied. Subsequently the hold stage was analyzed to see how it influenced the solidification of the liquid nuggets ⁽⁸⁾.

From their study they found that machine stiffness (refers to the rigidity of the upper and or lower arm of the welding machine part) slightly improves weld quality in terms of weld strength and significantly raises welding expulsion limits ⁽⁸⁾. Further analysis as reported ⁽⁸⁾ was made on the influence of the machine stiffness on the characteristics of the welding force, electrode displacement, and electrode alignment. The work concluded based on the analysis carried out that “due to thermal expansion of the weldment, in a stiff machine, the electrode force increases higher than its preset value to accommodate the stiffness” ⁽⁸⁾. The increased electrode force imposes a forging force on the nugget, which is beneficial for preventing welding expulsion ⁽⁸⁾.

The study ⁽⁸⁾ also revealed that friction (condition of moving parts of the welding machine) was unfavourable for both steel and aluminium welding. And in some combinations of parameters because data ranges do overlap, the reduction in strength is not statistically significant. The influence of friction was reported to vary with welding conditions ⁽⁸⁾. The findings ⁽⁸⁾ were that the tensile-shear strength of welds and welding expulsion limits, were not significantly influenced by machine moving mass (weight of the cylinder head) for steel and aluminium welding alloys that were used for the experiment. However machine stiffness and friction do affect welding processes and weld quality ⁽⁸⁾.

Similar work was done by Satoh et al ⁽²⁶⁾ and Dorn et al ⁽²⁷⁾. These researchers have made valuable contributions to the understanding of the effects of machine characteristics on resistance welding. However, the results of these studies had been mainly descriptive ⁽²⁶⁾. The expressions of the influence are not explicit, but mostly comparative ⁽²⁶⁾.

2.5 Concluding Remarks

Dynamic resistance as presented by the recent work of Matsuyama ⁽²⁵⁾ and others is intimately related to the progress of the welding operation. It is possible to obtain information regarding the nugget growth by monitoring the parameters that are related to this variable. Dynamic resistance (varying contact diameter) therefore is a suitable and appropriate parameter that can be used for modelling and estimating the nugget formation process.

The effect of mechanical characteristics on weld quality has been descriptive, not very concrete and of some debate among researchers. Considering the unclear speculations and debate around this issue, this research will investigate the possibility of using only electrical characteristics data to accurately predict weld diameter (weld quality). Electrical characteristic parameters data is thought to in some ways reflect the welding state and mechanical characteristics of the welding machine.

CHAPTER 3

NEURAL NETWORKS

3.1 Introduction

The chapter introduces the fundamentals of neural networks, neural network types, learning rules, optimisation techniques and application in resistance spot welding process. Neural networks controllers and the theoretical steps for the design of the process controller are included in this chapter. Sensitivity analysis which is typically carried out in neural network modelling for determining the contributory effect of inputs to outputs in a neural network model is discussed.

3.2 Background

Artificial Intelligence (AI) provides several techniques that are used in manufacturing systems ⁽²⁸⁾. In the 1980's, knowledge based expert systems were the most popular artificial intelligence techniques, they have however become less effective with the continuously changing, complex and open environment of manufacturing systems ⁽²⁸⁾. Neural networks are identified as capable techniques that can be used in increasing manufacturing system's predictability because of its ability to learn, adapt and do parallel distributed computation ⁽²⁸⁾. Neural networks are robust systems ⁽²⁸⁾. Smith ⁽²⁹⁾ mentioned that applying neural networks techniques in manufacturing systems creates potential to increase product quality, improve system reliability and reduce the reaction time of a manufacturing system.

Nelson et al ⁽³⁰⁾ gave the historical trend of neural networks development as having started at conceptual level around 1890 with investigation and insights into brain activity. The development progressed to 1936 with the successful explanation of the brain as a computing paradigm by Alan Turing ⁽³⁰⁾. This explanation gave a deeper insight into

neural network concept. In 1943 Warren McCulloch and Walter Pitts presented a work⁽³⁰⁾ explaining how neurons might work by modeling a simple neural network using electrical circuits. This discovery by Warren McCulloch and Walter Pitts was used by John von Neumann for teaching theory of computing machines⁽³⁰⁾. In 1949, Donald Hebb presented the connection between psychology and physiology and explained how neural pathway is reinforced each time it is used⁽³⁰⁾. Following the improvement on hardware and software capability in the 1950s, research in this area progressed further. The period 1969 to 1981 recorded stunted growth because of reduced funding and diverted attention to artificial intelligence that looked more promising at that time⁽³⁰⁾. However from 1982 to date there was a marked turn around and renewed interest in research in the field of neural network and a period of unfolding application possibilities mostly due to the availability of capable computer hardware and better understanding of neural network capability⁽³⁰⁾.

Literature^(28, 31) described the basic components of a neural network as nodes (or neurons, adapted from a biological neuron) and adaptable weights⁽³¹⁾. These neurons are also referred to as processing elements^(28, 31). Weight in neural network refers to the adjustable parameter on each connection that scales the data passing through it⁽³¹⁾. The weights were presented by Hassoun⁽³¹⁾ as corresponding to biological synapses. Identified inputs referred to as signals are accumulated and put through the networks, adapted by the weights, and the sum passed to an activation function that determines the neurons response⁽³¹⁾. Neural networks learn by example⁽³¹⁾. Hung et al⁽²⁸⁾ presented neural networks as having the capability to solve problems without a detailed, explicit algorithm available for the solution procedure.

Hassoun⁽³¹⁾ mentioned that a neural network is configured for a specific application, such as pattern recognition or data classification, through a learning process. The research further described the neural network as having a remarkable ability to derive meaning from complicated data and is able to extract patterns and detect trends which are too complex to be noticed by either humans or other computer techniques⁽³¹⁾.

Martin ⁽³²⁾ reported two breakthroughs in neural networks use in the late 80's that have made growth of the application possible in the process industries. The first was reduction in training time even with large number of inputs. This was achieved by the basic change in the learning algorithm. The second was a deeper insight by the work of Caudill et al ⁽³³⁾ on the development of “*inverted*” or “*reversed*” neural networks ⁽³²⁾. These two mentioned breakthroughs have helped with solutions for large scale problems involving time series models and nonlinear multiple-input-multiple-output (MIMO) models ^(32, 33).

Principe et al and other authors ^(34, 35) listed what makes a neural network unique as follows:

- Nonlinear models
 - Many nonlinear models exist, but the mathematics required is usually involved or nonexistent.
 - Neural networks are a simplified nonlinear system (combinations of simple nonlinear functions).
- Trained from the data
 - No expert knowledge is required a priori
 - Each task does not need to be completely specified in code
 - They can learn and adapt to changing conditions online
- Universal approximators
 - They can learn any model given enough data and processing elements and time

3.2.1 How Artificial Neural Networks (ANN) Work

Leondes ⁽³⁵⁾ reported the work carried out on universal approximation theorem in 1984 by the research group in San Diego which described neural networks as a heuristic technique used to perform various task within the supervised or unsupervised learning paradigm. This consists of optimized training, selection of appropriate size of a network and prediction of how much data that are required to achieve particular generalization

performance. The sequence in using artificial neural networks consists of determining the input and output signals ^(34, 35). This is followed by using generated data set to train and validate the network. A neural network architecture made up of inputs, network layers with hidden layers and output is shown in Figure 3.1. Hidden layers are the layers in-between the input and output layers.

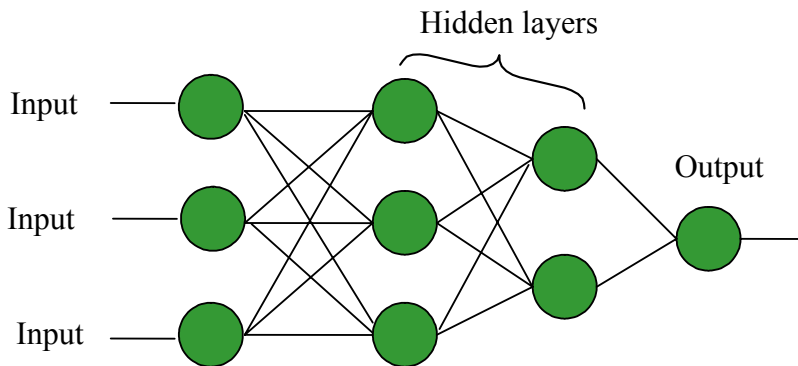


Figure 3.1: A neural network architecture [adapted ⁽³⁴⁾]

At the training stage, the data is presented to the network ⁽³⁴⁾. Figure 3.2 shows the adaptive process which takes place during the training stage of the neural network.

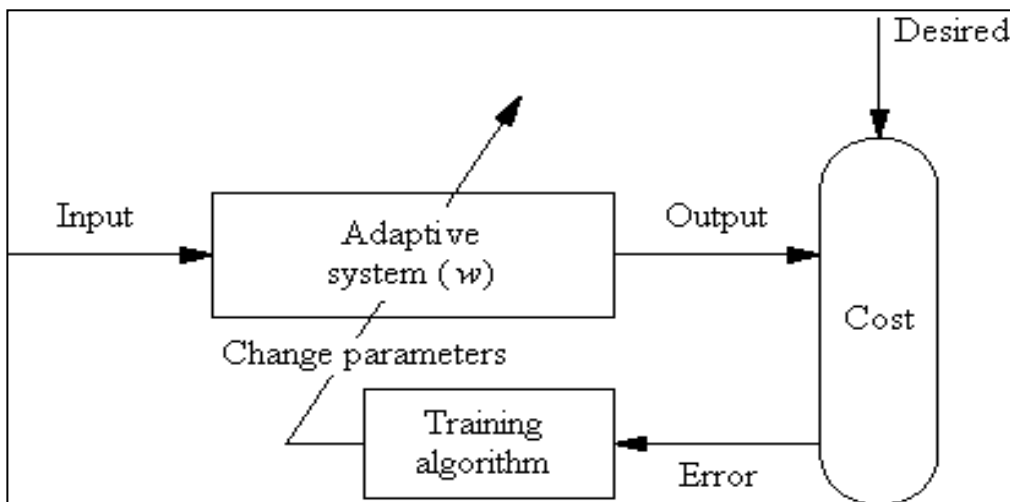


Figure 3.2: Neural Network Adaptive process ⁽³⁴⁾

The network computes an output which is compared to the desired output. Based on the level of error (difference between computed output and desired output) referred to as cost in neural network terms, the network weights are modified (adapted) to reduce the error⁽³⁴⁾ see Figure 3.2. The weight modification is done by passing the epoch through an iteration process. An epoch is a complete set of input/output data made up of elementary and exemplar. An exemplar is one individual set of input/output data while elementary is a complete set of input row. Presented in Figure 3.3 is a single neural network structure showing these terms.

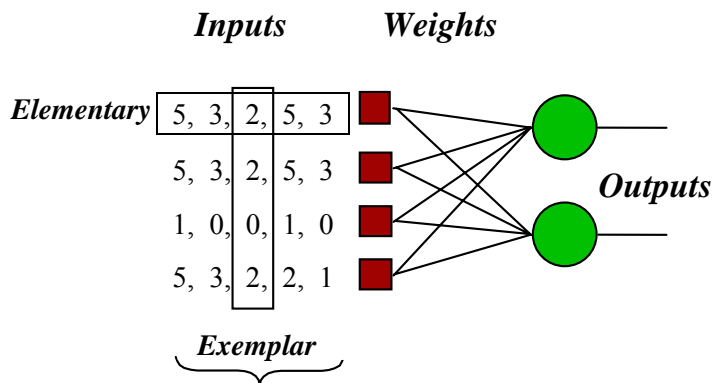


Figure 3.3: Single Layer Neural Network Structure [adapted⁽³⁴⁾]

To use the network a new set of data different from a test set are used to validate the network. The network then computes the output based on its training⁽³⁴⁾. The various aspects of the Neural Network models are as follows^(35,36):

- Neurons
- A state of activation for every unit, equivalent to the output of the unit.
- Connection between the units: each connection is defined by a weight which determines the signal of the unit.
- A propagation rule: determines the effective input of a unit from its external inputs.
- An external input or bias (threshold) for each unit.
- A learning rule and an environment within which the system should operate.

In a neural network structure as is shown in Figure 3.4, the processing element (*neuron*) has one scalar input (p) transmitted through a connection that multiplies its strength by the scalar weight (w), to form the product (wp), again a scalar ⁽³⁶⁾.

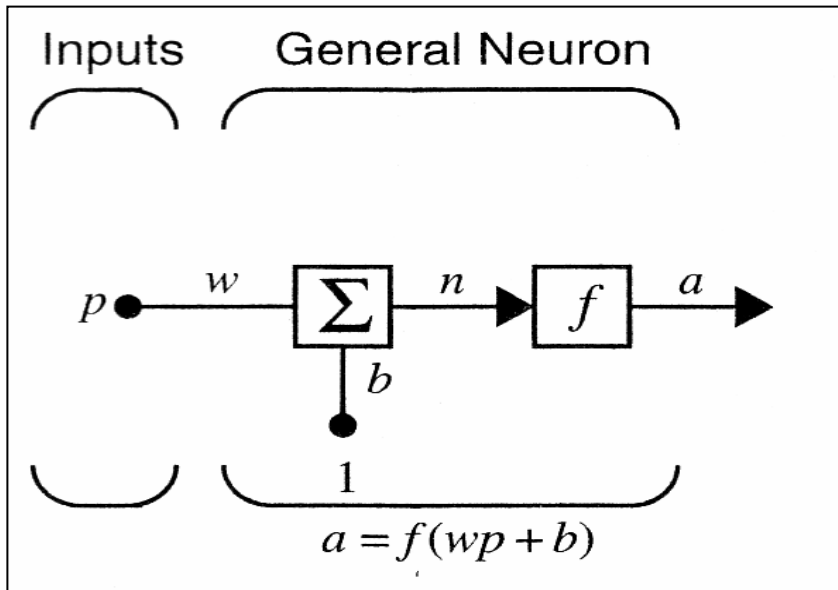


Figure 3.4: The Simple Neuron Model ⁽³⁶⁾

Here the weighted input plus the scalar bias (b) are the only argument ⁽³⁶⁾ of the transfer function (f), which produces the scalar output (a) such that:

$$a = f(wp + b) \tag{3.1}$$

This sum is the argument of the transfer function f . The parameters w and b are adjustable scalar parameters of the neuron ⁽³⁶⁾.

It is possible for a single neuron to have more than one input and thus more than one weight such that the parameters can be adjusted for the network to exhibit some desired behaviour ⁽³⁶⁾. This creates the possibility for a network to be trained to do a particular job by adjusting the weight or bias parameters ⁽³⁶⁾.

Many artificial neural networks (ANN) can be considered function approximator ^(34, 35). Function approximation approximates the function f when $y = f(x)$, given y and x (input & output respectively) ⁽³⁴⁾. Examples are:

- Linear regression
- Classification, where the output function is binary (on or off)

Artificial neural networks are good for function approximation because

- they are universal approximators
- they are efficient approximators
- they can be implemented as learning machines

Artificial neural networks use ensembles of simple functions to approximate complex functions ⁽³⁴⁾. For example in multilayer perceptron (MLP) and radial basis function (RBF) which will be discussed in later section, the MLPs approximates input-output function using a combination of functions like logistic or tanh while RBFs approximates input-output function using a combination of Gaussians ⁽³⁴⁾.

3.2.2 Benefits and Applications of Neural Networks

Huang et al ⁽²⁸⁾ mentioned that neural networks are being applied in many fields. Some of the benefits as given by Huang et al ⁽²⁸⁾ are as follows:

- High processing achieved through massive parallelism.
- Efficient knowledge acquisition through learning and adapting ability.
- It is robust, accurate and can operate in real time.
- Compact processors for space-constrained and power-constrained applications.
- Data analysis tasks time is significantly reduced.
- It is able to quickly and accurately solve difficult process problems that cannot be solved with conventional methods.
- In the presence of noise the nets are robust such that small changes in an input signal will not drastically affect a node's output.
- Can generalise from training data set.

Smith ⁽²⁹⁾ reported that neural networks have been implemented in broad areas in manufacturing, including the design phase, process planning, scheduling, process monitoring and quality assurance.

Artificial neural networks have specifically been applied in the following areas ^(37, 38):

Business

- Used to evaluate the probability of oil geological formations
- For Identifying corporate candidates for specific positions
- Recognition of hand written signatures

Environmental

- Used for weather forecasting

Financial

- For assessment of credit risk
- Identifying forgeries
- Analysing portfolios and rating investments

Manufacturing

- Automating robots and control systems (with machine vision and sensors for pressure, temperature, gas, etcetera)
- Controlling production line processes
- Inspecting for quality
- Selecting parts on an assembly line

Medical

- Analysing speech in hearing aids for the profoundly deaf
- Diagnosing/prescribing treatments from symptoms
- Monitoring surgery
- Predicting adverse drug reactions
- Reading X-rays
- Understanding cause of epileptic seizures

Military

- Classifying radar signals
- Creating smart weapons
- Optimising the use of scarce resources
- Recording and tracking targets

3.2.3 Neural Networks Limitations

Stergiou et al ⁽³⁹⁾ mentioned that it is only recently, that neural network techniques are finding its way into the industries ⁽³⁹⁾. According to Stergiou et al ⁽³⁹⁾, one of the major problems with neural networks in the early times was that neural network programs were unstable when applied to large scale problems ⁽⁴⁰⁾. This as explained by Yalcinoz ⁽⁴⁰⁾ was due to the “network solution having a local minimum which depends on the initial conditions and inefficient mapping method used to determine weights in the energy function”. Yalcinoz ⁽⁴⁰⁾ explained that the limitation was however overcome by an improvement in the energy function. This was done by modifying the algorithm, such that reliable feasible solutions were produced and various methods developed to escape from the local minima.

Presently, a limitation that is yet to be overcome is that neural networks function as black boxes whose rules are unknown. Results are presented as output without giving explainable mathematical function that was used to arrive at the answer ⁽⁴¹⁾. What this means is that while it presents an accurate output result, the knowledge representation is unclear and is not yet well understood ⁽⁴¹⁾.

Some other disadvantages of neural networks ^(29, 37), which hinder the optimal application of neural networks in certain areas, are:

1. Use of trial and error methods to find the proper neural network architecture for a given problem. This makes it usually time-consuming; this is though improved with the use of genetic algorithm.

2. Sometimes a particular neural network learning algorithms for a given problem may not be efficient enough for network convergence.
3. Acquisition of an optimal training set for a specific neural network application continues to be a challenge.

For neural networks to be used more effectively, there should be improvements in the following areas⁽³⁷⁾:

1. In knowledge representation, non-numerical operations, and symbolic reasoning which are areas that basic neural networks cannot deal with.
2. The determination of number of nodes, number of layers, connections, and initial weights of a neural network should be easier.
3. Possibility for determining the optimal network architecture while training by controlling the minimal number of nodes, weights, and layers during training.

While these limitations do not pose an immediate problem, overcoming them will make the technique more usable⁽³⁷⁾.

3.3 Neural Networks versus Other Methods

In this section neural network technique is compared with other methods used for the analysis and design of models and control systems. Specifically compared to the neural network techniques are the traditional linear statistics method that has been in use for long and the more recent techniques like fuzzy set theory and program algorithm. The reason for comparing, is to justify the appropriateness of the use of neural network techniques in solving the complex non linear resistance spot welding process modelling and control problem.

A very useful capability of a predictive modelling tool in a chaotic, non linear and dynamic process like the resistance spot welding process is the ability to learn and track changes⁽⁴¹⁾. Linear statistics are able to model nonlinear variables but do not have learning capability to track dynamic systems, compared to neural networks that are able

to learn and recognise patterns in complex, dynamic and chaotic events ⁽⁴¹⁾. Neural networks can create their own organization or representations of the information received during learning, with additional ability to represent any function and learn from representative examples ⁽⁴¹⁾. This capability has made neural network useful and superior to linear statistics and many other non-statistical techniques ⁽⁴¹⁾. In addition to this capability, neural networks because of its robustness can tolerate partial destruction of its network, though this could lead to a corresponding degradation of performance, some network capabilities can however, still be retained even with major network damage ⁽⁴²⁾. This robustness is absent in linear statistics method.

Fuzzy set theory is a technique that can be used like the neural network. Fuzzy set theory was developed with the capacity to deal with problems which were not solvable with traditional statistical methods ⁽⁴²⁾. However, the use of fuzzy set theory requires a good knowledge of rules for modelling a process, and sometimes closed-loop systems developed using fuzzy logic are unstable ⁽⁴²⁾. This burden of the knowledge of rules is absent with neural networks techniques ^(41, 42). Neural network systems are stable.

Neural networks models are predictive (models are accurate with reality) even though they are not descriptive ⁽⁴¹⁾. It is possible with neural networks to go straight from data to the model without the need for extra tools like recoding or simplification. This is not possible with other methods ⁽⁴¹⁾. Additional superiority of neural networks to other methods is the fact that it is extremely sensitive to noise or unreliable data. There is no restriction on the output type ⁽⁴¹⁾. Neural networks can output results of complex processes in a short computational time and can be done in real time ⁽⁴³⁾. Neural networks are able to generalise ⁽⁴¹⁾. That is when a trained neural network is presented with data that it has not seen before, it generates a reasonable response. Most methods are not able to accurately generate a reasonable response in most non linear, complex and chaotic relationships ^(41, 43).

Other methods on handling data have many drawbacks which neural networks do not possess⁽⁴³⁾. For instance statistical techniques imposes restrictions on the number of input data compared to neural network that can accept as much inputs and outputs as possible in a single network architecture. The regressions performed with statistical methods mostly uses simple dependency functions (linear and logarithmic), which are quite unrealistic⁽⁴³⁾.

Statistical techniques require intensive mathematical methods to transform data; this is not needed in the use of neural network techniques. Neural networks are non-linear hence are better able to account for complexity of human behaviour and real life situations⁽⁴³⁾. And they can give tolerance to missing values⁽⁴¹⁾.

3.4 Classification of Neural Networks

The two major kinds of network structures for the neurons making up the neural networks are feedforward and feedback network structures⁽⁴³⁾. Feedforward neural networks are biologically inspired classification algorithm made up of a number of simple neurons organised in layers⁽⁴⁴⁾. The signals can only travel in one direction from input to output. There is no feedback⁽³⁹⁾. Presented in Figure 3.5 is an example of a simple feedforward neural network.

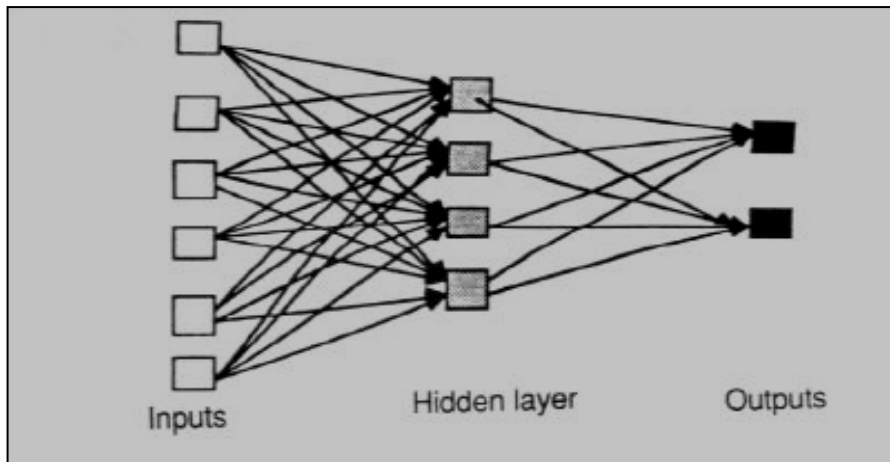


Figure 3.5: A Simple Feedforward Neural Network Diagram⁽³⁹⁾.

The layers arrangements are such that every unit layer is connected to all the units in the previous layer and each connection has a different strength or *weight* ⁽⁴⁴⁾. The weights on these connections encode the knowledge of a network ⁽⁴⁴⁾. There is no feedback between layers when it acts as a classifier ⁽⁴⁴⁾. This is because data enters at the inputs and passes through the network, layer by layer, until it arrives at the output (s). Feedforward neural networks usually produce a response to an input quickly ⁽⁴³⁾. Most feedforward neural networks can be trained using a wide variety of efficient conventional numerical methods in addition to algorithms invented by neural network researchers ⁽⁴³⁾.

Feedback neural networks are network structures where every neuron is potentially joined to every other neuron ⁽⁴⁶⁾, such that the output of one layer routes back to a previous layer ⁽⁴⁵⁾ forming cycles among the neurons in the network connections ⁽⁴³⁾ as is shown in Figure 3.6. They have signals travelling in both directions ⁽⁴³⁾.

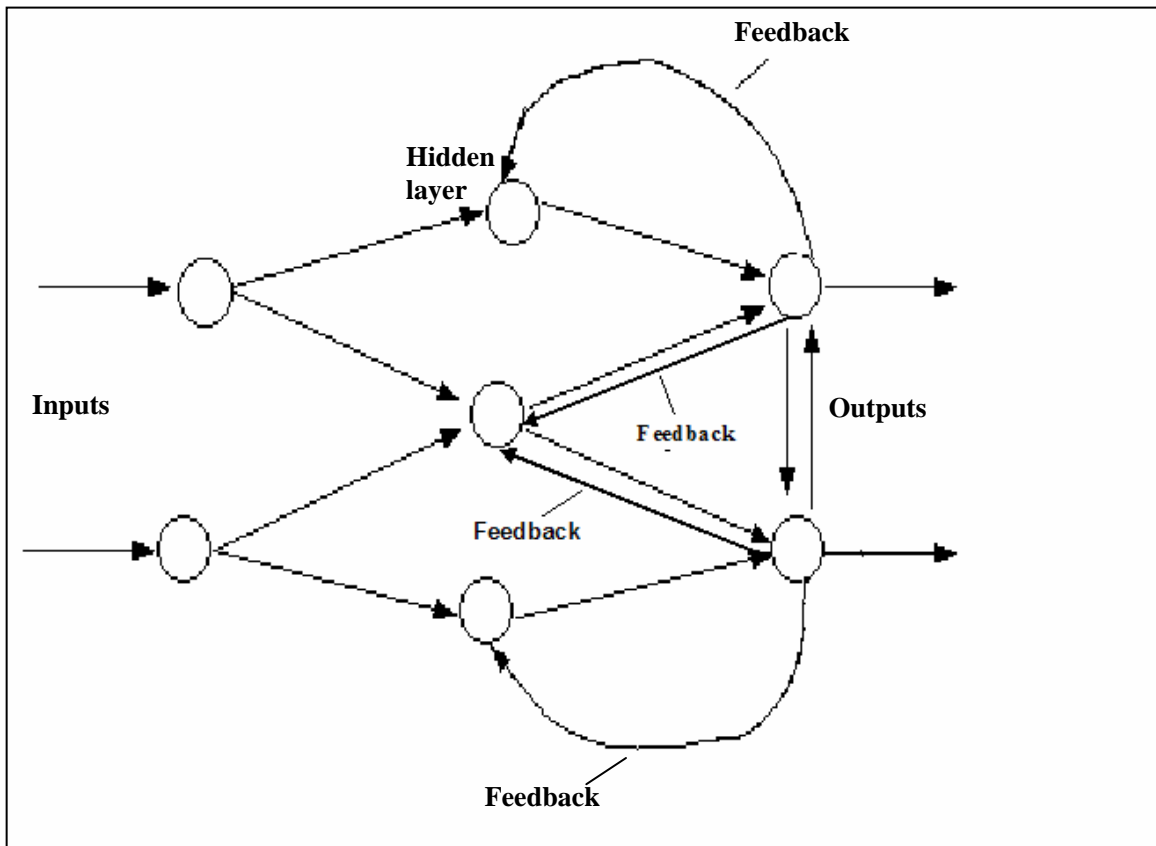


Figure 3.6: Simple Feedback Network Diagram [Adapted ⁽⁴⁵⁾]

Another unique behaviour of feedback neural network is its ability to update the activation of all neurons in parallel ⁽⁴⁶⁾. In some feedback neural networks, each time an input is presented, the neural network must iterate for a potentially long time before it produces a response ^(43, 47). Feedback neural networks are usually more difficult to train than feedforward neural networks ⁽⁴³⁾. It is possible to control the connections between the neurons ⁽⁴⁵⁾. Also, by changing the parameters that controls the connections ⁽⁴⁵⁾ the neuron in the network can be excited or inhibited.

Neural networks are also classified as supervised or unsupervised based on the training (teaching) method used ⁽⁴²⁾. In supervised learning the inputs and outputs are provided, and an input – output relationship is established. What this means is that the network processes the inputs and compares the resulting outputs against the desired output. While for unsupervised learning, only inputs are provided with no desired output. The neural network then decides for itself through a process of adaption or self organization what features it will use to group the input data ^(42, 48).

There are many classes of neural networks ⁽⁴²⁾. Several distinct neural network models can be distinguished both from their internal architecture and from the learning algorithms that they use ⁽⁴⁸⁾. Neural network architectures, learning algorithms, training and neural network controller model are further discussed.

3.4.1 Neural Network Architectures

Different kinds of neural network architectures exists ⁽⁴⁸⁾. The most commonly used ones are Multilayer Perceptron (MLP), Radial Basis Function (RBF), Self Organising Map (SOM) and Recurrent Neural Network (RNN). These are discussed in this section.

3.4.1.1 Multi-layer Perceptron (MLP)

Multilayer perceptron (MLP) architecture is a supervised neural network type with feedforward network structure where each unit receives inputs only from a lower layer

unit ^(34, 49). The network is termed supervised because desired targets are presented to the network during training. MLP are powerful models for solving nonlinear mapping problems.

The simplest network architecture consists of a single layer with directed inputs and weighted connections to the output unit ⁽⁴⁹⁾. The network is trained with standard backpropagation (simple learning algorithms which find the weights for linear and binary activation functions) algorithm ⁽³⁴⁾. However, these algorithms can only work for a limited number of functions. The limitations are overcome by adding one or more layers, known as hidden layers which are nonlinear units between the input and the output ^(44, 49). Presented in Figure 3.7 is a typical architecture of a multilayer perceptron network.

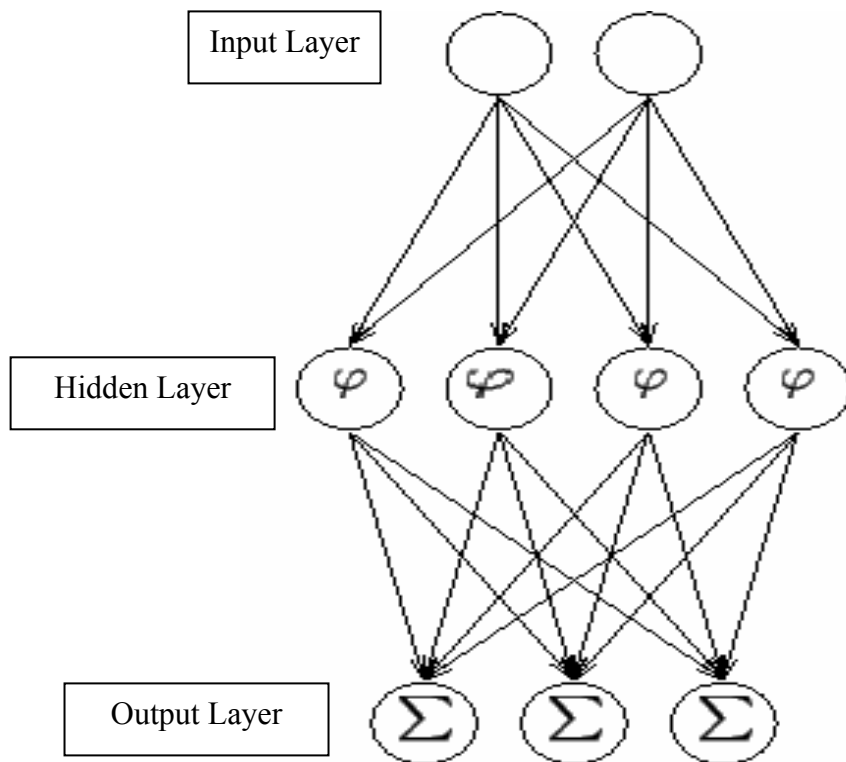


Figure 3.7: Architecture of a multi-layer perceptron network ⁽⁵⁰⁾

As shown in Figure 3.7, in the hidden layer is a nonlinear node with an elementwise nonlinearity function and the output layer with linear node. The computations performed

by the network with a single hidden layer with nonlinear activation functions and a linear output layer can be written mathematically as ⁽⁵⁰⁾:

$$x = f(s) = B \varphi (As + a) + b \quad (3.2)$$

where s is a vector of inputs and x a vector of outputs. A is the matrix of weights of the first layer, a is the bias vector of the first layer. B and b are the weight matrix and the bias vector of the second layer respectively, φ is the weight parameter.

Hagan et al ⁽³⁶⁾ explained that the principle of the network operation is that the network nodes perform calculations in successive layers until an output value is computed at each of the output nodes. This happens when data from an input pattern is presented at the input layer. Each layer of neurons may have a different number of neurons and a different transfer function ⁽³⁶⁾. The output of the MLP is expected to indicate the appropriate class of the input data. That is there should be a high output value represented with ones on the correct class node and a low output value on all the rest represented with zeros ⁽³⁶⁾.

The error function generally used in the neural network computation is the squared difference between the actual and desired outputs. The activities for each unit are computed by forward propagation through the network, for various training cases. Starting with the output units, backward propagation (chain rule) through the network is used to compute the derivatives of the error function with respect to the input received by each unit ^(36, 49).

The learning algorithm and number of iterations determines how good the error on the training set is minimized while the number of learning samples determines how good the training samples represent the actual function ⁽³⁶⁾. The different kinds of activation functions with their equations are shown in Table 3.1.

Table 3.1: Different Types of Activation Functions ⁽³⁶⁾.

Name	Linear	Sigmoid	Tanh	Softmax
Function	A	$\frac{1}{(1 + e^{-a})}$	$\frac{(e^a - e^{-a})}{(e^a + e^{-a})}$	$\frac{e^a}{\sum_j e_j^a}$

Perceptron learning rule is used in MLP. This learning rule is a method used for finding the weights in the network ⁽⁴⁹⁾. The perceptron has the property of searching for the existence of a set of weights which it uses to solve a problem ⁽⁴⁹⁾. This rule follows a linear regression approach, that is, given a set of inputs and output values, the network finds the best linear mapping from inputs to outputs ⁽⁴⁹⁾. Based on training, the network can predict the most likely output value ⁽⁴⁹⁾. This ability to determine the output for an input the network was not trained with is known as generalization ^(36, 49).

Multilayer perceptron networks are known as approximators (two-layer networks with a sigmoid transfer function in the hidden layer and linear transfer functions in the output layer) and can approximate any function provided a sufficient number of hidden units are available ⁽³⁶⁾. These hidden units make use of non-linear activation functions ⁽³⁶⁾. The performance of MLP function approximation does not degrade with increased input dimensionality unlike polynomial based function approximators ⁽³⁴⁾. Linear output is used for the multilayer perceptrons for function approximation with BiasAxon or LinearAxon as the transfer function. Each processing element in the Multilayer Perceptron architecture contributes to the global function of the network. A change in one weight may greatly affect the global function ⁽³⁴⁾.

The back-propagation algorithm used for solving learning problem of the MLP can take two forms; the forms are either forward pass or backward pass ^(36, 49). In the *forward pass* ⁽⁵⁰⁾, given inputs are used to predict output. In the *backward pass*, it is explained ⁽⁵⁰⁾ “that the partial derivatives of the cost function with respect to the different parameters are propagated back through the network”.

The same chain rule of differentiation which gives similar computational rules for the forward pass is same one for backward pass ⁽⁵⁰⁾. The network adapts weights by using any gradient-based optimisation algorithm ⁽⁵⁰⁾ and the iteration of the whole process is continued until the weights have converged ⁽⁵⁰⁾.

Though the MLP is a supervised neural network type, it can also be used for unsupervised learning. This is done by using *auto-associative* structure, a process of setting the same values for both the inputs and the outputs of the network ⁽⁵⁰⁾, such that the extracted sources can emerge from the values of the hidden neurons. This process approach is however computationally intensive ⁽⁵⁰⁾.

3.4.1.2 Radial Basis Function Networks

The radial basis function (RBF) neural network is a universal approximator for continuous functions given a sufficient number of hidden units. RBF have proven to be valuable alternative to multilayer perceptrons (MLPs) in many real world tasks ⁽⁵¹⁾. The tasks include speech recognition, data classification and chaotic time series prediction ⁽⁵²⁾. The RBF architecture consists of two-layer fully connected network, with an input layer performing no computations ^(51, 52). See Figure 3.8.

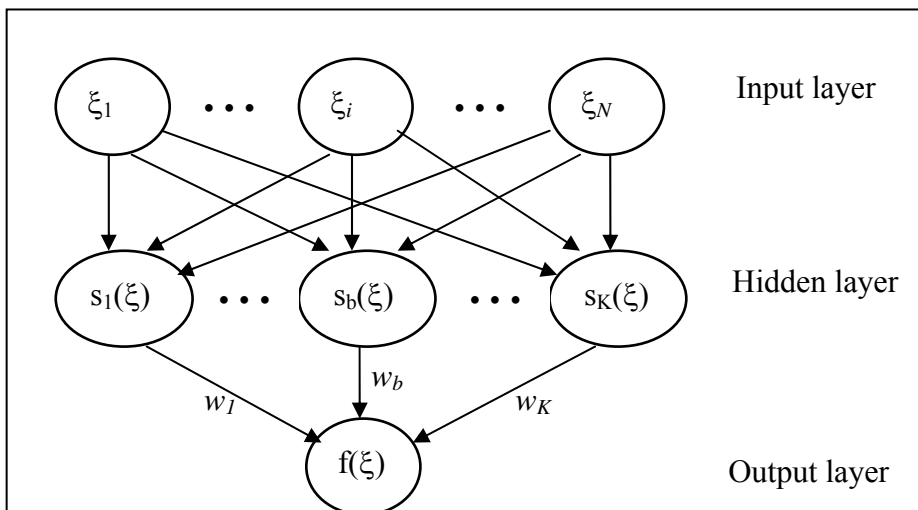


Figure 3.8: Radial basis function (RBF) network ⁽⁵²⁾

RBF is a commonly used neural network type ⁽⁵²⁾. The computation nodes of the hidden layers of radial base function network are different and serve a different purpose from the output layer of the network as opposed to the MLP where the hidden and output layers share a common neuron model ⁽⁵²⁾. The hidden layer of the RBF network is non-linear while the output layer is linear. This makes the network unable to approximate non-linear functions compared to MLP in which both hidden and output layers are non-linear ^(51, 52).

Radial basis function networks are feedforward neural networks. The distinguishing feature of an RBF network from other networks is that RBF network uses radial functions (i.e. the transfer functions of the hidden units) while other neural network types does not ⁽⁵²⁾. In the RBF structure each of the components of the input vector (ξ) feeds forward to the basis function (K). The outputs are linearly combined with weights, $w_1, w_2, \dots, w_b, \dots, w_K$, in the output layer of the network, $f(\xi)$ ⁽⁵²⁾. The general output of a RBF network is thus ⁽⁵²⁾:

$$f(\xi, w) = \sum_{b=1}^K w_b s_b(\xi) \quad (3.3)$$

where ξ is the vector applied to the input neurons and s_b represents the transfer function (basis function) b . RBF hidden layer neurons have a *receptive field* which has a *centre*: that is, a particular input value at which the neurons have a maximum output ⁽⁵²⁾. Their output tails off as the input value moves away from this point ⁽⁵¹⁾. The most commonly applied transfer function of an RBF network is the Gaussian and the output of the network is given by ⁽⁵²⁾:

$$f(\xi, w) = \sum_{b=1}^K w_b \left(\frac{-\|\xi - m_b\|^2}{2\sigma_b^2} \right) \quad (3.4)$$

where each hidden node is parameterized by two quantities: a centre \mathbf{m} in input space and width σ_b ⁽⁵²⁾. Generally radial basis network requires more neurons than most other neural network types ⁽³⁶⁾. Its simple structure and fast learning ability makes it very unique ⁽⁵³⁾.

3.4.1.3 Self-Organizing Maps (SOM)

Self-Organizing Map (SOM) was introduced by Teuvo Kohonen in 1982 ⁽⁵⁴⁾. The SOM (also known as the Kohonen feature map) algorithm is one of the best known artificial neural network algorithms ⁽⁵⁴⁾. In contrast to many other neural networks using supervised learning, the SOM is based on unsupervised learning ⁽⁵⁴⁾. In this unsupervised learning the network performs some kind of data compression, such as dimensional reduction or clustering ⁽⁴⁸⁾ by visualising high-dimensional data and converting it into simple low – dimensional display as is shown in Figure 3.9.

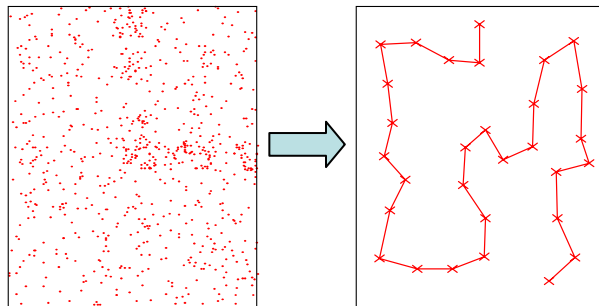


Figure 3.9: Dimensional Reduction of Data by Self-organising map [adapted ⁽³¹⁾]

The SOM can thus serve as a clustering tool of high-dimensional data. And can construct a topology preserving mapping from the high-dimensional space onto map units in such a way that relative distances between data points are preserved ⁽⁵⁶⁾. The map units, or neurons, usually form a two-dimensional regular lattice where the location of a map unit carries semantic information ^(55, 56), See Figure 3.9. It is made of a number of neurons

that are arranged in a predefined structure ⁽⁵⁶⁾. In most cases this structure is a regular grid of neurons of 1-, 2- or 3-dimensions ⁽⁵⁶⁾.

SOM neural network type is relatively easy to implement and evaluate, and is computationally not expensive ⁽⁵⁴⁾. However, it has the problem of overcrowding and underutilization of the neurons in the network due to the size and shape of the network that are fixed before the training phase begins ^(51, 55). Presented in Figure 3.10 is a Self-Organising Map architecture.

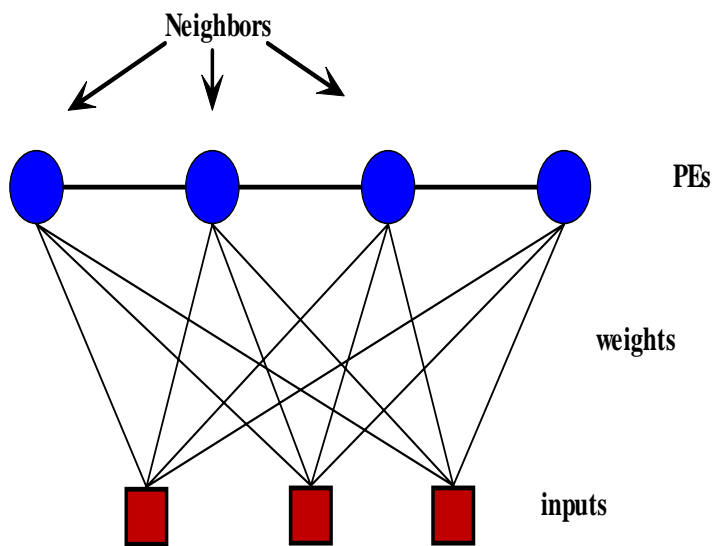


Figure 3.10: Self-organising map architecture ⁽³¹⁾

The weight of each processing element (PE) represents the center of its cluster as is shown in the Figure 3.10. Neighboring PEs has similar weights.

The SOM identifies a mapping from high dimensional input data space onto a regular array of neurons ⁽⁵⁴⁾. Every neuron i of the map is associated with an n -dimensional reference vector $m_i = [m_{i1}, \dots, m_{in}]^T$, where m denotes the dimension of the input vectors ⁽⁵⁴⁾. In essence the reference vector consists of the weights of the neurons. The reference vectors together form a codebook. The neurons of the map are connected to adjacent

neurons by a neighbourhood relationship, which dictates the topology, or the structure of the map ⁽⁵⁷⁾. The most common topologies in use are rectangular and hexagonal topology ⁽⁵⁷⁾. SOM is most suitable for classification problems as such will not be used for the application problem being investigated in this research.

3.4.1.4 Recurrent Neural Networks

Recurrent networks can have an infinite memory depth and thus find relationships through time as well as through the instantaneous input space ⁽³⁴⁾. Most real-world data contains information in its time structure. Recurrent networks are the state of the art in nonlinear time series prediction, system identification, and temporal pattern classification ⁽³⁴⁾. The human brain is a form of recurrent neural network ⁽⁵⁸⁾.

Recurrent neural networks are a kind of network with feedback connections ⁽⁵⁸⁾. They are computationally powerful and because of their ability to implement almost arbitrary behaviour they have found good use in adaptive robotics, music composition, speech recognition and other applications ⁽⁵⁸⁾. Backpropagation algorithm which is one of the best learning algorithms can not be easily used in the recurrent neural network architectures. This is because to use backpropagation algorithms in a network, the architecture has to be of feed-forward form ^(34, 51). This adds some computational expense.

The inputs and outputs of this architecture are lengthy sequence of vectors making handling of the input and outputs sometimes difficult to follow through ⁽⁵¹⁾. Presented in Figure 3.11 is a fully recurrent neural network.

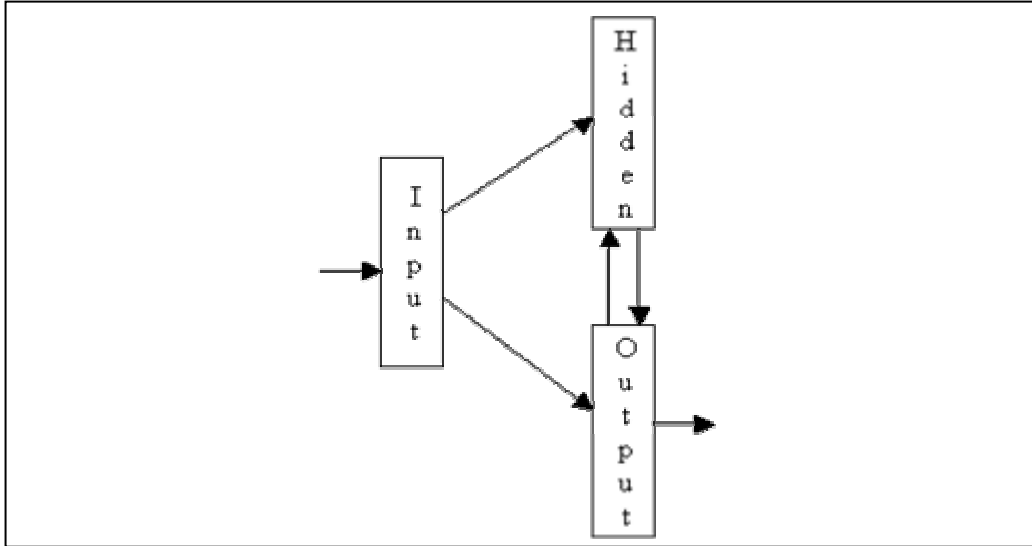


Figure 3.11: Fully recurrent neural networks ⁽⁵⁹⁾

Fully recurrent networks provide two-way connections between all processors in the neural network ⁽⁵⁹⁾. They are typically complex, dynamical systems, and exhibit instability ⁽⁵⁹⁾. Having, discussed the classification and architecture of neural networks. The next section is about how neural networks are trained.

3.4.2 Neural Network Training Methods

Training the neural network entails finding the network parameters (weights and biases) which would best approximate a given function ⁽⁴⁸⁾. Neural networks have the ability to learn from examples by adapting the weights on its connections in order to achieve a desired specification using specific learning rules ⁽⁴⁸⁾. During the learning process, the network embodies the complex relationships between the network inputs/explicative data and the network outputs/explicated data ⁽⁴⁸⁾. This learning process produces a statistical model which can determine an estimation of the likely outcome when fed with an input variable ⁽⁴⁸⁾.

When training the neural network, care is taken to ensure that they do not overfit the training data as this can prevent the network from generalizing ⁽⁴⁸⁾. The process is as

follows: Each example (data) is entered as input in the neural network. The values are propagated towards the output through a function. These are activation functions which are either the linear, logistic and softmax ⁽⁴⁸⁾. The prediction obtained at the network's output is called an error or cost function ⁽⁴⁸⁾. As explained earlier, the error value which is the difference between the expected value (real output) and the actual output value (what the network gives) are computed. This error value is then backpropagated by going upwards in the network and modifying the weights of each hidden unit based on the error contribution of each to the total error value. This mechanism is repeated for each value in the learning set ⁽⁴⁸⁾.

Neural network uses trial and error method of learning and finds the patterns associating inputs and outputs using a large set of training data where both inputs and outputs are known ⁽⁴⁸⁾. It initially begins with random weights and corrects mistakes by modifying the weight that it has given each input item ⁽⁴⁸⁾. The network works in feedback network form, whereby a given node output can be transmitted back to itself or to other previous nodes as another input ⁽⁴⁸⁾. The learning process is done using models and rules ⁽⁴⁸⁾. These rules are as follows:

- Biologically based rule such as Hebb's rule – one of the learning rules in which changes in synaptic strengths (weights) are proportional to the neuron activation (input) ⁽⁶⁰⁾.
- Grossberg Learning – a learning rule based on self-training and self-organisation which allows networks to adapt to changes in input data over time ⁽⁶¹⁾.
- Kohonen's Learning Law – an unsupervised learning rule, used when breaking down a system, via the Kohonen clustering algorithm, which takes a high-dimensional input and clusters ⁽⁵⁵⁾.

The practical approach to training a neural network is to know how to set stopping criteria during the training of the network ⁽³⁴⁾. Common stopping criteria include ⁽³⁴⁾:

- Using fixed number of epochs.
- Stop when the mean square error (MSE) gets below a certain point.

- Use of cross validation criteria to monitor performance. Cross validation helps to store best weights that gives best performance and not necessarily for stopping the network.

The aim during the training process is to maximize generalization ⁽³⁴⁾. The following can be done to achieve this ⁽³⁴⁾:

- Trying many possible networks and using the smallest network that meets the design criteria.
- Use of weight decay – a method that forces weights (discriminant functions) that are not necessary to zero.
- Use of cross validation by :
 - setting aside a subset of data to test the network
 - Monitoring the network to avoid memorizing. Memorizing occurs when the training set mean square error (MSE) continue to fall while the cross validation mean square error starts to rise.

The learning process is a trade-off made between the training speed and the weight quality (degree of error or convergence) ⁽⁴⁸⁾.

- If too fast, weights may not be effective for new data.
- If too slow, network will not be able to make accurate predictions.

There are two approaches to learning in supervised training ⁽⁴⁸⁾. The approaches depend on the nature of the target values which are ^(42, 43):

- 1). Based on the correctness of the decision (how accurate the results are compared to the target values).
- 2). Based on the optimization of a training cost function. (The least square error method).

In decision based neural networks, the target determines the correctness of the classification for each training pattern ⁽⁴¹⁾. The objective of the learning process is to find

a set of weights that gives an accurate classification ⁽⁴²⁾. In the first phase (retrieving phase) the objective is to determine which class the pattern belongs to based on the output values. The output values are function of the input values and network weights ^(41, 42). The learning process sequence consists of the input data propagated through the network to compute the system output. Error is computed and propagated backward through the network. Depending on the level of error the weights are modified accordingly ⁽⁴²⁾.

In optimisation based neural networks, the correctness of the training pattern is determined when the error or cost function has been minimised. This function is minimised by using the least square error method of optimisation ^(41, 42). The optimisation technique is used to find a set of design parameters ^(44, 49), that can be defined as optimal ⁽⁴⁴⁾. This could be in order to minimise or maximise a particular function such as an error function which is dependent on another variable. However, the function to be minimised might be subjected to constraints in the form of equality constraints or bounds ^(47, 62).

The optimization techniques used include the following ^(44, 49):

- Inverse Neural Network
- Brute-Force Method
- Fminbnd
- Descent Optimization
- Quasi-Newton Methods

A discussion of each of these optimisation techniques are given below.

3.4.2.1 Inverse Neural Network

The role of an inverse neural network is to predict the unknown inputs to a system such that it can produce a desired output. Psaltis et al ⁽⁶³⁾ proposed mathematical algorithms that can learn the inverse of target system mappings for the purpose of predicting unknown system inputs to produce the desired outputs.

Psaltis et al ⁽⁶³⁾ explained that in many real cases, learning the inverse of the system by mathematical algorithms was very difficult and time consuming. This complexity of modelling direct inverse systems has led to the derivation of inverse nonlinear mapping from a simple neural network multilayer perceptron (MLP) or radial basis function (RBF) which is trained as a simulator of a given system ^(64, 65).

Williams ⁽⁶⁶⁾ and Linden et al ⁽⁶⁷⁾ developed the first methods of inverting feed forward neural networks. It was an inversion algorithm of feedforward neural networks which is based on numerical *gradient descent search* method (similar to back-propagation) in which a candidate inverse is iteratively refined to decrease the error between its output and the target ^(66, 67).

The use of inverse neural networks has over the years emerged as a useful technique in neural network application ⁽³⁴⁾. Inverse neural network models are used for solving process optimization and product quality control problems as well as simple predictions ⁽³⁴⁾. To use inverse neural networks the target values take the role of the input while the input takes the role of the target values. Upon training the network a relationship of the output-to-input is obtained rather than input-to-output. This can then be used to adapt the network to correct the output to the required output. The algorithm is as shown below ⁽³⁴⁾:

- Desired output value, y_d is entered
- The current position, y_{act} is also entered
- The difference between the two, $y_1 = y_d - y_{act}$ is obtained
- The absolute of this difference is $y_2 = abs(y_1)$ required to update the position. This absolute is passed through the inverse neural network to get the required input, x_1 which gives this position.
- This input is then passed through the neural network to get the position, y_3 .
- y_3 is compared with y_2 while updating the input value, until the point where the two are equal or less than an error value. This input is then returned as the required input value which would set the actual output value to the required output hence minimizing the difference between the two, which is the optimization process.

An obvious problem associated with network inversion arises when a many-to-one function must invert from one to many targets ^(31, 68, 69). What this means is that in a typical neural network structure a number of input variables are used to generate one output ⁽³¹⁾, whereas in Inverse neural networks model it is required that the output be used to determine the inputs. While this is possible it could be very difficult ⁽⁶⁸⁾. The manipulation requires a large computational cost to find an exact inverse of the target even on neural networks of moderate size ^(31, 69). Inversion therefore, only yields estimate inverses which approximate the inverse of the target to a certain degree ⁽⁶⁹⁾.

Additionally, the use of inverse neural network optimisation technique takes a long time to find the optimal position, hence would not be practical for a large data training set ⁽⁶⁹⁾. The reason it takes a lot of time could be attributed to the fact that if the signal is a random signal or a non-linear relationship the value could lie within a small range such that the method keeps fluctuating around this point (due to the gradient of search) ^(31, 69). This disadvantage makes this technique inappropriate in the resistance spot welding process modelling problem.

There are though several techniques or algorithms that have been developed for improving inverse neural network accuracy ⁽²⁸⁾. These algorithms are based on fields such as numerical optimization methods (e.g. gradient descent search method and nonlinear programming) and other methods such as fuzzy logic and evolutionary methods ⁽²⁸⁾.

3.4.2.2 Brute Force Method

In this method input arrays and values are defined from the start of the data range set to the end of the data range set ⁽⁴⁴⁾. Different values of the input are then tested until at the point where a particular input value gives the required output or an output less or greater than the input by the error value ^(44, 47). One major drawback of this technique is that in the algorithm an array of input values are created with incremental steps chosen as a

result if the increments are too large the solution would be skipped and if it is too small the method would converge too slowly⁽⁴⁷⁾.

Similarly, if there are too many inputs in the array, it would take a lot of time before finding the possible solution and if the input in the array is too small the solution would not be found for small accuracies⁽⁴⁷⁾. It is for this reason that this method is discouraged.

3.4.2.3 Bounded Minimisation Technique (Fminbnd)

This method is from the MATLAB 6.2 toolbox⁽⁴⁷⁾. The optimisation technique is a mean square error minimisation function⁽⁴⁷⁾. The function is minimised by finding the optimum parameter that gives the minimum turning point(s) of the function to be minimised or the minimum point of the function within bounds specified for the parameter⁽⁴⁷⁾. Such that⁽⁴⁷⁾:

$$[X, Fval, Exitflag, Options] = \text{fminbnd}(@Fun, x_L, x_U, Options) \quad (3.5)$$

where:

- Fun is the function to be minimized
- x_L is the lower bound for the parameter
- x_U is the upper bound for the parameter
- Options can be used to specify the accuracy and displays what the function should do.
- X is the optimum value
- Fval is value of the function
- Exitflag is a convergence criterion.

This optimisation technique returns the optimum value onto X, the value of the function at this optimum value is also returned to fval. It is reported⁽⁴⁷⁾ that the Exitflag takes on a

value of 1 if the method converges, 0 if it does not converge and -1 if the number of iterations is exceeded.

This method however has the following limitations ⁽⁷⁰⁾:

- The function to be minimized must be continuous.
- Fminbnd may only give local solutions.
- Fminbnd often exhibits slow convergence when the solution is on a boundary of the interval.
- Fminbnd only handles real variables.

The Fminbnd uses either the Line search, Golden search or Parabolic search techniques to determine optimum values ^(47, 70). In using line search techniques, the search starts from a point with an assumption that the function should decrease along the line ⁽⁷¹⁾. This assumption is sometimes misleading and can yield inaccurate results. With the Golden search method no assumption is made about the function ⁽⁴⁷⁾. The interval is divided in the ratio of 1:τ where τ is a number greater than 1, which ensures that best reduction occurs within the interval per step ^(47, 70). A principle of scale similarity (dividing the interval in the same manner at each stage) is then used. This method of search is very effective because it is robust ⁽⁷⁰⁾. It however requires a continuous function in order to work properly. It has linear convergence properties and as a result may take a long time to converge. The parabolic method makes use of the assumption that the function is able to find the optimum point by itself ⁽⁷⁰⁾. The algorithm is as follows ⁽⁷⁰⁾:

- Divide the interval into three points
- The method fits a parabola to the three values which have the values f_L, f_m, f_U .
The parabola to be fitted takes a function of the form:

$$f(x) = m(x - X_{new})^2 + c \quad (3.6)$$

where m is the gradient and c the intercept.

- The new point X_{new} then becomes the minimum of the function. The point X_{new} is then given by:

$$X_{\text{new}} = \frac{1}{2} \left(\frac{f_L(X_U^2 - X_m^2) + f_m(X_L^2 - X_U^2) + f_U(X_m^2 - X_L^2)}{f_L(X_U - X_m) + f_m(X_L - X_U) + f_U(X_m - X_L)} \right) \quad (3.7)$$

- The value of the function at this new value, $f(X_{\text{new}})$ is then calculated.
- Say the interval X_L to X_m was the larger interval, if $f(X_{\text{new}}) > f(X_U)$ then the new interval becomes $(X_L, X_m, X_{\text{new}})$, otherwise the new interval is $(X_m, X_{\text{new}}, X_U)$.
- The accuracy is then checked. If $f(X_{\text{new}})$ has the accuracy required, the method stops otherwise the method returns to the second step and goes through all the steps again until an accurate value is obtained.

The parabolic search method on its own becomes inaccurate when there are two solutions because it tries to oscillate between the two solutions ⁽⁷⁰⁾. Another problem is that sometimes the points may lie on the function but the middle interval may not really lie on the lowest point on the function to be minimised so the parabolic search would get stuck on this point ⁽⁷⁰⁾. To cater for the two problems above, the parabolic search is combined with the golden search method ⁽⁷⁰⁾.

3.4.2.4 Descent Optimisation Methods

In this method, the optimisation approach is to minimise the function along a particular direction ⁽⁴⁹⁾. The algorithm for the descent methods is as follows ⁽⁴⁹⁾:

- 1 Start at some given point X_1
- 2 Assign $i = 1$,
- 3 Choose a search direction D_i
- 4 Use line minimization techniques such as golden search method to minimize $f(X_i + \lambda D_i)$ by varying the scalar λ .
- 5 Update $X_{i+1} = X_i + \lambda_{\min} D_i$

6 Check for convergence. If no convergence return to point 3.

There exist three kinds of descent methods, which are ⁽⁴⁹⁾:

1. Alternating variables,
2. Steepest Descents
3. Conjugate Gradient methods.

The alternating variable method is an iterative method for minimizing a function jointly over all variables. It is limited by the fact that even though the step sizes get smaller and smaller as the minimum point is approached, this value is never reached, hence the method is deemed to be non-convergent ⁽⁴⁹⁾. For the steepest descent method, the function is minimized along the direction with the greatest slope ⁽⁴⁹⁾. The steepest gradient descent methods have a fast convergence initially, but convergence slows down as the minimum point is reached. It also, needs an infinite number of steps in order to converge on a quadratic surface ⁽⁴⁹⁾.

In the steepest descent method the function is minimized along the direction with the greatest slope which is the negative gradient. The steepest gradient descent method has a fast convergence initially but slows down close to the minimum point. These methods need an infinite number of steps in other to converge on a quadratic surface.

The conjugate gradient method makes use of search directions ⁽⁴⁹⁾. The search directions are chosen based on information gained from previous searches ⁽⁴⁹⁾. It should be noted that for an n-dimensional space quadratic surface, conjugate gradient method would converge in n steps or less ⁽⁴⁹⁾. In conjugate gradient methods, the directions are conjugate to the Hessian matrix (a matrix and the determinant of that matrix) but do not need to be calculated ⁽⁴⁹⁾. The draw back in this method is that the gradient of the error function with respect to the inputs and thus the weights at times requires complex mathematical computations ⁽⁴⁹⁾.

3.4.2.5 Quasi-Newton Method

Quasi-Newton method ⁽⁴⁹⁾ is the most used optimisation method. The curvature of the function is computed at each iteration, in order to formulate the quadratic model of the problem of the form ⁽⁴⁹⁾:

$$\min_x \frac{1}{2} x^T H x + c^T x + b, \quad (3.8)$$

where H is the Hessian matrix, which is a positive definite matrix, c is a constant vector and b is a constant. The optimal solution is reached when the partial derivative of equation 3.8 goes to zero ⁽⁴⁹⁾.

The conventional Newton method calculates H and proceeds in a direction of descent to minimise the function after a number of iterations ⁽⁴⁹⁾. This method is, however computationally intensive for calculating the Hessian matrix ⁽⁴⁹⁾. The BFGS (Broyden Fletcher Goldfarb and Shanno) methods are used to update the Hessian matrix, so reducing the computational time ⁽⁴⁹⁾.

Learning rate and learning algorithms which affects the performance of neural networks are further discussed.

3.4.2.6 Learning Rates

The learning rate determines by how much the weights at each step has to be changed and how long it takes the network to converge ⁽³⁴⁾. Learning rates can be set based on the following ⁽³⁴⁾:

- Normalized learning rates – achieved by dividing the number of exemplars per update. This provides consistent learning between batch and online.
- The closer the processing elements (PE) are to the output PE, the lower should the learning rate be set because of error decay.

- NeuralExpert (programmed software) can be used to pick theoretically best initial weights.

An alternative to determining learning rate is to use adaptive learning rates ⁽³⁴⁾. An example is the delta-bar-delta adaptive learning rate. What this does is that if there are consecutive errors of same sign the delta-bar-delta will increase the learning rate (add) and if they are of different signs it will decrease the learning rate ⁽³⁴⁾.

3.4.2.7 Learning Algorithms

Neural networks fundamentally use two kinds of learning algorithms, namely; supervised and unsupervised learning ⁽⁴⁸⁾. In supervised learning as earlier explained, the known target values or desired outputs (correct results) are presented to the neural network during training. The neural network adjusts its weights and tries to match its outputs to the target values ⁽⁴⁸⁾. The learning algorithms are further classified under four kinds of learning algorithms, these are:

- a. Backpropagation Algorithm
- b. Conjugate Gradient Algorithm
- c. Quasi-Newton Algorithm and
- d. Levenberg-Marquardt (LM) Algorithm.

(a) Backpropagation Algorithm

Backpropagation algorithm is a gradient descent optimization procedure whereby the mean square error performance index is minimized ⁽⁷²⁾. This method makes use of a set of data which includes the input and output of the actual plant to be modelled by the neural network ⁽⁷³⁾. As the inputs are applied to the network, the network output is computed and is compared with the actual plant output. The algorithm then adjusts the network parameters such that the sum of the squared error between the actual plant

output, and the neural network output can be minimized ^(72, 73). The numerical performance of the backpropagation method depends on these three ⁽⁷²⁾:

- (1) The frequency of update which can be done in two ways; Block adaptive, or Data adaptive.
- (2) The direction of update which is either first order or second order methods.
- (3) The data adaptive method used.

(b) Conjugate Gradient Algorithm

In conjugate gradient algorithm, a search is performed along conjugate directions ⁽⁷⁴⁾. This method generally produces faster convergence compared to the steepest descent directions ⁽⁷⁴⁾. A search is made along the conjugate gradient direction to determine the step size that minimizes the performance function along that line ⁽⁷⁵⁾. The first step of the conjugate gradient algorithms is to search in the steepest direction, and then a line search is performed along the current search direction which optimizes the function ⁽⁷⁵⁾. The next search is done such that it is the conjugate of the previous search direction. The general procedure for determining the new search direction is to combine the new steepest descent direction with the previous search direction ⁽⁷⁴⁾. The Scaled Conjugate Gradient (SCG) algorithm is however now being used to avoid this time consuming nature of the line search ^(74, 75). The key principle of this algorithm is to combine the model trust region approach (where the solution is likely to be found) with the conjugate gradient approach ⁽⁷⁵⁾.

(c) Quasi-Newton Algorithm

Newton's method is an alternative to Conjugate Gradient Algorithm methods for fast optimization ⁽⁷⁶⁾. Newton's method uses the following formula ⁽⁷⁵⁾:

$$x_{k+1} = x_k - A_k^{-1} g_k \quad 3.9$$

where A_k is a matrix of the second derivatives of the performance index at the current weight values. Newton's method converges faster than the conjugate gradient methods but it is computationally intensive ^(75, 76). In Quasi-Newton algorithm, an approximate second derivative matrix is updated at each iteration of the algorithm ⁽⁷⁵⁾.

(d) Levenberg-Marquardt (LM) Algorithm

The LM algorithm was designed to approach second order training speed without having to compute the Hessian Matrix ⁽⁷⁵⁾. When the performance function has the form of the sum of squares, the Hessian matrix can be approximated to ⁽⁷⁵⁾:

$$H = J^T J \quad 3.10$$

and the gradient is

$$g = J^T e \quad 3.11$$

Where J is the Jacobian matrix, which contains first derivatives of the network errors with respect to the weights, and e is a vector of network errors ⁽⁷⁵⁾.

3.5 Neural Network Design Formulation

It is important to select and organise the neural network architecture in such a way that the production process problem would be solvable by neural network techniques. This section deals with the approach for formulation of the neural network architecture in order to apply it in this problem area.

Hagan ⁽³⁶⁾ pointed out that it is sometimes misbelieved that neural networks can be used to learn anything, and that they can do all the work related to an application. His suggestion is that the neural network application developer must make a number of decisions and perform a number of activities related to the application prior to making a

decision ⁽³⁶⁾. The choices made will affect the quality of the results achieved. Hagan ⁽³⁶⁾ summarizes these choices as follows:

1. Determination of the task to be performed by the network in the application.
2. Analysis of the data available for the application.
3. Choice of the inputs to the neural network.
4. Proper pre-processing of the data for input to the network.
5. Choice of the desired outputs of the network, including post-processing of the outputs.
6. Choice of the neural network learning method and algorithm (learning rule) to be used for training. Setting of the parameters associated with the network chosen, including number of processing elements in each layer, type of processing elements and learning constants.
7. Training of the neural network on the training data.
8. Verification of the trained network on test data.
9. Analysis of the results and possible retraining of the network or modifications of parameters or pre-processing.

In formulating neural network architecture, the input data to the network are determined and pre-proposed in order to achieve accurate output. Discussed below are classes of data, input data selection and pre-processing techniques.

3.5.1 Input Data Processing

According to Freeman et al ⁽⁴⁴⁾, the single best way to handle data in a neural network task is to study it. If a neural network is expected to learn and generalize from a set of training data, a user should, in a general way, be able to also do that to some extent. The goal in this analysis is to learn more about the problem, and to improve the representation of the data to the network. In general the smaller the neural network is the less data that is needed to achieve good generalization and overall network performance ⁽⁴⁷⁾.

Neural networks differ in the kinds of data they accept⁽⁴³⁾. There are two major kinds of data, namely categorical and quantitative data⁽⁴³⁾. Categorical variables take only a finite number of possible values, and they are usually several or more cases falling into each category. Categorical variables may have symbolic values⁽⁴³⁾ (e.g., "male" and "female", or "red", "green" and "blue") that must be encoded into numbers before being given to the network. Both supervised learning with categorical target values and unsupervised learning with categorical outputs are called "classification."⁽⁴³⁾ Quantitative variables are numerical measurements of some attribute, such as length in metres⁽⁴³⁾. The measurements have to be made in such a way that at least some arithmetic relations among the measurements reflect analogous relations among the attributes of the objects that are measured⁽⁴³⁾. A supervised learning with quantitative target values⁽⁴³⁾ is called "regression."

Some variables can be treated as either categorical or quantitative, such as number of children or any binary variable⁽⁴³⁾. Most regression algorithms can also be used for supervised classification by encoding categorical target values as 0 or 1 binary variables and using those binary variables as target values for the regression algorithm⁽⁴³⁾.

Having studied the available data, certain variables should appear more important than others⁽³⁶⁾. In addition there is a trade off between having a lot of inputs and therefore a large network and having a small number of inputs at the expense of reduced performance due to information loss. However there is no easy way to handle this trade-off as explained by Hagan⁽³⁶⁾.

As pointed out by Hush et al⁽⁶²⁾, for generalization purposes, the number of training samples should be approximately ten times the number of weights in the multi-layer propagation network. For a three-layer back-propagation network with inputs (I), outputs (O), neurons (A) in the hidden layer and training samples (P), the number of weights can be estimated thus⁽⁶²⁾:

$$W = [(I+1) * A + (A+1) * O] \quad (3.12)$$

And

$$10 * [(I + 1) * A + (A + 1) * O] = P \quad (3.13)$$

With this information, a more intelligent choice of architecture can be made.

Hagan ⁽³⁶⁾ state that any operation, which linearizes the input data, is usually beneficial. By studying the available data, such characteristics and improvements can be discovered. The learning rule in a processing element (neuron) usually employs each input in the calculation of the gradient with respect to the weights ⁽³⁶⁾. As a result, if the dynamic range of an input is large, the weight adjustments associated with that input are also large ⁽³⁶⁾. However, in some cases the adjustments are too large, causing the neurons to saturate its output ⁽³⁶⁾. When this happens, the neuron stalls ⁽³⁶⁾, making learning extremely slow if not impossible. If some inputs have very small dynamic ranges, their information content may be lost or not effectively used by the network ⁽²⁸⁾.

The solution to this problem is to pre-process all inputs so that they have the same dynamic range. This can usually be achieved without loss of information and with improved performance of the trained network in almost every case ⁽³⁶⁾.

In determining the network output, one of the best ways is to analyze how the performance of the network will be judged in the particular application it was designed for. As in what exactly should the output be doing and the measures that will show that it is doing well ⁽³⁶⁾.

There are some variations like statistical noise and overfitting that can affect the performance of the neural network ⁽³⁶⁾. The next section discusses these variations and their effect on neural network performance. This is followed by the application of neural networks in resistance spot welding and the process controller model design.

3.6 Noise and Generalization

‘Statistical noise’ refers to the variation in the target values that is unpredictable from the inputs of a specific network, regardless of the architecture or weights⁽⁷⁷⁾. ‘Physical noise’ refers to variation in the target values that is inherently unpredictable regardless of what inputs are used⁽⁷⁸⁾. Noise in the inputs usually refers to measurement and data capturing error⁽⁷⁸⁾. Noise in the actual data is not a good thing, since it limits the accuracy of generalization that can be achieved⁽⁷⁸⁾, no matter how extensive the training set was⁽⁷⁹⁾. On the other hand, injecting artificial noise (jitter) into the inputs during training is one of the several ways to improve generalization for smooth functions when only small training sets are present^(78, 79).

Certain assumptions about noise are necessary for theoretical results⁽⁷⁸⁾. Usually, the noise distribution is assumed to have mean and finite variance^(78, 79). The noise in different cases is usually assumed to be independent or to follow some known stochastic model⁽⁷⁸⁾, such as an autoregressive process⁽⁷⁹⁾. The more that is known about the noise distribution, the more effective the network can be⁽⁷⁸⁾.

If the noise is present in the target values, what the network learns depends mainly on the error function⁽⁷⁸⁾. For example, if the noise is independent with finite variance for all training, a network that is well-trained using least squares will produce outputs that approximate the conditional mean of the target values^(78, 79).

Noise in the inputs limit the accuracy of generalization in a more complicated way than noise in the targets⁽⁷⁸⁾. In a region of the input space where the function (weight, bias and activation function) being learned is fairly flat, input noise will have little effect⁽⁷⁹⁾. In regions where that function is steep, input noise can degrade generalisation severely⁽⁷⁹⁾.

Furthermore, if the target function is $Y = f(X)$, but noisy inputs $X + D$ are observed; (where D represents noise and X represents actual input values) it is unlikely that the network obtain an accurate estimate of the function $f(X)$ given $X+D$, no matter how large

the training set is. The network will according to White ⁽⁷⁹⁾ not learn $f(X)$, but will instead learn a convolution of $f(X)$ with the distribution of the noise D .

3.7 Overfitting

When developing neural networks it is imperative that the network is able to generalize, that is ensuring that the network will accurately predict output for cases that are not included in the training set ⁽⁷⁷⁾. A problem usually arises when a network is not complex enough to detect the signal in a complicated data set. This can lead to underfitting. Also, when a network is too complex that it fits the signal and the noise in the signal it will lead to overfitting ^(79, 80). Overfitting is a major problem in that it can cause the network to give predictions that are beyond the training data set range ⁽⁸⁰⁾. Overfitting leads to excessive variance in the outputs whereas underfitting produces excessive bias ⁽⁷⁷⁾. Overfitting can however be avoided by using a large set of training data. If there are only few training data set available, any of the following can be done ^(80, 34):

- Model Selection (selecting the right number of weights, that is, the number of hidden units and layers). This is done by trial and error.
- Early stopping during the training. Using the cross validation curve to see when the curve is turning away from the normal downward trend and stopping it immediately.
- Weight decay plot and monitoring of performance. A drop down curve of the plot indicates good performance.
- Combining networks to improve performance.
- Using Bayesian Learning to improve learning performance.

It is important to ensure that there is no underfitting or overfitting of the training data set by the network. The easiest way to do this is by choosing the appropriate number of hidden units and hidden layers ^(77, 80). This is done by trial and error and by comparing the network architecture to obtain the combination that presents the least mean square error.

3.8 Reconditioning of Neural Networks

Overfitting as discussed in the previous section is a condition that occurs when the trained neural network follows the actual outputs perfectly⁽⁸⁰⁾. This results in the network being unable to predict future behaviour. Another problem is when the network is not properly trained such that the neural network is not a representation of the true output⁽⁸⁰⁾. This usually results due to ill-conditioning of the network⁽⁸⁰⁾.

Depending on the application problem the network is usually trained using standard gradient descent methods⁽⁸⁰⁾. These methods make use of learning rates (η). If this rate is too slow, the network will take a long time to converge to the error tolerance and may not converge within the specified training steps⁽⁸⁰⁾. The Training steps are adjusted by trial and error in an attempt to obtain an optimal learning rate. If the rate is too fast the network will diverge and will not give accurate result as well⁽⁸⁰⁾. A network therefore is seen as ill-conditioned when the global learning rate can not be used to train the network. That is each weight requires different learning rates that differ so much from one another that a global rate can not be used to train the entire network⁽⁸⁰⁾. The major causes of ill-conditioning are⁽⁸⁰⁾:

- Network architecture (when there are both large and small layers in the network, the learning rate difference would be significant).
- Initial weights (if the initial weights are too large or too small that there are significant differences in the learning rates of the weights).

The above causes of ill-conditioning can be catered for as follows⁽⁸⁰⁾:

Large inputs and outputs values are normalized⁽⁸⁰⁾. Normalizing the values would make them lie between 0 and 1. Normalizing the input ensures that it has an average of zero and a standard deviation of 1⁽⁸⁰⁾. When dealing with large values small learning rate should be used. This would mean using a lot of steps to move the bias across the network⁽⁸⁰⁾. The outputs and the hidden units are normalized as well⁽⁸⁰⁾, this help to adjust the weight condition to suit the network intended performance. The reason for this is that if the initial values of the weights are too small, the activation and error signals

will fade out as they go through the network ⁽⁸⁰⁾ and if they are too large, the activation function which is the *tanh* with a maximum of ± 1 would be saturated giving a derivative close to zero ⁽⁸⁰⁾. This prevents the error signal from being backpropagated through the nodes, a phenomenon known as paralysis ⁽⁸⁰⁾. The appropriate learning rate can be computed mathematically ⁽⁸⁰⁾.

3.9 The application of Neural Networks in Resistance Spot Welding

The use of neural networks to predict weld quality in resistance spot welding has gained attention because of the highly non-linear processes prevalent in resistance spot welding process and the ability of neural networks to model such phenomena ^(4, 5). The common factor in these methods is the relation of pertinent information to weld quality ⁽⁴⁾. The quality of a model depends directly on the parameters selected and the dataset used. Aravinthan et al ⁽¹⁵⁾ carried out research in which he selected dynamic resistance as the only input to the neural network model to predict weld strength. The weld strength was taken as the value of the shear stress at the point of the spot weld failure. The accuracy of the prediction and repeatability of weld quality was not given in the findings ⁽¹⁵⁾.

Matsuyama ⁽⁵⁾ conducted similar research to estimate nugget size and to detect the occurrence of expulsion during welding using neural network prediction. The research involved the use of welding current values and reducing rate of dynamic resistance. Uncoated steel sheet of 1 mm thickness was used. Electrode force and weld time were not included as inputs in the neural network. The research concluded that neural network can predict nugget formation and detect the occurrence of expulsion during welding, on the condition that the adaptable range for accurate output should be within the training dataset range.

The outcome of the findings by Matsuyama ⁽⁵⁾ created the possibility for using neural networks to predict a variable in the resistance spot welding process which will help control expulsion. However, difficulty still exists with getting an accurate weld quality prediction in the use of dataset not used in the training of the neural network. This is

mostly due to the extreme inconsistent nature of the dynamic resistance variable during the welding process^(3, 4). Also these variables change from one machine to another⁽⁴⁾. If this dynamic resistance variable is modelled (made linear), managing it and using it to predict weld quality for any resistance spot welding machine will be possible and the accuracy should improve by using neural network capability.

The need therefore is to further the research and to accurately determine the effective weld current that can be used to achieve a desired weld diameter, with possibility for reproducibility of same level of weld quality in any resistance spot welding machine.

Exploring more literature in this application area, an earlier study was carried out by Monari et al⁽⁴⁾ on extracting physical features from the three phases of welding based on statistical verification of the pertinence of each feature of the welding process. These phases are⁽⁴⁾: positioning, welding and forging. Different input parameters were identified in these phases and used as inputs in a neural network model⁽⁴⁾. The research concluded by suggesting that future work in using neural network techniques should concentrate on obtaining a model that can predict the quality of spot welds for a given machine under a reasonable range of welding conditions⁽⁴⁾. Emphasis was on adapting a welding parameter which can be controlled towards achieving good joint quality⁽⁴⁾.

On the issue of selecting the best inputs to the neural network, Brown et al⁽⁸¹⁾ proposed a method of optimising the process of selecting the inputs. In their investigations, data associated with each weld nugget diameter was collated and features of the various electrical signals extracted as potential neural network inputs. A feature extraction method was then used to statistically analyse and rank the inputs according to their ability to distinguish between different weld sizes⁽⁸¹⁾. The features which were observed to give the best performance were selected for use as inputs to the neural network models⁽⁸¹⁾. The features were value of the electrode to electrode resistance, rate of rise of resistance at different half cycle of current flow, the difference between the minimum and maximum resistance value, the resistance drop from the peak to the last half cycle value of current flow, the areas under the energy curve and the resistance curve respectively.

The study concluded that by using an extracted feature of the input data it was possible to predict weld diameter more accurately than using the entire resistance waveform ⁽⁸¹⁾. They also found that there were practical difficulties associated with accurately approximating the rate of change of resistance over small regions of the dynamic resistance curve, as such only few input combinations were selected ⁽⁸¹⁾. The prediction accuracy using this model was inconclusive.

This research will concentrate on the development of an empirical model for curve fitting the inconsistent dynamic resistance variable. The dynamic resistance output from the empirical model will be trained using neural networks. This output in combination with other identified input parameters generated from the resistance spot welding process will be used to create the neural network model for predicting weld quality (weld diameter) and for the design of the process controller. The next section will discuss the choice and methodology for designing the process controller.

3.10 Neural Network Process Controller Model Design

Process controller can be described as a device that is used to monitor and control the activity and resources of a system ⁽⁴⁷⁾. Berenji ⁽⁸²⁾ mentioned that Fuzzy logic and neural networks provide new methods for designing control systems. Most of the proposed approaches to control applications use neural networks (typically feedforward neural networks) as black-box representations of plants and/or controllers trained using supervised learning ⁽⁸³⁾. These approaches are justifiable for control of nonlinear systems ⁽⁸³⁾.

Hines ⁽⁸⁴⁾ in reviewing the work of Werbos mentioned that there are five general methods for implementing neural network controllers. These are ⁽⁸⁴⁾:

- (a) Model based Controller (predictive control)
- (b) Direct Inverse Control
- (c) Neural Adaptive Control
- (d) Back-Propagation Through Time (BPTT)

These methods are further discussed below:

3.10.1 Model based controller (Predictive Control)

This is a neural network based method that is used to implement advance industrial algorithm⁽⁴⁷⁾. A Model Predictive Control Toolbox controller automates a target system (the plant) by combining a prediction and a control strategy⁽⁴⁷⁾. An approximate plant model provides the prediction. The control strategy compares predicted plant signals to a set of objectives and then adjusts available actuators to achieve the objectives within the plant's constraints⁽⁴⁷⁾.

Soeterboek⁽⁸⁵⁾ mentioned that predictive controllers are used to control a wide variety of processes like non minimum phase and unstable processes and in the design the designer does not have to take special precautions. Predictive controllers are easy to tune and process constraints can be handled systematically⁽⁸⁵⁾. Predictive controller belongs to the class of model-based controller design concept and has four major features in common as given by Soeterboek⁽⁸⁵⁾. They are⁽⁸⁵⁾:

1. A developed model of the process to be controlled. The model is used to predict the process output over the prediction horizon.
2. The criterion function that is minimized in order to obtain the optimal controller output sequence over the prediction horizon. Usually, a quadratic criterion which weights tracking error and controller output is used.
3. The reference trajectory for the process output.
4. The minimization procedure itself.

In order to predict the process output over the prediction horizon an i-step-ahead predictor is required. An i-step-ahead prediction of the process output is the function of all the data up to $t = k$ (defined as the vector ℓ), the future controller output sequence μ and a model of the process ∇ . Such an i-step-ahead predictor can be described by the equation given below⁽⁸⁵⁾:

$$Y(k+i) = f(\mu, \ell, \nabla) \quad (3.14)$$

where f is a function. Clearly, i -step-ahead predictors depend heavily on the model of the process.

The model predictive controller will be the most appropriate control model in this problem area because it uses a model of the process. The starting point is to develop an appropriate model of the process to be controlled by the controller. Of equal importance is that it is predictive and accepts set points from the controlled variables⁽⁸⁵⁾. It is robust and can compensate an inaccurate model such that the model will not tremendously affect the performance of the controller⁽⁸⁶⁾.

The selection of a model predictive controller design technique in neural networks is based on evaluation of the applicability of other techniques^(87, 88). For instance there exist conventional techniques like the Continuous Frequency Domain Techniques for the design of controller⁽⁸⁷⁾. A lot of research done shows that the frequency domain method is very stable and robust⁽⁸⁷⁾. However due to the fact that there is currently exceeding needs for adaptive designs which are able to learn and store data, these methods are being replaced by artificial intelligent related methods. There exist quite a number of continuous control techniques. Amongst these are prominent techniques such as^(86, 88):

- Quantitative Feedback Theory (QFT),
- H-infinity Controller Designs, and
- Fuzzy-Logic Designs.

These techniques are more appropriate for the design of controllers for a linear plant and need specifications which the overall system must meet in terms of stability and responses⁽⁸⁸⁾. Real time controllers become difficult to design with these methods⁽⁸⁶⁾.

3.10.2 Direct Inverse Control

Here the neural network is trained to model the inverse of a plant (target system)⁽⁸⁴⁾. First the neural network learns the inverse model which is used as a forward controller. This

methodology only works for a plant that can be modeled or approximated by an inverse function (F^{-1}). Since $F(F^{-1}) = 1$, the output ($y(k)$) approximates the input ($u(k)$)⁽⁸⁴⁾.

An inverse model neural network controller is implemented as an approximation of an inverse nonlinear function, where the neural network is employed to approximate the inverse function⁽⁸⁴⁾. The neural network is trained off-line with system states as network input and system inputs as network output. The training continues until either the learning error is below a specific goal or the learning curve flattens with no further decrease in learning error. Once the network is trained, it is used to calculate the input signal to the system so that the system follows a desired state space trajectory⁽⁸⁴⁾.

Presented in Figure 3.12 is a Neural Inverse Controller⁽³⁴⁾.

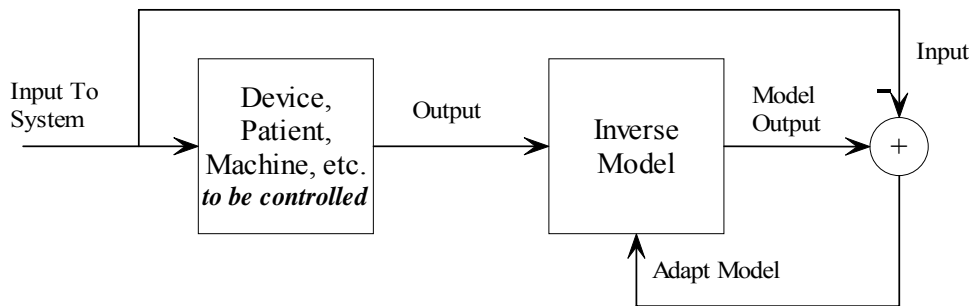


Figure 3.12: Neural Network Inverse Controller⁽³⁴⁾

The Figure shows an inverse model of the system to be controlled being trained. The inverse model then finds the input that created the system output. The inverse model is the “optimal” controller and determines the system input required to create the desired system behavior as is shown in Figure 3.13.

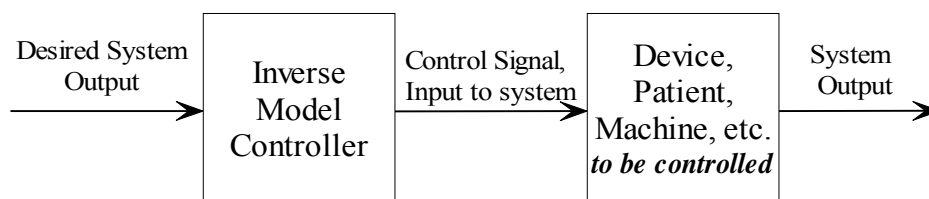


Figure 3.13: Inverse Model Optimal Controller ⁽³⁴⁾

Disturbance could be a problem in inverse model controller. This is because Inverse controller do not have direct feedback (feedback is only through training). To correct a disturbance therefore in inverse model controller the difference between the plant (target system) and model of the plant is passed through the inverse model in order to determine how much control is required for correction. An inverse model controller with disturbance correction is shown in figure 3.14.

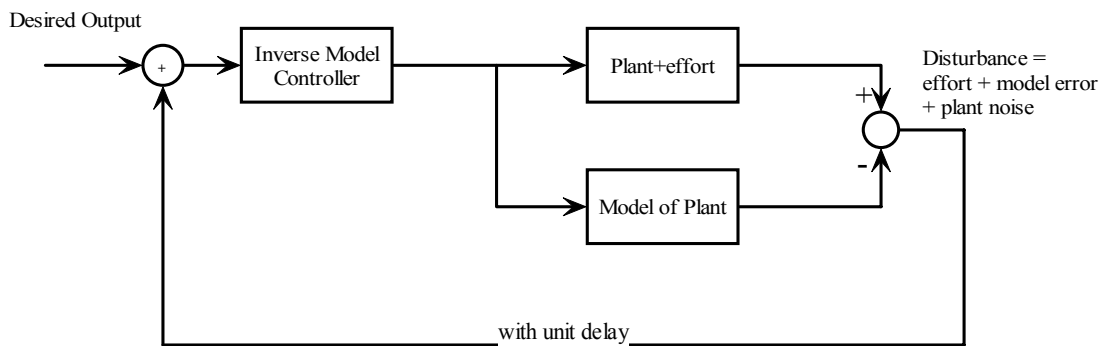


Figure 3.14: Inverse controller with disturbance correction ⁽³⁴⁾

3.10.3 Neural Adaptive Control

Neural adaptive control may be the best technique to use for a plant model that changes with time due to wear, temperature effects, etc. Hines ⁽⁸⁴⁾ mentioned that Model Referenced Adaptive Control (MRAC) which is a class of neural network adaptive control is known to have the capability to adapt the controller characteristics so that the controller/plant combinations perform like a reference plant (target system) ⁽⁸⁴⁾.

The plant lies between the neural network and the error term such that there is no method to directly adjust the controller weights in order to reduce the error. This leaves the option of using indirect control. In indirect adaptive control, an artificial neural network (ANN) identification model is used to model a non-linear plant ⁽⁸⁴⁾. If necessary, this model may be updated to track the plant. The error signals can then be backpropagated through the identification model to train the neural controller so that the plant response is equal to that of the reference model. This method uses two neural networks, one for system identification and one for MRAC ⁽⁸⁴⁾.

3.10.4 Back-Propagation Through Time (BPTT)

BPTT is a neural network controller that can be used to move a system from one state to another state in a finite number of steps (if the system is controllable). First a system identification neural network model is trained so that the error signals can be propagated through it to the controller. Next the controller is trained with BPTT paradigm ⁽⁸⁴⁾. BPTT training takes place in two steps; the plant motion stage, where the plant takes k time steps, secondly the weight adjustment stage, where the controller's weights are adjusted to make the final state approach the target state. In BPTT there is only one set of weights to adjust because there is only one controller ⁽⁸⁴⁾.

3.10.5 Adaptive Critic Methods (ACM)

In the ACM method, a critic evaluates the results of the control action: if it is good, the action is reinforced, if it is poor, the action is weakened. This is a trial and error method and uses active exploration when the gradient of the evaluation system in terms of the control action is not available. This is an approximate method and is only used when a more exact method is not available ⁽⁸⁴⁾. Often a decision has to be made without an exact conclusion as to its effectiveness (e.g. chess), but an approximation of its effectiveness

can be obtained. This approximation can be used to change the control system ⁽⁸⁴⁾. This type of learning is called reinforcement learning.

There are three classes of learning that can be used in neural network control ⁽⁸⁹⁾. These are supervised, unsupervised and reinforcement learning ⁽⁸⁹⁾. In supervised learning, at each time step, a teacher provides the desired control objective to the learning system. In unsupervised learning, the presence of a teacher or a supervisor to provide the correct control response is not assumed ⁽⁸⁹⁾. In reinforcement learning, the teacher's response is not as direct and informative as in supervised learning and it serves more to evaluate the state of the system. Once a neural network has been trained with a set of data, it can interpolate and produce answers for the cases not present in the data set ⁽⁸⁹⁾.

The task of neural network based system identification is to build mathematical model of a dynamic system based on empirical data. In neural network based system identification, the internal weights and biases of the neural network are adjusted to make the model outputs similar to the measured outputs ⁽⁸⁴⁾.

The resistance spot welding process control problem is considered a sampled-data control system which is characterized (perhaps only approximately) by the first-order difference equation where the output variable is a specified real and single valued function of the state variable ⁽⁸⁴⁾. The control variable (decision variable) is indicative of time, but not necessarily directly proportional to time ⁽⁹⁰⁾. The control variable is constrained to be an element of a given set of values. In order for a solution to exist to the problem, it is necessary that control actions exist which drive the values of the function of the state variable and the control variable to zero as the integer approaches infinity ⁽⁹⁰⁾. An optimal controller produces the absolute minimum of the sum of the function of the state variable and the control variable ⁽⁹⁰⁾.

3.11 Pole Assignment (Placement) in Control Systems

Pole assignment is the placement of pole for the synthesis of feedback control systems ⁽⁹¹⁾. It is relevant in this research because of the control system that will be designed for

the synthesis of the neural network feedback system that will be used for predicting the resistance spot welding parameter. Previous research ⁽⁹¹⁾ has confirmed that when all of the state variables of a system are completely controllable and measurable, the closed – loop poles of the system (the roots of characteristic equation) can be placed at the desired locations on the complex plane with state feedback through appropriate gains ⁽⁹¹⁾.

Whereas the transient behaviour of a feedback control system is largely determined by its closed-loop poles, pole placement is a very effective state-space approach for designing feedback control systems, especially for multivariable systems ⁽⁹¹⁾.

In some specific applications, some states in the linear system may not be available for feedback, because they are not measurable or such a measurement is too slow, too costly, or some other reason. In this case, a state estimator (observer) has to be used to estimate the unavailable states ⁽⁹¹⁾. A state estimator (observer) estimates the state variable of a dynamic system based on the measurements of the output and input (control) variables. For linear dynamic systems, the state estimator design task can be reduced to finding an output gain matrix. The output matrices in most linear state estimators are time-invariant. For time-varying dynamic systems, state estimators with time-invariant output matrices cannot follow the variation of system parameters, hence real-time gain updating of the output matrices of state estimators is necessary ⁽⁹¹⁾.

In conventional approaches to state estimator synthesis for linear dynamic systems via pole assignment, the output gain matrix L is usually obtained through off-line computation ⁽⁹¹⁾. In many real-time applications, the system dynamics are time-varying. In such applications, the time-varying nature of the plants entails on-line state estimation and hence complicates the computation ⁽⁹¹⁾.

3.12 Design Steps for the Neural Network Predictive Controller

In this design linear neural network and Scaled Conjugate Gradient algorithm as the optimization algorithm are chosen ⁽⁸⁸⁾. The network was trained using multi layer

perceptron. The input and output values were normalized before training the network so as to decrease the errors and also to enhance generalization.

After training the neural network, the network was validated using data which was not used to train the network. The best performing neural network architecture was employed in the development and design of the controller. An example of a predictive controller where optimization block and a neural network model block were used is shown in Figure 3.15.

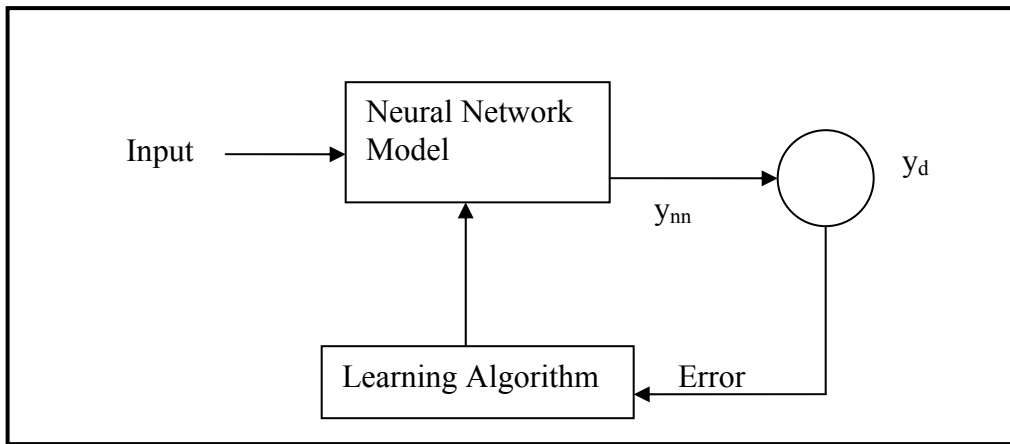


Figure 3.15: Data Generation and Training of Neural Network Diagram ⁽⁸⁸⁾

The optimization is implemented by minimizing the function ⁽⁸⁸⁾.

$$f = (y_d - y_{nn})^2 \quad (3.15)$$

The point of optimizing this function is in order to get the input value, which ensures that the error function f gets minimized, that is, the error between the desired value and the actual neural network process output is close to zero ⁽⁸⁸⁾.

3.13 Sensitivity Analysis

Sensitivity defines the relative importance of each input to the output ⁽³⁴⁾. Sensitivity analysis is a procedure used to assess sensitivity of the outcome of an alternative to changes in its parameters ⁽⁹²⁾. Sensitivity analysis is used to check the quality of a model. The effect of the input parameters to the output is measured by the response of the output to small changes in the input ⁽⁹³⁾.

Sensitivity analysis allows the determination of inputs that are important to the output solution. It is used to reduce the number of inputs that are of real importance in the model ⁽³⁴⁾. The essence is that inputs that do not contain useful information can then be eliminated ⁽³⁴⁾.

To test for input parameters sensitivity about mean ⁽³⁴⁾:

- Each input is varied independently between its mean +/- a user defined number of standard deviations.
- A report is generated relating the variation of each output with the variation in each input:
 - A table and three dimensional column plot of the sensitivity of each input is made.
 - A plot is created for each input showing the network output(s) over the range of the varied input.

3.14 Concluding Remarks

This section has discussed the different neural network architectures. These are Multilayer Perceptron (MLP), Radial Basis Function (RBF), Recurrent Neural Network (RNN) and Self Organising Map (SOM). Each of these neural network architectures except self organising maps (SOM) were tested in this application to find the most appropriate neural network architecture. The SOM which is based on unsupervised learning is considered inappropriate for this problem, because supervised learning is applied to this problem.

The inverse neural network optimisation method would be used based on theoretical applicability to this problem area. The fminbnd (bounded minimization technique) is limited by its instability and the requirement to define boundary parameters and condition. The brute force method is discouraged due to the fact that it is very uncertain and lies on extremes. Quasi-Newton is considered computationally expensive and for Conjugate Gradient methods the gradient of the error function with respect to the inputs and thus the weights were going to be required which is quite complex to calculate and is therefore not used in this application problem.

The required inputs and output for the neural networks, methodology for structuring the neural network, based on the choice of the number of neurons (processing elements) and hidden layers are considered in the modelling. There is some trial and error used to determine the most appropriate and optimal number of hidden layers that would be most suitable in the selected neural network type that would be used. To optimize the training convergence the network would be trained with different number of iterations while checking the error function. If that function converges before the iterations have been exceeded, then the network will be retrained with the number of iterations being decremented to the value of the iteration at which the error function converged. Sensitivity Analysis will be carried out to give the contributions of each input to the output. It will also show the importance of each input parameter to the output.

Neural networks techniques are presented by previous researcher ⁽⁶⁾ as an application that can be applied in the resistance spot welding process, with the ability to learn the pattern in the welding process data such that it can predict desired variable. In this research neural network will be trained with the identified welding process parameters to accurately predict effective weld current required to achieve any desired weld diameter. This is because effective weld current is a parameter that can be controlled in the welding process in other to achieve desired weld. Same electrode and material type used in the welding process will be used to set the boundary conditions for the model prediction.

CHAPTER 4

TEST CONDITION

4.1 Introduction:

The aim of the test was to generate relevant (identified) process parameter data from the resistance spot welding process. This data was used for the modelling of the welding process. Four different welding machines with instrumentation for capturing the welding process data were used. The data captured during the welding process were peak values of dynamic voltage and corresponding peak values of dynamic current for twenty half wave cycles (weld time) of each of the welded plate samples. These values were then used to calculate peak dynamic resistance generated from each of the welded sample. The other data captured are effective current (RMS) and applied electrode force. After the spot weld is made the weld diameter which is the measure of weld quality achieved during the welding process was determined. The same thickness of metal plate was used for the entire samples welded.

4.2 Materials Selection

Galvanized low carbon steel designated DC04 was selected ⁽⁹⁴⁾ for this investigation, following ISO 14373 standards ⁽⁹⁵⁾. The specific chemical composition and mechanical properties of the material are shown below in Tables 4.1 and 4.2 respectively.

Table 4.1: Chemical Composition of the galvanised plain Carbon Steel

%C	%Si	%Mn	%P	%S	%Al	%N	%Cu	%Cr	%Ni	%Nb	%Ti	%B
0.003	0.009	0.114	0.007	0.008	0.027	0.0038	0.031	0.039	0.031	0.002	0.06	0.0002

Table 4.2: Mechanical properties of the galvanised plain Carbon Steel ⁽⁹⁴⁾

Yield Strength (MPa)	Ultimate Tensile Strength (MPa)	% Elongation
139	298	46

A copper electrode with rounded tip, defined as electrode material A16 by DIN ISO 5821⁽⁹⁴⁾ specification, of electrode cap type A, width diameter 16mm and length 20mm was selected⁽⁹⁴⁾.

4.3 Welding of Plate Samples

Prewelding preparation was first carried out by cutting up the galvanized low carbon steel sheet into plates of 60mm by 40mm of 0.88mm thickness, as shown in Figure 4.1 below.

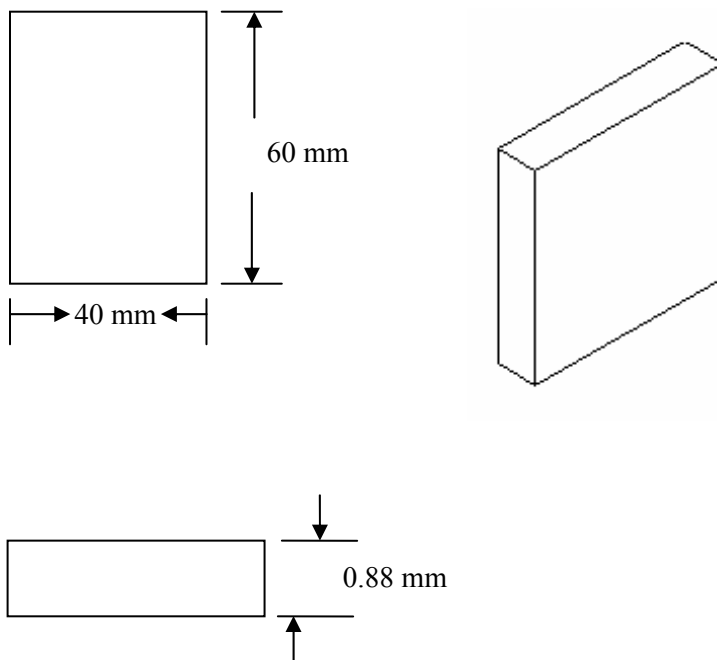


Figure 4.1: Shape and size of the sample plates welded

The sheets were cleaned with dry rags. Two separate plates of equal dimension were selected and placed together in-between two electrode tips ⁽¹⁷⁾ (upper and lower electrode pick-ups) of the welding machine (centralized adequately).

Using ISO 669 as a guide ⁽⁹⁶⁾, the welding of the samples was performed on four 50 Hz power supply ⁽⁹⁴⁾ alternating current electric resistance spot welding machines made available by the Federal Institute of Materials Research (BAM) and Technical University (TU) Berlin, Germany. Four different resistance spot welding machines were used in order to have a range of variability for the quality process modelling and to investigate the effect of the welding machines on weld quality. The machines were C-Gun, Dalex Gun 25, Dalex PMS 14-4, and Dalex Gun 35. These machines were one mobile (Dalex Gun 25) and three stationary resistance spot welding machines (C-Gun, Dalex-25, PMS 14-4, and Dalex Gun 35) with settings for simultaneous reading of weld time and effective current (RMS).

The stationary machines were fixed in one place while the mobile can be moved around and can be attached to a robot should the need arise. Figures 4.2 and 4.3 respectively show the pictures of the stationary and mobile resistance spot welding machines.

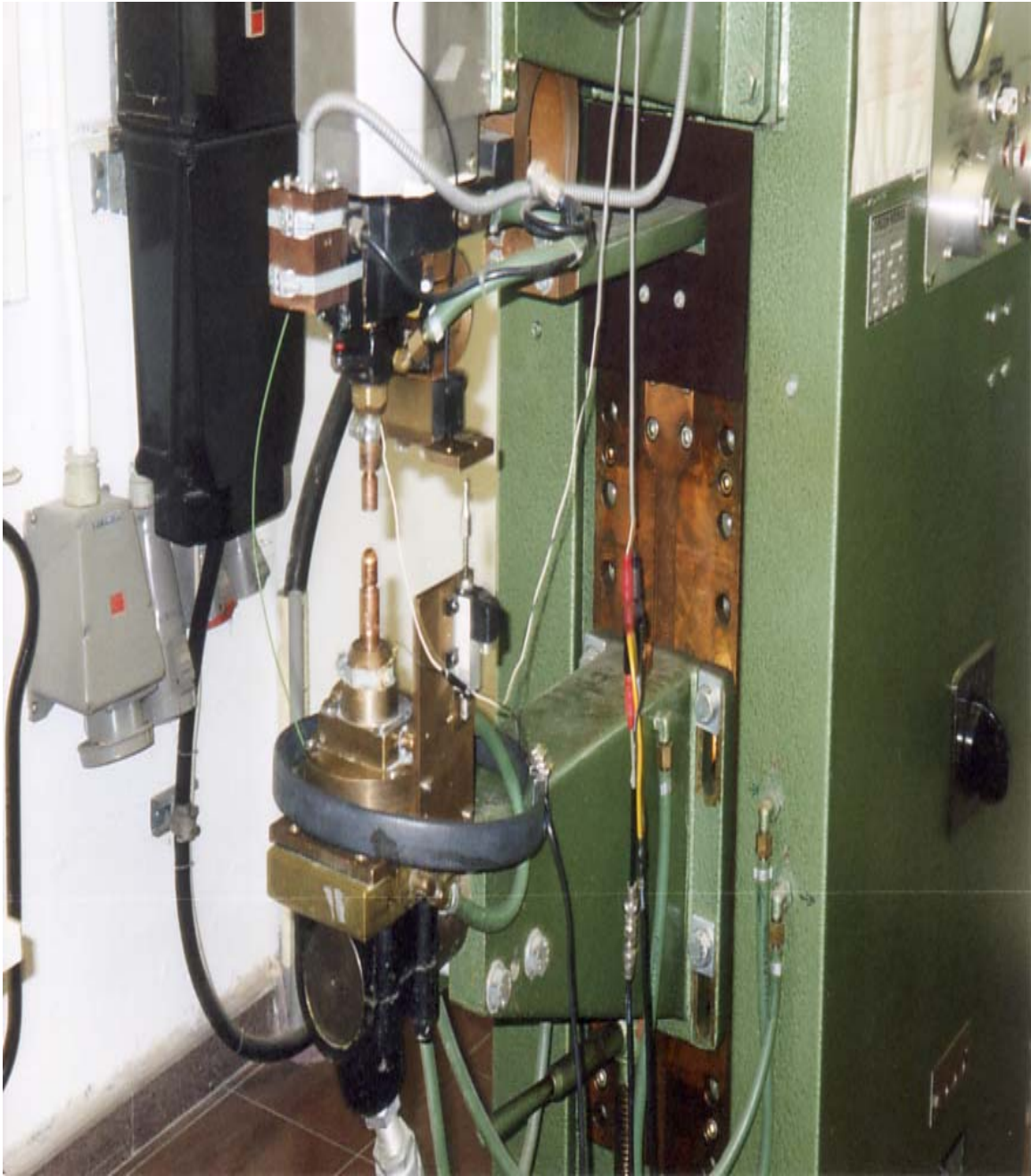


Figure 4.2: PMS-stationary Resistance spot welding machine

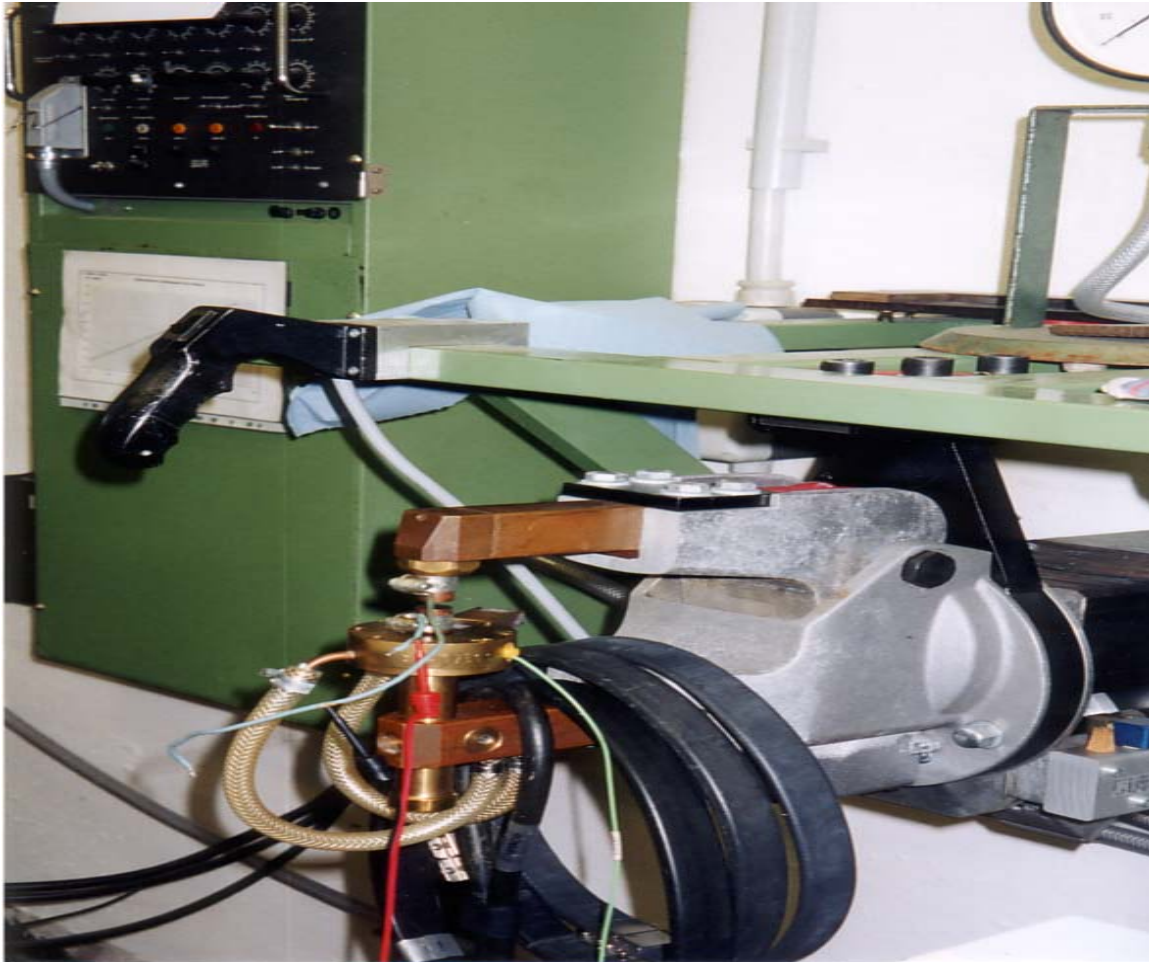


Figure 4.3: Dalex-25, Mobile Resistance spot welding machine

The welding parameters consisting of the welding period, applied electrode force (pressure), current level and squeeze time were set before commencement of the welding. The electrode force was set at the required value by using a pneumatically operated force gauge. To establish the effect of electrode force changes on weld quality in the process modelling, three force ranges which were 2.2 kN, 2.6 kN and 3.0 kN were selected for all four welding machines. These applied electrode force range are typically within the range used in these machine types for making spot welds for this material type and thickness^(94, 95, 96). However to be able to see how a small deviation from this range will affect the weld quality output, particularly in validating the neural network model that was developed, an additional range of values of 1.76 kN, 2.16 kN and 2.46 kN of applied electrode forces were selected for Dalex-25 welding machine.

The setting of the effective current range was by trial and error. This is because the effective weld current required to give the best weld quality is not known. The guide was to select a current range that meet and at least exceed the stick limit value of weld diameter by a value greater than $4\sqrt{t}$ or equal/less than $5\sqrt{t}$ where t is weld thickness. With $t = 0.88\text{mm}$, stick limit is expected to be ≥ 3.7 mm, while maximum boundary is the effective current that can maximize weld diameter before an expulsion occurs. The choice of current was by finding the range that gives a weld diameter of at least 3.7 mm as the lower limit and the current range before expulsion as the upper limit. Similarly the number of welding cycles was determined by trial and error. The selection was to determine the welding cycle period that would give a good weld quality for a given welding current range.

So pre-welding preparations of the plate samples and setting of the welding machine parameters was done and the welding was then carried out. The value of the parameters used to achieve each weld diameter was noted. In some cases there was expulsion indicating a poor weld quality. Similarly achieved weld diameters less than 3.7 mm were classified as poor weld quality^(18, 19).

The welding of the samples involved a selection of combination of the parameters from the ranges of applied electrode force and weld current. Welding time was fixed for 20 cycle periods for the welding of each specimen. The predetermined current range between stick limit and expulsion limit was divided into six welding steps for every selected applied electrode force. This is a grouping of the effective welding current into six ranges from low to high. The opinion of the operator based on experience, work from previous researchers on achieving good weld quality and some suggestions from the ISO 8166^(97, 98) were useful guides for making some of these selections and decisions.

The welding program was made up of six time steps for each specified applied electrode force category (value). Time steps explained in the literature is the total welding process time required to make a number of spot welds. In each time steps eight plate samples were spot welded. Twenty halfwave cycles time explained in the literature were required to weld each of the plate samples.

Instrumentation was set up for monitoring the welding process. This was done by connecting one end of the instrumentation wire to the electrode head of the welding machine and the other end to a computer for capturing the dynamic values of half wave voltage between electrodes and sheet. Also captured on the computer display is the value of the applied electrode force used in the welding operation. Effective current (RMS) is similarly picked up by a sensor device; the signal is amplified, converted and displayed as effective current on a recorder. The obtained potential difference value for each of the welded sample was converted to an equivalent dynamic current value (kilo ampere) by multiplying each of the halfwave potential difference value with 6.4483 (this is an instrument correction factor) ⁽⁹⁴⁾. Peak values of halfwave dynamic voltage and corresponding peak halfwave dynamic current were captured and displayed on the computer screen. Peak halfwave dynamic values of voltage and current were taken to avoid the effect of inductance (inaccurate resistance in the circuit due to voltage drop) ⁽⁹⁹⁾. The peak values of the dynamic current and dynamic voltage waveforms were used to calculate the halfwave dynamic resistance for the entire welded sample.

After welding, each single spot welded plate sample was opened up using Instron torsion machine. The Torsion machine generated the torque stress needed for separating the joined plates, exposing the fracture surface of the spot weld (formed nugget). ISO 14324-2003 was used as guide ⁽¹⁰⁰⁾. The type of fracture after shear of each sample was observed, fracture types were either plug failure (A) or shear fracture (S). Plug and shear failure describes the fracture surface failure mode. A plug failure mode also called button failure typically looks like a button as shown in Figure 4.4 while a shear failure is an interface failure shown in Figure 4.5.

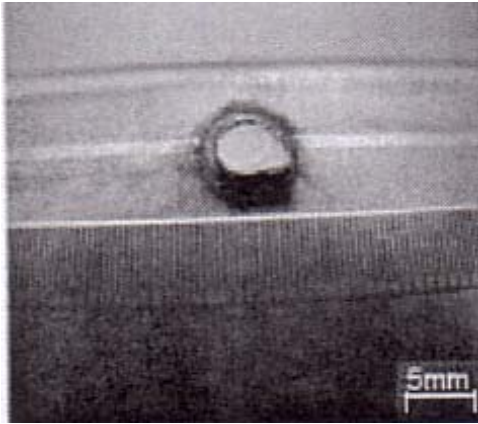


Figure 4.4: Plug failure [adapted ⁽¹⁰¹⁾]

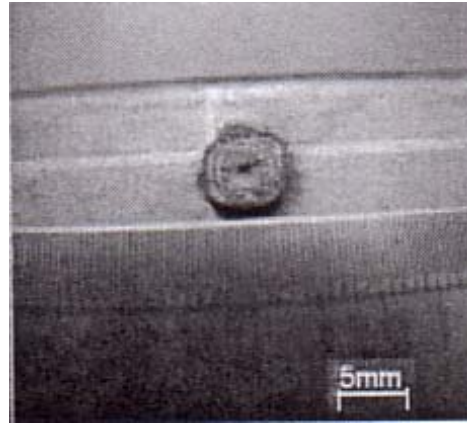


Figure 4.5: Shear failure [adapted ⁽¹⁰¹⁾]

The opening of the spot welded plates was to determine the achieved weld diameter (weld quality) by measuring the cross section of the exposed nugget surface using calibrated magnified ruler. Randomly selected samples from each welding step were taken for metallographic examination and estimation of nugget size. This was necessary, as a means of comparing weld diameter results obtained using the calibrated magnified ruler to the labour intensive metallographic nugget estimated result. Figures 4.6 and 4.7 shows the Instron torsion machine and one of the spot welded plates.



Figure 4.6: Instron torsion machine

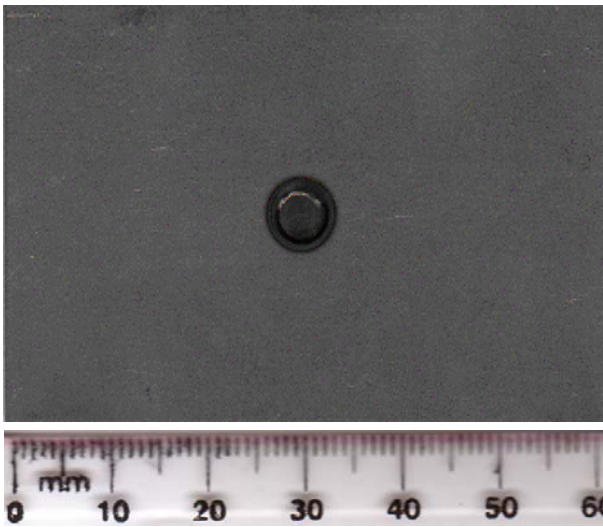


Figure 4.7: Double Plate with welded spot

Estimation of nugget size by metallographic examination was done using opened (separated) spot welded double plate samples with exposed nuggets. The exposed nugget was polished using emery paper and then etched (acid attack). The etching was done using 2 percent nital. The acid attack on the surface exposed the fusion and heat-affected zones of the weld as is shown in Figure 4.8. The image of the nugget was scanned into a computer and the nugget size and weld depth measured by drawing a line across the nugget and measuring. In each sample several measurements were taken and the average of these was considered as the final nugget diameter for a particular sample.

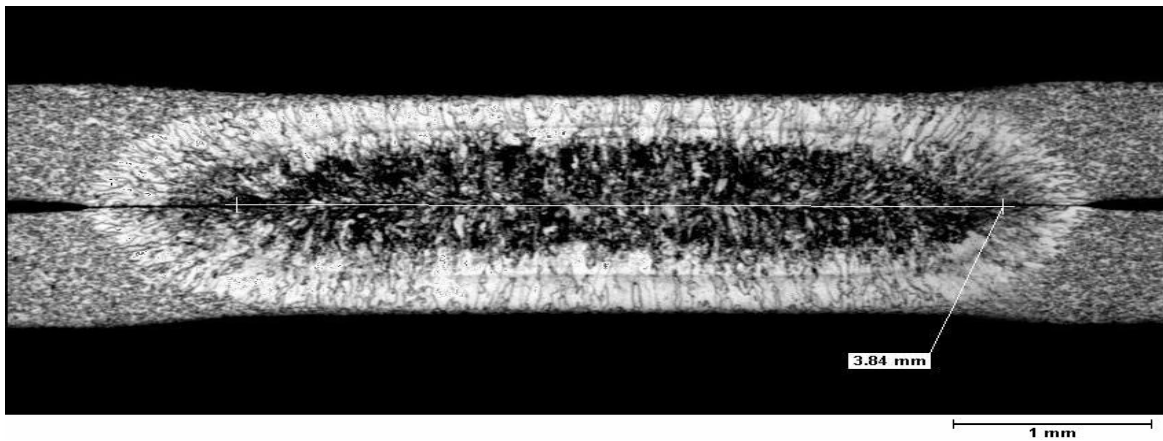


Figure 4.8: Microstructure of a spot weld nugget

4.4 Concluding Remarks

In this experiment electrical characteristics made up of halfwave dynamic voltage, halfwave dynamic current and effective current (RMS) were obtained. Equally corresponding weld diameter for each spot welded sample was determined and applied electrode force used for the welding of the samples was recorded.

CHAPTER 5

RESULTS: DATA SET GENERATED

5.1 Introduction

Presented in this chapter is the data obtained from the resistance spot welding process. These are dynamic voltage (peak halfwave voltage), dynamic current (peak halfwave current), calculated halfwave dynamic resistance, effective weld current (RMS) (Instantaneous current) and the weld diameter of each welded sample. A table showing the selection of the weld diameter used to determine good weld quality range based on observed expulsion limits is included in this Chapter. Also presented are micrographs of some spot welded samples. The micrographs were used for determining nugget size.

5.2 Dynamic Voltage and Dynamic Current Data

Dynamic halfwave voltage and dynamic halfwave current data were obtained in the welding process by instrumentation readings as described in chapter 4. The welding program as previously explained, consists of twenty halfwave welding cycles (HW) for each sample welded. Eight samples were welded under each time step and there were six time steps for each applied electrode force used. Dynamic voltage and dynamic current dataset therefore consists of twenty halfwaves made up of ten troughs (negative values) and ten peaks (positive values), for each welded sample.

The dynamic halfwave values of voltage and current for time step 1 to step 6 using applied electrode force of 2.2 kN obtained using C-Gun welding machine are presented in Appendix A. Figure 5.1 show a plot of dynamic voltage for Dalex-25 Gun machine at an applied electrode force of 2.2 kN. Corresponding values of halfwave dynamic current of same applied electrode force with same welding machine are presented in Figures 5.2.

Similar results were obtained for the welding steps one to six for the entire samples welded in all the four welding machines for all the applied electrode forces used.

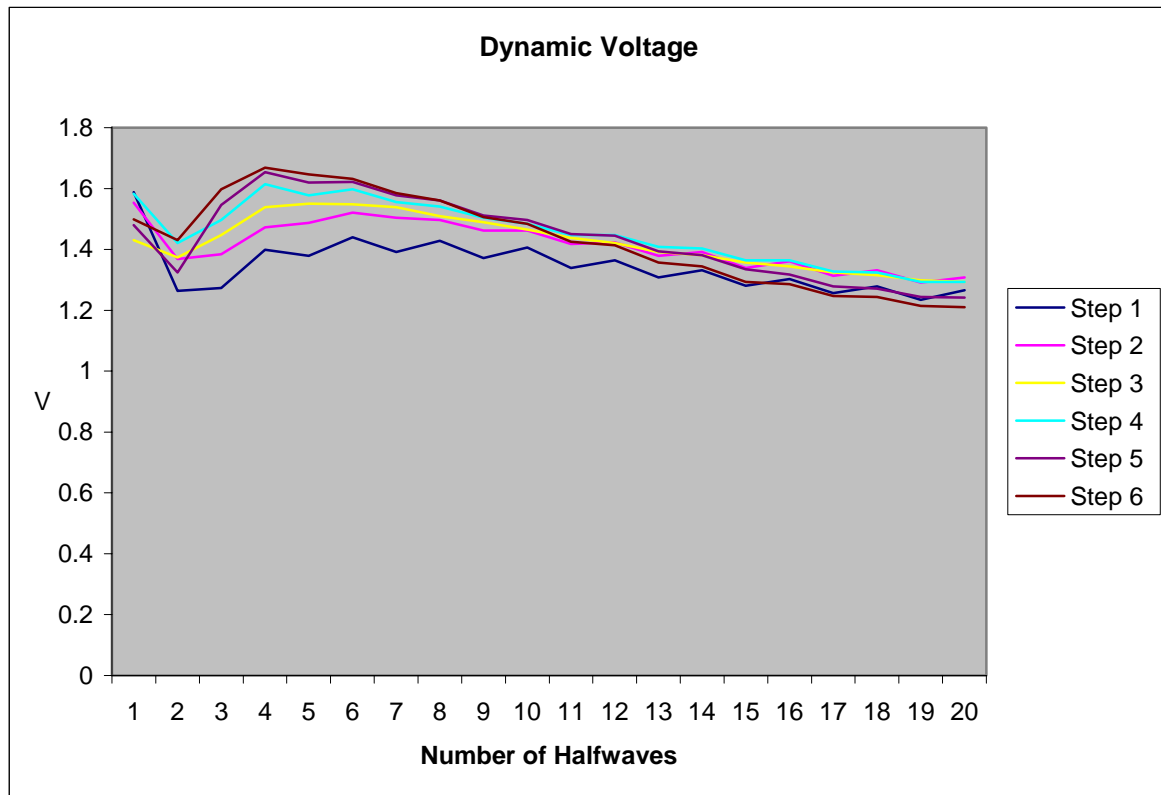


Figure 5.1: Dynamic Voltage step 1- 6 for Dalex-Gun 25 applied force 2,2kN.

The dynamic voltage values of steps 5 and 6 are higher than the dynamic voltage values of steps 1 and 2, with step 3 and 4 in-between as can be seen in Figure 5.1. The higher time steps 5 and 6 are carried out at higher welding current compared to the lower time steps of 1 and 2, hence higher dynamic voltage. The dynamic voltage at between the first two halfwave cycles was high (steep), with a sudden drop and then incremental rise to a peak at about halfwave four before gradually lowering down as shown in Figure 5.1. This behaviour typically shows the response of the welded material to the effect of increasing voltage during the welding process. This behaviour will be extensively discussed under the dynamic resistance modelling section in the next Chapter.

The higher dynamic current values for the higher time steps 5 and 6 and lower dynamic current values for the lower time steps 1 and 2, with time steps 3 and 4 in-between as

shown in Figure 5.2. The dynamic current for each of the time steps in Figure 5.2 showed an initial increase up to the second halfwave, then a sharp drop to halfwave four and gradual increase from that point to the twentieth halfwave.

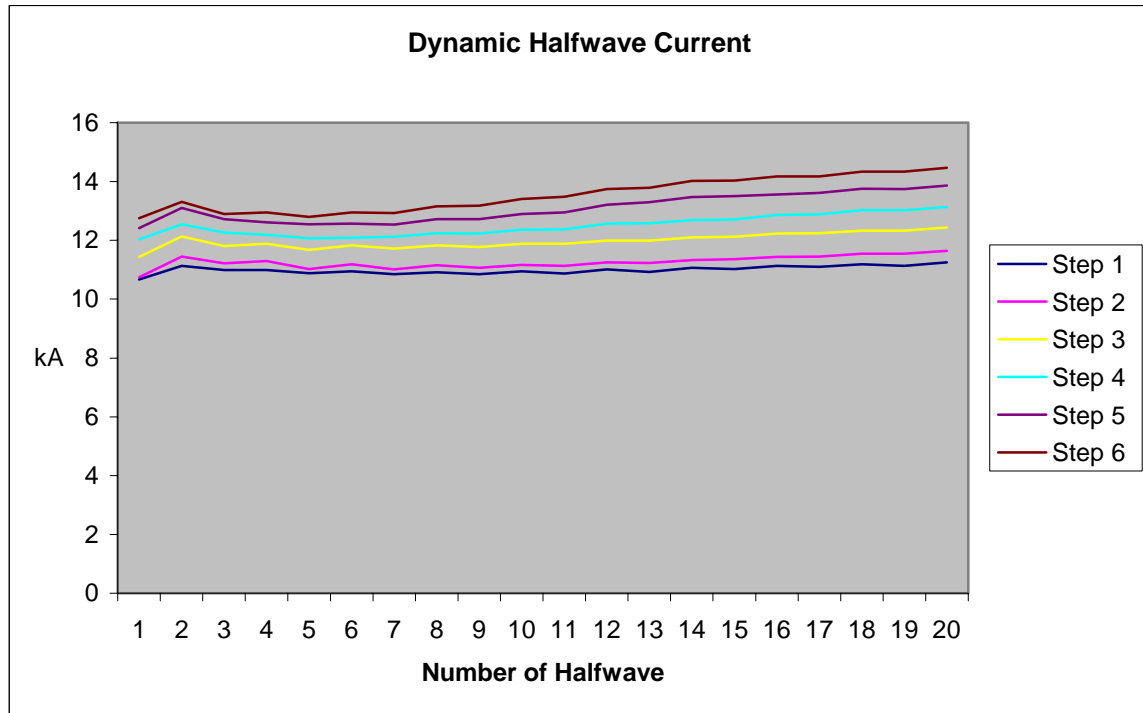


Figure 5.2: Dynamic Current step 1- 6 for Dalex-Gun 25 applied force 2,2kN.

5.3 Dynamic Resistance Data

The generated peak halfwave dynamic voltage and peak halfwave dynamic current values were used to calculate peak halfwave dynamic resistance values for the entire welded samples using the relationship:

$$V = IR \tag{5.1}$$

where V is peak dynamic voltage (V), I is peak dynamic current (kA) and R is peak dynamic resistance (mΩ). Dynamic resistance calculated using the dynamic voltage and current obtained from C-Gun welding machine at applied electrode force of 2.2 kN is

presented in Figure 5.3. Similar values obtained for the entire applied electrode force and for all four welding machines used are presented in Appendix B.

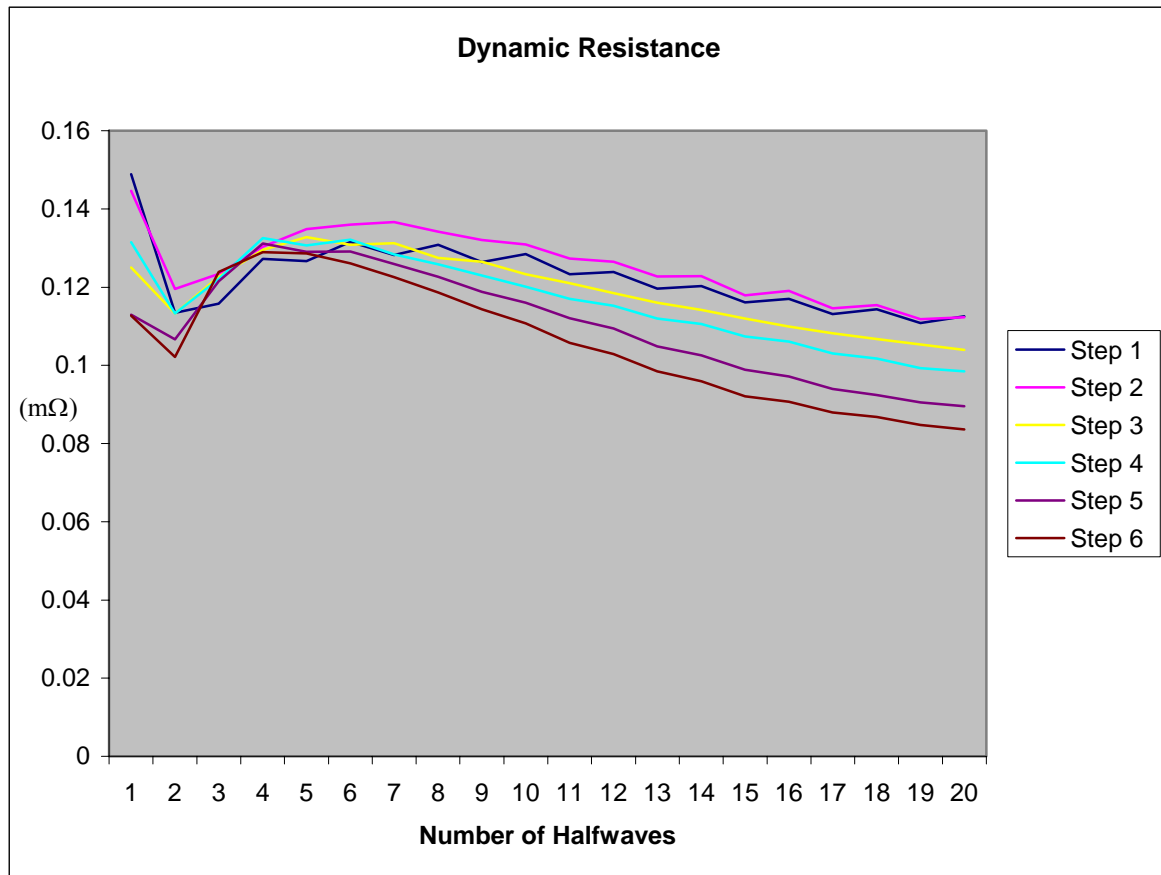


Figure 5.3: C-Gun (2.2 kN) steps 1-6, Dynamic Resistance plot

Figure 5.3 shows a common trend in the dynamic resistance behaviour of the welded samples generated from the C-Gun welding machine, at 2.2 kN force, and time steps 1 to 6. The plots of each of the sample dynamic resistance graph showed an initial high dynamic resistance value at the first halfwave, followed by sudden sharp drop at about the second halfwave and gradual increase in resistance from the second halfwave point to a peak point and then a gradual decrease from the peak point. The initial high dynamic resistance at the first halfwave is due to the effect of the contact resistance of the material, this effect is not sustained and within the second halfwave with increase in heat generated the contact resistance effect is overcome ⁽¹⁰²⁾. The dynamic resistance due to the solid state effect of the material resistance and inter-contact resistance effect between the

welded material (plates) causes the dynamic resistance to increase to the peak point, with a change of state from solid to a mixture of solid and liquid, the dynamic resistance drops⁽¹⁰²⁾. This state accounts for the sudden change in dynamic resistance. The liquid state of the weld accounts for a decrease in dynamic resistance as is noted with the downward trend of the dynamic resistance curve⁽¹⁰²⁾.

It was observed from the graphs of the dynamic resistance curves shown in Appendix B, that the dynamic resistance curves of all the welded sample have similar trend like the ones in Figure 5.3, with some samples however showing some slight deviation. The slight variation is expected because of some variability that may have arisen from the machine or machine settings or instrument readings etcetera^(3, 10).

It is observed that the peak points in the dynamic resistance curve of Figure 5.3 did not all occur at the same halfwave cycle time in all the time steps. Some of the peak points are seen to be reached at earlier halfwave cycles times than others. The peak point of the dynamic resistance curves for welding time steps 4-6 occurred at about the fourth halfwave cycle (HW 4) and welding time steps 1-2 at about the sixth halfwave cycle (HW 6). This can be explained as the effect of increased welding current at the higher time steps, such that the peak dynamic resistance are reached within the first few cycle times, compared to the reduced welding current of steps 1-2 which takes longer halfwave cycle time to reach the peak points⁽⁹⁴⁾. This observation will be further discussed in modelling section of Chapter 6.

5.4 Effective Weld Current (RMS) and Weld Diameter Dataset

The modelling of the resistance spot welding process parameters will require dynamic resistance, effective weld current (RMS), weld diameter and applied electrode force. Having determined dynamic resistance values for given applied electrode forces from the previous section, this section presents effective weld current and weld diameter data needed for the modelling process. Presented in Table 5.1 are effective weld current and weld diameter dataset for C-Gun welding machine at an applied electrode force of 2.2kN.

Similar results were obtained for the entire samples welded. Figures 5.4 and 5.5 shows the effective weld current (RMS) and weld diameter achieved for time steps 1 and 6.

Table 5.1: Additional Generated Data for Step 1 and 6, of C-Gun Machine at 2.2kN Force

Specimens.nr.	Fe (kN)	I _s (kA)	d _p (mm)	d _{pk} (mm)	M _t (Nm)	Win. (Deg)	BA	Step
15-1	2.2	5.75	4.8	3.8	6.6	2.9	S	Step 1
15-2	2.2	5.76	4.8	3.6	7.0	34.4	S	Step 1
15-3	2.2	5.76	4.8	3.6	6.8	14.2	S	Step 1
15-4	2.2	5.73	4.8	3.7	7.4	12.7	S	Step 1
15-5	2.2	5.73	4.8	3.4	6.8	33.9	S	Step 1
15-7	2.2	5.74	4.9	3.5	8.0	15	S	Step 1
15-8	2.2	5.76	4.9	4	6.7	6.7	S	Step 1
17-1	2.2	7.27	5.7	4.2	13.6	78.6	S	Step 6
17-2	2.2	7.32	5.6	4.4	14.4	65.7	A	Step 6
17-4	2.2	7.6	4.9	4	9.6	64.8	A	Step 6
17-5	2.2	7.34	5.9	4.4	14.3	62	A	Step 6
17-6	2.2	7.59	5	3.4	11.7	67.9	A	Step 6
17-7	2.2	7.37	5.7	4	18.1	68.4	A	Step 6
17-8	2.2	7.34	5.6	4.1	14.4	66.8	A	Step 6

Abbreviation terms as used in the table are as follows: **Fe**: Electrode force (kN), **I_s**: Welding current (kA), **d_p**: spot diameter with corona zone (mm), **d_{pk}**: spot-diameter (mm), **BA**: fracture type, **A**: plug failure, **S**: Interface fracture.

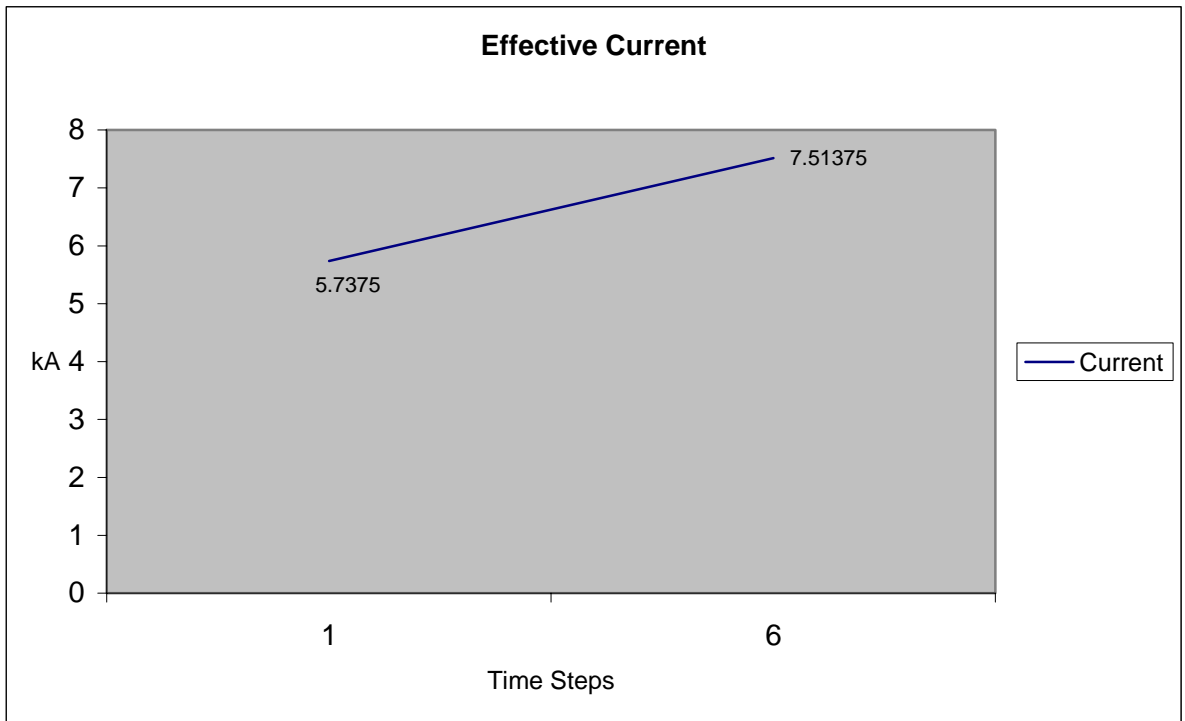


Figure 5.4: C-Gun (2.2 kN) Average Values of Effective Weld Current for steps 1 and 6

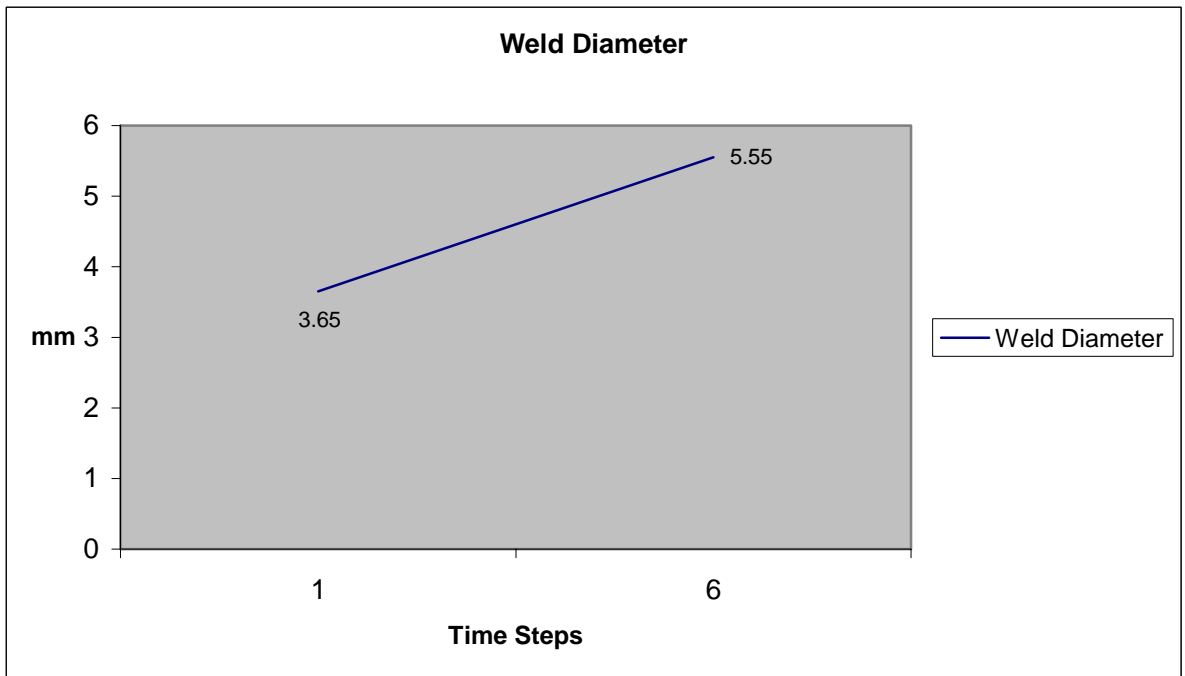


Figure 5.5: C-Gun (2.2 kN) Average Values of Weld Diameter for steps 1 and 6

The results of effective weld current and weld diameter in Figures 5.4 and 5.5 show that, the average size of the achieved weld diameter is larger in samples made at time step 6 than time step 1. The increase in weld diameter from step 1 to step 6 is because of the increase in current used from step 1 to step 6. Similarly, micrographs were obtained for a number of the samples welded. Presented in Figures 5.6 and 5.7 are micrographs of the nugget of some samples welded with Dalex PMS welding machine for step 1 and step 6 respectively.

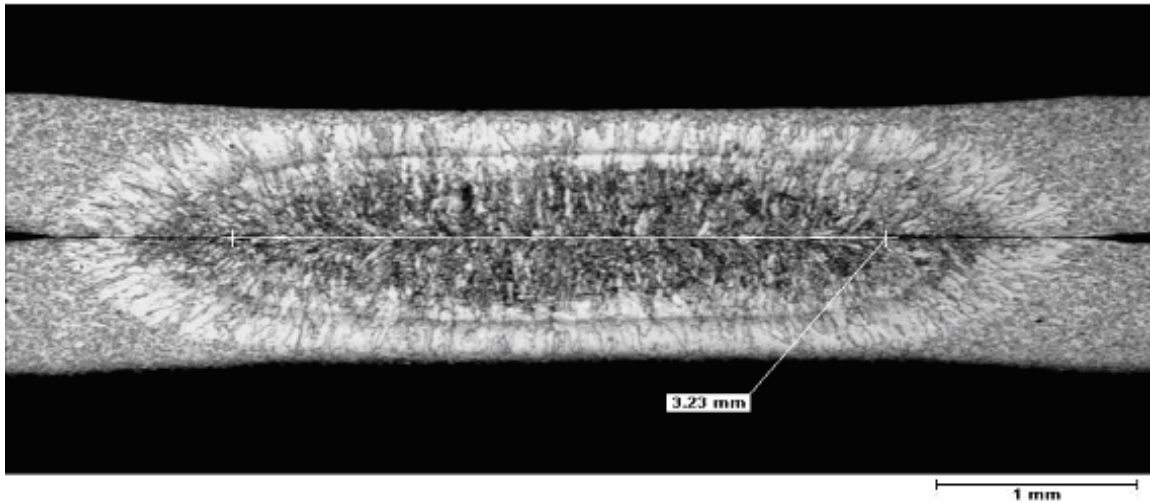


Figure 5.6: Metallography of weld spot nuggets of step 1, welded sample, Dalex PMS

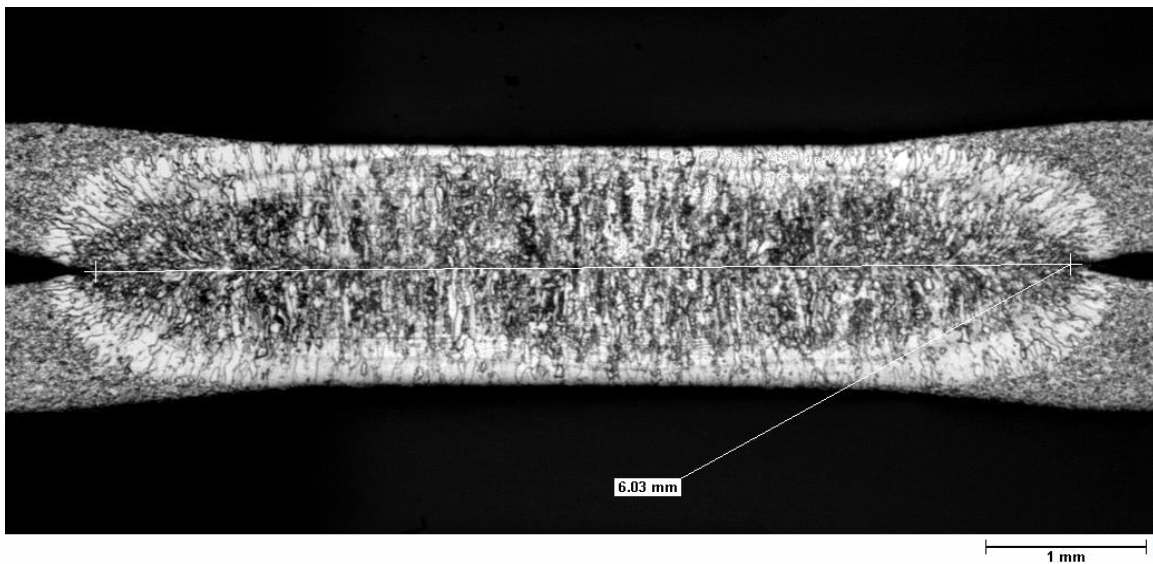


Figure 5.7: Metallography of weld spot nuggets of step 6, welded sample, Dalex PMS

These represent the two extremes of the time steps. The Figures show that the nugget sizes produced in step six are bigger in size (Figure 5.7) than the nugget sizes from step one (Figure 5.6). This agrees with the direct relationship between effective weld current and achieved weld diameter.

The selection of the good weld quality range using weld diameter cut off value based on observed expulsion limit is presented in Table 5.1.

Table 5.1: Observed Maximum Values: weld diameter, effective current and observed expulsion weld diameter

Machine Type	Applied Electrode Force (kN)	Maximum. Weld Diameter achieved (mm)	Corresponding Effective Current (kA)	Maximum Effective Current (kA)	Corresponding Weld diameter (mm)	Expulsion Weld Diameter (mm)
C-Gun	2.2	5.9	7.34	7.51	5.6	5.6
	2.6	6.1	8.32	8.41	6.0	None
	3.0	6.2	8.62	8.66	6.1	None
DZ	2.2	5.6	7.41	7.43	5.3	None
	2.6	6.0	8.39	8.39	6.0	None
	3.0	6.6	9.39	9.42	6.2	None
PMS	2.2	6.60	8.33	8.58	6.15	5.8
	2.6	6.50	8.76	8.84	6.2	None
	3.0	6.80	9.24	9.34	6.3	None
Dalex	1.76	5.4	7.04	7.04	5.4	5.25
	2.16	5.9	7.69	7.69	5.9	5.4
	2.2	6.0	7.63	7.73	5.7	5.5
	2.46	5.9	7.85	7.85	5.9	None
	2.6	6.1	7.95	7.95	6.1	None
	3.0	6.3	8.55	8.57	5.9	None

In defining weld quality, weld diameter less than 3.7 mm was considered a bad weld because it is below the stick limit. Theoretically, the weld diameter is expected to be between 3.7mm and 4.7mm to be considered a satisfactory weld quality for the electrode wear class used ⁽¹⁹⁾. Maximising the size of the weld diameter to a possible large size before expulsion point will give better weld quality (weld diameter).

Based on observation as shown in Table 5.1, weld diameter between 3.7 mm and less than 5.25 mm was considered good weld. With less than 5.25 mm weld diameter as the better spot weld quality. Less than 5.25 mm weld diameter was taken as a cut-off point because an expulsion was observed to occur at 5.25 mm during the welding process as shown in the Table. This observation shows that there is no guarantee that expulsion will not occur at a weld diameter above 5.25 mm.

5.5 Concluding Remarks

By using the equation ⁽¹⁹⁾ $4\sqrt{t} \leq d < 5\sqrt{t}$, it was possible to have a guide to what defines a good or poor quality weld. The nugget sizes produced in step six are bigger in size than the nugget sizes from step one because of higher current range applied. This agrees with the direct relationship between effective weld current and achieved weld diameter. Effective weld current achieved, in the time steps 6 are higher than in the steps one.

No expulsion was observed at below 5 mm weld diameter. This means that high chance exist to push the current up to the point of producing this weld diameter without expulsion. The earliest expulsion was with Dalex 25 welding machine with a weld diameter of 5.25 mm at an applied electrode force of 1.76 kN. Expulsions were frequent as noticed at the lower applied electrode force than at higher applied electrode force. This may be because at the lower applied electrode force, larger gap exist between the plates contact surfaces which creates higher resistance. During the welding process with fast heat generation mostly due to higher resistance and rapid growth of the nugget ⁽²³⁾, without adequate constraints chance for expulsion occurring will be very high.

The non linear nature of dynamic resistance variables makes it difficult to use in predicting weld quality. It is therefore important to model this variable in other to use it for predicting weld quality.

CHAPTER 6

MODELLING THE PROCESS PARAMETERS

6.1 Introduction

Presented in this Chapter are the models used for estimating the process parameters in the resistance spot welding process. These process parameters are dynamic resistance, applied electrode force, effective weld current and weld diameter. Dynamic resistance generated from each welded sample showed non linear and complex behaviour in having twenty halfwave dynamic resistance values per sample. An empirical model was developed and used to curve fit the dynamic resistance curve, such that the twenty halfwave dynamic resistance per sample was reduced to just one resistance value for each sample welded. This estimated resistance per sample will be referred to as sample resistance in this thesis. The level of error in the estimation was determined for each of the samples using the root mean square error and sum of square criteria ⁽¹⁰³⁾.

The prediction capability of the empirical model was improved by passing the outputs from the model through neural network learning for intelligent and accurate prediction. The predicted sample resistance from the neural network with applied electrode force and effective weld current were used as in inputs in a second neural network model to predict weld diameter.

Four neural network types which are generalized feed forward, multilayer perceptron (MLP), radial basis function (RBF) and recurrent neural network (RNN) types were trained and tested to find the one with least error and best generalization capability, for predicting sample resistance and the weld diameter. Such that for any desired weld diameter it was possible to determine the optimum parameters that will be needed to achieve the weld diameter.

6.2 Empirical Model for the Dynamic Resistance Parameter

An empirical (mathematical) model that explains the pattern of the dynamic resistance behaviour ⁽¹⁰²⁾ was developed. The purpose was to use it to linearise the nonlinear dynamic resistance curve and to be able to estimate a resistance value for each welded sample. This is because a linear input parameter to the neural network model would help improve the neural network prediction accuracy as discussed earlier in the literature section. In developing this model the dynamic resistance curve was broken up into three stages as is shown in Figure 6.1.

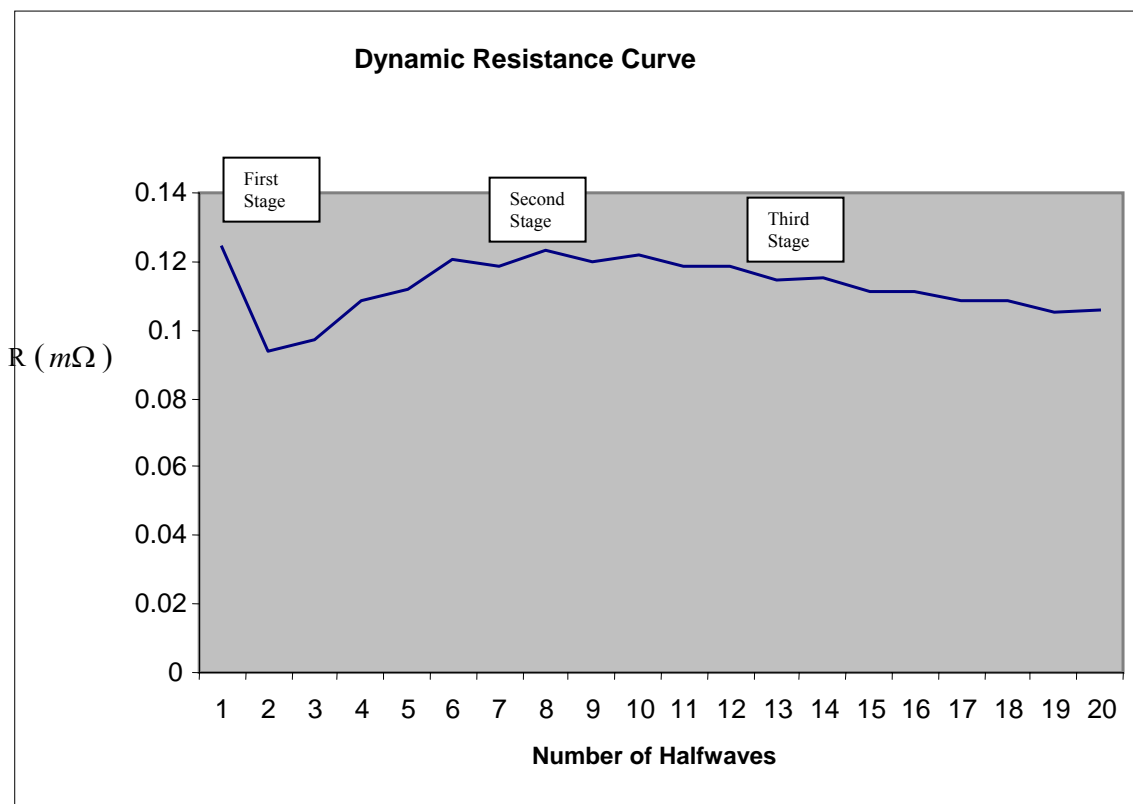


Figure 6.1: Trend Pattern of Dynamic Resistance Curve

The first stage is the early stage of the resistance change from its initial value up to the peak point. The second stage is the peak point and the third stage is the dynamic resistance from the peak point to welding completion.

6.2.1 First Stage

Figure 6.1 shows that in the first few initial halfwave cycle times there is significant drop in the dynamic resistance followed by a gradual increase. Peak point is reached after few time halfwave cycles depending on the welding current intensity ⁽¹⁰²⁾. With the dynamic resistance there is a corresponding increase in temperature and amount of energy generated ^(23, 102). This is because resistivity increases with temperature. It can be concluded that changes in welding cycle time corresponds to changes in temperature and generation of heat energy as the dynamic resistance progresses up to the peak point.

Based on observation of the dynamic resistance curve, it can be stated that the dynamic resistance behaviour of the spot welded sample from the first halfwave cycle time to the peak point is directly related to the number of halfwave cycles plus the initial resistance at first halfwave cycle time. Expressed mathematically:

$$R_1 \propto N_c + R_0 \quad (6.1)$$

Such that

$$R_1 = M \times N_c + R_0 \quad (6.2)$$

where R_1 is a function that accounts for the resistance from first time cycle up to the resistance at the peak point. N_c is the number of half waves. R_0 is the surface resistance of the sample. Parameter M is a function of temperature which depends on the material resistance (R_s) during current flow ^(94, 102), expressed by

$$R_s = \beta \frac{l}{A} \quad (6.3)$$

with β = specific electrical resistance (temperature dependant), l = length of current flow in work piece and A = current area (electrode contact area). As is shown in Figure 6.2.

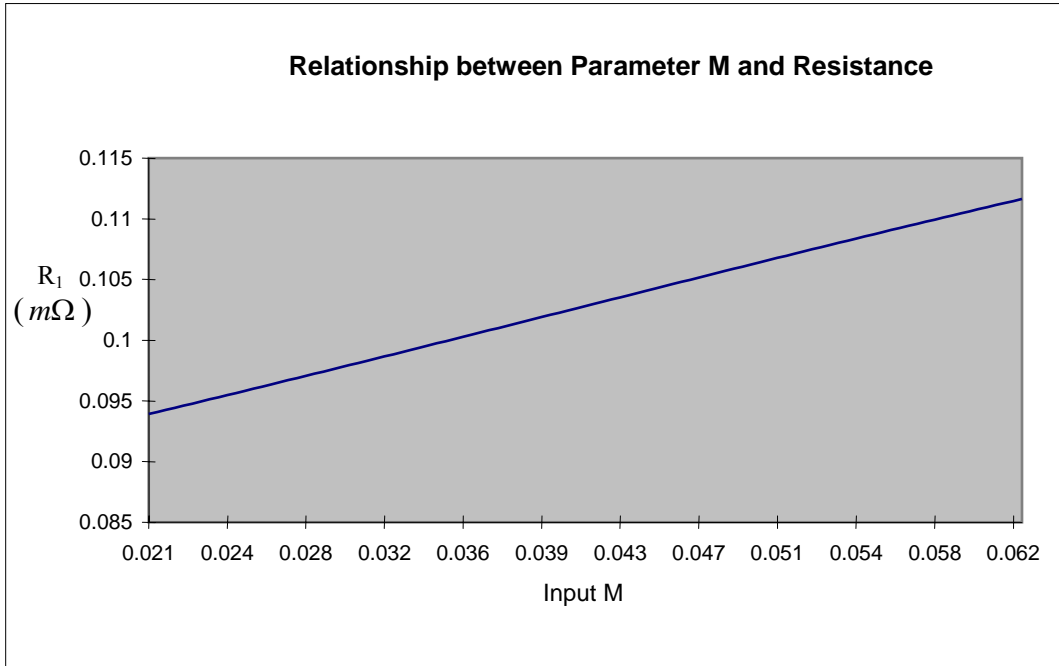


Figure 6.2: Influence of Parameter M on Resistance

The figure shows that increasing the input parameter M generates an increase in the value of the sample resistance (R). The effect of the initial resistance which is due to the contact resistance between the surfaces of the welded plate in contact disappears after the first few welding halfwave cycles. This agrees with Matsuyama⁽²⁴⁾ findings in which he concluded that the resistance due to the interface contact resistance is not very important in normal resistance spot welding.

6.2.2 Second Stage

The second phase is the peak point of the dynamic resistance curve. This peak point is referred to by most researchers as the β peak^(94, 102). In explaining the formation of the β peak, De et al⁽⁹⁴⁾ in reviewing the work by Dickinson⁽¹⁰²⁾ in this area mentioned that

at the peak point there is decreased interface resistance which is influenced by the increased bulk resistivity with temperature. This eventually leads to an overall decrease in the sample resistance away from the peak point ⁽⁹⁴⁾, such that the peak point stands out. This view is consistent with the views of other researchers ⁽¹⁰²⁾. However, at this β peak there is no change in dynamic resistance and welding cycle time hence:

$$\frac{dR}{dN_c} = 0$$

With the change in dynamic resistance to the change in welding cycle time being equal to zero $\frac{dR}{dN_c} = 0$ at this β peak it is possible to estimate the parameter M . The parameter

M in equation (6.2) is determined by taking the second order partial derivative of the same equation (6.2).

6.2.3 Third Stage

The third phase corresponds to the downward slope from the β peak of the dynamic resistance curve, Figure 6.3.

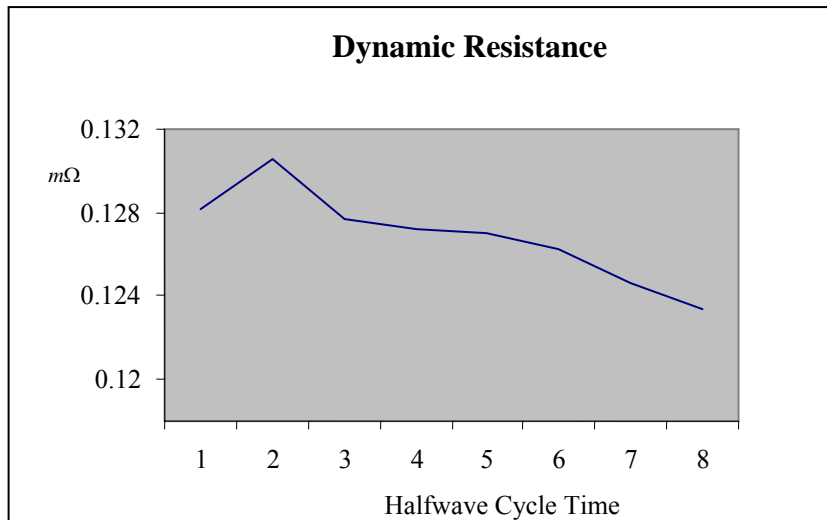


Figure 6.3: Dynamic resistance trend from the peak point downwards Slightly away from the β peak is a marked decrease in dynamic resistance sloping downwards as the welding cycle time progresses. The drop in dynamic resistance is due

to a change in contact diameter (contact resistance) because of the change of state from solid to liquid of the sheet surfaces in contact and increase in the cross sectional area ^(23, 94).

Estimating the change in cross sectional area of the contact surfaces is difficult because the contact diameter is not constant during welding ⁽²³⁾, Matsuyama ⁽²³⁾ used simulation method to determine contact diameter but only at a particular time (t). Contact diameter change at plate interface ⁽²³⁾ during the welding process is dependent on time. The change in cross sectional area (contact diameter) affects the downward slope of the curve from the β peak ⁽¹⁰²⁾.

The downward slope of the dynamic resistance curve from the β peak is observed to follow a mathematical function of inverse relationship between the dynamic resistance downward slope (R_2) and the welding cycle time (N_c) raised to power index “n” (n is an index that ranges between 0 and 1) and strongly influences the downward slope from the β peak .

Represented thus:

$$R_2 \propto N_c^n \quad (6.4)$$

Such that,

$$R_2 = \frac{K}{N_c^n} \quad (6.5)$$

Where R_2 is the dynamic resistance of the downward slope from the β peak, N_c is the welding cycle time, n is power index and K is a constant. The power index n describes the steepness of the slope. The physical cause of the downward slope is due to drop in interface resistance as a result of change of state from solid to liquid as the faying surface melts ⁽¹⁰⁴⁾. K directly influences the sample resistance. Increasing K leads to an increase in sample resistance as is shown in Figure 6.4.

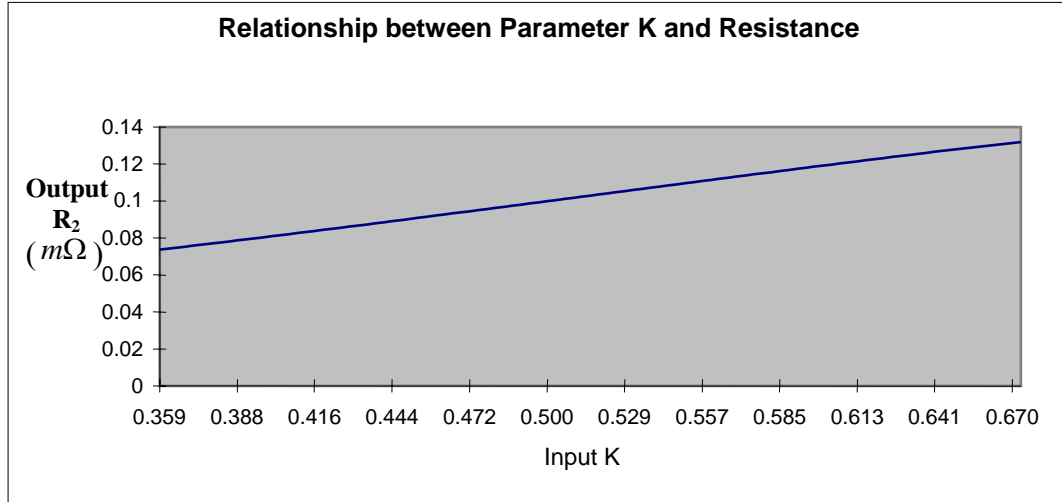


Figure 6.4: Influence of Parameter K on Resistance

6.2.4 Total Resistance

The mathematical function that describes the dynamic resistance will then be the total of R_1 and R_2 acting in parallel, such that

$$\frac{1}{R} = \frac{1}{R_1} + \frac{1}{R_2} \quad (6.6)$$

R is total resistance; R_1 and R_2 are defined earlier.

Substituting equations (6.2) and (6.5) into equation (6.6), the expression becomes;

$$\frac{1}{R} = \frac{1}{(M \times N_c + R_0)} + \frac{N_c^n}{K} \quad (6.7)$$

such that,

$$\frac{1}{R} = \frac{K + ((N_c^n) \times (M \times N_c + R_0))}{K(M \times N_c + R_0)} \quad (6.8)$$

By making R the subject of the equation;

$$R = \frac{K \times M \times N_c + K \times R_0}{((K + (N_c^n \times M \times N_c) + (N_c^n \times R_0))} \quad (6.9)$$

R_0 and N_c are known for each sample welded, K and M can be estimated. To determine the unknown parameter n (power index), the effect of change of n on the slope of the dynamic resistance curve was evaluated by taking n values from 0 to 1 and substituting into a plot of equation 6.9.

The value of n is incrementally increased to see the effect on the model. By increasing n to 0.2, the drop in resistance is noticeable but far from actually fitting the dynamic resistance curve. Further increasing n to 0.5 correctly fits the curve as is shown in Figure 6.5.

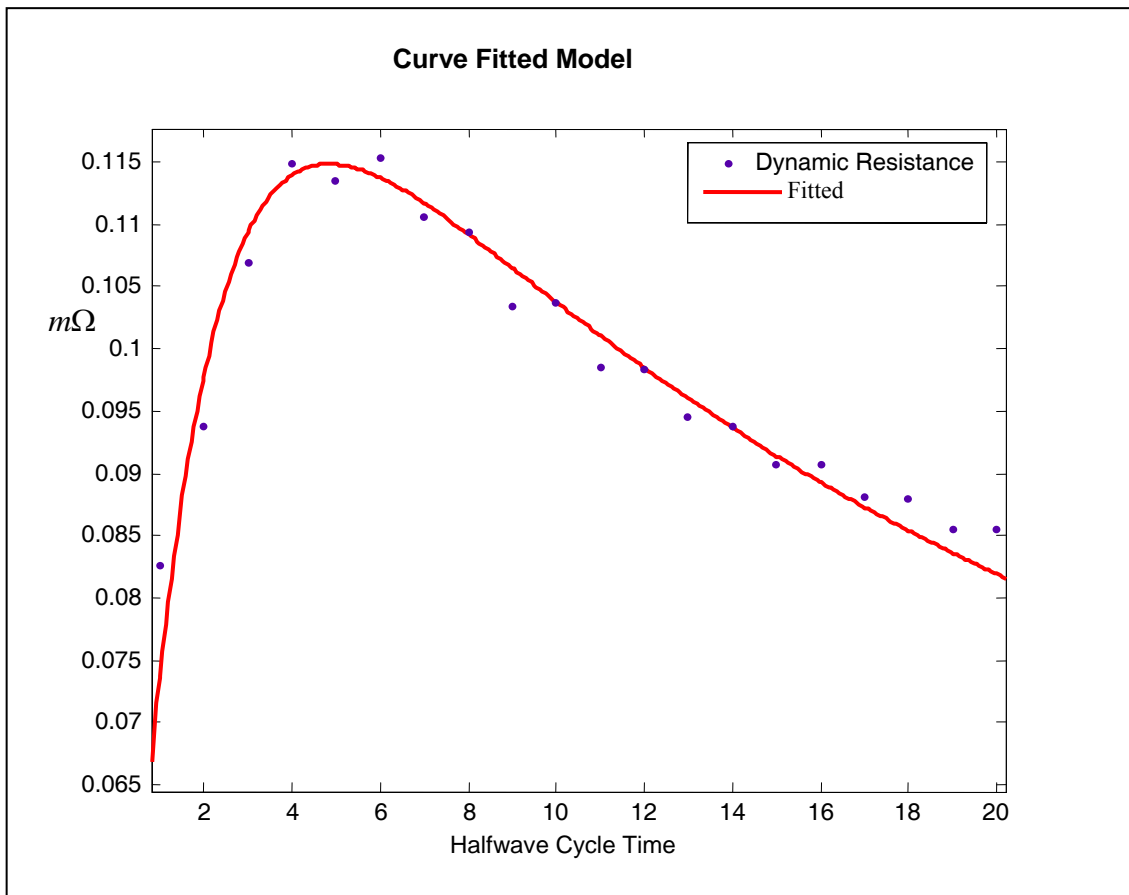


Figure 6.5: Curve fitted Model at $n = 0.5$

The power index n was taken as 0.5 in this model due to best fit. It is observed that the dynamic resistance curve fitting model responds to this power index n by some unknown non linear relationship function. This relationship is assumed to be depending on the contact area of the sheet surfaces during the welding process⁽²³⁾.

To calculate sample resistance R , the parameters K and M have to be determined. M and N can be estimated by taking partial derivatives of equation (6.7) at the β peak where

$$\frac{dR}{dN_c} = 0, \text{ such that;}$$

$$\frac{-(1/R^2)dR}{dN_c} = \frac{-(M/(M \times N_c + R_0)^2) + N^{(n-1)}}{nK} \quad (6.10)$$

$$\frac{dR}{dN_c} = R^2 \frac{M/(M \times N_c + R_0)^2 - N^{(n-1)}}{nK} \quad (6.11)$$

Maximum at $\frac{dR}{dN_c} = 0$, when $N_c = N_p$, N_p is the cycle number at β peak

$$\frac{M/(M \times N_p + R_0)^2 - N_p^{(n-1)}}{n \times K} = 0$$

$$\frac{N_p^{(n-1)}}{n \times K} = \frac{M}{(M \times N_p + R_0)^2}$$

$$\frac{1}{K} = \frac{n \times M}{N_p \times (n-1)(M \times N_p + R_0)^2}$$

$$K = \frac{N_p^{(n-1)} \times (M \times N_p + R_0)^2}{n \times M}$$

The equation will be

$$K = \frac{2(M \times N_p + R_0)^2}{\sqrt{N_p}} \quad (6.12)$$

Similarly parameter M will be

$$M = \frac{(K^2 N_p - 2R_0)}{2N_p} \quad (6.13)$$

Such that once parameter M is estimated K can be determined and vice versa. The total resistance (R) can therefore be determined by the equation:

$$R = \frac{K \times M \times N_c + R_0}{K + (M \times N_c^{1.5})} + R_0 \times N_c^{0.5} \quad (6.14)$$

This equation is the model that can be used for curve fitting the dynamic resistance curve and for determining the sample resistance (R), once the parameters K and M are estimated. This model equation (6.14) was used to test one hundred and seventy samples per machine for all four machines used. This was to confirm the model suitability for curve fitting the dynamic resistance curves and for estimating the resistance of welded samples.

The curve fitting and estimation of the unknown parameters were done for each welded sample in MATLAB⁽¹⁰⁵⁾. This was done by first making a plot of the dynamic resistance curve in MATLAB, followed by the equation (6.14) of the model being written in the MATLAB curve fitting custom solution option⁽¹⁰⁵⁾. The confidence interval was set at 95%. Initial parameter values were assumed and supplied⁽¹⁰³⁾ before starting iteration process for determining the final value of the parameters. Assuming initial parameter values were because the iteration process can not proceed without some initial values supplied. These initial values were randomly generated in MATLAB, and the correct parameter values were determined through the iteration process⁽¹⁰³⁾.

Through the iterative process the K and M parameters which curve fitted (best fits) the dynamic resistance curve were determined. With the parameters K and M known it was

possible to determine the sample resistance for each of the welded samples. This was done by substituting the values of the parameters K and M generated, and R_0 , which is the initial dynamic resistance value into the model expression of equation (6.14).

Presented in Figure 6.6 is the result of the curve fitting of the dynamic resistance curve for one of the samples taken from DZ machine under applied electrode force of 3.0 kN, using the model (equation 6.14) to make the fit.

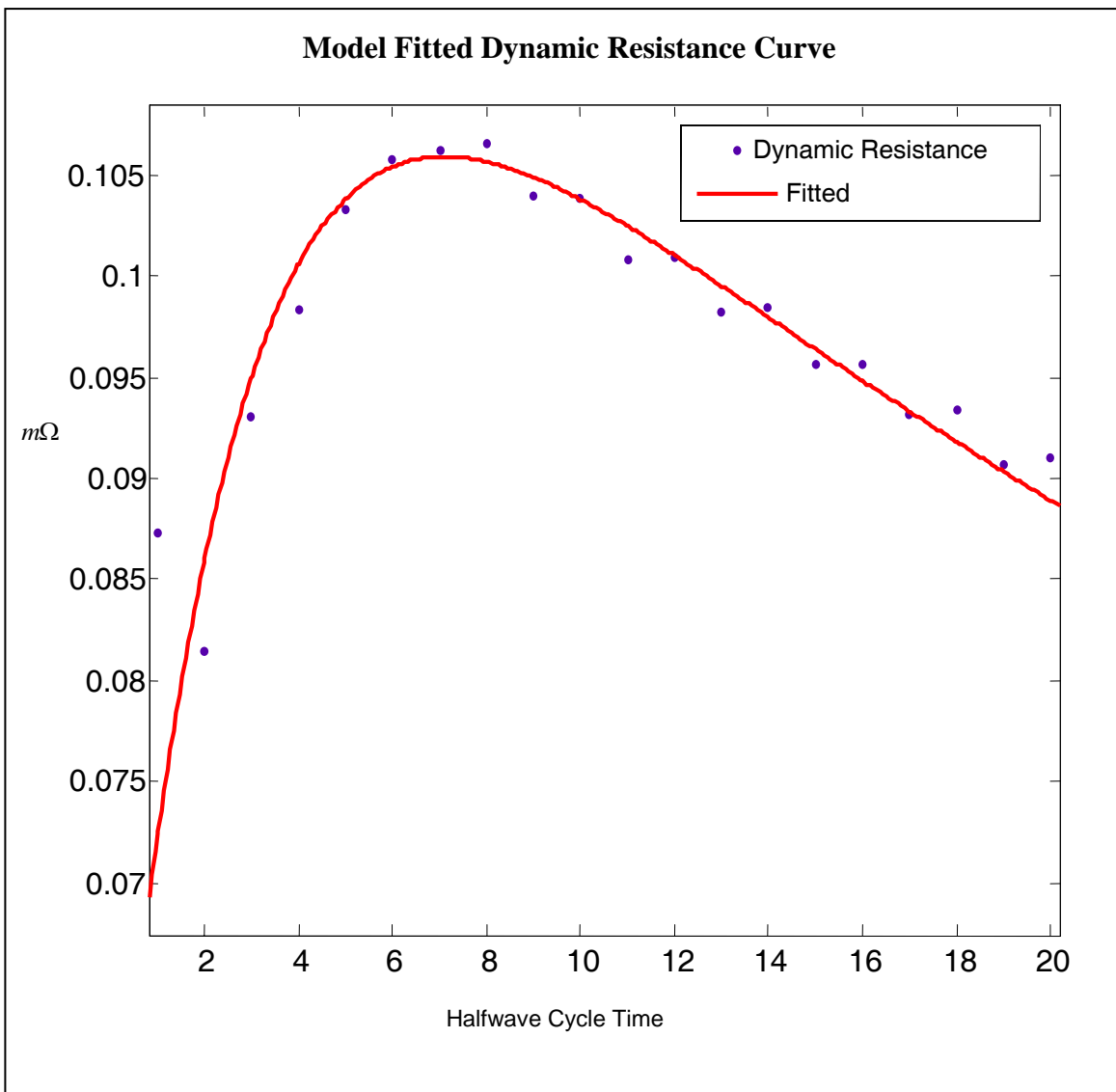


Figure 6.6: Fitted Dynamic Resistance Curve: DZ machine at 3.0 kN Force.

Similar results were obtained for all the welded samples. Presented in Appendix C are the results of the curve fit of some samples taken from all four welding machines, for different applied electrode force.

6.3 Applying the Empirical Model

The primary purpose of the empirical model (equation 6.14) was to linearise the inconsistent nonlinear dynamic resistance parameter. Additionally, the model is being explored for estimating sample resistance in an unknown welding condition.

The empirical model is applied by determining the parameters K , M and R_o and substituting these values into the model equation to estimate sample resistance. The sum of square error and root mean square error in each of the sample resistance estimated were determined ⁽¹⁰³⁾. In all the cases the sum of square error and root mean square error were significantly less than one ⁽¹⁰³⁾. This shows a good estimation. Presented in Table 6.1 are the K , M and R_o values determined for some samples welded in C-Gun machine which were used to determine the sample resistance (R).

Table 6.1: Estimated sample resistance (R)

Effective Current (kA)	Weld Diameter (mm)	K	M	Sum of Squares	RMSE	Ro ($m\Omega$)	R ($m\Omega$)
6.48	3.7	0.5391	0.029	0.001	0.008	0.106	0.101
6.48	3.7	0.6395	0.021	0.0002	0.004	0.085	0.11
6.52	3.7	0.5928	0.022	0.0005	0.005	0.091	0.104
6.5	3.7	0.5886	0.023	0.0005	0.005	0.092	0.105
6.53	3.9	0.5961	0.021	0.0003	0.004	0.086	0.105
6.52	3.7	0.5845	0.023	0.0004	0.005	0.089	0.104
6.52	3.7	0.5942	0.022	0.0005	0.005	0.091	0.105
6.51	3.7	0.6391	0.019	0.0004	0.004	0.086	0.108
6.99	4	0.5125	0.029	0.0004	0.005	0.093	0.097
7.01	4	0.5598	0.024	0.0526	0.054	0.087	0.102
6.99	4	0.5394	0.024	0.0529	0.054	0.085	0.099
6.97	4	0.5507	0.025	0.0003	0.004	0.086	0.101
6.93	4	0.5823	0.024	0.0002	0.004	0.085	0.105
6.96	4	0.5394	0.026	0.0003	0.004	0.083	0.1
6.97	4	0.5164	0.025	0.1194	0.081	0.089	0.096
7	4	0.5598	0.024	0.0005	0.006	0.092	0.102
7.35	4	0.5536	0.027	0.0002	0.003	0.082	0.102
7.34	4.4	0.5164	0.031	0.0002	0.004	0.089	0.099
7.36	4.4	0.5132	0.029	0.0002	0.004	0.087	0.097
7.33	4.3	0.537	0.027	0.0002	0.003	0.083	0.1
7.28	4.5	0.5536	0.031	0.0632	0.059	0.084	0.105
7.31	4.5	0.5628	0.027	0.0002	0.003	0.085	0.104
7.36	4.5	0.5281	0.028	0.0002	0.003	0.082	0.099
7.39	4.5	0.5267	0.028	0.0002	0.003	0.083	0.099
7.71	5.7	0.5334	0.03	0.0001	0.002	0.081	0.101
Effective Current	Weld Diameter	K	M	Sum of Squares	RMSE	Ro ($m\Omega$)	R ($m\Omega$)

(kA)	(mm)						
7.74	5.5	0.5123	0.032	0.0001	0.003	0.085	0.098
7.7	5.5	0.4893	0.035	0.0564	0.056	0.083	0.096
7.7	5.6	0.5003	0.033	0.0577	0.057	0.082	0.097
7.75	5.6	0.489	0.035	0.0002	0.003	0.086	0.096
7.73	5.6	0.4893	0.035	0.0002	0.003	0.088	0.096
7.73	5.5	0.489	0.035	0.0003	0.004	0.091	0.096
7.76	5.5	0.5003	0.033	0.0002	0.003	0.085	0.097
8.18	6	0.4944	0.036	9.80E-05	0.002	0.083	0.097
8.2	5.9	0.4709	0.042	0.0490	0.052	0.084	0.094
8.14	5.9	0.4721	0.039	0.0001	0.002	0.084	0.094
8.15	5.9	0.4702	0.039	8.68E-05	0.002	0.084	0.093
8.13	5.9	0.46	0.036	0.1166	0.08	0.084	0.091
8.12	5.8	0.4709	0.04	8.08E-05	0.002	0.084	0.094
8.16	6	0.4552	0.042	0.0001	0.003	0.086	0.092
8.18	6	0.46	0.041	0.0001	0.002	0.084	0.092
8.59	6	0.4348	0.042	0.0001	0.003	0.079	0.088
8.62	6	0.4128	0.046	0.0001	0.002	0.081	0.084
8.61	5.9	0.4186	0.046	9.16E-05	0.002	0.081	0.085
8.6	5.6	0.4358	0.046	0.0028	0.013	0.08	0.089
8.66	6.1	0.4095	0.045	9.56E-05	0.002	0.083	0.084
8.63	6	0.4186	0.042	0.0415	0.048	0.079	0.085
8.62	6.2	0.4256	0.043	9.66E-05	0.002	0.079	0.086
8.59	6.2	0.4358	0.043	6.81E-05	0.002	0.081	0.088

As is shown in Table 6.1, it is possible to use the empirical model to estimate sample resistance once K and M parameters are determined through an iteration process and R_o known.

To predict sample resistance R without going through an iteration process, graphs of values of the parameters are plotted and used for estimation needed values of M and K and R_o for a desired weld diameter. Presented in Figure 6.7 is a plot of the parameters M and K of one of the welding machines.

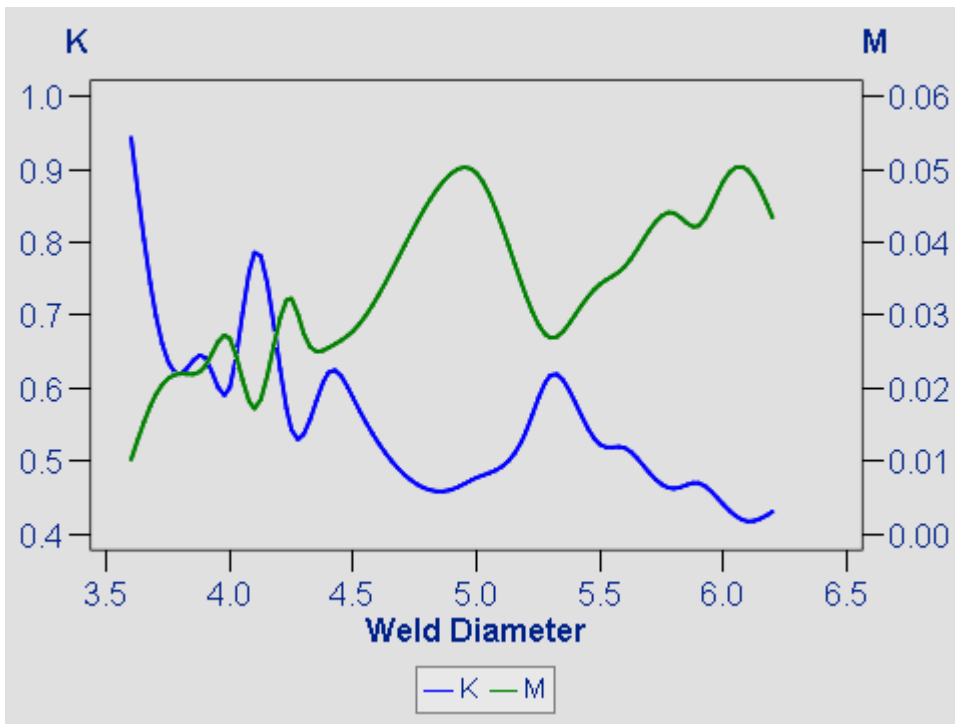


Figure 6.7: Machine C-Zange – Parameters M and K and Applied electrode force 2.2KN

To test if this is able to estimate sample resistance.

The parameters are estimated from the graph of Figures 6.7 at a desired weld diameter of 5.3 mm. The values for M and K were determined from the graph as $K = 0.6561$, $M = 0.02623$. Initial dynamic resistance R_o at first halfwave for this welding machine average is 0.094448.

Substituting these values into the model equation (6.13);

$$R = (K * (M * Nc + Ro)) / ((K + (M * Nc^{1.5})) + (Ro * (Nc^{0.5})))$$

$$R = (0.6561 * (0.02623 * 20 + 0.007563)) / ((0.6561 + (0.02623 * 20^{1.5})) + (0.007563 * (20^{0.5})))$$

$$R = 0.101 \text{ m}\Omega$$

To validate the above estimate, this value was compared to the actual value of the dynamic resistance at weld diameter of 5.3 mm for this machine and applied electrode force. Four values of sample resistance (R) were obtained. The values were 0.116201,

0.115402, 0.115902 and 0.112434. Percentage accuracy in estimating was 85%, 86%, 85.5% and 88.9% respectively.

Similarly compared for weld diameters of 5.9 mm, the parameters were estimated from the graphs of Figures 6.7, the value of R obtained was $0.1013\text{ m}\Omega$. Compared to actual value of R which was $0.10126\text{ m}\Omega$, a percentage accuracy of 99.98%. This was done for all the samples and the accuracies were all above 85%.

The applicability of this model was further verified to any of the welding machines without an identifier using data set generated from all the welding machines. The essence of this was to see how the graph can be used to accurately estimate sample resistance for a desired weld diameter in an unknown situation (unknown machine). Graphs were developed using the data generated from the model expression for different weld diameters. Presented in Figure 6.8 and 6.9 are the plots of K , M and R_o parameter values for different weld diameters for a number of samples welded at different applied electrode force using the four welding machines. These parameters were used for estimating sample resistance for a desired weld diameter in unknown welding machines.

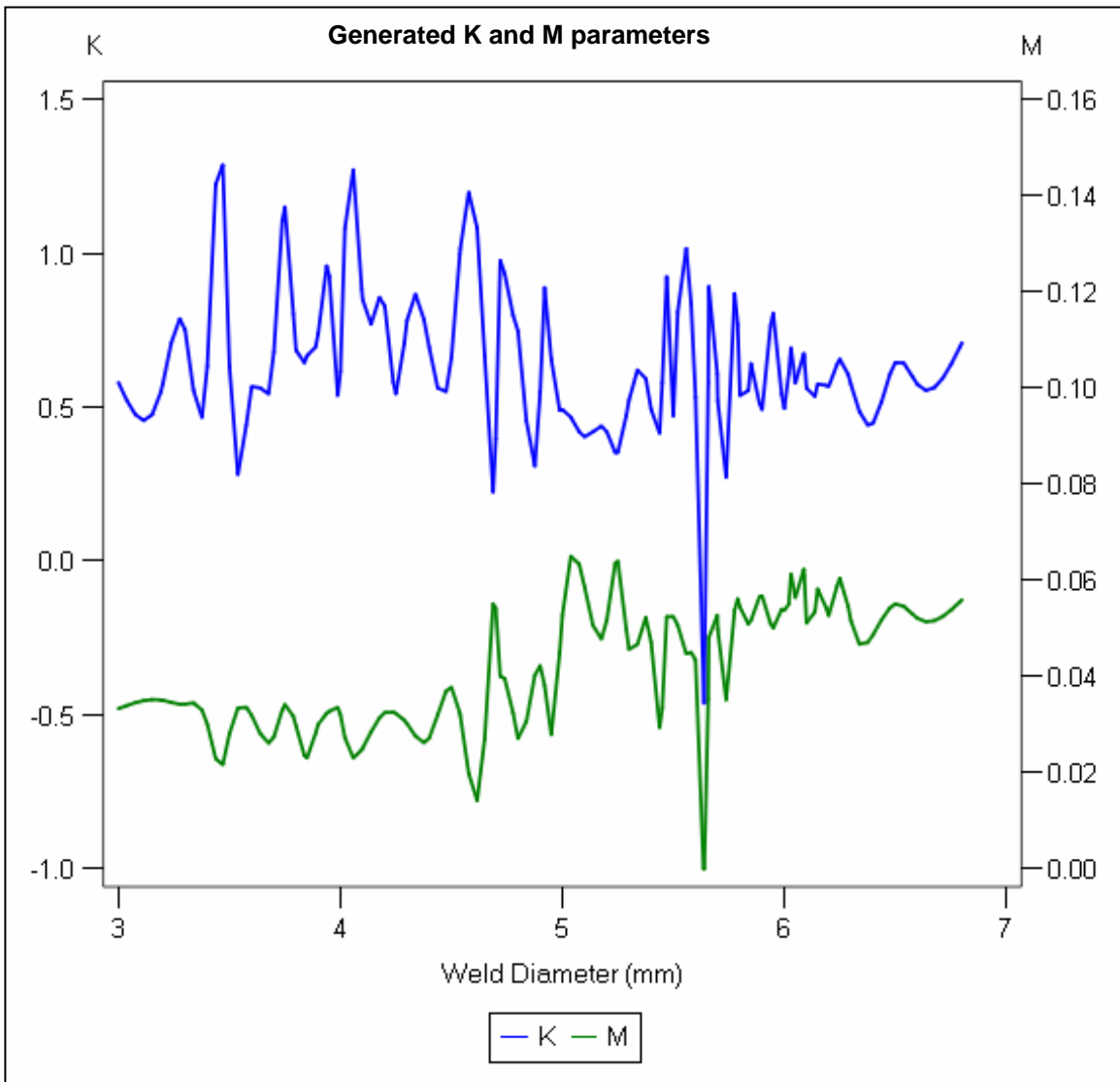


Figure 6.8: Parameters K and M Generated

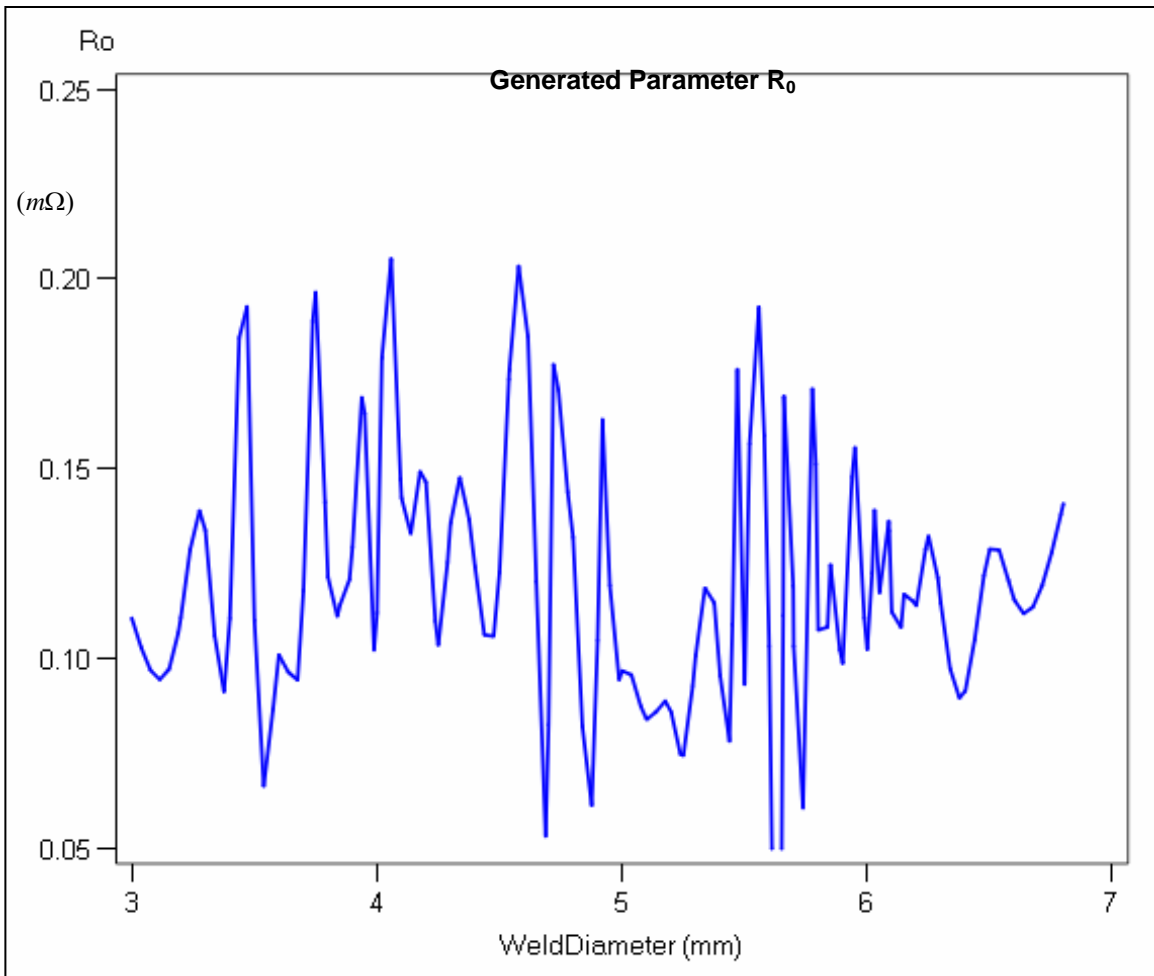


Figure 6.9: Parameter R_0 Generated

The obtained result of the sample resistance was compared with the actual values of sample resistance obtained. Presented in Figure 6.10 is the estimation of sample resistance for samples welded in an unknown welding machine.

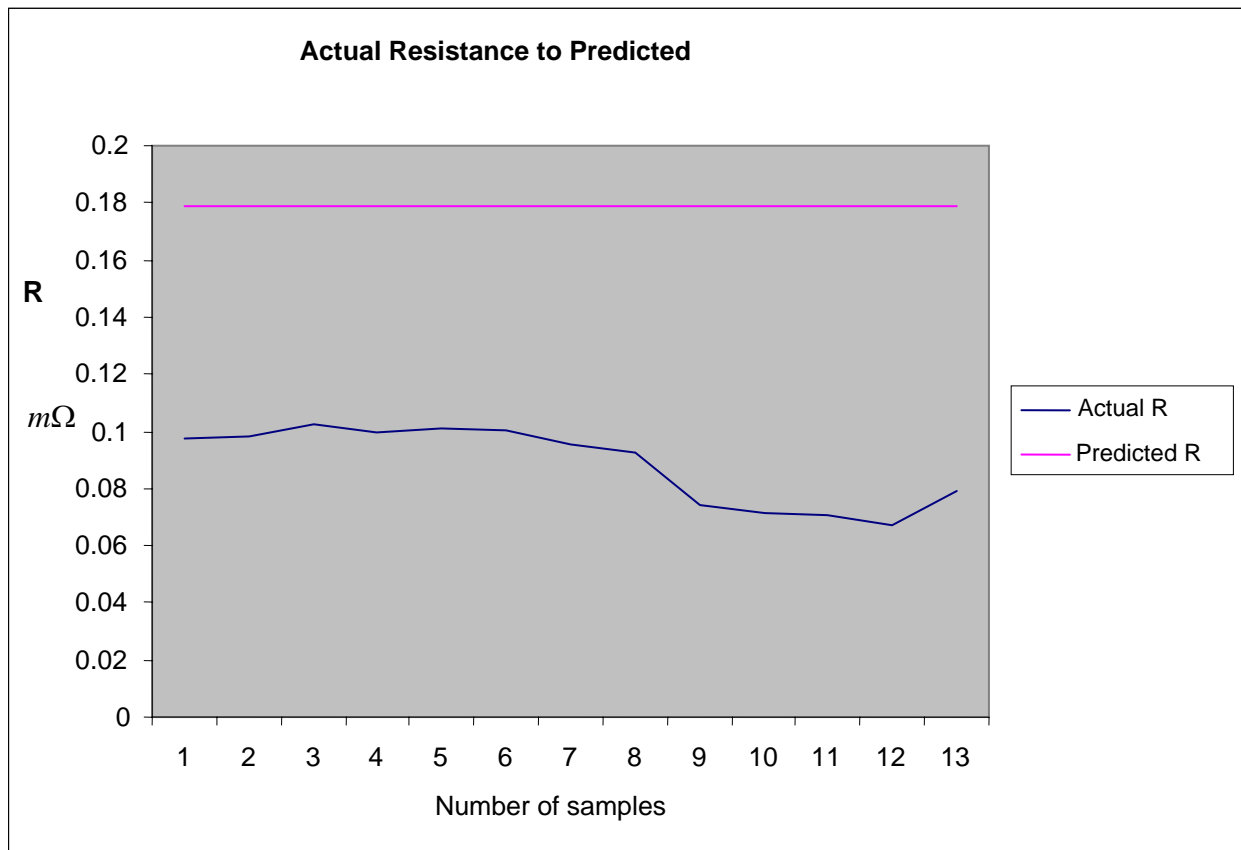


Figure 6.10: Predicted Resistance to actual in Dalex Machine

The Figure shows the actual resistance compared to the predicted. The predicted is not following the actual. Similar estimations were made without identifying (unknown) the welding machines. The percentage difference (error) of the predicted to the actual ranged between 16% to 149%. The large prediction error as is shown in figure 6.10 may be because the model can only track linear changes and is not able to follow nonlinear dynamic and complex changes in new situation. Statistical analysis will be carried out to determine the relationships between the parameters. If nonlinear relationships are confirmed to exist between the parameters and the sample resistance then neural network techniques will be the most appropriate method to use in modelling the process.

The cause of this error was investigated by carrying out correlation analysis and multiple regression analyses between the parameters and sample resistance R. Presented in Table 6.2 is the correlation of the parameters to one another.

Table 6.2: Correlations Matrix

	Current (kA)	Weld Diameter (mm)	K	M	Ro	R
Current (kA)	1.000					
Weld Diameter (mm)	0.951	1.000				
K	-0.943	-0.884	1.000			
M	0.959	0.921	-0.956	1.000		
Ro ($m\Omega$)	-0.648	-0.569	0.457	-0.479	1.000	
R ($m\Omega$)	-0.912	-0.830	0.979	-0.922	0.466	1.000

The table shows significant linear correlation between the parameters. Strong linear correlation exists between current and all the parameters and between weld diameter and all the parameters with slight reduction with Ro. The linear correlation coefficient between the parameters K, M and Ro are about 0.5 and are considered significant. The prediction error is therefore not due to lack of linear correlation between the parameters. Further investigation was done using multiple linear regression analysis to ascertain the relationship between the predicted variable R (sample resistance) to the other variables. Presented in Table 6.3 is the result of the multiple regression for sample resistance (R).

Table 6.3: Multiple Correlations Matrix

Results of multiple regression for R ($m\Omega$)						
Summary measures						
Multiple R	0.9840					
R-Square	0.9683					
Adj R-Square	0.9645					
StErr. of Est.	0.0012					
ANOVA Table						
Source	df	SS	MS	F	p-value	
Explained	5	0.0020	0.0004	256.6746	0.0000	
Unexplained	42	0.0001	0.0000			
Regression						

coefficients							
		Coefficient	Std Err	t-value	p-value	Lower limit	Upper limit
	Constant	0.0146	0.0215	0.6797	0.5004	-0.0287	0.0579
	Current (kA)	0.0001	0.0019	0.0759	0.9399	-0.0038	0.0041
	Weld Diameter (mm)	0.0014	0.0007	2.1295	0.0391	0.0001	0.0027
	K	0.1279	0.0124	10.2839	0.0000	0.1028	0.1531
	M	0.0146	0.1090	0.1336	0.8944	-0.2055	0.2346
	Ro	0.0996	0.0757	1.3159	0.1954	-0.0531	0.2523

The R-Square, adjusted R-Square, high F value and low standard error shows good estimation accuracy. The p-value gives indication of clear linear relationship existing only between the sample resistance (R) and weld diameter, K and Ro. While the relationship between R and current and M parameter are not seen as linear as indicated by the high p value. The relationships were combinations of linear and non linear relationships among the parameters. The level of estimation error in the result obtained by using the graph suggests that the technique is not appropriate for an accurate result. The values were further linearised using logarithm function ⁽⁸⁹⁾ but the improvement in estimation accuracy was little.

It can be concluded that the sample resistance of a desired weld diameter in an unknown welding machines can be predicted using the graphs. This is however with high level of prediction inaccuracy mostly because of the nonlinear and complex relationship that exists between the sample resistance R and some of the parameters. To improve the prediction accuracy neural network technique will be employed to learn the pattern in the data and to be able to make accurate prediction ⁽⁶⁾.

6.4 Improving the Empirical Model using Artificial Neural Networks

The generated parameters from the empirical model were passed through neural network learning in other to improve the prediction accuracy. Such that for any desired weld diameter in any of the welding machines the sample resistance will be determined (known), without the need to conduct the welding experiment or going through the

iteration process of determining the parameters K , M and R_o . The inputs are weld diameter and parameters K , M and R_o . Sample resistance was the output. The result was validated (tested) and further cross validated on dataset not used for the training and then used to make prediction on dataset not seen before.

Four neural network types which are generalized feed forward, multilayer perceptron (MLP), recurrent network and radial basis function (RBF) were tested to find the best predictor to be used for improving the empirical model.

6.4.1 Training using Generalized feed forward neural network

Generalized feedforward networks are a generalization of the MLP such that connections can jump over one or more layers⁽³³⁾. The inputs for this network as mentioned earlier are desired weld diameter and applied electrode force, while linearised sample resistance from the empirical model is the output.

The dataset were randomised to achieve even spread. Then the columns were tagged as inputs and outputs. 70% of the data set (exemplars) was set apart (tagged) for training, 15% for training and another 15% for cross validation. 20 exemplars were kept as production data for production testing.

The generalized feed forward network design was made up of 2 inputs processing elements, 1 output processing element, 502 exemplars, 3 hidden layers, with first hidden layer made up of 16 processing elements, TanhAxon transfer function, with momentum learning rule. The second hidden layer was made up 8 processing elements, TanhAxon transfer function and momentum learning rule. The third hidden layer was made up of 5 processing elements, TanhAxon transfer function and momentum learning rule also. The outer layer consists of one processing element, BiasAxon transfer function and conjugated gradient learning rule. 3000 epochs were specified for the training iterations.

The generated architecture design showing input and out put files with the hidden layers and transfer functions is presented in Figure 6.11.

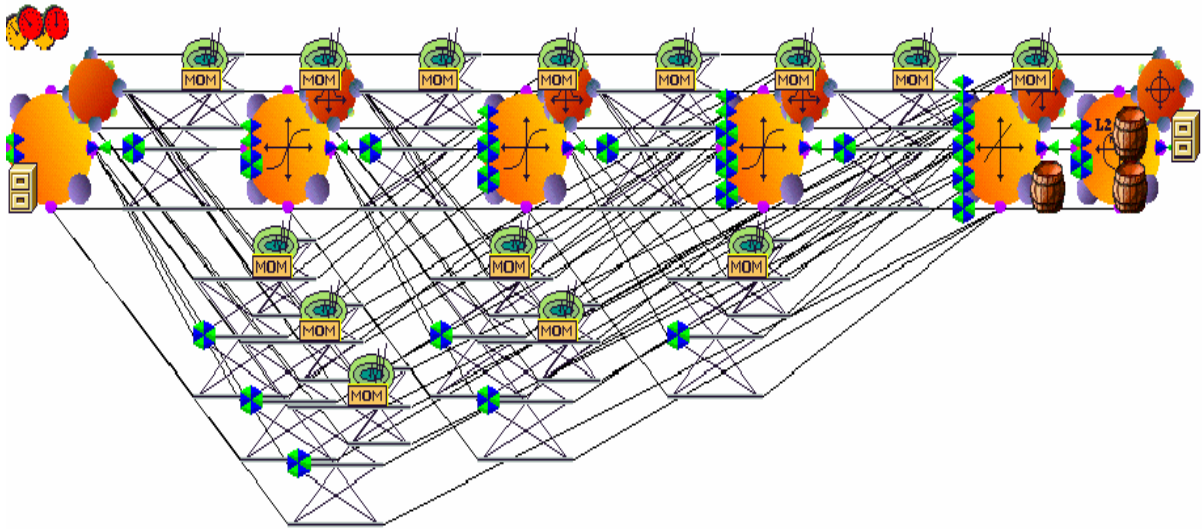


Figure 6.11: Generated generalized feedforward network architecture design ⁽¹⁰⁶⁾

The results of the training and cross validation are presented in Figure 6.12.

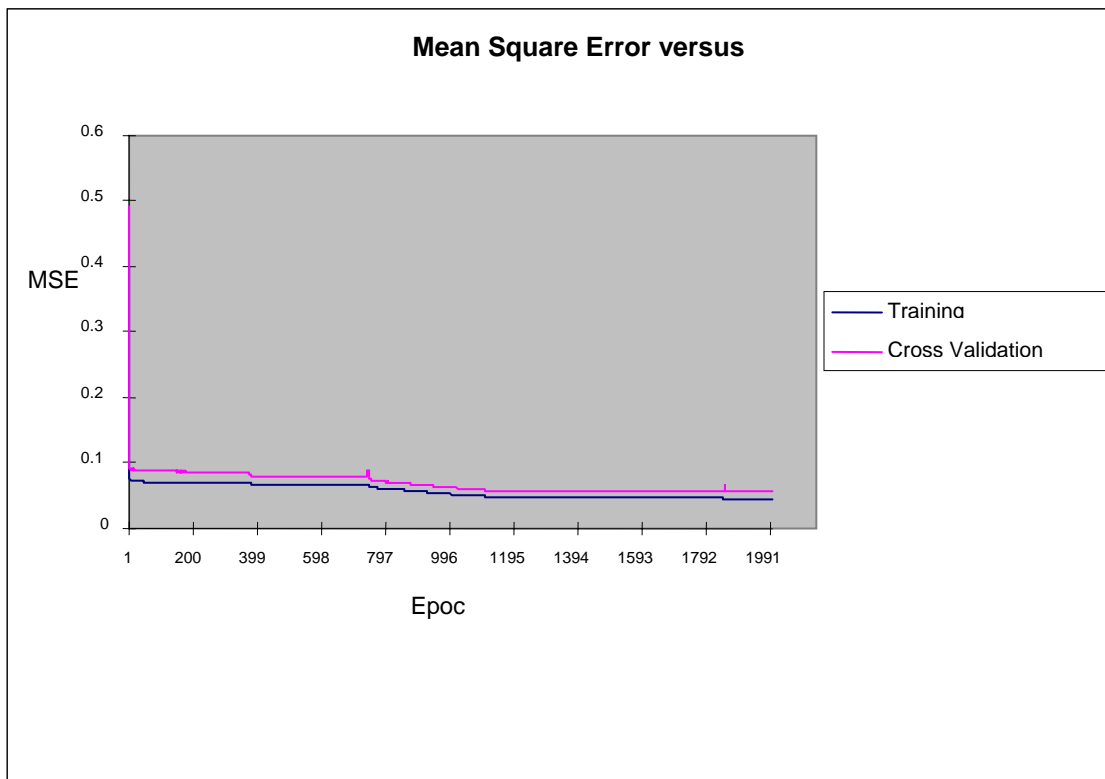


Figure 6.12: Training performance of the generalized feedforward network

The result of the training performance shows a good performance and a small error of about 0.05 at training epochs of 2000. The training was therefore stopped at 2000 epochs. The mean square error MSE curve showed a downward slope (weight decay) indicative of good performance. The network was tested to validate the consistency of the performance.

The testing error is measured by the linear correlation coefficient (r), mean absolute error (MAE), normalised mean squared error (NMSE) and mean squared error (MSE). These statistical parameters give an acceptable measure of the level of control and performance quality of the network ⁽⁹³⁾. How closely the predicted resistance lines are following the actual resistance was determined as is shown in Figure 6.13.

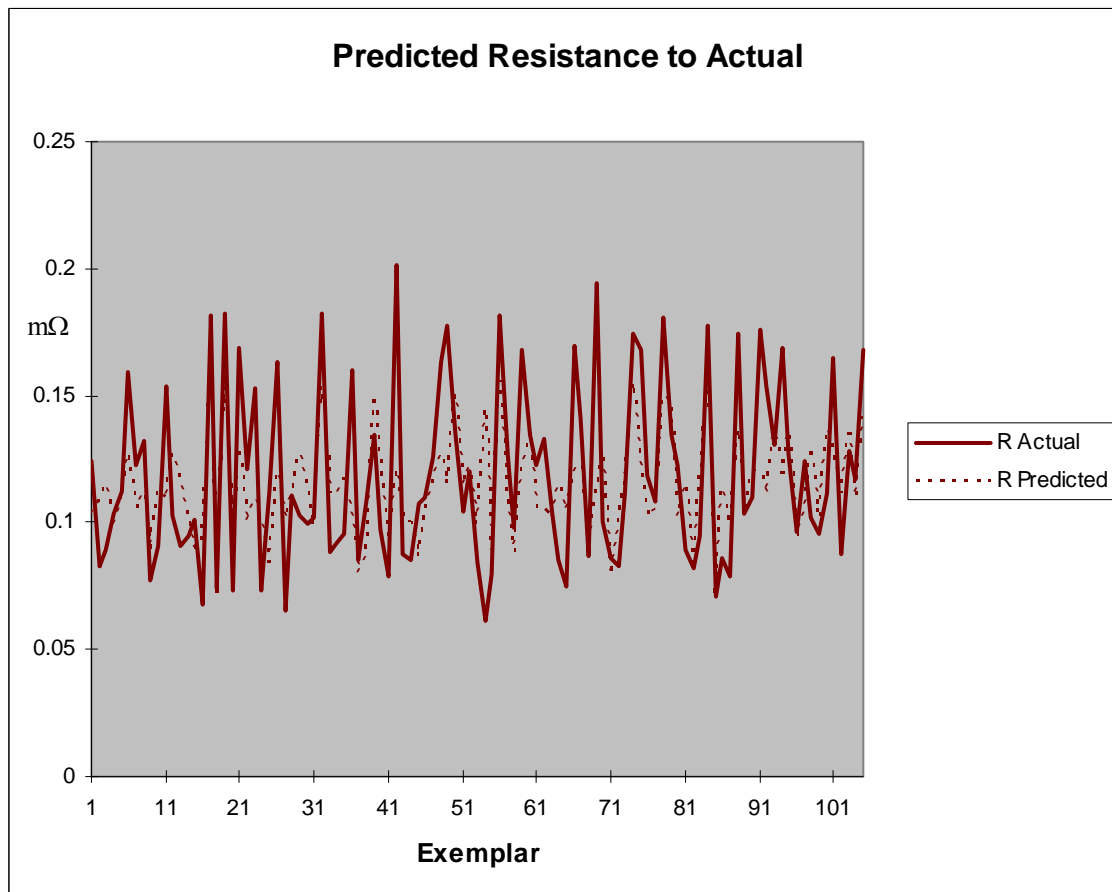


Figure 6.13: Testing performance of the generalized feedforward network.

The result of the testing performance gave a mean sum of squares of 0.001, and mean absolute error (MAE) of 0.03. This indicates a good performance. The normalised mean squared error (NMSE) was about 0.83 and the linear correlation coefficient was 0.52. A linear correlation coefficient of 0.52 shows that the set of point are not close to a straight line, which indicates a poor correlation. The graph in Figures 6.13 shows that estimated resistance is not closely following the actual resistance value. The performance of the network will be further validated by presenting data not seen before by the network to see how well it can generalize. Table 6.4 shows the predicted resistance (R) to the estimated resistance, and the estimation accuracy using the generalized feedforward neural network type.

Table 6.4: Predicted Resistance to Actual Resistance using generalized feedforward Neural Network type.

Machine Type	Applied Force (kN)	Weld diameter (mm)	R predicted mΩ	R actual mΩ	Difference	% Difference
PMS	3	3.7	0.1186	0.1079	0.0107	9.9222
C-Gun	3	4.4	0.117	0.1662	-0.049	-29.591
Dalex-35	3	4	0.1191	0.089	0.03	33.741
Dalex-25	2.46	5.7	0.0986	0.0716	0.0271	37.799
Dalex-35	3	4	0.1191	0.1017	0.0174	17.116
PMS	2.2	5.3	0.0959	0.1154	-0.019	-16.88
Dalex-25	2.46	4	0.1123	0.0739	0.0384	51.949
Dalex-25	3	3.7	0.1186	0.1015	0.0171	16.892
C-Gun	2.2	4.4	0.1063	0.1178	-0.012	-9.8047
Dalex-25	2.46	3.6	0.1115	0.084	0.0275	32.693
Dalex-25	2.46	5.5	0.0991	0.0714	0.0277	38.754
C-Gun	2.2	3.5	0.1087	0.1053	0.0035	3.3057
Dalex-25	2.46	3.8	0.1124	0.0828	0.0295	35.67
Dalex-35	3	6.3	0.1079	0.1378	-0.03	-21.708
Dalex-25	2.16	5.4	0.1001	0.0578	0.0423	73.055
C-Gun	3	6.5	0.1103	0.1408	-0.031	-21.665
Dalex-25	2.46	3.6	0.1115	0.0889	0.0226	25.467
PMS	2.6	3.8	0.1167	0.1262	-0.009	-7.5071
Dalex-25	1.76	4	0.1034	0.0966	0.0068	7.0807

Table 6.4 shows marked differences between the predicted resistances to the actual, with prediction error of about 3% to 73%. The prediction output of this network using real

data not used for training the network is presented in Figure 6.14. This is to further evaluate how well the network is able to generalize.

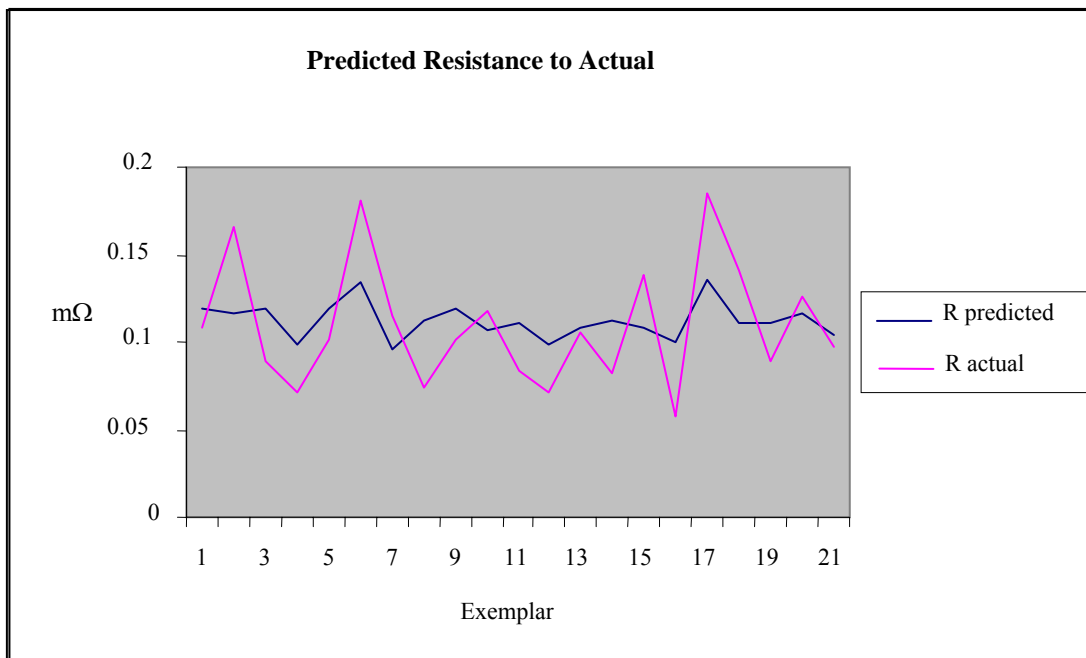


Figure 6.14: Validation performance of the generalized feedforward network.

The graph showed that the generalisation is very poor. The network was not able to predict accurate output for data that it has not seen before. Though a large error of 3% to 73%, it is an improvement from the earlier estimation error of about 16% to 149%. To achieve reliable and usable process model this error is considered high and unacceptable. Other neural network types will be tested.

6.4.2 Training using Multilayer Perceptron neural network type

Multilayer perceptrons (MLP) are layered feedforward networks architecture which is typically trained with static backpropagation⁽³³⁾. In this network architecture there are 2 input processing elements (desired weld diameter and applied electrode force), 1 output processing elements (linearised sample resistance), 487 exemplars and 1 hidden layer.

The hidden layer has 16 processing elements, TanhAxon transfer function with momentum learning rule. The output layer uses BiasAxon transfer function with conjugate gradient learning rule. The hidden layer and the process elements were determined by trial and error and by comparing the error output. The generated network architecture is shown in Figure 6.15.

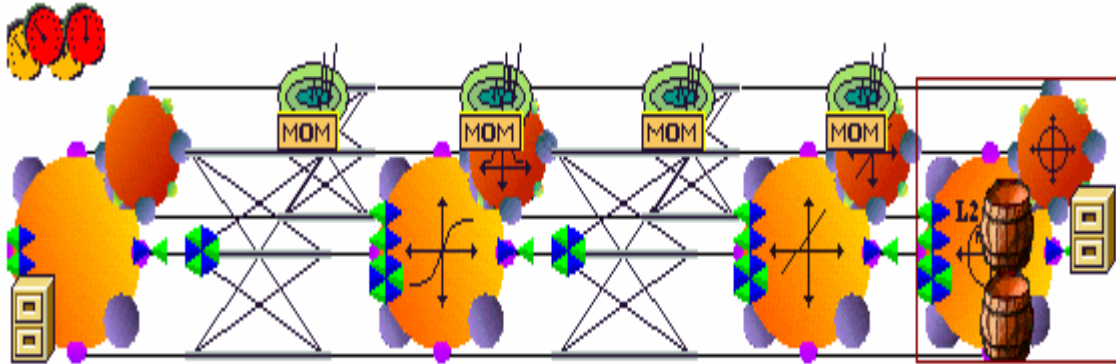


Figure 6.15: Generated multilayer perceptrons (MLP) network architecture design ⁽¹⁰⁶⁾

The levels of errors for the training and cross validation are shown in Figures 6.16.

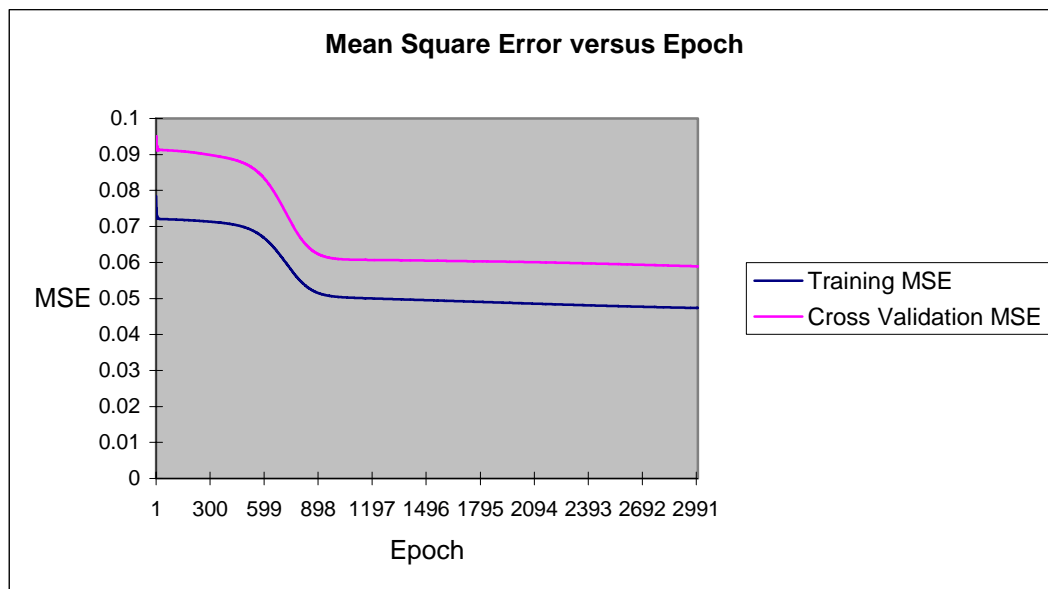


Figure 6.16: Training performance of the multilayer perceptrons (MLP) network

Similar to the generalised feedforward neural network type, the result of the training performance of the multilayer neural network showed good performance with an error output of about 0.05 at training epochs of 3000 and cross validation error of 0.06 at same epoch of 3000. The downward slope (weight decay) however did not indicate a good training and cross validation performance, as the slope did not show a significant drop. The overall network performance was confirmed by the testing performance result. The testing performance of the multilayer perceptron neural network used is presented in Figure 6.17.

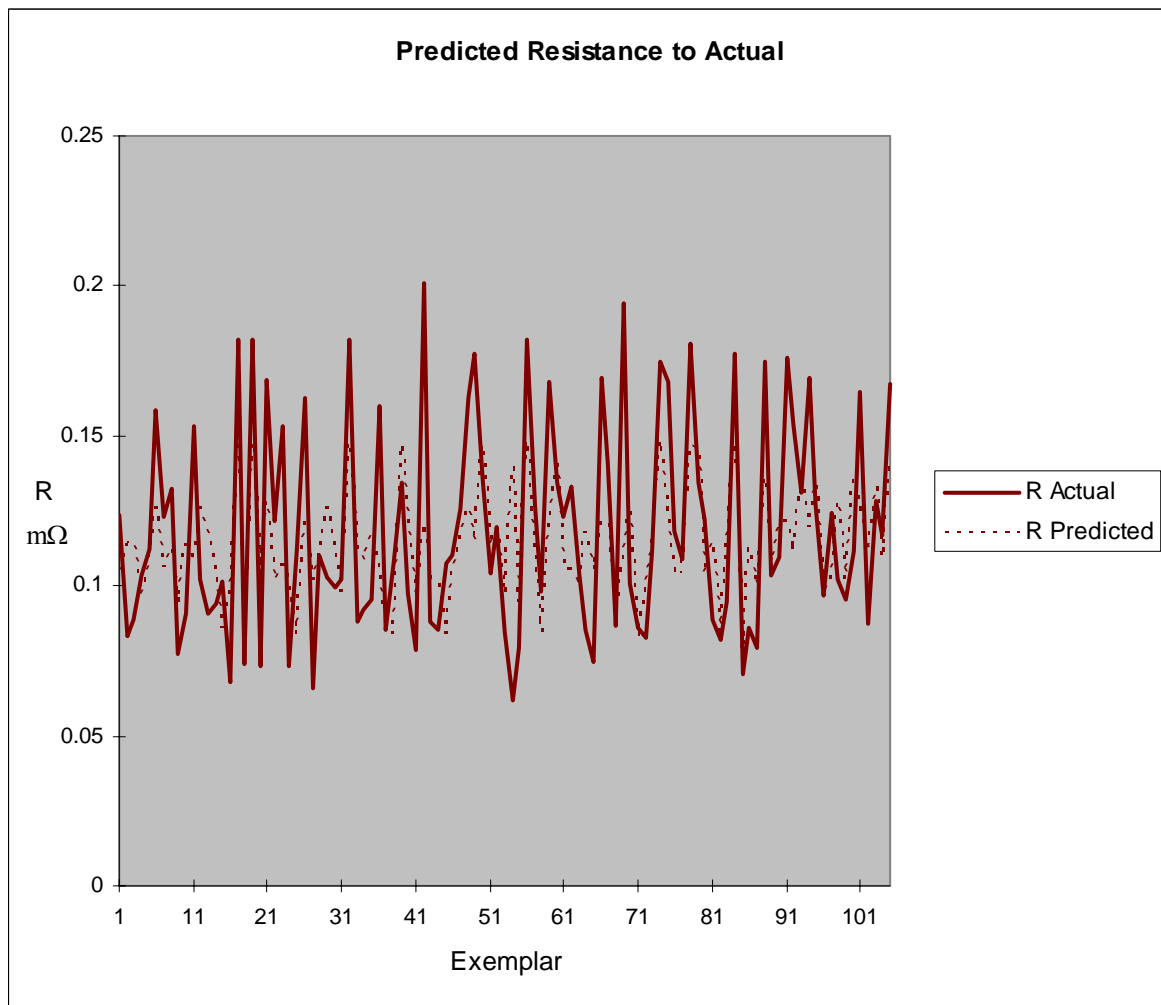


Figure 6.17: Testing performance of the multilayer perceptrons (MLP) network. The test performance result gave a mean sum of squares of 0.008, mean absolute error (MAE) of 0.02 indicating good performance. Normalised mean squared error (NMSE) of

0.67 and linear correlation coefficient of 0.6. In the graph of Figure 6.17, the estimated resistance is not closely following the actual resistance value, it is however performing better than the feedforward neural network type. The performance of the network will be validated using data set not seen before by the multilayer perceptron neural network. Table 6.5 shows the predicted resistance (R) to the estimated resistance, and the estimation accuracy using the multilayer perceptron neural network type.

Table 6.5: Predicted Resistance to Actual Resistance using multilayer perceptron neural network type.

Machine Type	Applied Force (kN)	Weld diameter (mm)	R predicted (mΩ)	R actual (mΩ)	Difference	% Difference
PMS	3	3.7	0.1134	0.1079	0.0055	5.1089
C-Gun	3	4.4	0.1212	0.1662	-0.045	-27.09
Dalex-35	3	4	0.1175	0.089	0.0285	32.023
Dalex-25	2.46	5.7	0.0766	0.0716	0.005	7.0184
Dalex-35	3	4	0.1175	0.1017	0.0159	15.612
PMS	2.2	5.3	0.0837	0.1154	-0.0317	-27.446
Dalex-25	2.46	4	0.0951	0.0739	0.0212	28.619
Dalex-25	3	3.7	0.1134	0.1015	0.0119	11.773
C-Gun	2.2	4.4	0.1042	0.1178	-0.0136	-11.527
Dalex-25	2.46	3.6	0.0877	0.084	0.0037	4.3658
Dalex-25	2.46	5.5	0.0758	0.0714	0.0044	6.1602
C-Gun	2.2	3.5	0.0998	0.1053	-0.0054	-5.1532
Dalex-25	2.46	3.8	0.0918	0.0828	0.009	10.833
Dalex-35	3	6.3	0.1077	0.1378	-0.0301	-21.858
Dalex-25	2.16	5.4	0.096	0.0578	0.0381	65.951
C-Gun	3	6.5	0.1129	0.1408	-0.0279	-19.828
Dalex-25	2.46	3.6	0.0877	0.0889	-0.0012	-1.3175
PMS	2.6	3.8	0.1229	0.1262	-0.0033	-2.6032
Dalex-25	1.76	4	0.0978	0.0966	0.0012	1.285

Table 6.5 shows a prediction error of 1% to 65% using real data not used for training the network. This generalization is presented in graph form in Figure 6.18. The graph showed that the generalisation is slightly improved from the generalized feedforward neural network type. It is still considered generally poor.

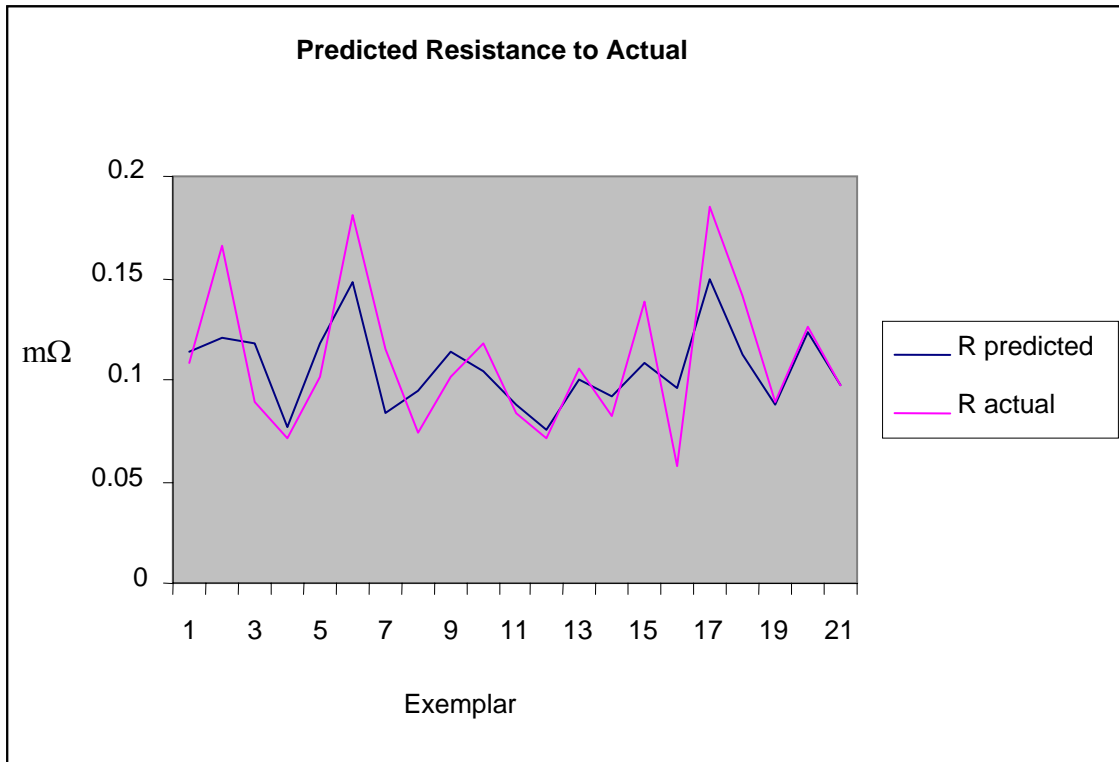


Figure 6.18: Validation performance of the multilayer perceptrons (MLP) network

Radial basis neural network type and Recurrent neural network were explored to see if there will be further improvement in the prediction of sample resistance.

6.4.3 Training with Radial Basis Function Neural Network

Radial basis function (RBF) networks are nonlinear hybrid networks typically containing a single hidden layer of processing elements (PEs). This layer uses gaussian transfer functions. The centres and widths of the gaussians are set by unsupervised learning rules, and supervised learning is applied to the output layer. These networks tend to learn much faster than MLPs⁽³³⁾.

The radial basis function network architecture design to be used here is made up of 2 input processing element with 1 output processing element, 487 exemplars, with no

hidden layer, 10 cluster centres, using consciencefull competitive learning with Euclidean metrics ⁽⁹²⁾. The output layer uses the conjugate gradient learning rule and Bias Axon transfer function. 100 epochs of iteration is done for the unsupervised learning with a set rate of decay and 1000 epochs for the supervised learning. The generated network architecture design is shown in Figure 6.19.

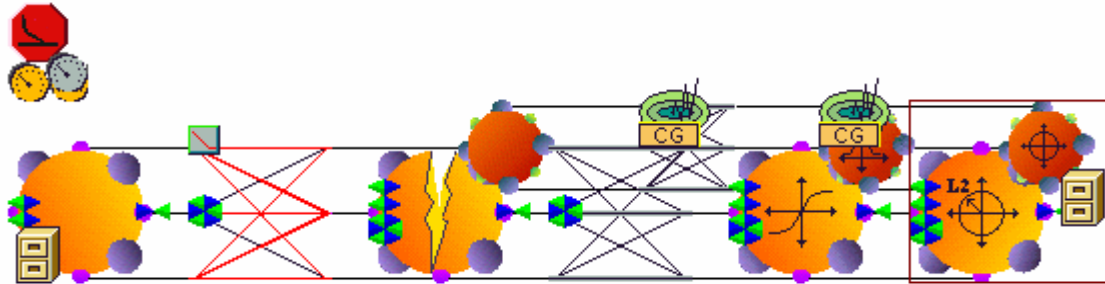


Figure 6.19: Generated Radial basis function (RBF) network architecture design ⁽¹⁰⁶⁾

This Radial basis function network architecture was trained and cross validated. The result of the training performance and cross validation is shown in Figure 6.20.

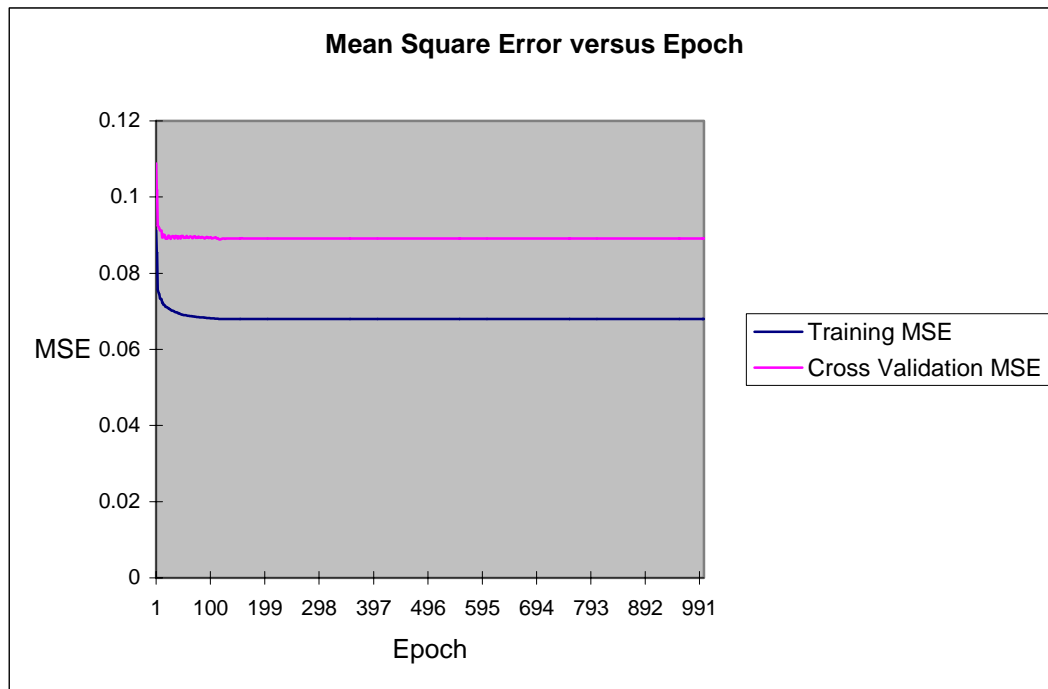


Figure 6.20: Training performance of the Radial basis function (RBF) network

The Radial basis function training performance result shows a mean square error output of about 0.07 at a training epoch of 180 and cross validation error of 0.09 at an epoch of 117. The downward slope (weight decay) did not indicate a good training and cross validation performance. The network will be tested to confirm overall performance of the network. The Radial basis function network was further validated by testing its performance. The result of the test performance is presented in Figure 6.21.

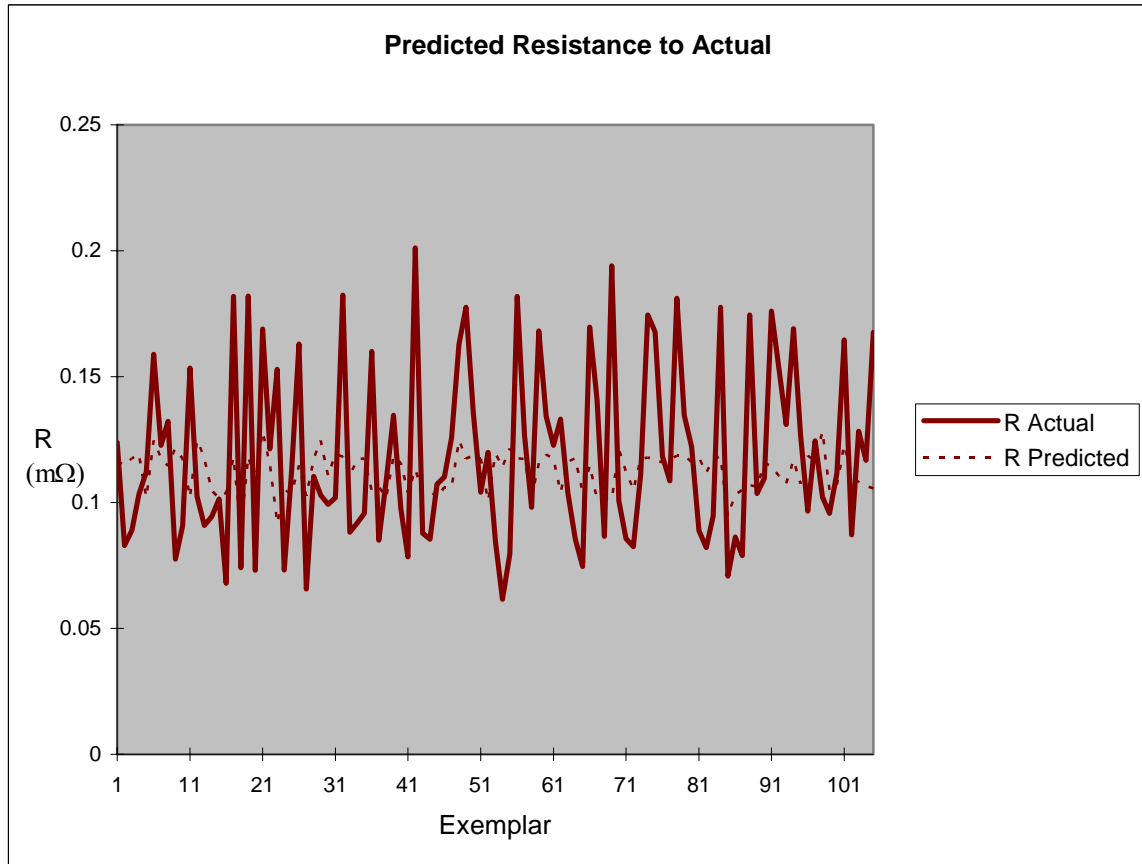


Figure 6.21: Testing performance of the Radial basis function network

The test performance result is poor. Though with a good mean sum of squares of 0.001, and mean absolute error (MAE) of 0.02. The performance is not consistent as the normalised mean squared error (NMSE) was 0.98 and linear correlation coefficient was 0.24. The graph (Figure 6.21) shows the estimated resistance is not closely following the actual resistance value at all. The performance of the network validated using data set not

seen before by the Radial basis function neural network is presented in Table 6.6 and Figures 6.22 respectively.

Table 6.6: Predicted Resistance to Actual Resistance using Radial basis function neural network type.

Machine Type	Applied Force (kN)	Weld diameter (mm)	R predicted m Ω	R actual m Ω	Difference	% Difference
PMS	3	3.7	0.1174	0.1079	0.0095	8.8182
C-Gun	3	4.4	0.1156	0.1662	-0.0506	-30.429
Dalex-35	3	4	0.1175	0.089	0.0285	32.024
Dalex-25	2.46	5.7	0.0945	0.0716	0.023	32.088
Dalex-35	3	4	0.1175	0.1017	0.0159	15.612
PMS	2.2	5.3	0.1037	0.1154	-0.0117	-10.143
Dalex-25	2.46	4	0.1215	0.0739	0.0475	64.314
Dalex-25	3	3.7	0.1174	0.1015	0.016	15.718
C-Gun	2.2	4.4	0.116	0.1178	-0.0018	-1.4936
Dalex-25	2.46	3.6	0.1089	0.084	0.0249	29.596
Dalex-25	2.46	5.5	0.0899	0.0714	0.0184	25.808
C-Gun	2.2	3.5	0.1161	0.1053	0.0109	10.34
Dalex-25	2.46	3.8	0.1152	0.0828	0.0324	39.089
Dalex-35	3	6.3	0.1037	0.1378	-0.0341	-24.738
Dalex-25	2.16	5.4	0.1045	0.0578	0.0466	80.637
C-Gun	3	6.5	0.1029	0.1408	-0.0379	-26.924
Dalex-25	2.46	3.6	0.1089	0.0889	0.02	22.539
PMS	2.6	3.8	0.1171	0.1262	-0.0091	-7.2037
Dalex-25	1.76	4	0.1186	0.0966	0.022	22.776

The table shows the predicted resistance (R) to the estimated resistance, and the estimation accuracy. Table 6.6 shows a prediction error of about 1.5% to 80% using real data not used for training the network. The graph of Figure 6.22 shows that the generalisation is poor, as the predicted resistance is not following the actual resistance.

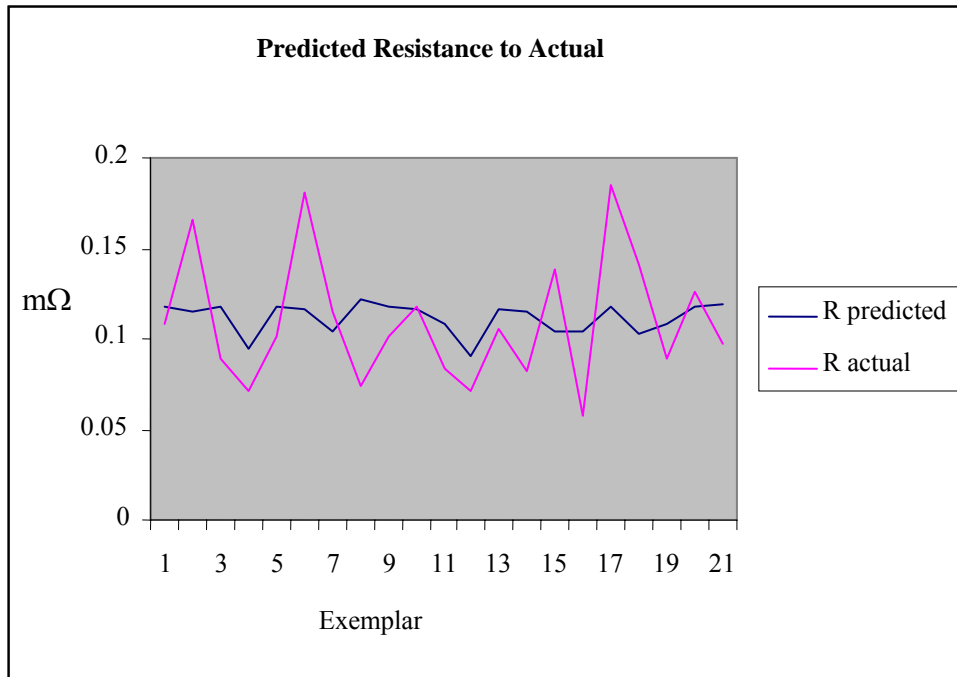


Figure 6.22: Validation performance of the Radial basis function (RBF) network

6.4.4 Training with Recurrent Network

Recurrent neural networks was used for training the data set and for predicting output. Recurrent neural networks can have an infinite memory depth ⁽³³⁾ and thus find relationships through time as well as through the instantaneous input space ⁽³³⁾. Most real-world data contains information in its time structure. Recurrent networks are the state of the art in nonlinear time series prediction, system identification, and temporal pattern classification ⁽³³⁾. Though the set of data presented to the network is not a typical time series prediction dataset, it is however a time dependent variable event.

The recurrent network architecture used here is made up of 2 input processing elements with 1 output processing element as in other earlier architectures used. There are 480 exemplars, with 1 hidden layer and an input layer Axon. There are 16 processing elements in the hidden layer and uses TanhAxon transfer function and momentum learning rule. The output layer consists of BiasAxion Transfer function and conjugate

gradient learning rule. 1000 epochs was used for the supervised learning. The network architecture design is shown in Figure 6.23.

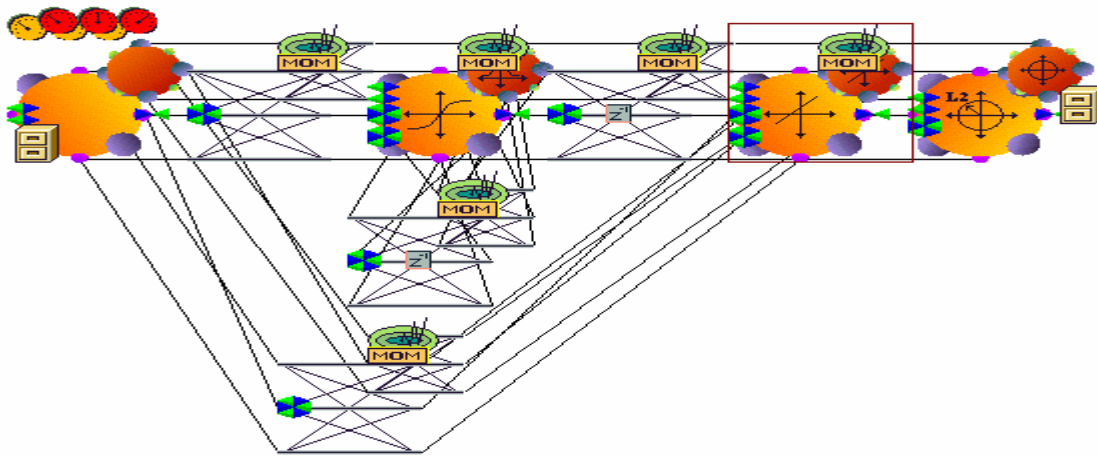


Figure 6.23: Generated Recurrent network architecture design ⁽¹⁰⁶⁾

This Recurrent network architecture was trained and cross validated. The result of the training performance and cross validation is shown in Figure 6.24.

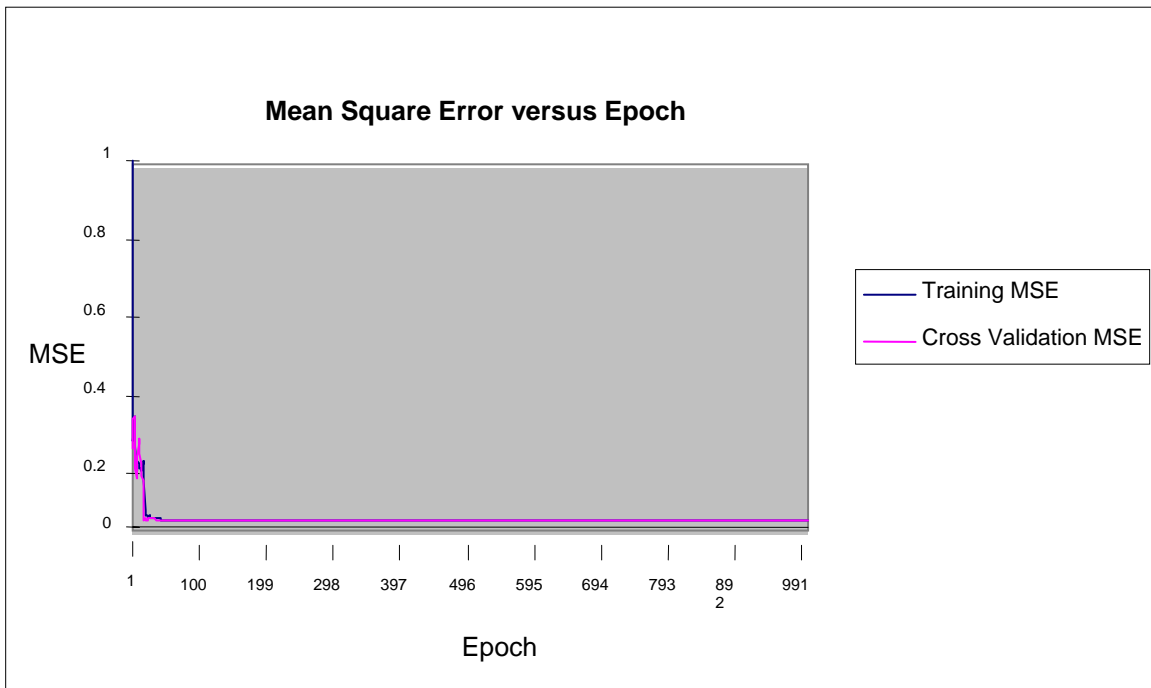


Figure 6.24: Training performance of the Recurrent neural network

The recurrent network training performance result gave a mean square error output of about 0.08 at a training epoch of 830 and cross validation error of 0.08 as well at an epoch of 910. The downward slope (weight decay) is substantial but not very good. The network was further tested to confirm overall performance. The testing performance of the Recurrent network is presented in Figure 6.25.

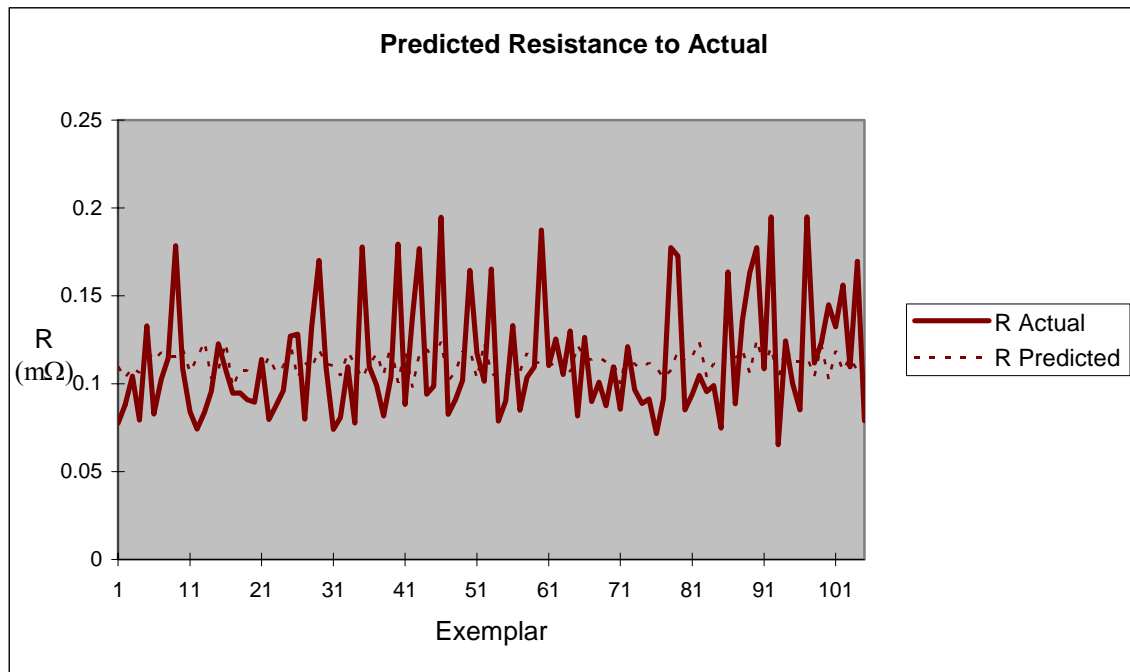


Figure 6.25: Testing performance of the Recurrent network architecture.

The test performance result is considered generally poor like with the radial basis function. It though showed a good mean sum of squares of 0.001, and mean absolute error (MAE) of 0.03. The performance is however not consistent, as the normalised mean squared error (NMSE) achieved was 0.96, with linear correlation coefficient of 0.2. The graph (Figure 6.25) shows the estimated resistance not closely following the actual resistance value. The performance of the network validated using data set not seen before by the Recurrent neural network is presented in Table 6.7 and Figures 6.26 respectively.

Table 6.7: Predicted Resistance to Actual Resistance using Recurrent

neural network type.

Machine Type	Applied Force (kN)	Weld diameter (mm)	R predicted mΩ	R actual mΩ	Difference	% Difference
PMS	3	3.7	0.118	0.108	0.01	9.238
C-Gun	3	4.4	0.106	0.166	-0.0603	-36.3
Dalex-35	3	4	0.11	0.089	0.0213	23.93
Dalex-25	2.46	5.7	0.101	0.072	0.0294	41.06
Dalex-35	3	4	0.116	0.102	0.0146	14.31
PMS	2.2	5.3	0.109	0.18	-0.0715	-39.7
Dalex-25	2.46	4	0.11	0.115	-0.0058	-5
Dalex-25	3	3.7	0.119	0.074	0.0449	60.68
C-Gun	2.2	4.4	0.115	0.101	0.0137	13.47
Dalex-25	2.46	3.6	0.108	0.118	-0.01	-8.52
Dalex-25	2.46	5.5	0.118	0.084	0.0335	39.88
C-Gun	2.2	3.5	0.104	0.071	0.0326	45.66
Dalex-25	2.46	3.8	0.121	0.105	0.016	15.2
Dalex-35	3	6.3	0.116	0.083	0.0329	39.71
Dalex-25	2.16	5.4	0.1	0.138	-0.0377	-27.4
C-Gun	3	6.5	0.115	0.058	0.0571	98.68
Dalex-25	2.46	3.6	0.118	0.185	-0.0665	-36
PMS	2.6	3.8	0.101	0.141	-0.0397	-28.2
Dalex-25	1.76	4	0.127	0.089	0.0379	42.7

The results in Table 6.7 shows a prediction error of about 5% to 98% using real data set not used for training the network. The graph of Figure 6.26 confirms this high prediction inaccuracy. It is seen in the graph (Figure 6.26) that the predicted resistance is not following the actual resistance accurately.

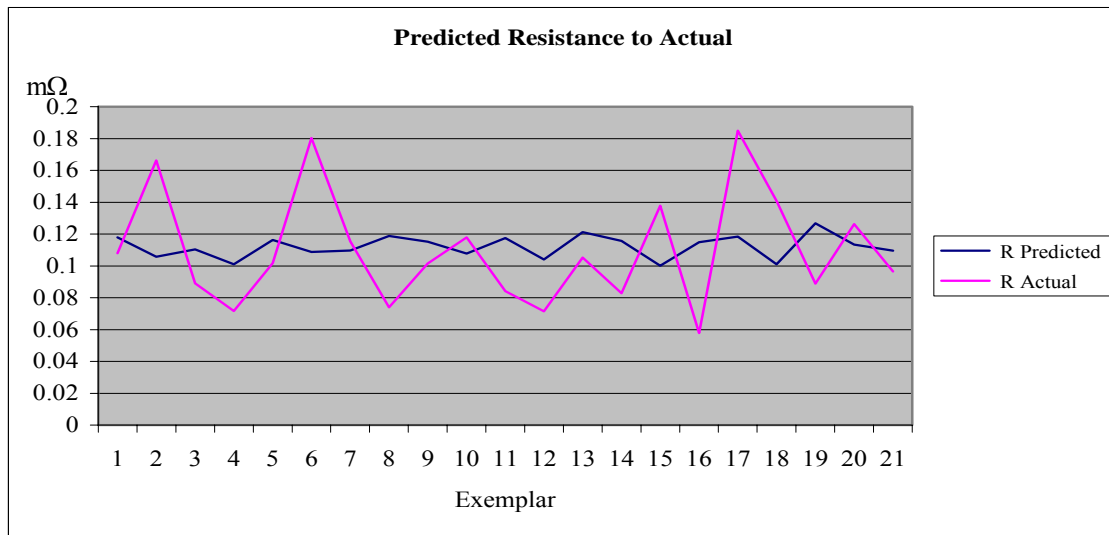


Figure 6.26: Validation performance of the Recurrent network

A summary of the performance of all four neural network architectures used are presented in Table 6.8. Of the four neural network architectures compared here the multilayer perceptron (MLP) is the best performer, though with high prediction inaccuracy. To further reduce this substantial error in the prediction of the sample resistance, the neural network architecture will be refined by increasing the number of input parameters ⁽³³⁾.

Table 6.8: Comparism of performance results of the four neural network types used.

Neural Network Type	Training MSE	Testing MSE	Linear Correlation Coefficient (r)	%Error Range Predicting Production Data
Generalized Feed Forward	0.045	0.001	0.52	3% - 73%
Multilayer Perceptron	0.047	0.008	0.60	1% - 65%
Redial basis Function	0.067	0.001	0.24	1.5% - 80%
Recurrent Network	0.079	0.001	0.52	5% - 98%

6.5 Improving Prediction Accuracy using Multilayer Perceptron Neural Network Architecture

To further reduce the prediction error, the number of parameters to be used as inputs to the neural network architecture was increased by including the parameters K, M and Ro from the empirical model to the earlier inputs which were desired weld diameter and applied electrode force. Linearised sample resistance is the output. The multilayer perceptron architecture considered a better performer of the four neural network architectures tested was selected.

The architecture design is a 5 input processing elements, 1 output processing elements, 488 exemplars and 1 hidden layer Multilayer perceptron architecture. The hidden layer has 8 processing elements with TanhAxon transfer function, using momentum learning rule. The output layer uses BiasAxon transfer function with conjugate gradient learning rule. The architecture is shown in Figure 6.27.

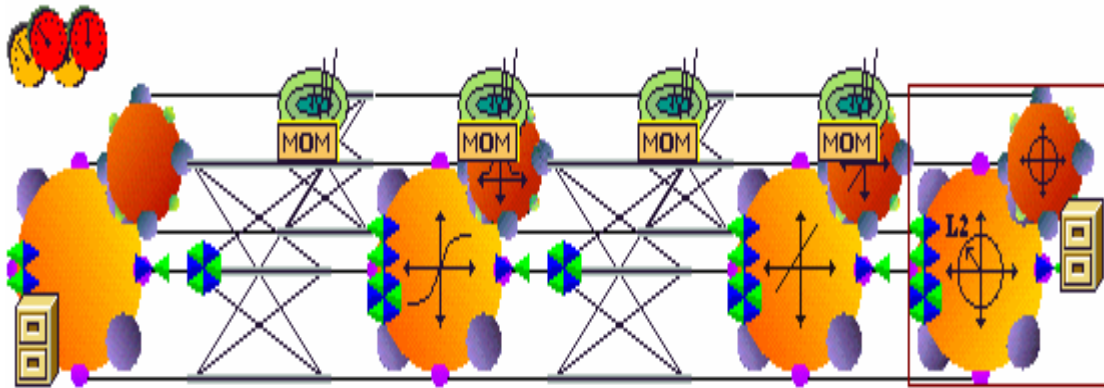


Figure 6.27: Generated Multilayer perceptron network with more input parameters ⁽¹⁰⁶⁾.

The network was trained and cross validated. The result of the training performance and cross validation is shown in Figure 6.28.

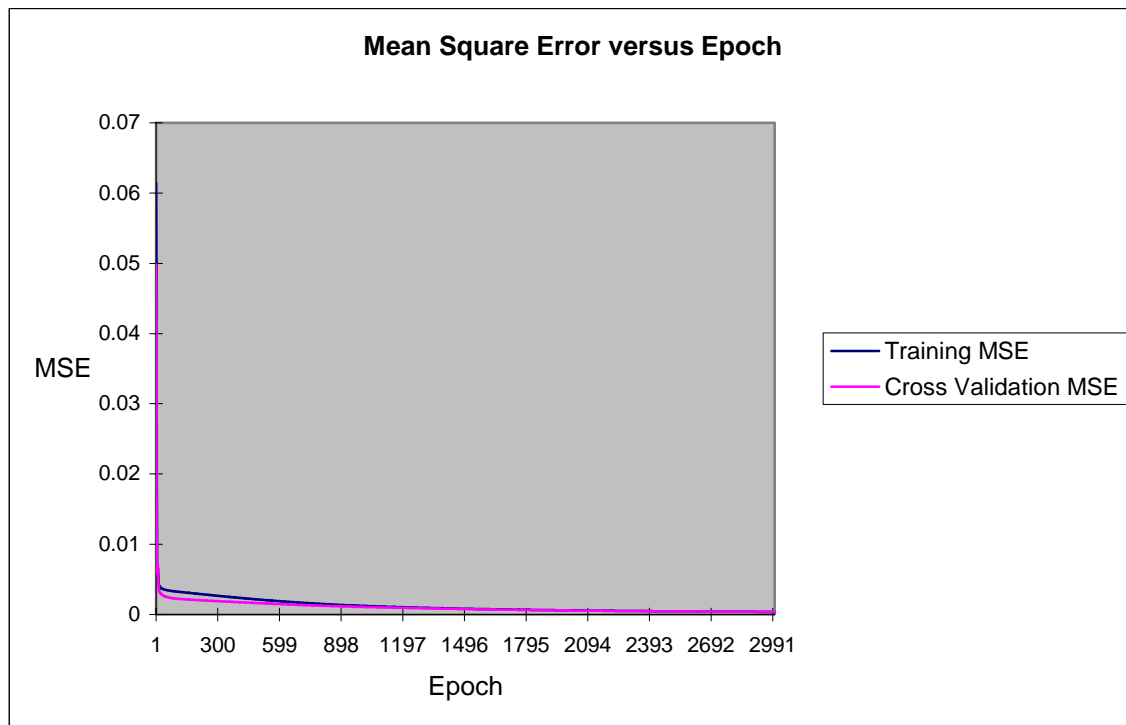


Figure 6.28: Training performance of the MLP network with more input parameters.

Training performance result of this multilayer perceptron architecture is better than the previous. The training mean square error output was 0.0004 at a training epoch of 3000 and 0.0004 for the cross validation error output at an epoch of 3000. The downward slope (weight decay) is very good. The network will be further tested to confirm overall performance. The testing performance of the multilayer perceptron with more input parameters is presented in Figure 6.29.

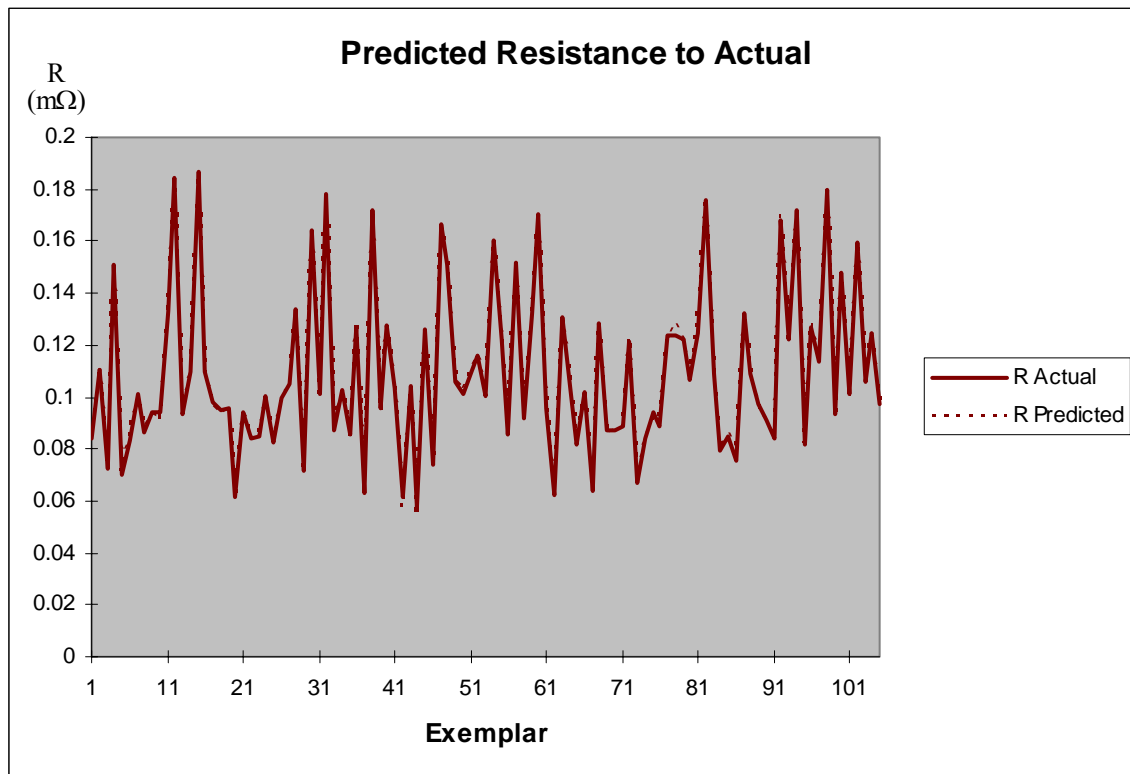


Figure 6.29: Testing performance of the MLP network with more input parameters.

The test performance result of this network is consistent with the training performance. The Mean sum of squares is $2.28614\text{E-}06$, mean absolute error (MAE) is 0.001173088. The normalised mean squared error (NMSE) is 0.00234, with linear correlation coefficient of 0.99884. The performance is outstanding. The graph (Figure 6.29) shows the estimated resistance is accurately following the actual resistance. The performance of the network was validated using data set not seen before by the multilayer perceptron. The result is presented in Table 6.9 and Figures 6.30 respectively.

Table 6.9: Predicted Resistance to Actual Resistance using Multilayer perceptron with more input parameters.

Machine Type	Force (kN)	Diameter (mm)	K	M	Ro	R predicted mΩ	R Actual mΩ	% Difference
PMS	3	5.9	0.46	0.0356	0.0841	0.0908	0.09076	0.04676
C-Gun	3	4.2	0.697	0.0148	0.0837	0.113799	0.11102	2.50259
Dalex-35	3	4.4	0.516	0.0314	0.0891	0.097824	0.09886	-1.0435
Dalex-25	3	4.4	0.61	0.0213	0.0847	0.107378	0.10787	-0.45268
Dalex-25	2.46	3.6	0.428	0.047	0.1268	0.088637	0.08736	1.45592
PMS	2.6	3.3	1.1	0.0384	0.2107	0.194962	0.19403	0.48232
Dalex-35	3	4	0.554	0.0266	0.0818	0.100916	0.10237	-1.41895
PMS	3	3.7	0.455	0.0332	0.0898	0.088333	0.08914	-0.90842
C-Gun	2.6	4	0.879	0.0345	0.1695	0.159946	0.15926	0.43179
PMS	3	3.9	0.464	0.0299	0.0981	0.088331	0.08964	-1.45683
Dalex-25	2.16	5.4	0.38	0.0646	0.1102	0.080149	0.08	0.18339
Dalex-25	1.76	5.1	0.39	0.0644	0.1475	0.083353	0.08199	1.65961
C-Gun	2.2	4.5	0.693	0.0197	0.0961	0.119565	0.11796	1.3594
Dalex-35	2.2	3.7	0.78	0.025	0.1002	0.110687	0.11458	-2.88982
Dalex-25	2.16	3.8	0.448	0.0438	0.1301	0.091104	0.09091	0.21214
C-Gun	3	5.6	0.436	0.0459	0.08	0.087492	0.08862	-1.27284
Dalex-25	2.2	5.6	0.55	0.0332	0.093	0.106392	0.10591	0.45528
PMS	2.6	6	0.402	0.0607	0.1182	0.085126	0.08402	1.31829
Dalex-25	1.76	5.3	0.388	0.0702	0.1323	0.083277	0.08194	1.63661
Dalex-25	2.16	4.5	0.398	0.0564	0.1203	0.083765	0.08306	0.85326

The network was validated using real data set not used for training the network. The result in Table 6.9 shows a good prediction with error of 0.1% to 2.9%. Similarly the plot of the actual predicted resistance to the predicted gave a very good match as is shown in Figure 6.30.

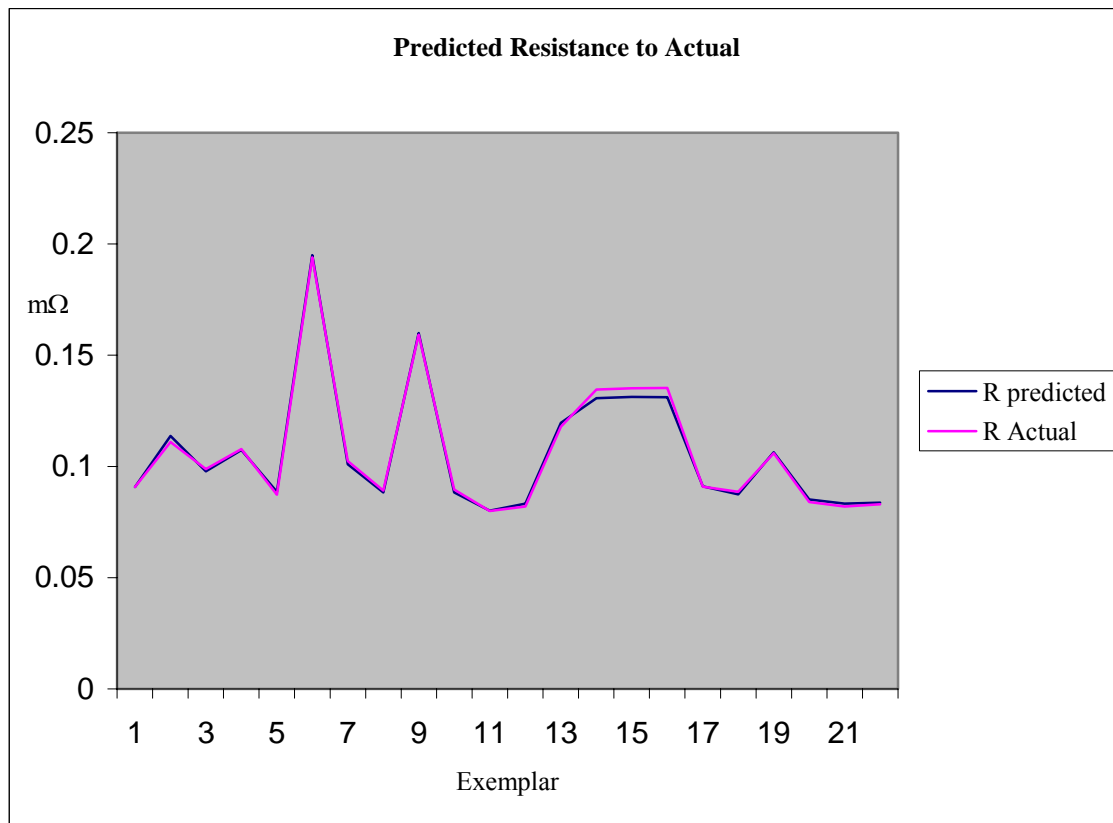


Figure 6.30: Validation performance of the Multilayer perceptron neural Network Using Production Dataset.

This neural network model for predicting sample resistance accurately tracked the actual sample resistance. The performance of the network was outstanding with a prediction accuracy of 97% to 99.9%. Sensitivity Analysis will be conducted carried out, to establish the contribution of each of these inputs to the output.

6.6 Sensitivity analysis of the Result

Sensitivity analysis of these parameters (weld diameter, applied electrode force, K, M and Ro parameters) was carried out to determine the influence of these parameters to the sample resistance. Sensitivity Analysis ⁽³⁴⁾

- First, train the network with all inputs
- Second, compute the relative importance of each input to the overall response -- called sensitivity

- In NeuroSolutions, this is done by fixing the weights, adding a dither to each input, and computing the difference in the result
 - Controller has a sensitivity button
 - Criterion has a sensitivity access point
- This is the sensitivity for the current solution. Should average over multiple training runs.

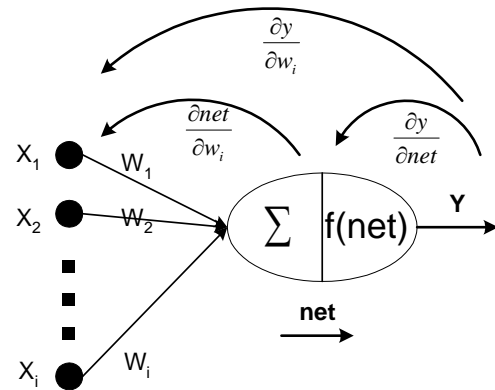
$$S_k = \frac{\sum_{p=1}^P \sum_{i=1}^o (y_{ip} - \bar{y}_{ip})^2}{\sigma_k^2}$$

An output $y(k)$ at an arbitrary time step k influences both the plant dynamics and the inverse dynamics ⁽³⁴⁾. The Delta Rule was used for computing the sensitivity of the output to each weight using the chain rule as follows ⁽³⁴⁾:

$$y = f(\text{net}) = f\left(\sum_i w_i x_i\right)$$

$$y = f(g(x)) \quad \Rightarrow \quad \frac{\partial y}{\partial x} = \frac{\partial y}{\partial g} \frac{\partial g}{\partial x}$$

$$\frac{\partial J}{\partial w_i} = \frac{\partial J}{\partial y} \frac{\partial y}{\partial \text{net}} \frac{\partial \text{net}}{\partial w_i} = -\varepsilon f'(\text{net})x_i$$



The performance index (J) for each possible value of the system parameters (weights) is computed. New update equation is same as old one with derivative of nonlinearity included, such that:

$$w_i(n+1) = w_i(n) + \eta \varepsilon_p(n) x_{ip}(n) f'(\text{net}_p(n))$$

This equation was used for computing the relative importance of each input to the overall response and determining the difference in the result using neurosolution software package⁽⁹²⁾. The result of the sensitivity analysis is presented in Figure 6.31.

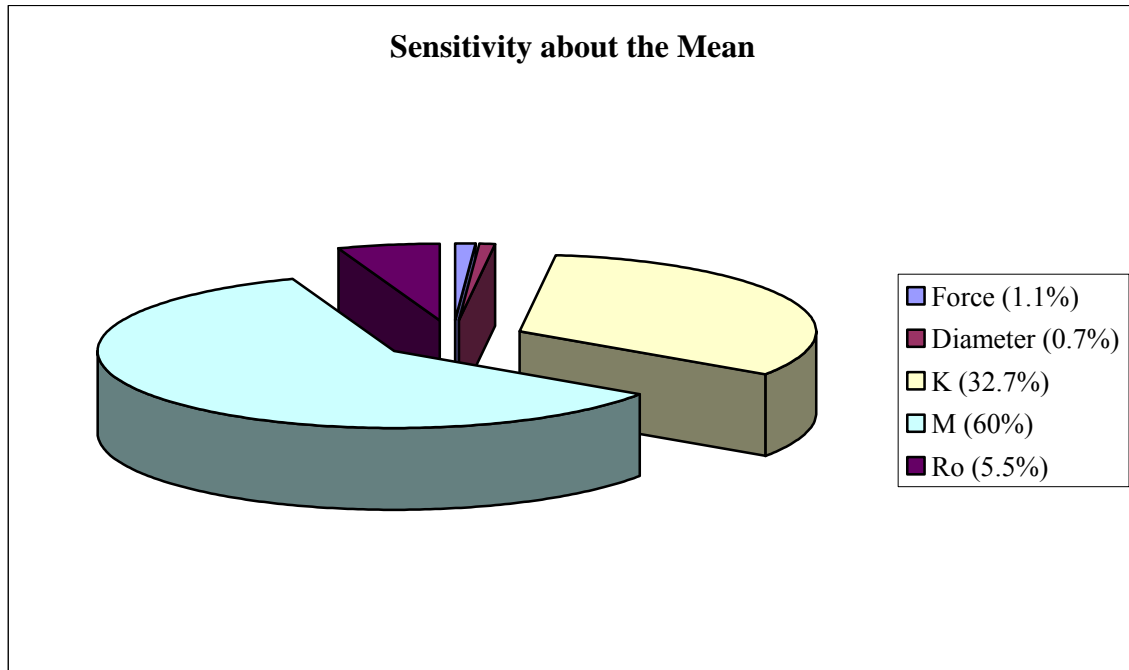


Figure 6.31: Sensitivity Analysis of the Input Parameters to the Output.

The result shows the contribution of each input to the overall resistance output. The parameters estimated from the empirical model are shown to have strong influence on the output, Figure 6.31. Applied electrode force contributed 1.1% to the output sample resistance. Desired weld diameter 0.7% and parameter Ro 5.5%. The parameters K and M estimated from the empirical model (equation 14) show large contributions of 32.7% and 60% respectively to the output (sample resistance). These two parameters are considered critical for estimating the sample resistance.

Having developed a model that can predict sample resistance, the intension of this research is to be able to use this predicted sample resistance in combination with applied electrode force to determine the effective weld current (RMS) that will be required for a desired weld diameter. The overall welding process will therefore be modelled using these mentioned process parameters.

6.7 Modelling the Overall Welding Process

The overall welding process was modelled in order to determine required effective weld current needed to achieve desired weld diameter in any of the resistance spot welding machines. First step in modelling the overall process model was to determine the capability of the neural network to predict weld quality (weld diameter) using the process parameters which are predicted sample resistance (predicted from dynamic resistance), applied electrode force and effective weld current. Based on the performance of the neural network, the same neural network model feedforward architecture was inverted to be able to predict the effective weld current needed to achieve desired weld quality (weld diameter) in any welding machine. Such that the output of the neural network model is effective weld current and the inputs are predicted sample resistance, applied electrode force and desired weld diameter. This inverted feedforward neural network model was used for predictive estimation and control of the resistance spot welding process. So that for any desired weld diameter it was possible to determine the required effective weld current to achieve the weld quality.

Result of sensitivity analysis carried out to establish the relationship between the inputs to the output parameters is also presented.

6.7.1 Neural Network Model for the Overall Welding Process

Four neural network types which are generalized feed forward, multilayer perceptron (MLP), radial basis function (RBF) and recurrent neural network architectures as previously used were trained and tested using input process parameters which are predicted sample resistance, applied electrode force and effective weld current to output weld diameter. The neural network architectures were validated using similar dataset not used for the training or testing to confirm prediction accuracy of the network. The best

performing neural network architecture using least error and prediction accuracy criteria was selected ⁽³³⁾.

Presented in Table 6.10 is a summary of the performance of each of the neural network types considered.

Table 6.10: Comparison of performance results of four neural network types.

Neural Network Type	Training MSE	Testing MSE	Linear Correlation Coefficient (r)	%Error Predicting Production Data
Generalized Feed Forward	0.0129	0.127	0.92	11.5
Multilayer Perceptron	0.0067	0.050	0.972	7.05
Radial basis Function	0.0146	0.1412	0.91	12
Recurrent Network	0.0154	0.1618	0.91	12

From the performance result shown in Table 6.10, the multilayer perceptron (MLP) outperformed the other four neural network types. It is therefore chosen as the neural network that will be used for developing the predictive controller model for the welding process. This multilayer perceptron neural network architecture consists of 3 inputs which are predicted sample resistance, applied electrode force and effective weld current, with output as weld diameter. There were 474 exemplars and 2 hidden layers. The first hidden layer has 11 processing elements, TanhAxon transfer function with momentum learning rule, the second hidden layer has 5 processing elements, TanhAxon transfer function with momentum learning rule. The output layer uses BiasAxon transfer function with conjugate gradient learning rule. The learning iteration was 3991 epochs, this was

because no lower epoch could give a good performance. The figure of the generated network architecture is shown in Figure 6.32.

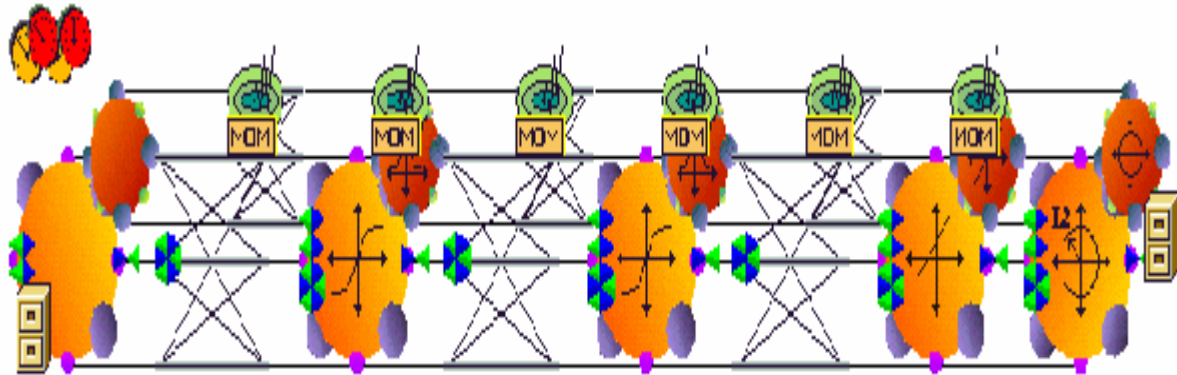


Figure 6.32: Generated multilayer perceptron (MLP) network architecture design ⁽¹⁰⁶⁾

Result of the network training performance and cross validation is shown in Figure 6.33.

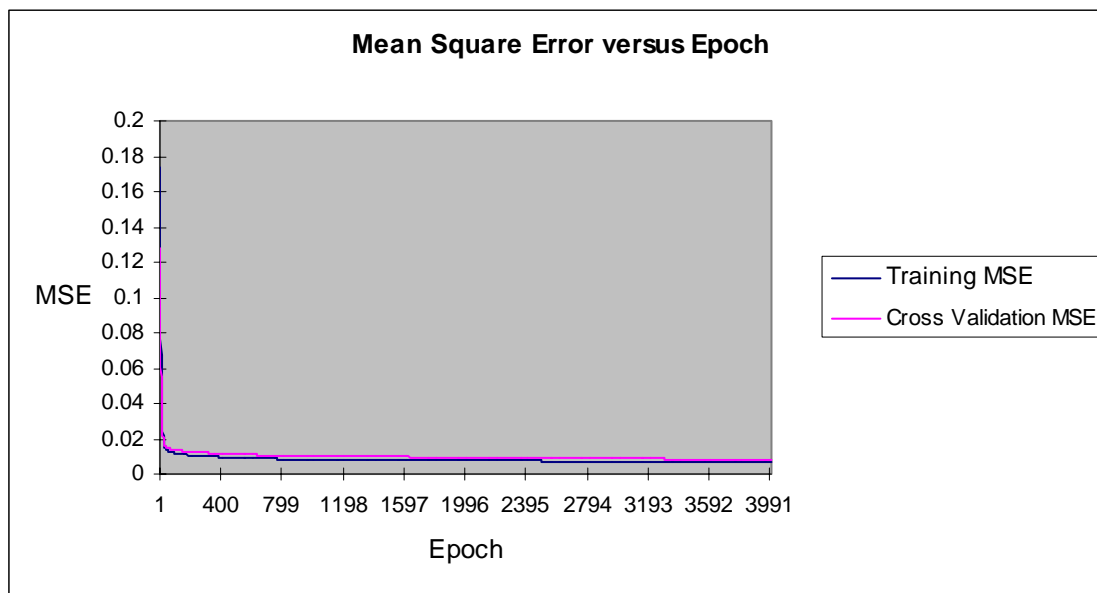


Figure 6.33: Training performance of the multilayer perceptron (MLP) network design. The training epoch for best result was at 3991 epochs with a mean square error output of 0.0067 for the training and 0.008 for the cross validation as is shown in Figure 6.33. Weight decay (downward slope) of the training and cross validation plot is substantial.

The network test performance result using data set not seen before by the network is presented in Figure 6.34.

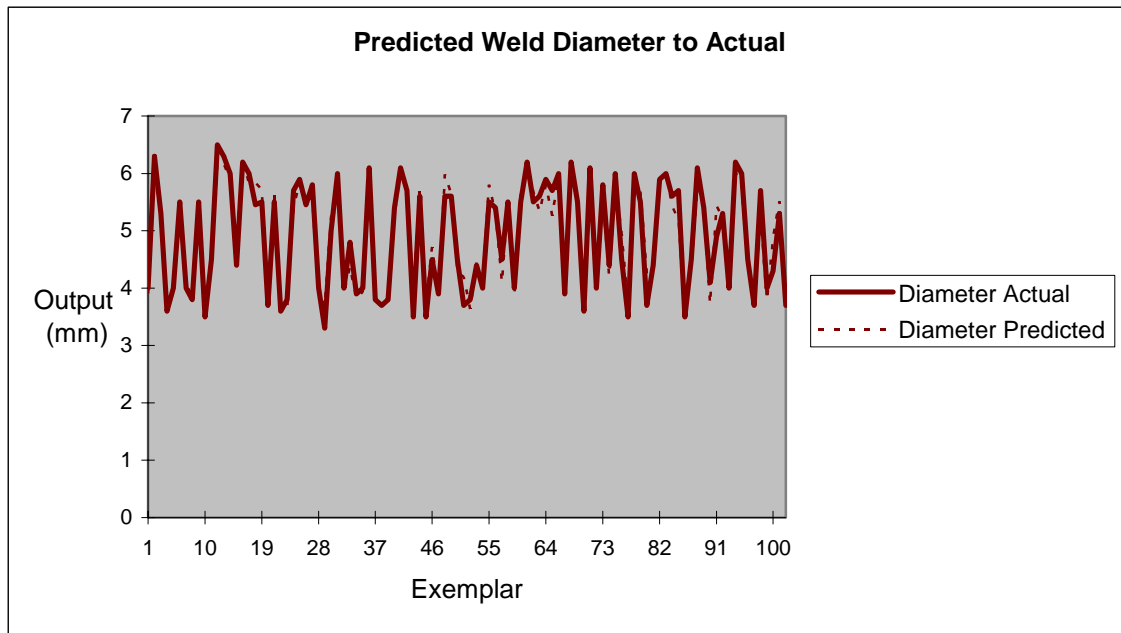


Figure 6.34: Testing performance of the multilayer perceptron network

The result of the testing shown in Figure 6.34 gives a mean sum of squares of 0.05, mean absolute error (MAE) of 0.18, normalised mean squared error (NMSE) of 0.06, and linear correlation coefficient is 0.97. This performance is outstanding and consistent with the training performance result. The graph in Figure 6.34 shows the estimated weld diameter is closely tracking the actual weld diameter. The validated performance result of the network using production dataset not known to the network is presented in Figures 6.35.

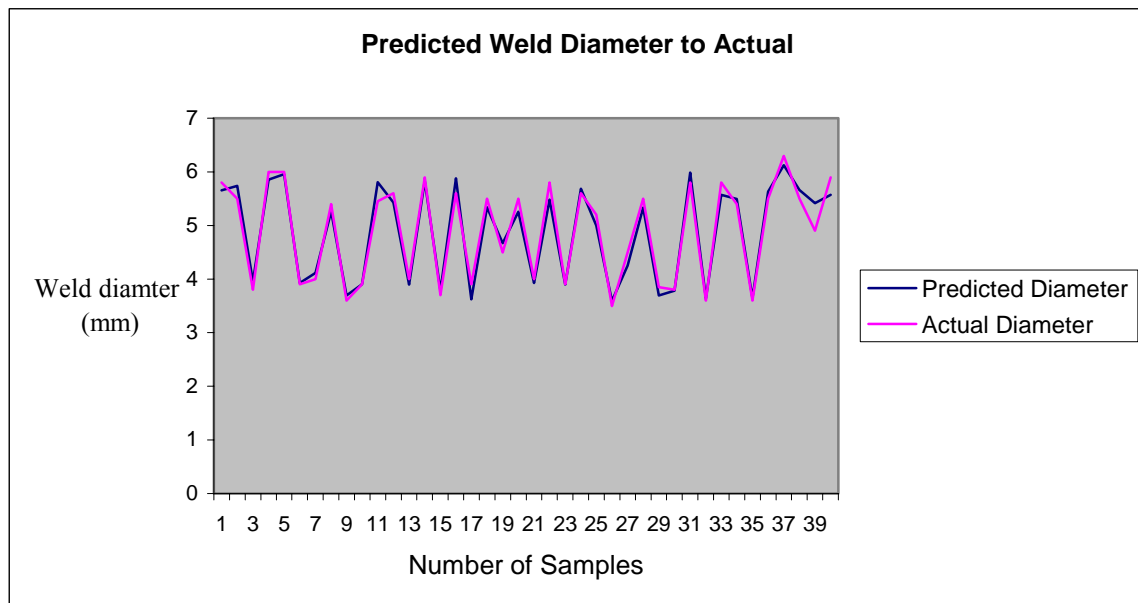


Figure 6.35: Validation performance of the multilayer perceptron network

The result confirms the good performance result of the training and testing of the network, with the predicted weld diameter seen to be tracking the actual weld diameter. The prediction error of the estimated weld diameter to the actual weld diameter is presented in Table 6.11.

Table 6.11: Predicted Weld Diameter to Actual Weld Diameter using multilayer Perceptron network

Machine Type	Force (kN)	Current (kA)	Resistance	Diameter Predicted (mm)	Diameter Actual (mm)	Difference	% Difference
Dalex-25	2.16	7.36	0.0716	5.656	5.8	-0.144	-2.483
C-Gun	2.2	7.57	0.0874	5.737	5.5	0.237	4.3089
Dalex-35	3	6.71	0.1813	3.9558	3.8	0.1558	4.1002
PMS	3	8.18	0.0967	5.8585	6	-0.141	-2.358
Dalex-25	2.6	8.3	0.0895	5.9558	6	-0.044	-0.737
PMS	2.6	6.74	0.1001	3.9277	3.9	0.0277	0.7105
Dalex-25	2.46	6.57	0.0796	4.1165	4	0.1165	2.9116
Dalex-25	2.46	6.91	0.0749	5.2619	5.4	-0.138	-2.557
C-Gun	3	6.39	0.108	3.6963	3.6	0.0963	2.6764
PMS	2.2	6.6	0.1797	3.9005	3.9	0.0005	0.0126
Dalex-25	3	8.12	0.1101	5.8079	5.45	0.3579	6.567
Dalex-25	2.16	6.89	0.0792	5.4285	5.6	-0.172	-3.063
C-Gun	2.6	6.79	0.1253	3.8974	4	-0.103	-2.564

Dalex-25	2.46	7.85	0.063	5.8313	5.9	-0.069	-1.165
Dalex-35	2.6	6.29	0.1949	3.7818	3.7	0.0818	2.2111
C-Gun	2.6	7.89	0.1119	5.8775	5.6	0.2775	4.9548
Dalex-25	2.2	5.75	0.1129	3.6247	3.9	-0.275	-7.06
PMS	3	7.73	0.0955	5.3371	5.5	-0.163	-2.962
Dalex-25	2.6	7.04	0.1021	4.6689	4.5	0.1689	3.7525
Dalex- 25	3	7.7	0.0956	5.2567	5.5	-0.243	-4.423
Dalex-25	3	7.02	0.1073	3.928	4	-0.072	-1.8
C-Gun	3	7.72	0.0832	5.4812	5.8	-0.319	-5.497
Dalex-35	3	6.95	0.1076	3.8958	3.9	-0.004	-0.108
PMS	2.2	7.41	0.1098	5.6851	5.6	0.0851	1.519
Dalex-25	1.76	6.17	0.0857	4.9997	5.2	-0.2	-3.852
PMS	2.6	5.92	0.1077	3.5941	3.5	0.0941	2.6889
Dalex-25	2.6	7.15	0.1636	4.254	4.5	-0.246	-5.466
Dalex-25	2.16	6.78	0.0811	5.3311	5.5	-0.169	-3.071
C-Gun	2.6	6.38	0.1255	3.6919	3.85	-0.158	-4.107
PMS	2.6	6.29	0.1948	3.7816	3.8	-0.018	-0.484
Dalex-25	2.2	7.77	0.1676	5.9859	5.8	0.1859	3.2054
Dalex-25	2.16	5.77	0.0908	3.6378	3.6	0.0378	1.0499
C-Gun	3	7.75	0.079	5.5707	5.8	-0.229	-3.953
Dalex-25	2.2	7.11	0.1139	5.494	5.4	0.094	1.74
Dalex-35	2.2	5.98	0.1238	3.6449	3.6	0.0449	1.2471
Dalex-25	2.46	7.24	0.0741	5.6291	5.5	0.1291	2.3467
Dalex-25	3	9.29	0.0865	6.1245	6.3	-0.175	-2.785
PMS	2.6	7.47	0.0983	5.6617	5.5	0.1617	2.9405
Dalex-25	3	6.39	0.108	3.6963	3.6	0.0963	2.6764
Dalex- 25	2.2	7.17	0.0938	5.5707	5.9	-0.329	-5.582

It is seen from the table that the prediction error is between 0.01% to 7.05%. That is an accuracy of about 99.99% to 93% in the prediction.

6.7.2 Relationship Analysis of the Process Parameters

Sensitivity analysis of the input parameters which are effective current, estimated sample resistance determined from the dynamic resistance and applied electrode force are tested to determine their contribution and relationship to the achieved weld diameter (quality measure). This is necessary to confirm the importance of the inputs to the output (solution). The neural network was first trained using the selected input parameters, followed by computing the relative importance of each input to the overall response. Presented in Figure 6.36 is a graph showing the sensitivity of the selected input parameters to the output. The result is however based on data correlation, which is a

linear function and does not necessarily show the true physical importance of the inputs to the outputs⁽³³⁾.

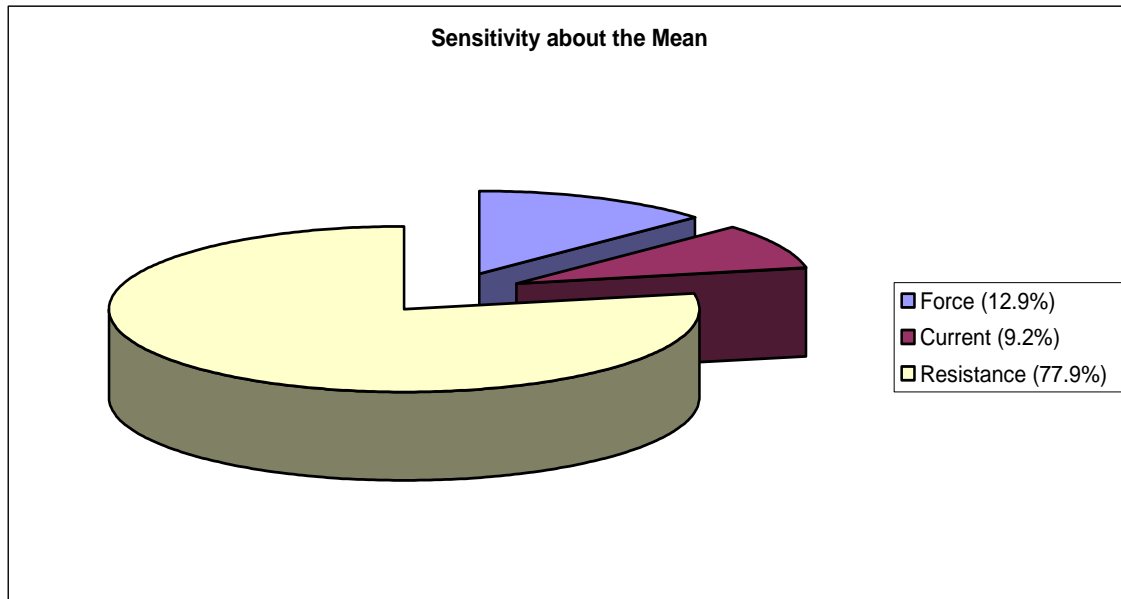


Figure 6.36: Sensitivity of the selected inputs parameters to the output.

The result shows that sample resistance significantly influenced the output (weld diameter). The input parameters used to determine the output in this neural network model are further analyzed to show the relationship between each of the input to the output (weld diameter).

6.7.2.1 Effect of Dynamic Resistance on Weld Quality

Presented in Figure 6.37 is the relationship between sample resistance and weld diameter.

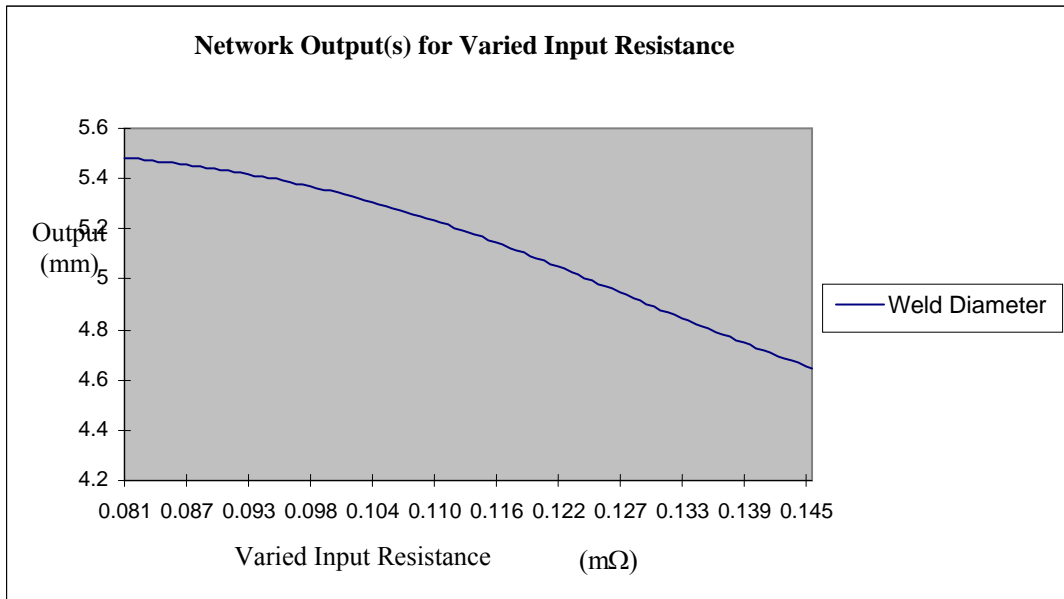


Figure 6.37: Sensitivity Result of the Varied Input Resistance to Weld Diameter

Figure 6.37 shows that, in comparing the two parameters, sample resistance contributed the most to the achieved weld diameter. This extreme influence of the resistance to the achieved weld diameter means that a small change in dynamic resistance during the spot welding process affects the weld diameter achieved. An increase in dynamic resistance leads to a decrease in achieved weld diameter.

To further analyse the effect of resistance on the welding process quality. Calculated sample resistance for applied electrode forces 2.2kN, 2.6kN and 3.0kN carried out on all the four welding machines over the six welding time steps are presented.

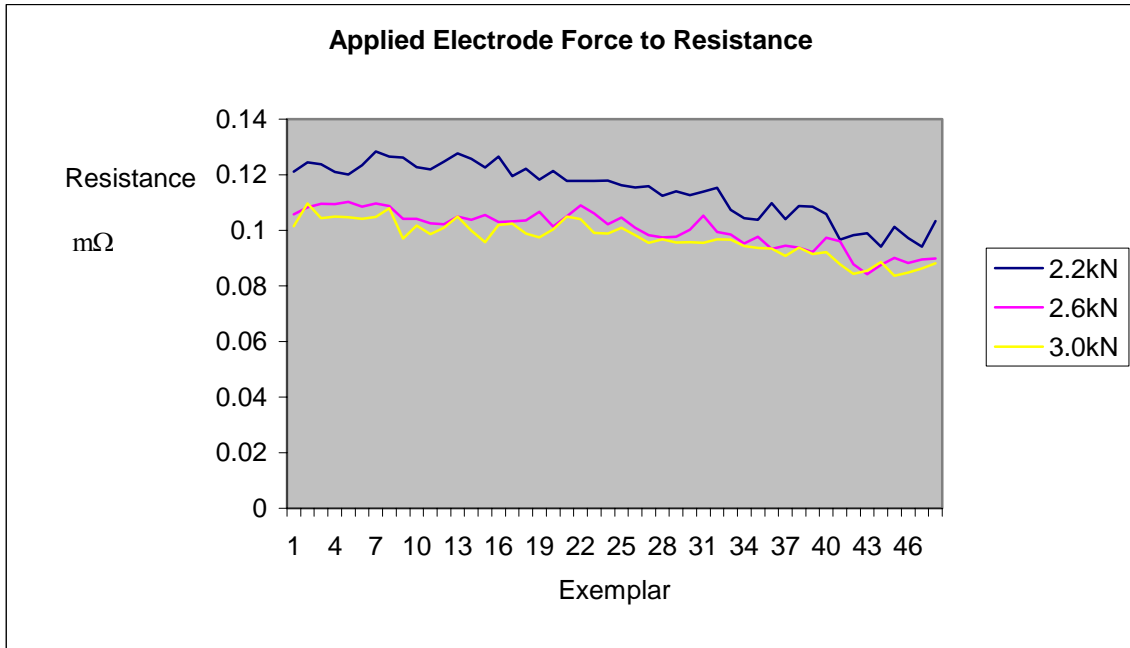


Figure 6.38: Calculated Sample Resistance welded with C-Gun Machine

The result of Figures 6.38 shows that resistance generated in using lower applied electrode force of 2.2kN was higher compared to the other two applied electrode forces 2.6kN and 3.0kN. This is expected because at lower applied electrode force less contact exists between the plate surfaces to be welded such that the resistance offered is higher compared to the surface under higher applied electrode force^(22, 23) like the 2.6 and 3.0kN applied electrode forces. This trend is similar to the sample resistance generated in the DZ welding machine in Figure 6.39.

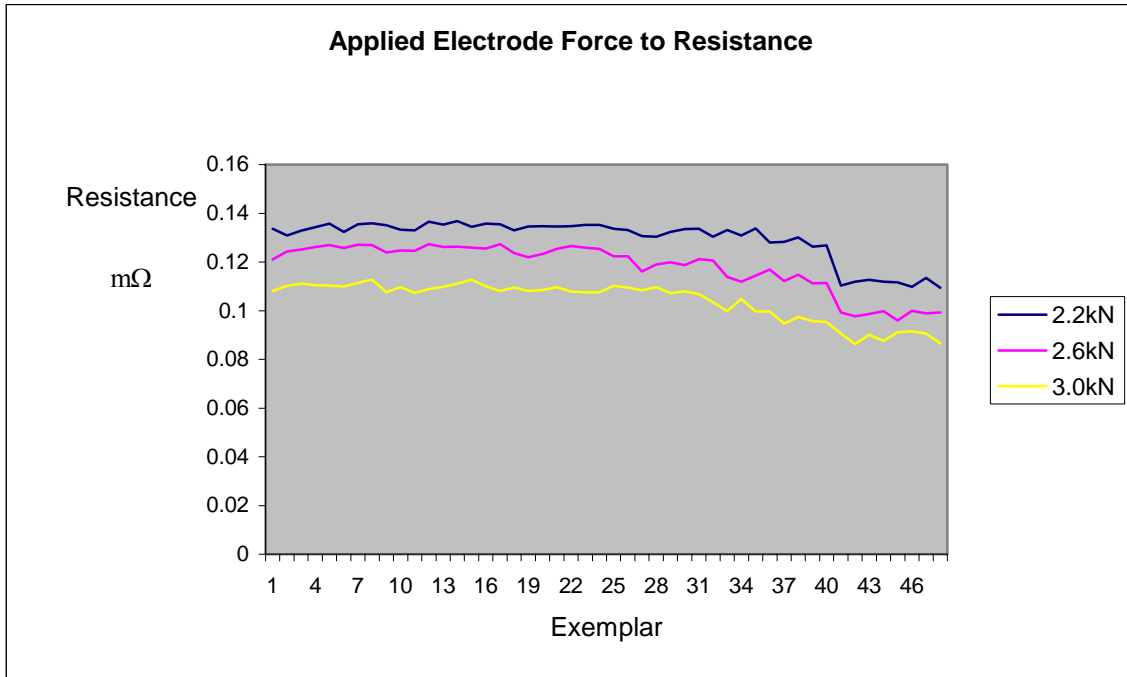


Figure 6.39: Calculated Sample Resistance welded with DZ Machine

With high resistance is a higher chance for generation of heat and fast nugget growth which can lead to expulsion of the nugget formed. It is therefore not necessarily advantageous to weld at a low applied electrode force. Equally at very high applied electrode force, less resistance is offered by contact surface between the plates with lower heat generation and slower nugget growth. This is also not an advantage as achieving maximum nugget size takes longer and the electrodes in contacts will have enough time to absorb some of the heat generated. It is important to use an optimal applied electrode force for best results. As shown in Figure 6.39 the resistance achieved in using applied electrode force of 2.6kN and 3.0kN for the C-Gun welding machine are very close. This is suggestive of an optimal point between 2.6kN and 3.0kN in welding with C-Gun machine.

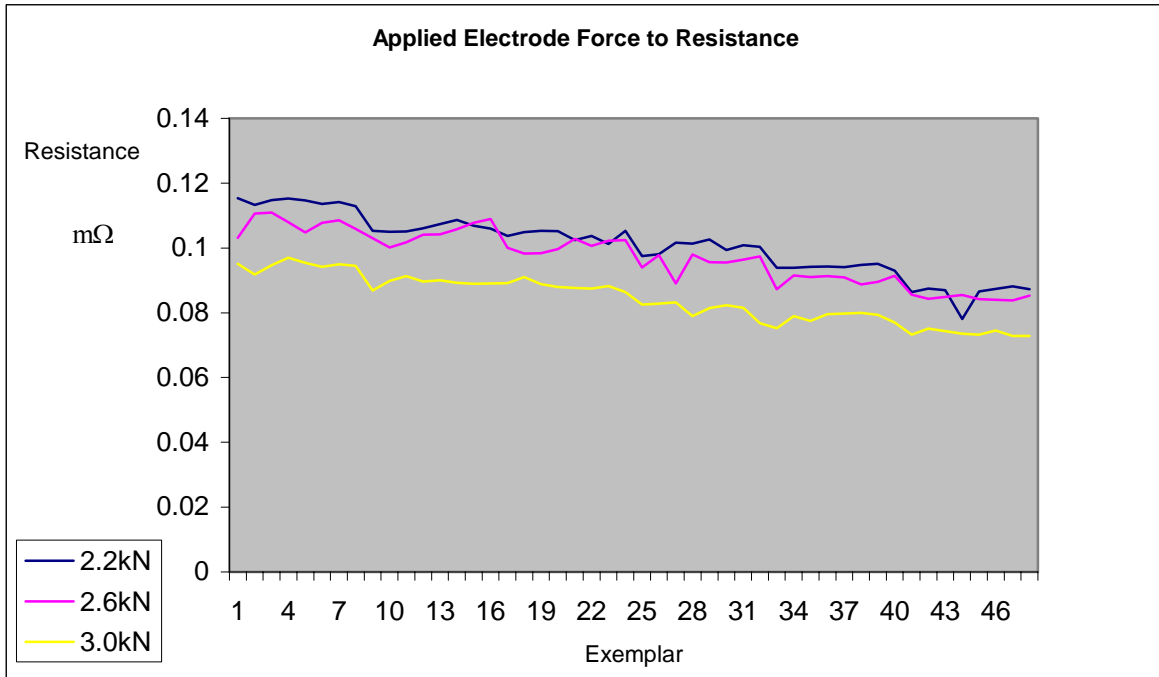


Figure 6.40: Calculated Sample Resistance welded with Dalex Machine

The calculated sample resistance trend in Dalex machine Figure 6.40 and Figure 6.41 are slightly different from the previous figures. Figure 6.40, welding using Dalex machine, there was close overlap between welding at an applied electrode force of 2.2kN and 2.6kN.

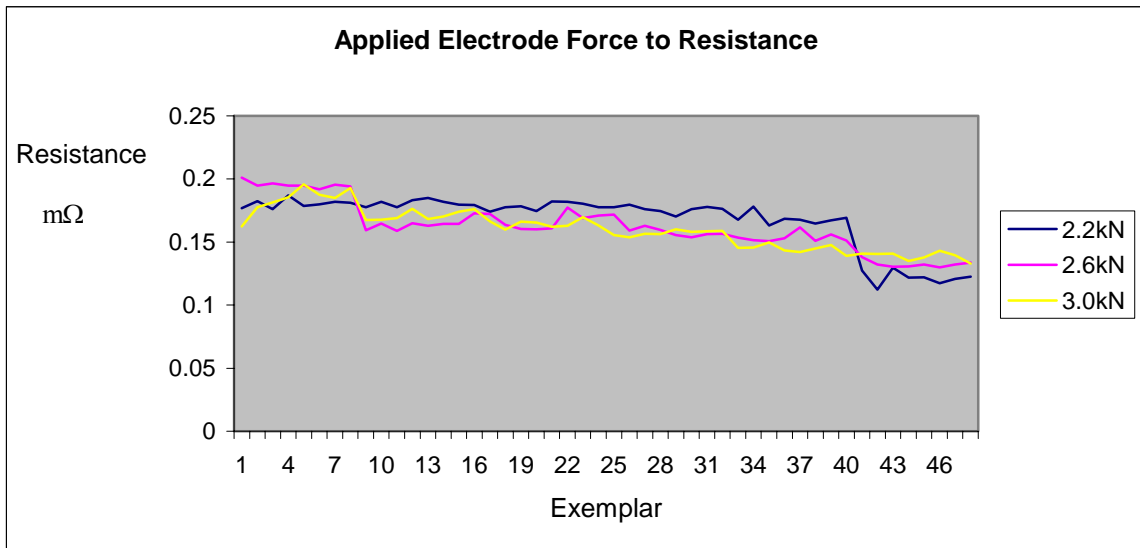


Figure 6.41: Calculated Sample Resistance welded with PMS Machine

In Figure 6.41, welding with PMS machine, the gap between all three applied electrode forces of 2.2kN, 2.6kN and 3.0kN are very close and overlapping at some points. In all the four welding machines, the calculated sample resistance decreases at the later welding time steps.

To investigate the effect of welding machines on the sample resistance (calculated), the calculated sample resistance at specific applied electrode forces of 2.2kN, 2.6kN and 3.0kN are compared in all the four welding machines used. Presented in Figures 6.42, 6.43 and 6.44 respectively are the sample resistance generated at specific applied electrode forces in all four welding machines.

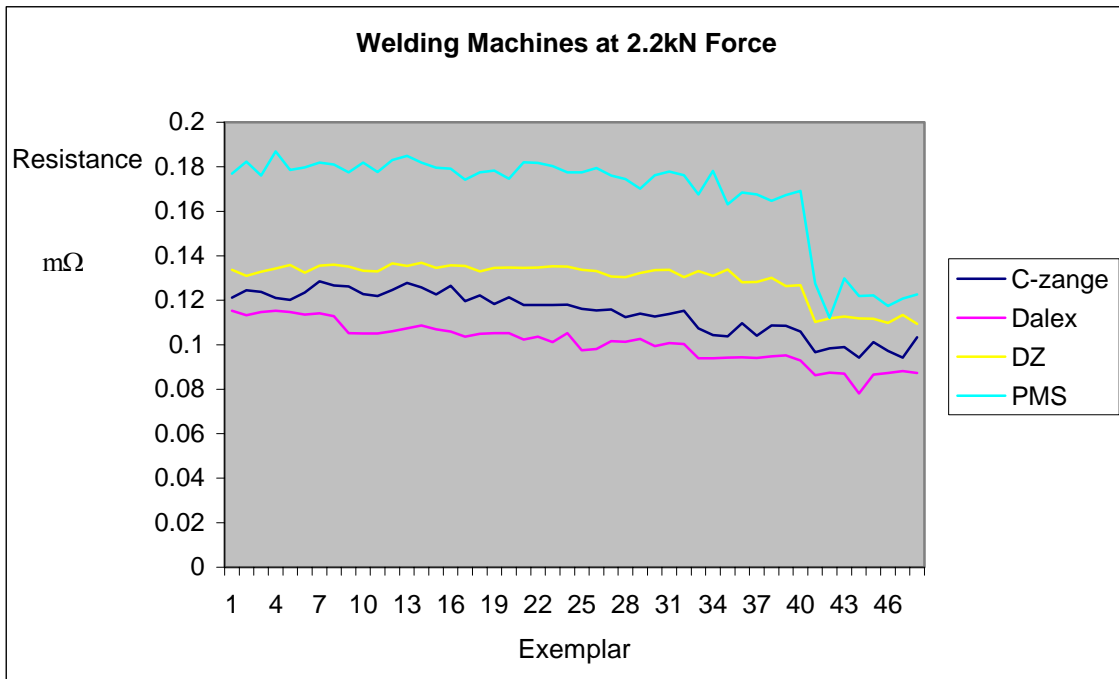


Figure 6.42: Calculated Sample Resistance in all four Machines at 2.2kN Force

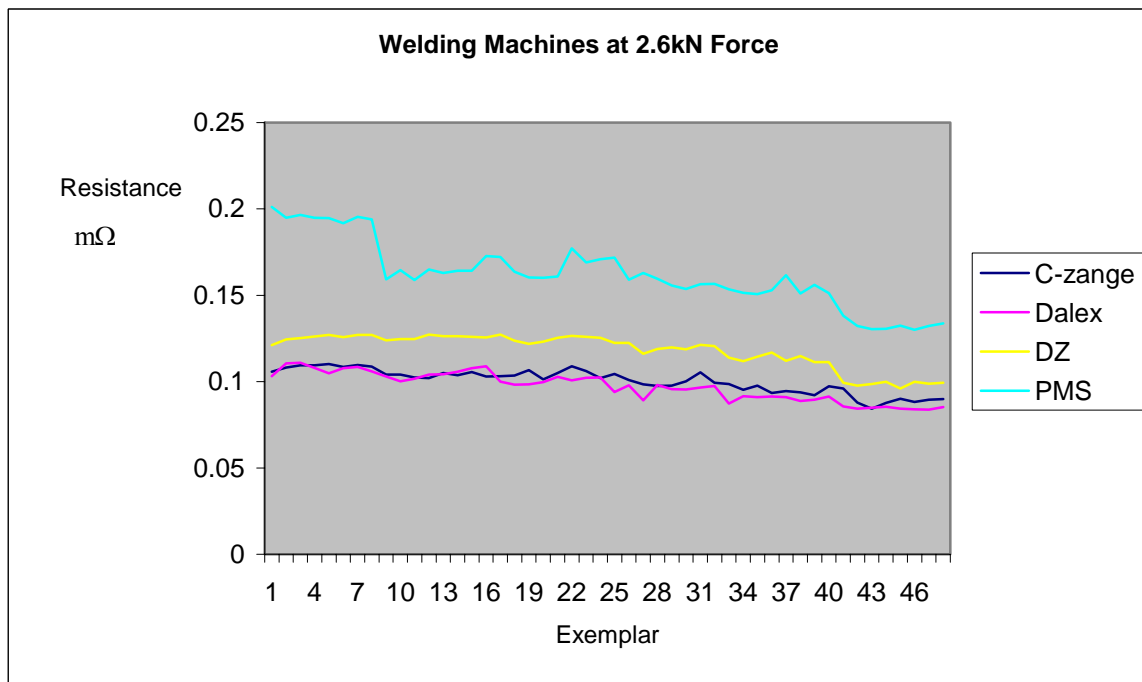


Figure 6.43: Calculated Sample Resistance in all four Machines at 2.6kN Force

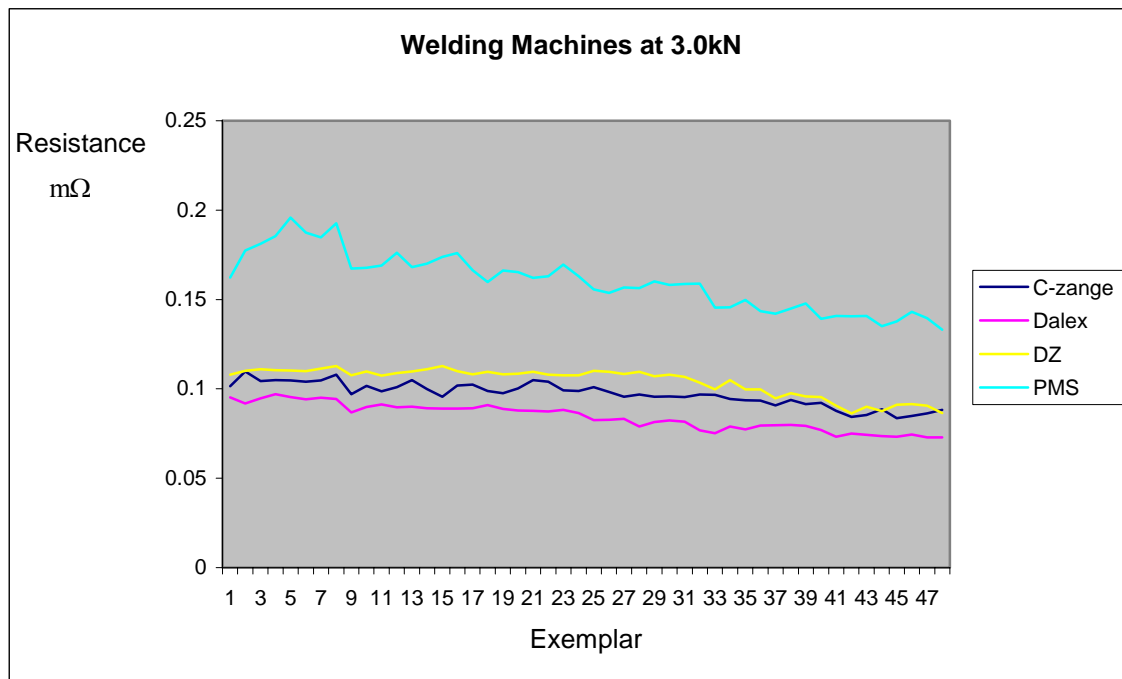


Figure 6.44: Calculated Sample Resistance in all four Machines at 3.0kN Force

The Figures show consistent behaviour of all the four machines under the applied electrode forces of 2.2kN, 2.6kN and 3.0kN. Sample resistance generated with the use of the PMS welding machines showed higher sample resistance in all the three applied force cases considered. The sample resistance in using PMS welding machine is substantial as can be seen by the large gap between the sample resistance lines from this machine compared to the other three welding machines. DZ machine, C-Gun and Dalex closely followed one another.

The plots of sample resistance in Figures 6.42 to 6.44 shows that for same applied electrode force, using same type of sample material and thickness it was not possible to generate the same value of dynamic resistance in all the welding machines. This means that each welding machine maintained unique but consistent dynamic resistance behaviour under particular applied electrode force.

With this unique behaviour it is possible to say that the resistance generated in each welding machine is able to provide some information about the welding machine from

which it was generated. This is very important as it shows that the resistance (electrical characteristic parameter) has some machine characteristics information, justifying the fact that in using sample resistance to model the welding process, reasonable information on the welding machine characteristics are provided as well in the model. Reasonable amount of information in the dynamic resistance data therefore exists to be able to give a good indication about mechanical characteristics of the welding machine, without having to generate specific mechanical characteristics data. The calculated sample resistance from the nonlinear halfwave dynamic resistance is considered a strong signal and will be used as one of the inputs in the neural network architecture for modelling and predicting weld diameter (weld quality).

6.5.2.2 Effect of Applied Electrode Force on Weld Quality

Applied electrode force affects weld diameter in some ways⁽⁹⁴⁾. Presented in Figure 6.45 is the effect of varied input force on weld diameter.

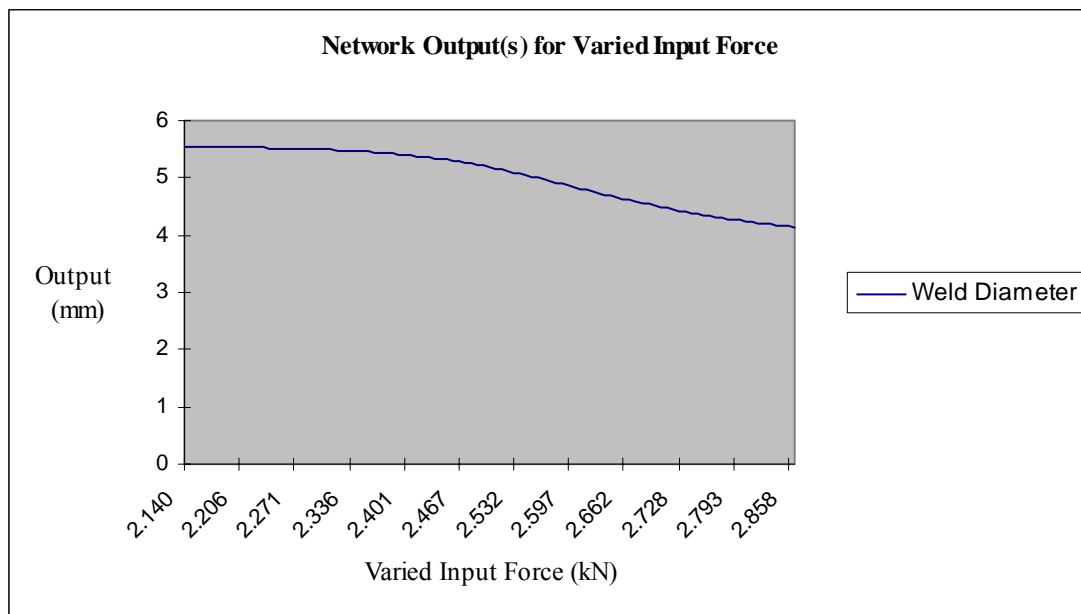


Figure 6.45: Result of the Varied Input Force to Weld Diameter

The Figure shows, that the varied input force to the weld diameter had almost no significant effect on the weld diameter at a low applied electrode force. By increasing the applied electrode force to a certain point at about 2.3 kN -2.45 kN the weld starts to

respond to the change. Increasing the applied electrode force to above a certain value leads to decrease in the achieved weld diameter size. This was explained by De et al ⁽⁹⁴⁾ in welding two plate surfaces at high applied electrode force, a large area of interface is established, which reduces the initial contact resistance, thereby reducing the heating and nugget growth ⁽⁹⁴⁾. This means that above an optimum point of applied electrode application, the effect becomes detrimental to the weld diameter produced.

6.5.2.3 Effect of Weld Current on Weld Diameter

Effective weld current is a process parameter that affects weld diameter. Presented in Figure 6.46 is a graph showing the effect of varied weld current on weld diameter.

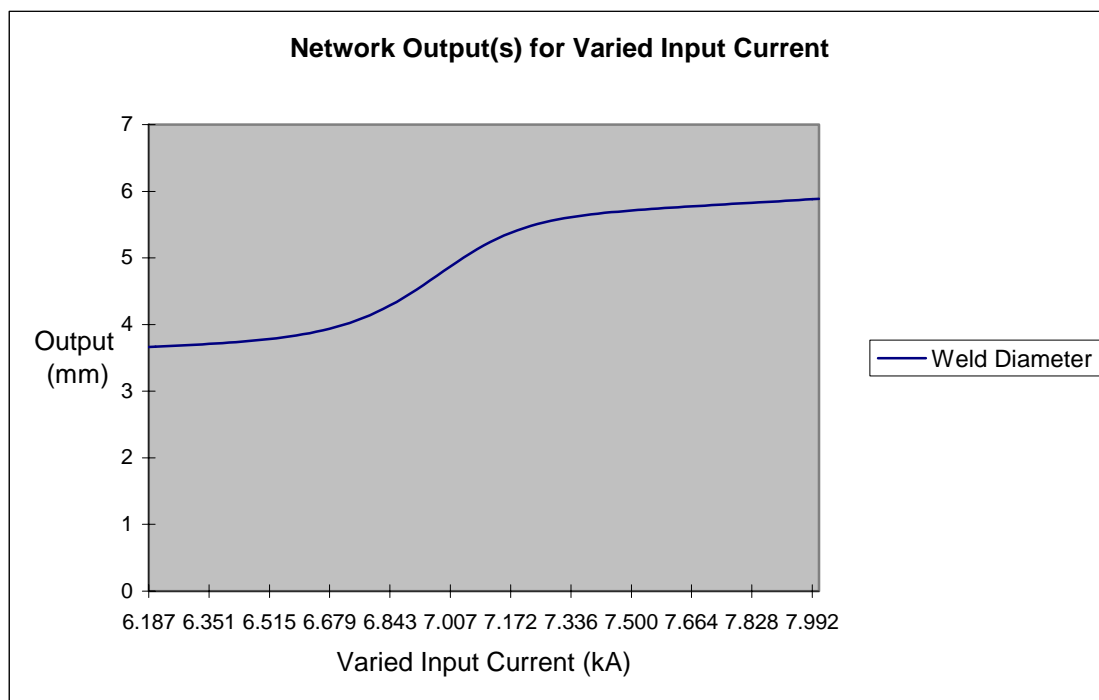


Figure 6.46: Result of the Varied Input Current to Weld Diameter

Figure 6.46 shows some direct relationship between weld diameter and weld current as is expected. Increasing the effective weld current leads to an increase in the size of weld diameter achieved. This creates opportunity to maximise the size of weld diameter that

can possibly be achieved. Increase in the welding current brings about increase in heat supply to plate sample welded, leading to a corresponding nugget growth. The graph shows that in the welding process increasing the weld current initially had a mild effect on the weld diameter with a sudden upward change. This point of change corresponds to the point of high resistance drop away from the β peak point ⁽¹⁰²⁾ (Figure 6.1). To continue increasing the effective weld current above a particular weld diameter will lead to expulsion. Optimum welding current that gives good weld quality has to be determined and selected in the resistance welding process.

6.8 Concluding Remarks

An empirical model that best fits the dynamic halfwave resistance curve was developed. The best fit parameters M and K for the dynamic resistance curve fit were estimated and goodness of fit was carried out to determine the level of error, using the least sum of square and root mean square error criteria. This agrees with Ratowski ⁽⁸⁹⁾ findings that the least sum of squares using an iterative method beginning with a set of initial parameter estimates is appropriate for non linear regression expression models. Using the model expression the parameters M and K was determined through an iterative process.

In all cases the curve fitting of each of the dynamic resistance curves for each welded sample and estimation of the parameters using the model yielded good results. By plotting a graph using these parameters M, K and R_o for given weld diameter and applied electrode force, it was possible to estimate the resistance for each sample welded. Plotting this graph and using it to predict sample resistance for any desired weld diameter in any welding machine did not yield accurate result. Neural network technique was employed in the prediction to improve the prediction accuracy. Different neural network types and architectures were investigated. The multilayer perceptron neural network using the parameters M, K and R_o as inputs yielded good result such that it was possible to accurately predict resistance for any of the welded sample in an unknown welding machine. Sensitivity analysis confirmed the contributory effect of these parameters on the output.

Relationship analysis was carried out on the identified input process parameters that are strong signals that affect weld quality. These input parameters are sample resistance, effective weld current (RMS) and applied electrode force. Weld diameter was taken as the output. Sample resistance showed the strongest influence on weld diameter, followed by effective current. Applied electrode force did not have much influence on the weld quality and above a certain point in the application of the force the effect was detrimental.

Each of the resistance spot welding machine used gave unique dynamic resistance curve. This shows that the electrical characteristics parameter particularly dynamic resistance is able to provide some information on the mechanical behaviour of the machine. This behaviour was confirmed using sensitivity analysis carried out to determine the influence of these three input parameters (applied electrode force, effective weld current and predicted sample resistance) on the output (weld diameter).

Four neural network types which were generalised feed forward neural network type, multilayer perceptron neural network, radial basis function neural network and recurrent neural network were trained, tested, validated and compared, in order to determine the most appropriate for modelling the welding process. Of all four neural networks tested, the multilayer perceptron (MLP) neural network which outperformed the other three was selected and used to model the overall process for predicting weld diameter. Using this network architecture, prediction accuracy of about 93% to 99.99% was obtained. The next Chapter will present implementation of the predictive controller.

CHAPTER 7

DESIGN AND IMPLEMENTATION OF THE PREDICTIVE CONTROLLER

7.1 Introduction

In this chapter, the selected neural network which showed best performance in training, testing and accurately predicting outcome was used for designing the predictive controller. The best performing neural network of all the neural network types tested as discussed in Chapter 6 was the feedforward multilayer perceptron (MLP) neural network. The inputs were predicted sample resistance, effective weld current and applied electrode force and output was weld diameter. However, because effective current is what must be controlled in the welding process, the neural network architecture was inversed and used in the controller model. This implies that for any desired weld diameter (based on choice of good weld) ⁽¹⁹⁾, given applied electrode force, and estimated (predicted) sample resistance, the effective weld current (RMS) to achieve the desired weld diameter can be predicted using this controller. The controller can be applied online such that the neural network training is done in real time and predictive control and adjustment of effective weld current also done in real time.

7.2 Design and Development of MLP Neural Network Model

The selected MLP network architecture was used for the design of the predictive controller. The feedforward neural network architecture consists of 3 input processing elements, 1 output processing element, 474 exemplars with 2 hidden layers. The architecture was designed such that desired weld diameter which is usually an output was made an input and effective current (originally an input) was made as output. Typically in the welding process weld diameter is the output from the combination of the process

parameters used. Effective current is a parameter that can be controlled to give a desired weld quality (weld diameter), hence the need to know what effective current that will be required for a desired weld diameter. The first hidden layer of the network architecture has 11 processing elements and uses TanhAxon transfer function with momentum learning rule. The second hidden layer has 5 processing elements, TanhAxon transfer function with momentum learning rule. The output layer uses BiasAxon transfer function with conjugate gradient learning rule. The learning iteration was 3000 epochs.

The multilayer perceptron network architecture is shown in Figure 7.1

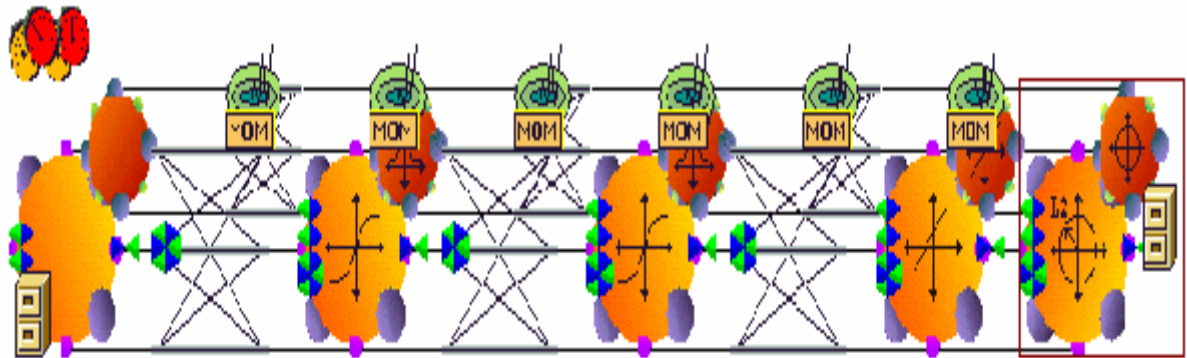


Figure 7.1: Generated Inverse MLP network architecture ⁽¹⁰⁶⁾

Presented in Figure 7.2 are the performance results of the network training and cross validation.

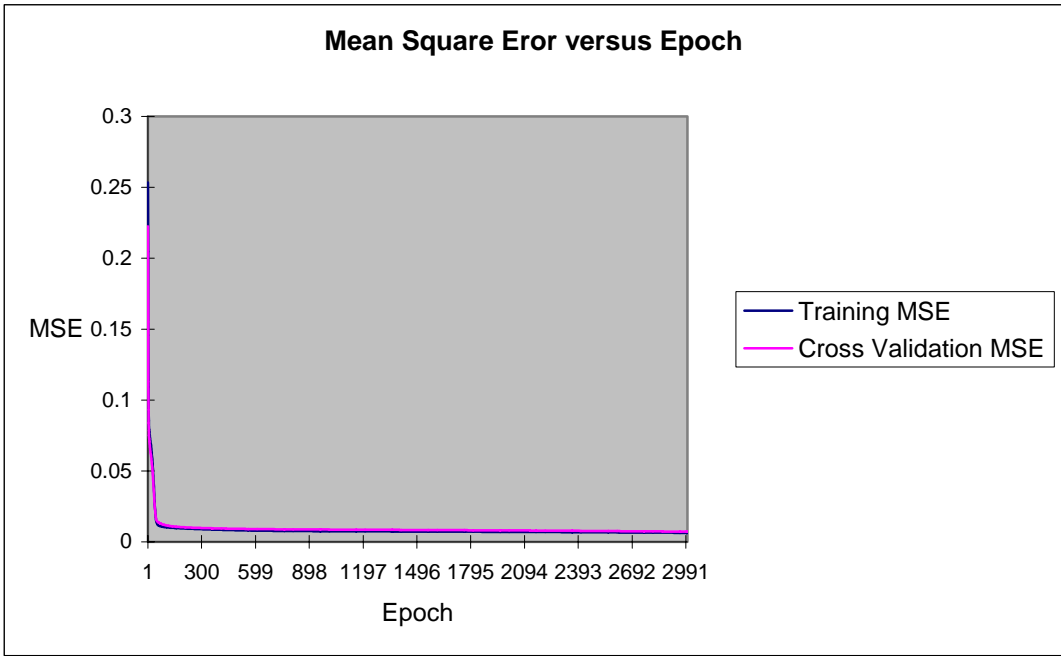


Figure 7.2: Testing performance of the multilayer perceptron (MLP) network design.

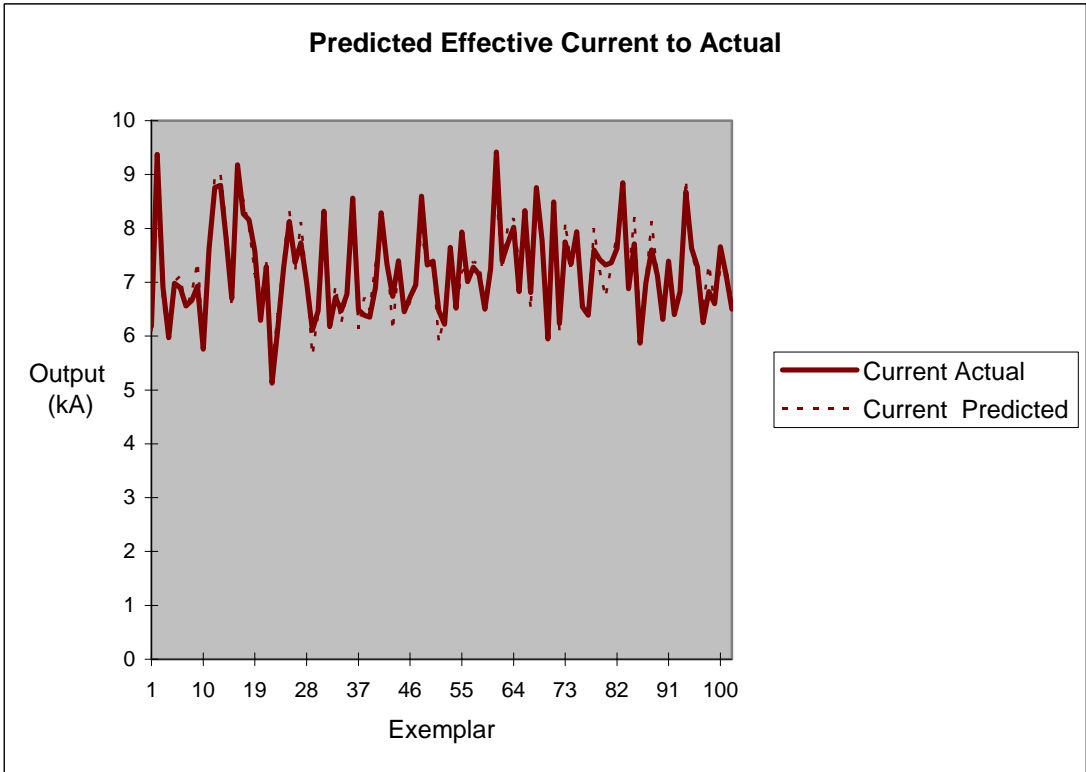


Figure 7.3: Testing performance of the inverse multilayer perceptron network

The mean square error output of 0.0063 at 3000 epochs was obtained for the training and 0.007 at same epochs for the cross validation as is shown in Figure 7.3. Weight decay (downward slope) of the training and cross validation plot is good. To determine overall performance of the network, the network was tested with data set not used for training the network. Presented in Figure 7.3 is the performance result of the network test.

The result of the testing shown in Figure 7.3 gives a mean sum of squares of 0.08, mean absolute error (MAE) of 0.23, normalised mean squared error (NMSE) of 0.11 and linear correlation coefficient is 0.94. This performance is quite good and consistent with the training performance result.

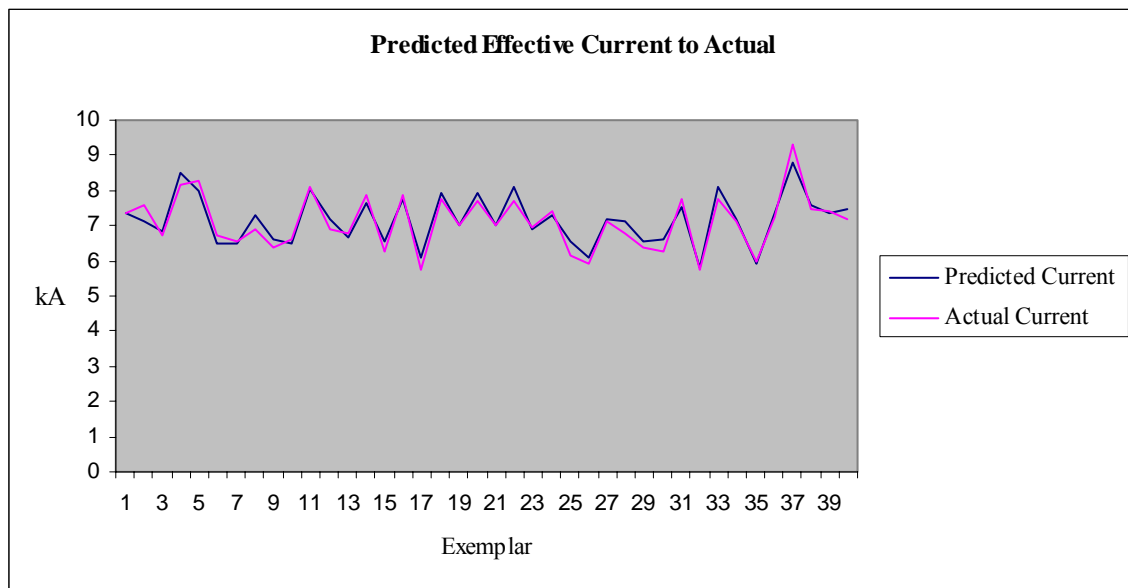


Figure 7.4: Validation performance of the multilayer perceptron network

This is corroborated by the result of the graph in Figure 7.4 showing the predicted effective weld current output closely following the actual effective weld current. The validated performance result of the network using production dataset not known to the network is presented in Figure 7.4. The result confirms the good performance result of the training and testing, with the predicted effective weld current seen to be tracking the actual effective weld current. The prediction error of the estimated effective weld current to the actual effective weld current is presented in Table 7.1.

Table 7.1: Predicted Effective Weld Current to Actual Effective Weld Current using
Multilayer Perceptron (MPL) network

Machine Type	Force (kN)	Resistance (mΩ)	Diameter (mm)	Predicted Current (kA)	Actual Current (kA)	Difference	% Difference
Dalex-25	2.16	0.072	5.8	7.329	7.36	-0.031	-0.421
C-Gun	2.2	0.087	5.5	7.140	7.57	-0.430	-5.685
Dalex-35	3	0.181	3.8	6.863	6.71	0.153	2.287
PMS	3	0.097	6	8.520	8.18	0.340	4.159
Dalex-25	2.6	0.089	6	7.981	8.3	-0.319	-3.838
PMS	2.6	0.100	3.9	6.499	6.74	-0.241	-3.574
Dalex-25	2.46	0.080	4	6.485	6.57	-0.085	-1.291
Dalex-25	2.46	0.075	5.4	7.318	6.91	0.408	5.909
C-Gun	3	0.108	3.6	6.600	6.39	0.210	3.281
PMS	2.2	0.180	3.9	6.522	6.6	-0.078	-1.178
Dalex-25	3	0.110	5.45	8.036	8.12	-0.084	-1.030
Dalex-25	2.16	0.079	5.6	7.173	6.89	0.283	4.108
C-Gun	2.6	0.125	4	6.673	6.79	-0.117	-1.729
Dalex-25	2.46	0.063	5.9	7.655	7.85	-0.195	-2.486
Dalex-35	2.6	0.195	3.7	6.567	6.29	0.277	4.411
C-Gun	2.6	0.112	5.6	7.771	7.89	-0.119	-1.510
Dalex-25	2.2	0.113	3.9	6.076	5.75	0.326	5.678
PMS	3	0.096	5.5	7.955	7.73	0.225	2.905
Dalex-25	2.6	0.102	4.5	7.009	7.04	-0.031	-0.447
Dalex- 25	3	0.096	5.5	7.955	7.7	0.255	3.312
Dalex-25	3	0.107	4	7.007	7.02	-0.013	-0.179
C-Gun	3	0.083	5.8	8.121	7.72	0.401	5.190
Dalex-35	3	0.108	3.9	6.913	6.95	-0.037	-0.533
PMS	2.2	0.110	5.6	7.296	7.41	-0.114	-1.538
Dalex-25	1.76	0.086	5.2	6.536	6.17	0.366	5.930
PMS	2.6	0.108	3.5	6.115	5.92	0.195	3.301
Dalex-25	2.6	0.164	4.5	7.176	7.15	0.026	0.361
Dalex-25	2.16	0.081	5.5	7.106	6.78	0.326	4.814
C-Gun	2.6	0.125	3.85	6.524	6.38	0.144	2.257
PMS	2.6	0.195	3.8	6.631	6.29	0.341	5.420
Dalex-25	2.2	0.168	5.8	7.549	7.77	-0.221	-2.843
Dalex-25	2.16	0.091	3.6	5.783	5.77	0.013	0.217
C-Gun	3	0.079	5.8	8.082	7.75	0.332	4.282
Dalex-25	2.2	0.114	5.4	7.175	7.11	0.065	0.919
Dalex-35	2.2	0.124	3.6	5.906	5.98	-0.074	-1.234
Dalex-25	2.46	0.074	5.5	7.374	7.24	0.134	1.846
Dalex-25	3	0.087	6.3	8.810	9.29	-0.480	-5.162
PMS	2.6	0.098	5.5	7.586	7.47	0.116	1.559
Dalex-25	2.6	0.122	4.9	7.350	7.4	-0.050	-0.675
Dalex- 25	2.2	0.094	5.9	7.463	7.17	0.293	4.085

The table shows that the prediction error is between 0.17% and 5.9%. That is an accuracy of about 99.83% to 94% for the prediction. This inverse multilayer neural network architecture was used as the process model for the controller design.

7.3 Design and Implementation of the Predictive Process Controller

The multilayer perceptron neural network architecture model developed previously was used for the design and implementation of the overall predictive process controller. Presented in Figure 7.5, is the design of the predictive controller using the inverse of the feedforward neural network model for predicting the effective weld current for desired weld diameter. The design was made by integrating this inversed MLP model and an earlier neural network model discussed in Chapter 6. The initial model was used for predicting sample resistance given the input parameters M, K and Ro. The predicted sample resistance was then used as an input with weld diameter and applied electrode force to predict the effective weld current in the controller model.

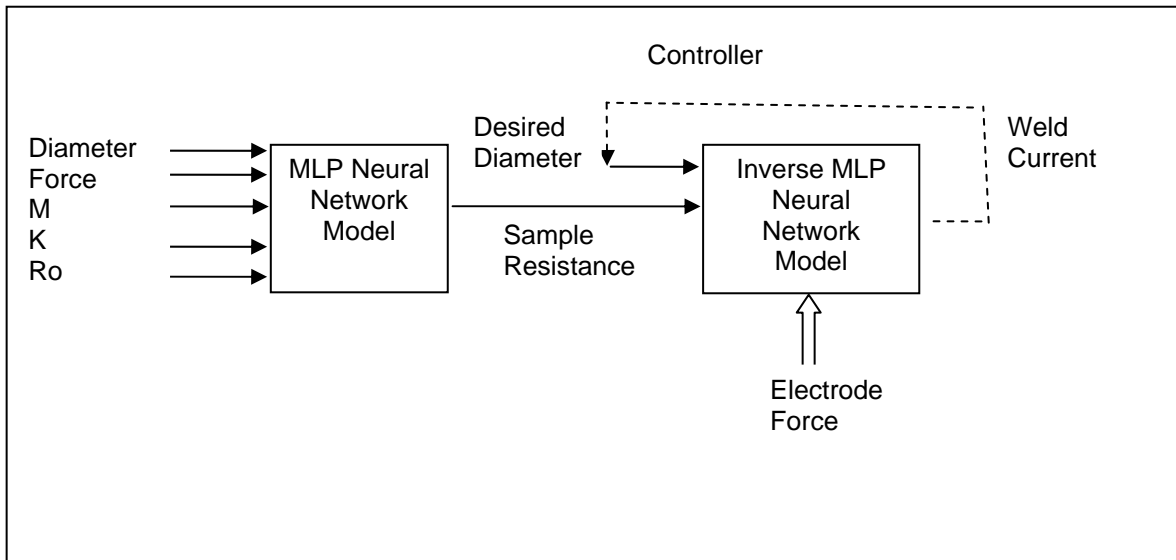


Figure 7.5: Neural Network Controller Design for Predicting Effective Current

To make this controller usable, a dialogue box was designed such that it was possible to input values into the predictive controller and by the push of a command button obtain

the output. This controller form was embedded into an excel application with input values from an original neurosolutions ⁽¹⁰⁷⁾ breadboard that have been loaded into an 'Input' worksheet, generated from the trained and tested neural network models. The network output is generated from a digital link library (DLL). On pressing the command button, the code used for running the controller becomes active such that the embedded controller form automatically calls up (predict) output(s) from the digital link library (DLL). The code for running the controller is presented in Appendix D.

Presented in Figure 7.6 is the controller designed form for capturing the inputs; force, weld diameter, and parameters K, M and Ro, for predicting sample resistance. (mΩ)

The image shows a software window titled "UserForm1" with a blue title bar and a close button. The window contains several input fields and a button. The fields are arranged vertically on the left side, each with a label and a text box containing a value. The labels and values are: "Force_" with "2.46", "Diameter" with "3.6", "K" with "0.4297", "M" with "0.03842", "Ro" with "0.11541", and "output" with "8.621889E-02". To the right of each text box is a unit label: "(kN)", "(mm)", "", "", "(mΩ)", and "(mΩ)" respectively. At the bottom right of the form is a button labeled "CommandButton".

Label	Value	Unit
Force_	2.46	(kN)
Diameter	3.6	(mm)
K	0.4297	
M	0.03842	
Ro	0.11541	(mΩ)
output	8.621889E-02	(mΩ)

Figure 7.6: Controller Model form for predicting Sample resistance

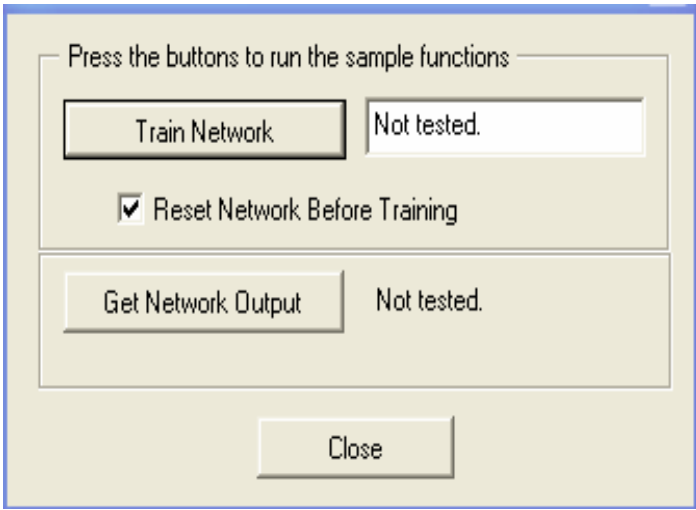


Figure 7.7: Controller form for generating network output.

In online situation new input can be trained such that most recent data are used. Figure 7.7 presents this option of retesting the inputs of the network or just calling up an already trained neural network as shown.

To predict effective weld current the generated (predicted) sample resistance from this controller form was combined with applied electrode force and desired weld diameter as inputs into another controller form also embedded in an excelXP⁽¹⁰⁷⁾ application for predicting effective current as is shown in Figure 7.8.

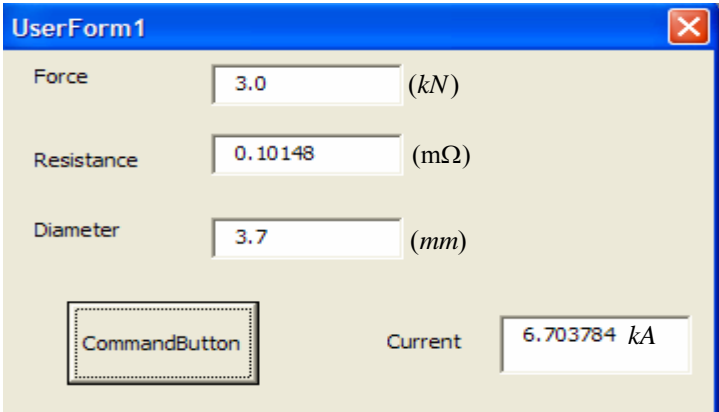


Figure 7.8: Effective Current Predicted for C-Gun Machine 3.0kN Applied Force

The design of the embedded controller used for predicting the effective current (RMS) for the welding process is presented in Figure 7.9.

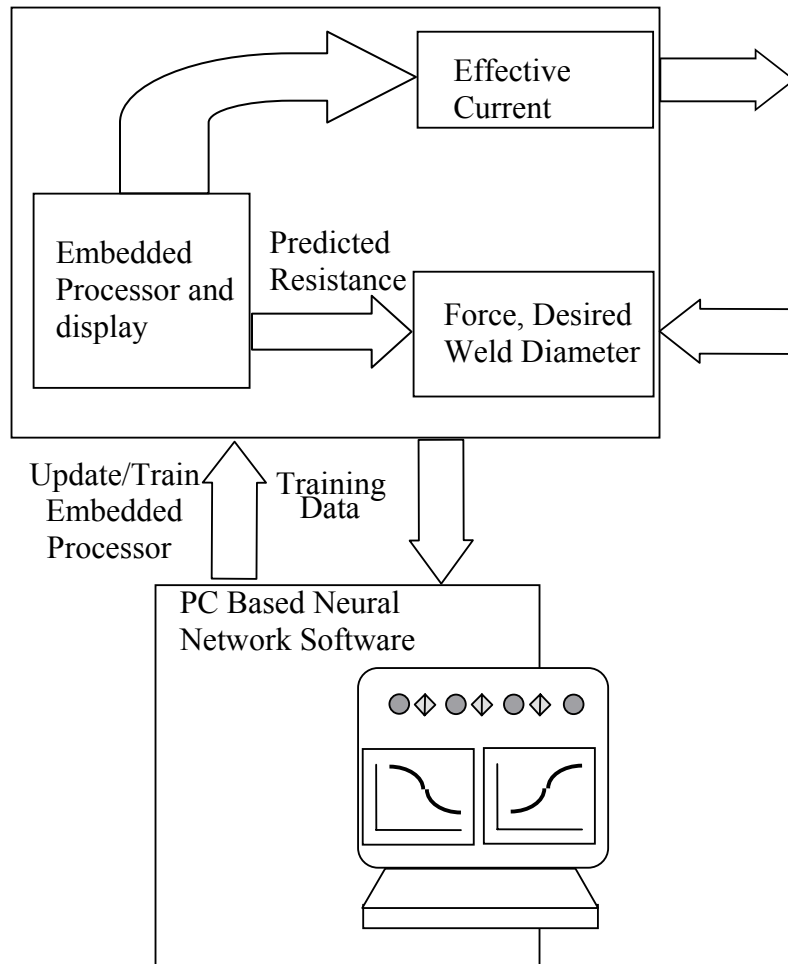


Figure 7.9: Embedded Controller for Predicting Effective Weld Current [Adapted ⁽³⁴⁾]

The code used for running the controller form is attached in Appendix E. The inputs values which are used for the training, validation and testing were used to create an original neurosolutions breadboard loaded into the 'Input' worksheet and used to generate outputs from the neural network digital link library (DLL). Like in the first controller the 'Output' worksheet receives the output values generated by the DLL.

By entering the inputs which are applied electrode force, desired weld diameter and sample resistance predicted and pressing the command button it automatically outputs

effective weld current required to achieve the desired weld diameter, called up from the digital link library stored in a breadboard.

The controller forms are tested with real production data to further confirm their performance in terms of prediction accuracy. Data sets which are not known to the neural networks were randomly selected from all the machines and effective weld current for the desired weld diameter were predicted using the neural network predictive controller form. The predicted result was compared to the actual production data obtained for the desired weld diameter. The prediction accuracy in predicting the effective current was determined for all the welding machines and applied electrode forces used. The results of the prediction grouped by the machine types, for different applied electrode forces are presented Table 7.2.

Table 7.2: Prediction of Effective Weld Current for Different Machines and Applied Electrode Force

Applied Electrode Force (kN)	Welding Machine Type	Predicted Weld Current (kA)	Actual Weld Current (kA)	Prediction Accuracy
3.0	C-Gun	6.704	6.48	96.55%
2.6	C-Gun	7.985	8.29	95.29%
2.2	C-Gun	7.122	7.10	99.66%
1.76	Dalex	5.383	5.18	96.86%
2.46	Dalex	6.388	6.58	97.04%
3.0	Dalex	8.359	8.49	97.97%
2.2	PMS	6.475	6.35	98.08%
2.6	PMS	7.986	7.68	95.28%
3.0	PMS	8.963	9.36	93.88%
3.0	DZ	7.326	7.61	95.61%
2.6	DZ	8.089	8.32	96.43%
3.0	DZ	6.074	6.49	93.58%

The forms (dialogue box) of the neural networks on which each of the result was generated are presented in Appendix F.

7.4 Concluding Remarks

Predictive controller design was developed for the sample resistance neural network model needed for predicting the sample resistance. This sample resistance was used as an input in the overall process predictive controller. The multilayer neural network type was used, as it was the best performer of the four neural networks tested. The network architecture consists of five inputs and one output. The inputs were applied electrode force, weld diameter and the parameters M , K and R_o . M , K and R_o were determined using the model expression that curve fitted the non linear dynamic resistance curve. The controller was embedded in an ExcelXP and calls up an output when an input is entered and command button pressed (activated).

Implementing the neural network model for predicting effective weld current output was similar to the sample resistance prediction controller. A multilayer perceptron type neural network, which was the best performing neural network, was selected and embedded into an excelXP application. The initial network architecture consists of three inputs and one output. The inputs were applied electrode force, effective weld current and predicted sample resistance. The output was the weld diameter. This network architecture was inverse such that applied electrode force, predicted sample resistance and weld diameter were used as inputs and effective weld current as output such that for any desired weld diameter, the effective weld current to achieve it can be determined. This is because the weld current is the parameter that can be controlled during the welding process.

This inverse neural network was used for implementing the predictive controller, such that by entering the inputs which are applied electrode force, desired weld diameter and sample resistance predicted and pressing the command button it automatically outputs effective current required to achieve the desired weld diameter, called up from the digital link library stored in a breadboard. Accuracy of the prediction was checked by predicting weld current output for production data set not known to the neural network. The prediction accuracy ranged between about 93.5% and 99.6%. The next Chapter presents full conclusion of the findings in this research.

CHAPTER 8

CONCLUSIONS

8.1 Introduction

This final chapter highlights the major conclusions made in this study and the future work that could be attempted as a direct result of this study. The work is seen as having a positive influence on the future of resistance spot welding and application of neural network in developing predictive controller for desired spot weld quality reproducibility. Work directly pertaining to this study includes four articles that have been developed and are being reviewed for publication. The abstracts are presented in Appendix G, H, I and J.

8.2 Conclusion on Findings

The conclusions arising from this study are as follows:

1. Electrical parameter data set generated from the resistance spot welding process was sufficient data in combination with applied electrode force for modelling the welding process and predicting weld quality. The model developed was used in a predictive process controller to determine required effective current for desired weld diameter (weld quality) in any of the resistance spot welding machines. The input parameters used were predicted sample resistance from the half wave peak dynamic resistance generated, applied electrode force and the desired weld diameter, outputting required effective current (RMS).

The relationship analysis shows that the sample resistance generated in each welding machine used maintained consistent behaviour for all the applied electrode force ranges. This gives unique indication of the mechanical characteristic of the welding machine. It is concluded that the electrical parameter data have information on mechanical characteristic enough to model the resistance spot welding process and to good accuracy

predict weld quality (weld diameter). Using the electrical parameter data in the process model and in the predictive controller precludes the need to generate additional costly mechanical parameter data from the resistance spot welding machines for the process modelling. This verifies the argument in literature as to which of electrical and mechanical parameter data are most appropriate for modelling the resistance spot welding process.

2. The nonlinear dynamic resistance plot was curve fitted using an empirical three parameter equation expression given as:

$$R = \frac{K \times M \times Nc + Ro}{K + (M \times Nc^{1.5})} + Ro \times Nc^{0.5} \quad (6.14)$$

R is the sample resistance for each sample welded, Ro is the initial dynamic resistance value at step one welding halfwave cycle. N_c is the number of halfwave cycles, K and M are unknown parameters that are determined through an iterative process of the curve fitting. It can also be calculated at the β peak point of $dR/dNc = 0$ and by taking the second order partial derivative of the equation. The sample resistance (R) can be estimated using this model equation. Estimating sample resistance using plots of the parameters M , K and Ro for a given weld diameter and applied electrode force read off from developed graphs made of these parameters for a specific machine yielded an accuracy of about 85% to 99%. However, when machine identifiers were excluded so that sample resistance can be predicted for any unknown welding machine, maximum prediction error of about 149% was observed.

3. Neural network capability was employed to improve the prediction accuracy of the empirical model for estimating sample resistance. Four neural network types which are generalized feed forward neural network, multilayer perceptron (MLP), recurrent network and radial basis function (RBF) neural network were trained and tested to find the one with least error and best prediction capability to use for the estimation.

The networks architecture which consists of two inputs and one output which were weld diameter and applied electrode force as inputs and sample resistance as the output were trained tested and validated. The best performing neural network type with this architecture was the multilayer perceptron (MLP) with maximum estimation error of about 65%, an accuracy of about 35%.

To overcome this unacceptable prediction level, multilayer perceptron neural network with inputs made up of weld diameter, applied electrode force, M , K and R_o parameters from the empirical model expression was used to train and test the network. Multilayer perceptron neural network architecture prediction performance was excellent. It yielded a mean square error in training and cross validation of 0.00037 and 0.000390 with linear correlation coefficient in testing of 0.999 and maximum estimation error of about 0.1% to 3%. This is an accuracy of about 99.9% to 97%. This model was selected for the design and implementation of the controller for predicting overall sample resistance. Sensitivity analysis carried to confirm the influence of the parameters to the output (sample resistance) shows that the parameter M from the model expression is the most contributor, followed by K and R_o . Applied electrode and weld diameter had little effect. Development of the models and accurately predicting sample resistance in the resistance spot welding process is a unique contribution of this work to the body of knowledge.

4. Applied electrode force, dynamic resistance and effective weld current are presented as useful and strong input signals that can be used to model the resistance spot welding process as they all have significant relationship with weld diameter (weld quality). The effect of applied electrode is not so significant up to a point. Above a certain point the effect is significant and detrimental to the achieved weld diameter. Optimum applied electrode force value does exist for best yield, for this range of forces considered above about 2.45 kN the effect is seen as detrimental. There is direct relationship between effective current and achieved weld diameter. Increasing effective current achieves bigger size weld diameter all other conditions kept constant. Sample resistance has very significant effect on weld diameter. There is inverse relationship between the weld diameter and resistance. This work further verifies this understanding in the literature, on the relationship between these spot welding parameters.

5. Four neural network types were trained, tested and validated to determine the best performing neural network to use for the resistance spot welding process model. The Multi layer perceptron (MLP) neural network type used outperformed the others. The Multi layer perceptron (MLP) neural network architecture used as the process model consists of three inputs which are applied electrode force, dynamic resistance and effective weld current with weld diameter as the output. The performance result gave a mean square error in training and cross validation of 0.0067 and 0.05 with linear correlation coefficient in testing of 0.972 and maximum estimation error of about 7%. The predicted output from this model closely followed the actual observation. However because the parameter that can be easily controlled which affects weld diameter is effective current, the neural network architecture was inverse such that applied electrode force, weld diameter and sample resistance were used as inputs and effective current as output. So for any desired weld diameter, using a particular applied electrode force and sample resistance, the required effective current can be predicted.

6. The two multilayer perceptron neural network architectures, a forward form and an inverse form developed was employed for the design of the controllers. One controller was for predicting sample resistance using the parameters from the empirical model and another for predicting effective weld current required for any desired weld diameter. The controllers were implemented by embedding both controller forms in an excelXP application. When the inputs are entered and the command button on the controller form applied, it generates outputs from the neural network digital link library (DLL).

The controller designed using the inverse neural network model was tested with data which was not used during the training process and for data it had not seen before. The result yielded accurate, reliable, and repeatable prediction. The controller was found to be predicting well to an accuracy of about 93.5 to 99.9%. This controller is appropriate in this application problem. This is a unique contribution that has not been done before.

This work presents the possibility of employing the developed empirical model used for predicting sample resistance and the inverse multilayer perceptron neural network predictive controller model for predicting effective weld current (RMS) for any desired

weld diameter in any new resistance spot welding machine. Boundary condition will be the use of the same material (galvanised low carbon steel) with thickness of 0.88 mm. Other unique identifiers like mechanical characteristic need not be known to be able to predict weld quality using this controller for any new resistance spot welding machine, for this material type and thickness.

To obtain an accurate prediction using this controller it should be ensured that use of worn out electrodes are avoided, as data from completely worn out electrodes were not used in building and designing the process model and predictive controller. Copper electrode of material type A16 with electrode wear class V1 (transition state 1) corresponding to 900 to 1700 spot welds made with the electrode is the range used in this research. The welding cycle time used in the design of this model is 20 halfwave cycles. The controller can be used online or off-line.

8.3 Future Work

During the investigation undertaken in this study some other alternatives and ideas have emerged but unfortunately not all these could be investigated in this study

These alternative suggestions are:

1. The need to investigate the effect of other types of materials and thickness on the resistance spot welding process and to develop model(s) for predicting weld quality for such conditions. This will help confirm the effect of material types and changes in material thickness on weld quality and will give flexibility in the selection of materials types and thickness for use in the resistance spot welding.
2. There is the need to investigate and model the relationship between the failure modes of the welded samples to shear stress and the torque angle at the point of failure. This is because resistance spot welds under shear stress fails at different angles. A model should

be used to establish these relationships and to predict the shear stress and torque angle at which a spot weld can fail.

3. The developed predictive controller design from this work should be implemented on actual welding machine in order to evaluate and confirm its design performance in real welding condition.

REFERENCES

1. Russell RS and Taylor BW, 2000, Operations Management, 3rd Edition, Prentice-Hall, Inc, 2000, Chapt. 1 & 3.
2. Welding years made with Adobe Golive, www.Golive/weldingyears (last accessed 12th September 2002).
3. Feng Z, Babu SS, Riemer BW, Santella ML, Gould JE, Kimchi M, 1999, Modelling of Resistance Spot Welds – Process and Performance, Proceedings of the IIW – Doc. No III – 1132, pp 2-4.
4. Monari G, Dieraert O, Oberle H and Dreyfus G, 1998, Prediction of Spot Welding Diameter Using Neural Networks, Proceedings of the IIW – Doc. No III – 1108-98, p1.
5. Matsuyama K, 1997, Nugget Size Sensing of Spot Weld based on Neural Network Learning, Annual Meeting of IIW, San Francisco, Doc. No. III – 1081, p.1 &2.
6. Waller DN, and Knowlson PM, 1965, Electrode Separation Applied to Quality Control in Resistance Welding, Welding Journal, 12(4), pp 168 – 174.
7. Weber G, and Preß H, 1994, Description of the Electrical Processes in the Secondary Circuit of Resistance Welding Equipment, Welding in the World, Vol. 33, No. 1, pp. 8-13.
8. Tang H, Hou W, Hu SJ, Zhang HY, Feng Z, Kimchi M, 2003, Influence of Welding Machine Mechanical Characteristics on the Resistance Spot Welding Process and Weld Quality, Welding Research, pp. 116-s – 124-s.
9. Lipa M, 1992, Mechanical Properties of Resistance Spot and Projection Welding Machines, Welding International (8) pp. 661 – 667.
10. Wei L, Shaowei C, Hu SJ, Justin S, 2001, Statistical Investigation on Resistance Spot Welding Quality Using a Two-State, Sliding – Level Experiment, Journal of Manufacturing Science and Engineering, Vol. 123, p. 513.
11. Hagan M, Demuth H and De Jesus O, 2002, An Introduction to the Use of Neural Networks In Control Systems, International Journal of Robust and Non-linear Control, Vol. 12, No. 11, September 2002, pg 959 - 985

12. Houpis C, Sating R, Rasmussen S and Sheldon S, 1994, Quantitative Feedback Theory Techniques and Applications. International Journal of Control, 59 (1), pp 39-70.
13. Kumar M, Devendra PG, 2004, Intelligent Learning of Fuzzy Logic Controllers Via Neural Network and Genetic Algorithm, Proceedings of 2004 JUSFA Japan – USA Symposium on Flexible Automation, Denver, Colorado, pp 1-5.
14. Gupta O P and De A, 1998, An Improved Numerical Modelling for RSW Process and its Experimental Verification". Journal of Manufacturing Science & Engineering. pp 246-251.
15. Aravinthan A, Sivayoganathan K, Al-Dabass D, and Balendran V, A Neural Network System for Spot Weld Strength Prediction, <http://ducati.doc.ntu.ac.uk/uksim'01/Papers/NTU/AraviArumugam/paper.doc> (last accessed 21st October 2003).
16. Resistance spot welding, July 2000, TWI World Centre for Materials Joining Technology Document <http://www.twi.co.uk/j32k/getfile/kssaw001.html>, (last accessed 5th November 2002).
17. Gourd L, 1980 Principles of welding technology Spottiswoode Ballentyne Ltd, Colchester & London.
18. http://www.robot-welding.com/Welding_parameters.htm, (last accessed 12th July 2002).
19. Weber G, and Burmeister J, 2000, Online Process Monitoring by Fuzzy Classification during AC Resistance Welding, 53rd Annual Assembly of IIW Florence Italy July 2000, IIW Doc. No. III-1156, pp 1.
20. Dupuy T, Clad A, Oberle H and Bienvenu Y, 1998, The Degradation of Electrodes by Spot Welding Zinc Coated Steels, iiw Doc. No. III – 1107, pp 1-6.
21. De A, Dorn L, Gupta OP, 2000, Analysis and Optimisation of Electrode Life for Conventional and Compound Tip Electrodes during Resistance Spot Welding of Electrogalvanised Steels, Science and Technology of Welding and Joining 2000, Vol. 5 No. 1, pp 49 – 57.
22. Tsai CL, Dai WL, Dickinson DW and Papritan JC, 1991, Analysis and Development of a Real – Time Control Methodology in Resistance Spot Welding, Welding Research Supplement, pp 339 – 350.

23. Matsuyama K, 1996, Numerical Simulation of the Nugget Formation Process in Resistance Spot Welding Aluminium Alloys and its Application to the Quality Monitoring of Spot Welds, IIW Doc. No. III-1060-96, pp 1 - 11.
24. Matsuyama K, 2000, Computer Simulation of Nugget Formation Process in Resistance Spot Welding, Australasian Welding Journal – Volume 45, Fourth Quarter – 2000, pp.32 – 37.
25. Matsuyama K, Obert R, Chun JH, 2002, A Real-Time Monitoring and Control System for Resistance Spot Welding, Eleventh International Conference on Computer Technology in Welding, NIST Special Publication 973, pp. 183 – 200.
26. Satoh, T., Katayama, J., and Nakano, T. 1988. Effect of Mechanical Properties of Spot Welding Machine on Spot Welds Quality. IIW Doc. no. III-912, pp. 118–122.
27. Dorn, L., and Xu, P, 1993, Influence of the Mechanical Properties of Resistance Welding Machines on the Quality of Spot Welding. *Welding and Cutting*, No. 1, pp. 12–16.
28. Huang SH and Zhang H, 1994, Artificial Neural Networks in Manufacturing: Concepts, Applications, and Perspectives, IEEE Transactions on Components, Packaging, and Manufacturing Technology – Part A, Vol. 17, No. 2.
29. Smith L, 2001, Department of Computing and Mathematics, Centre for Cognitive and Computational Neuroscience, University of Stirling. www.cs.stir.ac.uk/~lss/, (last accessed 10th September 2002)
30. Nelson MM & Illingworth WT, 1990, A Practical Guide to Neural Networks, Addison-Wesley Publishing Company, Inc. USA, pg 26 – 32.
31. Hassoun, M.H, 1995, Fundamentals of artificial neural networks, MIT Press, Cambridge, Massachusetts.
32. Martin G, 1995, Neural Network Applications for Prediction, Control and Optimisation, ISA TECH/EXPO Technology Update Conference Proceedings, v50, pp 433 – 441.
33. Caudill, M and Butler, C, 1991, Understanding Neural Networks: Volume 1: Basic Networks, MIT Press, Cambridge Massachusetts, US.
34. Principe JC, Euliano NR, Lefebvre WC, 2000, Neural and Adaptive Systems, Fundamentals through Simulations, John Wiley & Sons, New York, chpt 1, 2 & 3.

35. Leondes CT, 1998 Algorithms and architectures, Volume 1 of Neural Network systems Techniques and Applications) Academic Press, San Diego.
36. Hagan M, Demuth H and Beale M, 1996, *Neural Network Design*, PWS Publishing Company, 1996, chpt 1, 2 & 14.
37. Matlab, Neural Network Toolbox version 6, The Math Works Inc 2000
38. <http://www.avaye.com/ai/nn/introduction/index.html>. (last accessed 3rd August 2002).
39. Stergiou C and Siganos D, Neural Networks, http://www.doc.ic.ac.uk/~nd/surprise_96/journal/vol4/cs11/report.html#Introduction%20to%20neural%20networks, (last accessed 10th September 2002).
40. Yalcinoz T and Halis A, 2000, Comparism of Simulation Algorithms for the Hopfield Neural Network: An Application of Economic Dispatch. Turk J Elect. Engin, Vol. 8, No. 1.
41. <http://www.cs.stir.ac.uk/~lss/NNIntro/InvSlides.html#what>, (last accessed 23rd July 2003).
42. <http://www.willamette.edu/~gorr/classes/cs449/>, (last accessed 8th August 2002).
43. <http://ftp.sas.com/pub/neural>, (last accessed 31st March 2002).
44. Freeman J.A and Skapura DM, 1991, *Neural Networks: Algorithms, Applications and programming techniques*, Addison Pub. Co, Reading Massachusetts, US.
45. Artificial Neural Networks Technology, <http://www.dacs.dtic.mil/techs/neural/neural2.html>, (last accessed 21st March 2003).
46. <http://big.mcw.edu/display.php/1660.html>, (last accessed 1st December 2002).
47. Matlab, Neural Network Toolbox version 6.2, The Math Works Inc 2000
48. <http://opim.wharton.upenn.edu/~opim101/fall98/lectures/f98-neuralnets/sld011.htm>, (last accessed 6th August 2002).
49. <http://www.bip.bham.ac.uk/osmart/msc/lect/lect2a.html>, (last accessed 10th August 2003).
50. <http://www.cis.hut.fi/ahonkela/dippa/node41.html>, (last accessed 5th September 2003).
51. DARPA Neural Network Study, 1988, AFCEA International Press, p. 60.

52. Freeman J, Orr M and Saad D, 1998, Statistical Theories of Learning in Radial Basis Functions Networks, Neural Networks Systems Techniques and Applications, Vol. 2 – Algorithms and Architectures, Academic Press.
53. Su C, Yang T and Ke C, 2002, Neural Network Approach for Semiconductor Wafer Post-Sawing Inspection, IEEE Transactions on Semiconductor Manufacturing, Vol. 15, No. 2.
54. Horowitz R and Alvarez L., 1996, Self-Organizing Neural Networks: Convergence Properties, Proceedings of the International Conference on Neural Networks, Vol. 1, Track I, Session L1.
55. Kohonen, T, 1982, Self-organized formation of topologically correct feature maps, Biological Cybernetics, 43, pp 59 – 69
56. Goppert J and Rosentiel W, 1996, Regularized SOM-Training: A Solution to the Topology-Approximation Dilemma, Proceedings of the International Conference on Neural Networks, Vol. 1, Track I, Session L2.
57. <http://207.158.222.5/nnintro.shtml>, (last accessed 31st March 2002).
58. Recurrent network. <http://www.willamette.edu/~gorr/classes/cs449/rnn1.html>, (last accessed 31st March 2002).
59. Neural Network Topologies
<http://www.netnam.vn/unescocourse/knowlegde/62.htm>, (last accessed 1st October 2002).
60. Hebb, D.O. 1949, The Organization of Behaviour: A Neuropsychological Theory, New York: John Wiley & Sons, p1.
61. Grossberg, S, 1982, Associative and competitive principles of learning and development: The temporal unfolding and stability of STM and LTM patterns. In S.I. Amari and M. Arbib (Eds.), Competition and cooperation in neural networks. New York: Springer-Verlag, pp 4 – 11.
62. Hush, LR and Horne BG, 1993, Progress in Supervised Neural Networks - IEEE Signal Processing Magazine, pp 8-39.
63. Psaltis D, Sideris A, and Yamamura A, 1988, A multilayered neural network controller, IEEE Control System Magazine, pp. 17–21.

64. Lee S, and Kil R.M., 1989, Inverse mapping of continuous functions using local and global information, [<http://amath.kaist.ac.kr/~nipl/paper2.html>], (last accessed 5th December, 2003).
65. Hoskins D.A.; Hwang J.N and Vagners J, 1992, Iterative inversion of neural networks and its application to adaptive control, IEEE Transactions on Neural Networks, vol. 3, pp. 292–301.
66. Williams RJ, 1986, Inverting a connectionist network mapping by back-propagation error, IEEE Transactions on Neural Network, pp 2.
67. Linden A, and Kindermann J, 1989, Inversion of multilayer networks, Proceedings of the International Joint Conference on Neural Networks, vol. 2, pp. 425–430.
68. Hwang JN and Chan CH, 1990, Iterative Constrained Inversion and its Applications, Proc. 24th Conf. Inform. Syst. Sci., Princeton, NJ, March 1990, pp. 754–759.
69. [Lu Bao-Liang](#); [Kita H](#) and [Nishikawa Y](#), 1999, Inverting Feedforward Neural Networks using Linear and Nonlinear Programming”, IEEE Transactions on Neural Networks, v 10, n 6, Nov, 1999, pp 1271-1290.
70. www.mathworks.com/access/helpdesk/help/techdoc/ref/fminbnd.html, (last accessed 10th August 2003).
71. Oliver Smart, Univariant Minimisation
<http://www.biochemistry.bham.ac.uk/osmart/msc/lect/lect2a.html>, (last accessed 31st March 2002).
72. <http://www.gc.ssr.upm.es/inves/neural/ann1/supmodel/Nbackpro.htm>. Last visited [2003-07-23](#)
73. S. Haykin. “Neural Networks, A Comprehensive Foundation”, Macmillan, pg 45 – 87, 1994.
74. http://www.netlib.org/linalg/html_templates/node20.html. Last visited 2003-08-09
75. <http://www.uwed.ucsb.edu/~weibin/nnet/linfil13.html>. Last visited 2003-07-29
76. <http://mathworks.de/access/helpdesk/help/toolbox/optim/tutorial4b.shtml>. Last visited 2003-08-09.

77. Bishop, CM, 1995, Neural Network for Pattern Recognition, Oxford University Press, Oxford.
78. McCullough, P, and Nelder, JA, 1989, Generalized linear models, 2nd Ed, London, UK, Chapman and Hall.
79. White, H, 1992, Artificial Neural Networks: Approximation and Learning Theory, Blackwell, London, UK
80. Ripley, BD, 1999, Statistical Ideas for Selecting Network Architectures, University of Oxford, Oxford, UK.
81. Brown JD, Rodd MG and Williams NT, 1998, Application of Artificial Intelligence Techniques to Resistance Spot Welding, Ironmaking and Steelmaking 25(3), pp. 199 – 204
82. Berenji HR, 1992 Fuzzy and Neural Control, Sterling Software Artificial Intelligence Research Branch, NASA Ames Research Center, Canada.
83. Jun Wang (1998) Control and Dynamic Systems Volume 7 of Neural Network Systems Techniques and Applications, academic Press, San Diego. Pg 76 – 77
84. Hines JW, 1997, Matlab Supplement to Fuzzy and Neural Approaches in Engineering, John Wiley & Sons Publication Canada, pg 131 – 135.
85. Soeterboek, R 1992, Predictive Control, A Unified Approach, Prentice Hall International (UK).
86. Chait Y, The QFT Frequency Domain Control Design Toolbox (For use with MATLAB), QFTDEMOS, qftex1.m, 1995 – 1998
87. Hagan M, Demuth H and De Jesus, O, 2002, “An Introduction to the Use of Neural Networks In Control Systems”, International Journal of Robust and Non-linear Control, Vol. 12, No. 11, September 2002, pp 959 – 985.
88. Houppis C, Sating R, Rasmussen S and Sheldon S, 1994, Quantitative Feedback Theory Techniques and Applications. International Journal of Control, 59 (1), pp 39-70.
89. Antsaklis PJ, Passino KM, 1992, An Introduction to Intelligent and Autonomous Control

90. Donald A. Pierre (1969), Optimization Theory with Applications, John Wiley & Sons, Inc publication, New York.pg 386 – 418
91. W.M Wonham. On Pole Assignment in Multi-input, Controllable Linear Systems, IEEE Trans. Automat. Control 12:660-665, 1967.
92. <http://www.llnl.gov/CASC/nsde/sensitivity.html>. Last visited 2003.03.12, (last accessed 21st June 2002).
93. http://pespmc1.vub.ac.be/ASC/SENSIT_ANALY.html. SENSITIVITY ANALYSIS, (last accessed 5th November 2003).
94. De A, Gupta OP, and Dorn L, 1996, An Experimental Study of Resistance Spot Welding in 1 mm Thick Sheet of Low Carbon Steel, Journal of Engineering Manufacture, Institute of Mechanical Engineers, Part B, Vol. 210, pp 341 – 347.
95. ISO/DIS 14373, 2001 Welding -- Resistance spot welds -- Procedure for spot welding of uncoated and coated low carbon and high strength steels Technical committee: [ISO/TC 44/SC 10](#) .
96. ISO 669, 2000, Resistance welding -- Resistance welding equipment -- Mechanical and electrical requirements, Technical committee / subcommittee TC 44/SC 6
97. ISO/FDIS 8166, 2003, Resistance Welding – Procedure for the Evaluation of the Life of Spot Welding Electrodes using Constant Machine, Draft European Standard publication, p8.
98. S Westgate-Resistance welding of sheet metals-a guide to best practice http://www.twi.co.uk/j32k/protected/band_8/bprwsms01.html, (last accessed 1st December 2002).
99. Cho Y and Rhee S, 2000, New Technology for Measuring Dynamic Resistance and Estimating Strength in Resistance Spot welding, Meas. Sci. Technology, pp 1173-1178. <http://ej.iop.org/links/q76/SVScwCuTfEsDVqqRDo+0Fg/e00811.pdf>, (last accessed 10th February 2003).
100. ISO 14324, 2003, Resistance spot welding -- Destructive tests of welds -- Method for the fatigue testing of spot welded joints, Technical committee / subcommittee, IIW, ISO Standard

101. Hambling SJ, Jones TB, Fournalist G, 2003, The Influence of Steel Strength and Loading Mode on the Fatigue Properties of Resistance Spot Welded H-Beam Components, Engineering Integrity, Vol. 14, pp 4.
102. Dickinson DW, Tsai CL and Jammal O, 1990, Modelling of Resistance Spot Weld Nugget Growth – Applications for the Automotive Industry, International Congress and Exposition, Detroit, Mich. Pp1-8.
103. Ratkowsky D, 1989, Handbook of Nonlinear Regression Models, Marcel Dekker, Inc, New York and Basel, pp.19 – 29.
104. Kaiser JG, Dunn GJ and Eagar TW, 1982, The Effect of Electrical Resistance on Nugget Formation During Spot Welding, AWS Welding Research Supplement, pg. 172.
105. Matlab, Curve Fitting Toolbox version 7, The Math Works Inc 2002
106. Lefebvre WC, Principe JC, 2004, NeuroSolution software Version 4.
107. Battaglia G, Mean Square Error, 1992, AMP Journal of Technology Vol. 5

Bibliography

1. Kaiser JG, Dunn GJ, and Eagar TW, 1982, The Effect of Electrical Resistance on Nugget Formation During Spot Welding, Supplement to the Welding Research Journal, June 1982, 167-s – 174-s.
2. Brown JD, Jobling CP, Williams NT, 1998, Optimisation of Signal Inputs to a Neural Network for Modelling Spot Welding of Zinc Coated Steels, IIW Doc. 1117, p1.
3. Nossley KM, Brown M, Harris CJ, 1995, Neurofuzzy Adaptive Modelling and Construction of Non-linear Dynamical Processes, IEE Neural Network Applications in Control, Chapter 12, p253.
4. BEATSON, E.V. 1977, An introduction to quality Control Systems in Resistance Welding. Resistance Welding Control and Monitoring Seminar, TWI.
5. Frawley W, Piatetsky-Shapiro G, Matheus C, 1992, Knowledge Discovery in Databases: An Overview”, AI Magazine, pages 213-228.
6. Aravinthan K, Sivayoganathan D, Al-Dabass D, A Neural Network System for Spot Weld Strength Prediction,
<http://ducati.doc.ntu.ac.uk/uksim/uksim'01/Papers/NTU/AraviArumugam/paper.doc> (last accessed 19th November 2003).
7. Bianchini M, Frasconi P, Gori M and Maggini M, 1998, “Optimal Learning in Artificial Neural Networks: A Theoretical View” in *Neural Networks Systems Techniques and Applications*, Vol. 2 – Algorithms and Architectures, Academic Press.
8. Demuth H and Beale M, 2000, Neural Network Toolbox User’s Guide: for use with MATLAB, Mathworks, Inc.
9. Huang SH and Zhang H, 1994, “Artificial Neural Networks in Manufacturing: Concepts, Applications, and Perspectives”, *IEEE Transactions on Components, Packaging, and Manufacturing Technology – Part A*, Vol. 17, No. 2.
10. Russell RS and Taylor BW, III, 2000, *Operations Management*, 3rd Edition, Prentice-Hall, Inc.
11. <http://koti.mbnet.fi/~phodju/nenet/NeuralNetworks/NeuralNetworks.html>, (last accessed 31th March 2003).

12. <http://europa.eu.int/en/comm/eurostat/research/supcom.95/16/result/node6.html>
(last accessed 3rd October 2003).
13. Hamid R. Parsaei and Mohammed Jamshidi, 1995, Design and Implementation of Intelligent Manufacturing Systems, Prentice Hall PTR.
14. Lefteri H. Touskalas, Robert E. Uhig, 1998, Fuzzy and Neural Approaches in Engineering, John Weiley & Sons, INC
15. C. Houpis, R. Sating, S. Rasmussen, and S. Sheldon, 1994, Quantitative Feedback Theory Techniques and Applications. International Journal of Control, No. 59, pp. 39-70.
16. Anguita D and Boni A, 2002, Improved Neural Network for SVM Learning, *IEEE Transactions on Neural Networks*, Vol. 13, No. 5, 2002, pp. 1243-1244.
17. Catelani M, Fort A and Nosi G, 1999, Application of Radial Basis Function Network to the Preventive Maintenance of Electronic Analog Circuits, *IEEE Instrumentation and Measurement Technology Conference*, Vol. 1, 1999, pp. 510-513.
18. Chen C, and Yan Q. 1991, Design of a case associative assembly planning system Intelligent Engineering Systems through Artificial Neural Networks, ASME Press, pp. 757-762.
19. Chryssolouris G and Park J, 1988, Sensor integration for tool wear estimation in machining, Proc. ASME on Sensors and Controls for Manufacturing, pp.115-123.
20. Chryssolouris G, Lee M and Domoroese M, 1991, The use of neural networks in determining operational policies for manufacturing systems, Journal of Manufacturing Systems, Vol. 10, No. 2, pp. 166-175.
21. Chryssolouris G, Lee M and Pierce J, 1990, Use of neural network for the design of manufacturing systems, *Manufacturing Review*, Vol. 3, No. 3, pp. 187-194.
22. Cristianini N and Shawe-Taylor J, 2000, *An Introduction to Support Vector Machines*, Cambridge University Press, 2000, chpt. 1.
23. Cser L, Kohonen A, Mantyla P and Simula O. 2000, *Data Mining in Improving the Geometric Quality Parameters of Hot Rolled Strips*, Helsinki University of Technology.

24. Du R, 1998, *Engineering Monitoring and Diagnosis*, Neural Networks Systems Techniques and Applications, Vol. 4 – Industrial and Manufacturing Systems, Academic Press, 1998, pp. 119-141.
25. Foote B, Tillinghast T, Tretheway S, Cheung J and Chang C, 1990, Application of neural networks to optimize plant layout problems, *Knowledge-based Systems and Neural Networks: Techniques and Applications*, Elsevier, pp. 229-235.
26. Freeman J, Orr M and Saad D, 1998, Statistical Theories of Learning in Radial Basis Functions Networks, *Neural Networks Systems Techniques and Applications*, Vol. 2 – Algorithms and Architectures, Academic Press, pp. 1-21.
27. Goppert J and Rosentiel W. 1996, Regularized SOM-Training: A Solution to the Topology-Approximation Dilemma?, *Proceedings of the International Conference on Neural Networks*, Vol. 1, Track I, Session L2, June 1996, pp. 87-90.
28. Hagan M, Demuth H and Beale M, 1996, *Neural Network Design*, PWS Publishing Company, 1996, chpt 1, 2 & 14.
29. Horowitz R and Alvarez L, 1996, Self-Organizing Neural Networks: Convergence Properties, *Proceedings of the International Conference on Neural Networks*, Vol. 1, Track I, Session L1, June 1996, pp. 7-12.
30. Huang SH and Zhang H, 1994, Artificial Neural Networks in Manufacturing: Concepts, Applications, and Perspectives, *IEEE Transactions on Components, Packaging, and Manufacturing Technology – Part A*, Vol. 17, No. 2, June 1994, pp. 212-228.
31. De A, Gupta OP, Dorn L, 1996, An Experimental Study of Resistance Spot Welding in 1mm Thick Sheet of Low Carbon Steel, *Journal of Engineering Manufacture*, Institute of Mechanical Engineers, Part B, Vol.210, pp 341 – 347.
32. Haykin, S. 1994, *Neural Networks: A comprehensive Foundation*, NY: Macmillan, p. 2
33. Demuth, H and Beal, M, 1998, *Neural Network toolbox: For use with MATLAB-Users guide Vol. 3*, MathWorks Inc, Natick, Massachusetts.

APPENDIX A

DYNAMIC VOLTAGE AND CURRENT DATASET

Table A1: Step-1 (HW 1-20): Halfwave Voltage Values for C-Gun Machine at Applied Force of 2.2kN

Voltage values step-1	HW 1 (V)	HW 2 (V)	HW 3 (V)	HW 4 (V)	HW 5 (V)	HW 6 (V)
Specimen 1	1.008455	-1.0869723	1.03544545	-1.239099	1.18021	-1.39123
Specimen 2	1.0403527	-1.0845186	1.02808439	-1.236645	1.17776	-1.39368
Specimen 3	1.05507469	-1.1066015	1.03299177	-1.24155	1.18267	-1.40104
Specimen 4	1.09678697	-1.1458602	1.06979668	-1.29799	1.22192	-1.43785
Specimen 5	1.001094	-1.1115089	1.04526	-1.2587286	1.19493	-1.4084
Specimen 6	1.04771	-1.1016943	1.0379	-1.2513676	1.19003	-1.41086
Specimen 7	1.0747	-1.121323	1.04526	-1.2660897	1.2072	-1.43539
Specimen 8	1.06488931	1.12132358	1.05507469	-1.26854	1.20966	-1.42803
Average:	1.04863283	-1.1099753	1.04372662	-1.2575012	1.1955475	-1.41331
Standard Deviation	0.0301	0.0187	0.0126	0.0190	0.0149	0.0172
step-1 (Continue)	HW 7 (V)	HW 8 (V)	HW 9 (V)	HW 10 (V)	HW 11 (V)	HW 12 (V)
Specimen 1	1.26364	-1.44766	1.31271	-1.4722	1.32498	-1.46974
Specimen 2	1.271	-1.46238	1.32988	-1.49919	1.35197	-1.50409
Specimen 3	1.28817	-1.47465	1.3397	-1.50655	1.35688	-1.50655
Specimen 4	1.31271	-1.49919	1.35197	-1.51391	1.35688	-1.50164
Specimen 5	1.29553	-1.47465	1.33234	-1.48447	1.33725	-1.4771
Specimen 6	1.28817	-1.48201	1.34951	-1.52372	1.3716	-1.52618
Specimen 7	1.31026	-1.50655	1.36669	-1.5409	1.38877	-1.54581
Specimen 8	1.3078	-1.50164	1.35933	-1.53354	1.37896	-1.53599
Average:	1.29216	-1.4810912	1.34276625	-1.50931	1.35841125	-1.5083875
Standard Deviation	0.0170	0.0192	0.0164	0.0221	0.0198	0.0250
step-1 (Continue)	HW 13 (V)	HW 14 (V)	HW 15 (V)	HW 16 (V)	HW 17 (V)	HW 18 (V)
Specimen 1	1.32498	-1.45993	1.32498	-1.44521	1.32007	-1.43294
Specimen 2	1.35688	-1.48937	1.34951	-1.46974	1.34215	-1.45748

Specimen 3	1.35688	-1.49183	1.34951	-1.4722	1.3397	-1.45502
Specimen 4	1.34951	-1.48201	1.3397	-1.45993	1.32498	-1.4403
Specimen 5	1.32988	-1.45748	1.32007	-1.4403	1.31026	-1.42312
Specimen 6	1.37405	-1.51391	1.36914	-1.49673	1.35688	-1.47465
Specimen 7	1.39123	-1.53354	1.38632	-1.51636	1.38141	-1.50409
Specimen 8	1.37896	-1.52372	1.3765	-1.509	1.36914	-1.49673
Average:	1.35779625	-1.4939737	1.35196625	-1.47618375	1.34307375	-1.4605412
Standard Deviation	0.0217	0.0262	0.0223	0.0266	0.0231	0.0274
step-1 (Continue)	HW 19 (V)	HW 20 (V)				
Specimen 1	1.31516	-1.42067				
Specimen 2	1.33234	-1.44275				
Specimen 3	1.32988	-1.4403				
Specimen 4	1.31516	-1.42558				
Specimen 5	1.30044	-1.41086				
Specimen 6	1.34951	-1.46238				
Specimen 7	1.37405	-1.49183				
Specimen 8	1.36424	-1.48201				
Average:	1.3350975	-1.4470475				
Standard Deviation	0.0240	0.0274				

Table A2: Step-2 (HW 1-20): Halfwave Voltage Values for C-Gun Machine at Applied Force of 2.2kN

Voltage values step-2	HW 1 (V)	HW 2 (V)	HW 3 (V)	HW 4 (V)	HW 5 (V)	HW 6 (V)
Specimen 1	1.09678	-1.21702	1.23665	-1.50409	1.44275	-1.65131
Specimen 2	1.0894259	-1.19248	1.14095	-1.38141	1.32007	-1.53599
Specimen 3	1.109055	-1.19248	1.15567	-1.40349	1.33725	-1.55562
Specimen 4	1.1262309	-1.194933	1.15322	-1.39859	1.33725	-1.55808
Specimen 5	1.13604557	-1.21947	1.16058	-1.39859	1.3397	-1.56053
Specimen 6	1.104147	-1.1998407	1.15322	-1.39613	1.3397	-1.56298
Specimen 7	1.08451867	-1.1703968	1.12868	-1.38141	1.33234	-1.55071
Specimen 8	1.12623095	-1.1998407	1.15077	-1.39368	1.33234	-1.56544
Average:	1.10905425	-1.1983076	1.1599675	-1.40717375	1.347675	-1.5675825
Standard Deviation	0.0176	0.0144	0.0304	0.0374	0.0364	0.0328

step-2 (Continue)	HW 7 (V)	HW 8 (V)	HW 9 (V)	HW 10 (V)	HW 11 (V)	HW 12 (V)
Specimen 1	1.509	-1.69303	1.53109	-1.68812	1.52863	-1.67585
Specimen 2	1.41086	-1.59488	1.44275	-1.60224	1.4403	-1.58752
Specimen 3	1.41822	-1.6096	1.45502	-1.61696	1.45502	-1.60224
Specimen 4	1.41822	-1.61206	1.45257	-1.61451	1.45011	-1.59979
Specimen 5	1.42558	-1.61942	1.46729	-1.63414	1.46974	-1.62187
Specimen 6	1.43049	-1.62432	1.46974	-1.62678	1.46238	-1.6096
Specimen 7	1.42312	-1.61206	1.45748	-1.61206	1.45011	-1.59243
Specimen 8	1.42067	-1.62923	1.45993	-1.6415	1.46484	-1.62678
Average:	1.43202	-1.624325	1.46698375	-1.62953875	1.46514125	-1.61451
Standard Deviation	0.0296	0.0277	0.0255	0.0251	0.0256	0.0264
step-2 (Continue)	HW 13 (V)	HW 14 (V)	HW 15 (V)	HW 16 (V)	HW 17 (V)	HW 18 (V)
Specimen 1	1.51882	-1.65622	1.52127	-1.6415	1.51146	-1.61206
Specimen 2	1.43539	-1.56789	1.42803	-1.55071	1.41576	-1.53354
Specimen 3	1.44766	-1.58507	1.44275	-1.56298	1.43049	-1.54581
Specimen 4	1.44766	-1.58507	1.44521	-1.57034	1.43785	-1.55562
Specimen 5	1.46484	-1.60224	1.45748	-1.58261	1.45502	-1.56544
Specimen 6	1.45502	-1.59243	1.44766	-1.5728	1.43539	-1.55071
Specimen 7	1.4403	-1.57034	1.42803	-1.54581	1.41331	-1.52372
Specimen 8	1.45993	-1.6096	1.45011	-1.58752	1.43785	-1.56544
Average:	1.4587025	-1.5961075	1.4525675	-1.57678375	1.44214125	-1.5565425
Standard Deviation	0.0245	0.0263	0.0277	0.0279	0.0290	0.0250
step-2 (Continue)	HW 19 (V)	HW 20 (V)				
Specimen 1	1.48692	-1.58261				
Specimen 2	1.4084	-1.51146				
Specimen 3	1.42558	-1.52863				
Specimen 4	1.44521	-1.54826				
Specimen 5	1.45257	-1.54826				
Specimen 6	1.42803	-1.53599				
Specimen 7	1.39859	-1.50409				
Specimen 8	1.42803	-1.54826				
Average:	1.43416625	-1.538445				
Standard Deviation	0.0258	0.0230				

Table A3: Step-3 (HW 1-20): Halfwave Voltage Values for C-Gun Machine at Applied Force of 2.2kN

Voltage values step-3	HW 1 (V)	HW 2 (V)	HW 3 (V)	HW 4 (V)	HW 5 (V)	HW 6 (V)
Specimen 1	1.1286845	-1.271	1.28081	-1.54581	1.4722	-1.68321
Specimen 2	1.12132	-1.28817	1.28081	-1.5409	1.47465	-1.69057
Specimen 3	1.09924066	-1.26364	1.27345	-1.53599	1.45748	-1.67094
Specimen 4	1.1458601	-1.29308	1.30044	-1.56544	1.48692	-1.70039
Specimen 5	1.153221	-1.29799	1.29553	-1.55808	1.48447	-1.69548
Specimen 6	1.1286845	-1.27836	1.28572	-1.54335	1.47465	-1.68812
Specimen 7	1.1605821	-1.28327	1.29553	-1.55317	1.47465	-1.67585
Specimen 8	1.11887	-1.2685433	1.28327	-1.54581	1.47465	-1.69057
Average:	1.13205786	-1.280506	1.286945	-1.54856875	1.47495875	-1.6868912
Standard Deviation	0.0188	0.0115	0.0087	0.0091	0.0083	0.0092
step-3 (Continue)	HW 7 (V)	HW 8 (V)	HW 9 (V)	HW 10 (V)	HW 11 (V)	HW 12 (V)
Specimen 1	1.53599	-1.7102	1.54335	-1.68812	1.52863	-1.65868
Specimen 2	1.54335	-1.71756	1.54826	-1.69793	1.53599	-1.67094
Specimen 3	1.52863	-1.70039	1.53109	-1.67585	1.51391	-1.64395
Specimen 4	1.54581	-1.71511	1.54581	-1.69303	1.52863	-1.66604
Specimen 5	1.54826	-1.7102	1.54335	-1.68076	1.52127	-1.65131
Specimen 6	1.5409	-1.70775	1.53845	-1.6783	1.51636	-1.64641
Specimen 7	1.53599	-1.70284	1.5409	-1.67585	1.50655	-1.6415
Specimen 8	1.53599	-1.70284	1.53599	-1.6783	1.51636	-1.64641
Average:	1.539365	-1.7083612	1.5409	-1.6835175	1.5209625	-1.653155
Standard Deviation	0.0060	0.0057	0.0052	0.0079	0.0090	0.0102
step-3 (Continue)	HW 13 (V)	HW 14 (V)	HW 15 (V)	HW 16 (V)	HW 17 (V)	HW 18 (V)
Specimen 1	1.509	-1.62678	1.48692	-1.59488	1.46484	-1.57034
Specimen 2	1.52863	-1.6415	1.51882	-1.61696	1.50409	-1.58752
Specimen 3	1.49673	-1.61451	1.47465	-1.58507	1.45748	-1.56298
Specimen 4	1.51882	-1.63659	1.509	-1.61206	1.49183	-1.58507
Specimen 5	1.49919	-1.61942	1.48447	-1.58997	1.46484	-1.56053
Specimen 6	1.49428	-1.61451	1.47465	-1.58507	1.45748	-1.55562
Specimen 7	1.48692	-1.60715	1.46974	-1.58016	1.45748	-1.56053
Specimen 8	1.49673	-1.61696	1.4771	-1.58752	1.45748	-1.56298
Average:	1.5037875	-1.6221775	1.48691875	-1.59396125	1.46944	-1.5681962
Standard Deviation	0.0131	0.0111	0.0166	0.0126	0.0170	0.0111

step-3 (Continue)	HW 19 (V)	HW 20 (V)
Specimen 1	1.44766	-1.54826
Specimen 2	1.48201	-1.56298
Specimen 3	1.4403	-1.5409
Specimen 4	1.4771	-1.56053
Specimen 5	1.45011	-1.5409
Specimen 6	1.43785	-1.53354
Specimen 7	1.4403	-1.53599
Specimen 8	1.4403	-1.5409
Average:	1.45195375	-1.5455
Standard Deviation	0.0164	0.0102

Table A4: Step-4 (HW 1-20): Halfwave Voltage Values for C-Gun Machine at Applied Force of 2.2kN

Voltage values step-4	HW 1 (V)	HW 2 (V)	HW 3 (V)	HW 4 (V)	HW 5 (V)	HW 6 (V)
Specimen 1	1.138499	-1.36424	1.4084	-1.66358	1.59488	-1.774
Specimen 2	1.1556748	-1.39368	1.43785	-1.68321	1.60224	-1.78872
Specimen 3	1.14831387	-1.41331	1.46484	-1.71756	1.63169	-1.82062
Specimen 4	1.1581284	-1.39368	1.45011	-1.70039	1.60715	-1.78872
Specimen 5	1.1679431	-1.40595	1.45993	-1.71511	1.61451	-1.79363
Specimen 6	1.16058218	-1.41331	1.46238	-1.71756	1.62187	-1.80344
Specimen 7	1.1703968	-1.39613	1.44275	-1.69548	1.61206	-1.78627
Specimen 8	1.14831387	-1.40595	1.44766	-1.68567	1.61206	-1.78872
Average:	1.1559815	-1.3982812	1.44674	-1.69732	1.6120575	-1.793015
Standard Deviation	0.0100	0.0149	0.0170	0.0181	0.0106	0.0129
step-4 (Continue)	HW 7 (V)	HW 8 (V)	HW 9 (V)	HW 10 (V)	HW 11 (V)	HW 12 (V)
Specimen 1	1.62678	-1.77154	1.61206	-1.74701	1.59243	-1.71756
Specimen 2	1.63169	-1.77891	1.61942	-1.74946	1.59243	-1.71266
Specimen 3	1.66358	-1.81816	1.65377	-1.79853	1.64395	-1.77154
Specimen 4	1.63414	-1.77891	1.61206	-1.7421	1.58507	-1.70039
Specimen 5	1.63414	-1.77891	1.61942	-1.74946	1.60469	-1.71266
Specimen 6	1.63659	-1.77645	1.61696	-1.7421	1.58016	-1.70284
Specimen 7	1.62678	-1.76664	1.60715	-1.73229	1.59243	-1.70284
Specimen 8	1.63659	-1.77645	1.61942	-1.7421	1.59243	-1.70775

Average:	1.63628625	-1.7807462	1.6200325	-1.75038125	1.59794875	-1.71603
Standard Deviation	0.0109	0.0147	0.0134	0.0189	0.0186	0.0217
step-4 (Continue)	HW 13 (V)	HW 14 (V)	HW 15 (V)	HW 16 (V)	HW 17 (V)	HW 18 (V)
Specimen 1	1.58016	-1.68321	1.56298	-1.64641	1.52863	-1.60224
Specimen 2	1.56789	-1.68076	1.54335	-1.64395	1.51391	-1.60469
Specimen 3	1.6096	-1.72492	1.54826	-1.65622	1.49428	-1.58752
Specimen 4	1.55808	-1.65622	1.52127	-1.6096	1.48692	-1.56789
Specimen 5	1.58261	-1.67094	1.54581	-1.62678	1.51146	-1.58261
Specimen 6	1.55071	-1.66113	1.52372	-1.61696	1.49183	-1.58016
Specimen 7	1.57034	-1.66358	1.55071	-1.62187	1.509	-1.57525
Specimen 8	1.57034	-1.6734	1.54581	-1.63659	1.51636	-1.60224
Average:	1.57371625	-1.67677	1.54273875	-1.6322975	1.50654875	-1.587825
Standard Deviation	0.0167	0.0202	0.0130	0.0151	0.0133	0.0129
step-4 (Continue)	HW 19 (V)	HW 20 (V)				
Specimen 1	1.47956	-1.56298				
Specimen 2	1.48447	-1.57034				
Specimen 3	1.46484	-1.54581				
Specimen 4	1.45011	-1.53354				
Specimen 5	1.46729	-1.54826				
Specimen 6	1.46484	-1.54581				
Specimen 7	1.46238	-1.53109				
Specimen 8	1.49428	-1.5728				
Average:	1.47097125	-1.5513287				
Standard Deviation	0.0132	0.0148				

Table A5: Step-5 (HW 1-20): Halfwave Voltage Values for C-Gun Machine at Applied Force of 2.2kN

Voltage values	HW 1 (V)	HW 2 (V)	HW 3 (V)	HW 4 (V)	HW 5 (V)	HW 6 (V)

step-5						
Specimen 1	1.180211	-1.49919	1.56053	-1.78136	1.6783	-1.83289
Specimen 2	1.1703968	-1.48692	1.55562	-1.77645	1.67585	-1.82062
Specimen 3	1.1679431	-1.49183	1.56544	-1.78627	1.6783	-1.83043
Specimen 4	1.14586	-1.45257	1.52618	-1.75437	1.6734	-1.83043
Specimen 5	1.16548955	-1.48447	1.55071	-1.774	1.6734	-1.82307
Specimen 6	1.16303586	-1.4771	1.56544	-1.77891	1.6783	-1.82307
Specimen 7	1.17285048	-1.49183	1.57034	-1.78872	1.68321	-1.84025
Specimen 8	1.18021142	-1.48937	1.56053	-1.78136	1.68321	-1.84025
Average:	1.16824978	-1.48416	1.55684875	-1.77768	1.67799625	-1.8301262
Standard Deviation	0.0103	0.0134	0.0129	0.0099	0.0036	0.0071
step-5 (Continue)	HW 7 (V)	HW 8 (V)	HW 9 (V)	HW 10 (V)	HW 11 (V)	HW 12 (V)
Specimen 1	1.68076	-1.8059	1.65377	-1.76418	1.62432	-1.71266
Specimen 2	1.66604	-1.78627	1.61942	-1.73229	1.5728	-1.66849
Specimen 3	1.66604	-1.79117	1.62678	-1.7421	1.24646	-1.2955335
Specimen 4	1.68812	-1.80344	1.65131	-1.76173	1.61451	-1.71756
Specimen 5	1.65622	-1.77645	1.60715	-1.72247	1.55808	-1.66113
Specimen 6	1.66849	-1.78627	1.63169	-1.73719	1.58997	-1.68567
Specimen 7	1.69548	-1.8108	1.65868	-1.76418	1.61942	-1.72492
Specimen 8	1.69303	-1.8108	1.64886	-1.75191	1.60224	-1.69548
Average:	1.6767725	-1.7963875	1.6372075	-1.74700625	1.553475	-1.6451804
Standard Deviation	0.0136	0.0122	0.0174	0.0149	0.1180	0.1339
step-5 (Continue)	HW 13 (V)	HW 14 (V)	HW 15 (V)	HW 16 (V)	HW 17 (V)	HW 18 (V)
Specimen 1	1.55071	-1.6415	1.50164	-1.58997	1.46729	-1.54826
Specimen 2	1.52618	-1.61206	1.48201	-1.56053	1.44766	-1.51636
Specimen 3	1.1924	-1.278357	1.1998407	-1.275904	1.190026	-1.22928
Specimen 4	1.5777	-1.66604	1.53599	-1.61206	1.49428	-1.57034
Specimen 5	1.51146	-1.60469	1.47465	-1.55562	1.44275	-1.51882
Specimen 6	1.5409	-1.61696	1.49183	-1.56544	1.43785	-1.51146
Specimen 7	1.58752	-1.66358	1.51391	-1.60224	1.4771	-1.56053
Specimen 8	1.56053	-1.6415	1.48692	-1.56789	1.44766	-1.52863
Average:	1.505925	-1.5905858	1.46084884	-1.54120675	1.425577	-1.49796
Standard Deviation	0.1208	0.1199	0.1003	0.1021	0.0908	0.1035
step-5 (Continue)	HW 19 (V)	HW 20 (V)				
Specimen 1	1.43785	-1.51882				

Specimen 2	1.41576	-1.48692
Specimen 3	1.145806	-1.21947
Specimen 4	1.45993	-1.53845
Specimen 5	1.41822	-1.48937
Specimen 6	1.4084	-1.48201
Specimen 7	1.43785	-1.51146
Specimen 8	1.42067	-1.49428
Average:	1.39306075	-1.4675975
Standard Deviation	0.0947	0.0955

Table A6: Step-6 (HW 1-20): Halfwave Voltage Values for C-Gun Machine at Applied Force of 2.2kN

Voltage values step-6	HW 1 (V)	HW 2 (V)	HW 3 (V)	HW 4 (V)	HW 5 (V)	HW 6 (V)
Specimen 1	1.20720172	-1.60224	1.66358	-1.86724	1.74946	-1.88687
Specimen 2	1.24400663	-1.63169	1.68567	-1.88196	1.75437	-1.88441
Specimen 3	1.2587286	-1.65622	1.7102	-1.90159	1.774	-1.90895
Specimen 4	1.22683107	-1.60469	1.66849	-1.8746	1.75191	-1.88932
Specimen 5	1.31761658	-1.65868	1.71266	-1.9114	1.78872	-1.93103
Specimen 6	1.31025553	-1.68321	1.72983	-1.93103	1.77645	-1.91386
Specimen 7	1.29307997	-1.65622	1.71266	-1.9114	1.77891	-1.90404
Specimen 8	1.32988489	-1.69057	1.74701	-1.94821	1.8059	-1.95311
Average:	1.27345062	-1.64794	1.7037625	-1.90342875	1.772465	-1.9089487
Standard Deviation	0.0426	0.0307	0.0272	0.0262	0.0184	0.0223
step-6 (Continue)	HW 7 (V)	HW 8 (V)	HW 9 (V)	HW 10 (V)	HW 11 (V)	HW 12 (V)
Specimen 1	1.70775	-1.81816	1.63169	1.7421	1.56544	1.65868
Specimen 2	1.7102	-1.82062	1.62923	-1.73719	1.56544	-1.66113
Specimen 3	1.75682	-1.85742	1.67585	-1.78136	1.60469	-1.69303
Specimen 4	1.71511	-1.82798	1.63905	-1.74455	1.56053	-1.65868
Specimen 5	1.76909	-1.88196	1.68567	-1.79363	1.61942	-1.7102
Specimen 6	1.72983	-1.84025	1.6415	-1.74701	1.56053	-1.66113
Specimen 7	1.72247	-1.82062	1.62187	-1.72002	1.54581	-1.63414
Specimen 8	1.80835	-1.91386	1.73719	-1.84025	1.68321	-1.75928
Average:	1.7399525	1.84760875	1.65775625	-1.76326375	1.58813375	-1.6795337
Standard Deviation	0.0331	0.0325	0.0368	0.0367	0.0428	0.0372

step-6 (Continue)	HW 13 (V)	HW 14 (V)	HW 15 (V)	HW 16 (V)	HW 17 (V)	HW 18 (V)
Specimen 1	1.49919	-1.58752	1.45257	-1.53354	1.41576	-1.49183
Specimen 2	1.509	-1.59243	1.45748	-1.53845	1.42067	-1.49673
Specimen 3	1.53845	-1.61942	1.48692	-1.56053	1.44275	-1.51882
Specimen 4	1.50409	-1.59243	1.45257	-1.53354	1.40595	-1.48447
Specimen 5	1.56053	-1.63905	1.50409	-1.57525	1.45748	-1.52863
Specimen 6	1.50164	-1.59488	1.45502	-1.53599	1.41331	-1.49183
Specimen 7	1.47956	-1.56298	1.42803	-1.50164	1.38632	-1.46238
Specimen 8	1.58507	-1.66604	1.52127	-1.60469	1.47956	-1.56298
Average:	1.52219125	-1.6068437	1.46974375	-1.54795375	1.427725	-1.5047087
Standard Deviation	0.0335	0.0307	0.0292	0.0294	0.0283	0.0291
step-6 (Continue)	HW 19 (V)	HW 20 (V)				
Specimen 1	1.38877	-1.46238				
Specimen 2	1.39368	-1.4722				
Specimen 3	1.41822	-1.48937				
Specimen 4	1.3765	-1.45257				
Specimen 5	1.42558	-1.49919				
Specimen 6	1.39123	-1.46729				
Specimen 7	1.35442	-1.42558				
Specimen 8	1.45011	-1.52618				
Average:	1.39981375	-1.474345				
Standard Deviation	0.0282	0.0287				

Table A7: Step-1 (HW 1-20): Halfwave Current Values for C-Gun Machine at Applied Force of 2.2kN

Current values step-1	HW 1 (kA)	HW 2 (kA)	HW 3 (kA)	HW 4 (kA)	HW 5 (kA)	HW 6 (kA)
Specimen 1	10.5345877	-12.262022	11.4065268	-12.2620228	11.2956161	-12.135313
Specimen 2	10.4877086	-12.357070	11.4382525	-12.3095468	11.2956161	-12.166974
Specimen 3	10.5035069	-12.341272	11.4699136	-12.293684	11.3273417	-12.119450
Specimen 4	10.4243218	-12.29368	11.3907285	-12.2303616	11.216431	-12.103588

Specimen 5	10.6144177	-12.420457	11.4857764	-12.4363203	11.3748657	-12.181677
Specimen 6	10.7094656	-12.372933	11.4540508	-12.3254096	11.3590029	-12.198636
Specimen 7	10.4877086	-12.341272	11.4699136	-12.3729336	11.2956161	-12.166974
Specimen 8	10.5827565	-12.388796	11.4382525	-12.293684	11.3114789	-12.182837
Average:	10.5430592	-12.347188	11.4441768	12.3154953	11.309496	-12.156931
Standard Deviation	0.0838	0.0475	0.0306	0.0603	0.0451	0.0315
step-1 (Continue)	HW 7 (kA)	HW 8 (kA)	HW 9 (kA)	HW 10 (kA)	HW 11 (kA)	HW 12 (kA)
Specimen 1	11.121383	-11.992677	11.0579962	-11.9451533	11.0263351	-11.913492
Specimen 2	11.0579962	-11.992677	10.9154243	-11.8659682	10.8995615	-11.786783
Specimen 3	11.0263351	-11.92935	10.9154243	-11.8659682	10.9312871	-11.818444
Specimen 4	11.0263351	-11.929355	10.9470855	-11.881831	10.8995615	-11.865968
Specimen 5	11.0897219	-12.056064	10.9946094	-11.9134922	10.9470855	-11.881831
Specimen 6	11.1372458	-12.056064	11.0579962	-12.0085401	11.1055202	-11.992677
Specimen 7	11.0579962	-11.976879	10.9312871	-11.8501054	10.8995615	-11.834307
Specimen 8	11.0579962	-12.040265	10.9470855	-11.929355	10.9312226	-11.897629
Average:	11.0718762	-11.996667	10.9708636	-11.9075517	10.9550169	-11.873891
Standard Deviation	0.0384	0.0480	0.0554	0.0494	0.0691	0.0598
step-1 (Continue)	HW 13 (kA)	HW 14 (kA)	HW 15 (kA)	HW 16 (kA)	HW 17 (kA)	HW 18 (kA)
Specimen 1	11.0421334	-11.865968	11.0421334	-11.9134922	11.073859	-11.929355
Specimen 2	10.9946094	-11.802581	10.9946094	-11.8659682	10.9788111	-11.897629
Specimen 3	10.9788111	-11.850105	10.9788111	-11.8659682	11.0421334	-11.865968
Specimen 4	11.0104723	-11.897629	11.0104723	-11.9610162	11.0421334	-11.961016
Specimen 5	11.0421334	-11.929355	11.0421334	-11.9451533	11.0579962	-11.929355
Specimen 6	11.1847698	-11.992677	11.1847698	-12.0402658	11.2480921	-12.103588
Specimen 7	10.9788111	-11.802581	10.9788111	-11.881831	10.9946094	-11.834307
Specimen 8	11.0263351	-11.897629	11.0263351	-11.8976294	11.0263351	-11.913492
Average:	11.0322594	-11.879815	11.0322594	-11.9214155	11.0579962	-11.929338
Standard Deviation	0.0617	0.0600	0.0623	0.0555	0.0776	0.0756
step-1 (Continue)	HW 19 (kA)	HW 20 (kA)				
Specimen 1	11.121383	-11.913496				
Specimen 2	10.9788111	-11.897629				
Specimen 3	11.073859	-11.913492				
Specimen 4	11.1055202	-12.040201				
Specimen 5	11.121383	-11.945153				
Specimen 6	11.2956161	-12.103588				
Specimen 7	11.0421334	-11.834307				

Specimen 8	11.073859	-11.945153
Average:	11.1015706	-11.949127
Standard Deviation	0.0856	0.0795

Table A8: Step-2 (HW 1-20): Halfwave Current Values for C-Gun Machine at Applied Force of 2.2kN

Current values step-2	HW 1 (kA)	HW 2 (kA)	HW 3 (kA)	HW 4 (kA)	HW 5 (kA)	HW 6 (kA)
Specimen 1	11.5333004	-13.371001	12.3254096	-12.974946	11.976879	-12.800649
Specimen 2	11.1372458	-12.848173	11.9451533	-12.68980	11.6758723	-12.578892
Specimen 3	11.0104723	-12.848173	11.9134922	-12.721464	11.6916707	-12.563029
Specimen 4	11.0104723	-12.816512	11.881831	-12.673940	11.6916707	-12.531368
Specimen 5	10.9946094	-12.800649	11.881831	-12.705601	11.6758723	-12.547166
Specimen 6	11.0579962	-12.848173	11.8976294	-12.658077	11.6916707	-12.483844
Specimen 7	11.0897219	-12.911560	11.9451533	-12.73732	11.7075335	-12.515505
Specimen 8	10.9788111	-12.800649	11.8501054	-12.705601	11.6441467	-12.515505
Average:	11.1015787	-12.905611	11.9550757	-12.733345	11.7194145	-12.566995
Standard Deviation	0.1706	0.1791	0.1432	0.0943	0.0989	0.0926
step-2 (Continue)	HW 7 (kA)	HW 8 (kA)	HW 9 (kA)	HW 10 (kA)	HW 11 (kA)	HW 12 (kA)
Specimen 1	11.7867831	-12.673940	11.7075335	-12.6264162	11.7709203	-12.705601
Specimen 2	11.4857764	-12.420457	11.4540508	-12.3729336	11.4382525	-12.420457
Specimen 3	11.5649616	-12.436320	11.4223897	-12.3729336	11.4223897	-12.404594
Specimen 4	11.4065268	-12.372933	11.3590029	-12.3095468	11.34314	-12.277885
Specimen 5	11.4540508	-12.372933	11.4065268	-12.3095468	11.34314	-12.293684
Specimen 6	11.4382525	-12.341272	11.34314	-12.2620228	11.34314	-12.309546
Specimen 7	11.4857764	-12.388796	11.4223897	-12.3887964	11.4065268	-12.357070
Specimen 8	11.4540508	-12.388796	11.34314	-12.3254096	11.4223897	-12.388796
Average:	11.5095223	-12.424431	11.4322717	-12.3709507	11.4362374	-12.394704
Standard Deviation	0.1134	0.0982	0.1109	0.1043	0.1319	0.1275
step-2 (Continue)	HW 13 (kA)	HW 14 (kA)	HW 15 (kA)	HW 16 (kA)	HW 17 (kA)	HW 18 (kA)
Specimen 1	11.8501054	-12.68980	11.9134922	-12.7056014	11.8976294	-12.768988
Specimen 2	11.5174376	-12.420457	11.5649616	-12.4679815	11.6124855	-12.531368
Specimen 3	11.5333004	-12.404594	11.5174376	-12.3887964	11.5649616	-12.420457
Specimen 4	11.4065268	-12.293684	11.4382525	-12.293684	11.4699136	-12.357070
Specimen 5	11.3907285	-12.277885	11.4699136	-12.2778856	11.4857764	-12.262022

Specimen 6	11.4223897	-12.357070	11.4699136	-12.3254096	11.5015748	-12.404594
Specimen 7	11.4857764	-12.388796	11.5333004	-12.4521187	11.6441467	-12.467981
Specimen 8	11.4540508	-12.404594	11.4540658	-12.3412724	11.5332359	-12.372933
Average:	11.5075395	-12.404610	11.5451672	-12.4065937	11.5887155	-12.448177
Standard Deviation	0.1381	0.1186	0.1449	0.1303	0.1299	0.1421
step-2 (Continue)	HW 19 (kA)	HW 20 (kA)				
Specimen 1	11.929355	-12.832374				
Specimen 2	11.7075335	-12.499642				
Specimen 3	11.5808244	-12.420457				
Specimen 4	11.4382525	-12.309546				
Specimen 5	11.4857764	-12.325409				
Specimen 6	11.5649616	-12.357070				
Specimen 7	11.7075335	-12.499642				
Specimen 8	11.5333004	-12.388796				
Average:	11.6184422	-12.454117				
Standard Deviation	0.1475	0.1579				

Table A9: Step-3 (HW 1-20): Halfwave Current Values for C-Gun Machine at Applied Force of 2.2kN

Current values step-3	HW 1 (kA)	HW 2 (kA)	HW 3 (kA)	HW 4 (kA)	HW 5 (kA)	HW 6 (kA)
Specimen 1	11.5808244	-13.402662	12.3570707	-13.1491799	12.0877897	-12.927422
Specimen 2	11.6758723	-13.371001	12.293684	-13.006608	12.0560641	-12.927422
Specimen 3	11.6124855	-13.418525	12.3254096	-13.0699948	12.0085401	-12.879898
Specimen 4	11.5649616	-13.355138	12.293684	-13.0224708	12.0719269	-12.911560
Specimen 5	11.5808244	-13.355138	12.3095468	-13.054132	12.1035881	-12.927422
Specimen 6	11.5649616	-13.339340	12.3254096	-13.1175188	12.1035881	-12.911560
Specimen 7	11.4699136	-13.228429	12.2144988	-12.9908097	11.9926773	-12.78485
Specimen 8	11.6441467	-13.386864	12.3570707	-13.054132	12.151112	-12.911560

Average:	11.5867488	-13.357137	12.3095468	-13.0581057	12.0719108	-12.897712
Standard Deviation	0.0576	0.0546	0.0427	0.0506	0.0488	0.0451
step-3 (Continue)	HW 7 (kA)	HW 8 (kA)	HW 9 (kA)	HW 10 (kA)	HW 11 (kA)	HW 12 (kA)
Specimen 1	11.881831	-12.848173	11.881831	-12.8798989	11.9451533	-12.927422
Specimen 2	11.8976294	-12.832374	11.881831	-12.8165121	11.976879	-12.864036
Specimen 3	11.8659682	-12.848173	11.929355	-12.8956972	11.9451533	-12.974946
Specimen 4	11.881831	-12.800649	11.881831	-12.8640361	11.929355	-12.864036
Specimen 5	11.976879	-12.911560	11.976879	-12.9115601	12.0560641	-12.974946
Specimen 6	11.9451533	-12.879898	11.929355	-12.8956972	12.0402658	-12.959084
Specimen 7	11.8501054	-12.753125	11.8501054	-12.8323749	11.9768145	-12.959084
Specimen 8	11.9293357	-12.848173	11.9610162	-12.9274229	12.0085401	-13.006608
Average:	11.9035916	-12.84026	11.9115255	-12.8778999	11.9847781	-12.941270
Standard Deviation	0.0403	0.0448	0.0415	0.0358	0.0434	0.0491
step-3 (Continue)	HW 13 (kA)	HW 14 (kA)	HW 15 (kA)	HW 16 (kA)	HW 17 (kA)	HW 18 (kA)
Specimen 1	12.0560641	-12.927422	12.1353137	-12.9749468	12.1669749	-13.069994
Specimen 2	12.0560641	-12.879898	12.0560641	-12.9115601	12.1035881	-12.959084
Specimen 3	12.0877897	-12.990809	12.2303616	-13.006608	12.2778856	-13.101655
Specimen 4	12.0402658	-12.864036	12.0719269	-12.8956972	12.1035881	-12.974946
Specimen 5	12.1669749	-13.069994	12.2620228	-13.054132	12.3095468	-13.117518
Specimen 6	12.0877897	-12.974946	12.1828377	-13.0224708	12.2778856	-13.149179
Specimen 7	12.0560641	-12.959084	12.151112	-13.006608	12.2303616	-13.069994
Specimen 8	12.0877897	-13.022470	12.2144988	-13.1175188	12.24616	-13.133381
Average:	12.0798503	-12.961083	12.1630172	-12.9986927	12.2144988	-13.071969
Standard Deviation	0.0372	0.0651	0.0689	0.0677	0.0752	0.0660
step-3 (Continue)	HW 19 (kA)	HW 20 (kA)				
Specimen 1	12.293684	-13.085857				
Specimen 2	12.2303616	-12.990809				
Specimen 3	12.3095468	-13.117518				
Specimen 4	12.1986554	-12.990777				
Specimen 5	12.3412724	-13.101655				
Specimen 6	12.2778856	-13.133381				
Specimen 7	12.198636	-13.054132				
Specimen 8	12.3570707	-13.133381				
Average:	12.2758891	-13.075939				
Standard	0.0574	0.0548				

Deviation		
-----------	--	--

Table A10: Step-4 (HW 1-20): Halfwave Current Values for C-Gun Machine at Applied Force of 2.2kN

Current values step-4	HW 1 (kA)	HW 2 (kA)	HW 3 (kA)	HW 4 (kA)	HW 5 (kA)	HW 6 (kA)
Specimen 1	12.3887964	-13.925490	12.8006493	-13.4185254	12.5788923	-13.323477
Specimen 2	12.3254096	-13.877966	12.8006493	-13.3710014	12.5471666	-13.339340
Specimen 3	12.293684	-13.909627	12.737327	-13.3393403	12.4996427	-13.355138
Specimen 4	12.2620228	-13.925490	12.8481733	-13.4501866	12.5946906	-13.355138
Specimen 5	12.24616	-13.925490	12.7214642	-13.4185254	12.5788923	-13.386864
Specimen 6	12.2778856	-13.877966	12.7689881	-13.4501866	12.6105534	-13.371001
Specimen 7	12.1669749	-13.798717	12.737327	-13.3551386	12.5155055	-13.339340
Specimen 8	12.3095468	-13.877966	12.7056014	-13.3710014	12.5471666	-13.323477
Average:	12.28381	-13.889839	12.7650224	-13.3967382	12.5590637	-13.349222
Standard Deviation	0.0603	0.0402	0.0453	0.0403	0.0361	0.0209
step-4 (Continue)	HW 7 (kA)	HW 8 (kA)	HW 9 (kA)	HW 10 (kA)	HW 11 (kA)	HW 12 (kA)
Specimen 1	12.4679815	-13.418525	12.5788923	-13.4185254	12.6264162	-13.450186
Specimen 2	12.4521187	-13.386864	12.5313683	-13.4501866	12.6264162	-13.481912
Specimen 3	12.4045947	-13.355138	12.4521187	-13.3393403	12.4679815	-13.402662
Specimen 4	12.4679815	-13.450186	12.5155055	-13.4977105	12.5946906	-13.545234
Specimen 5	12.4838443	-13.386864	12.5313683	-13.4501866	12.5946906	-13.481912
Specimen 6	12.5313683	-13.434388	12.6264162	-13.4977105	12.6739402	-13.576960
Specimen 7	12.4045947	-13.402662	12.5788923	-13.4185254	12.5788923	-13.466049
Specimen 8	12.4838443	-13.355155	12.5313038	-13.4343882	12.5947203	-13.545234
Average:	12.462041	-13.398723	12.5432332	-13.4383217	12.5947185	-13.49376
Standard Deviation	0.0396	0.0324	0.0487	0.0473	0.0555	0.0542
step-4 (Continue)	HW 13 (kA)	HW 14 (kA)	HW 15 (kA)	HW 16 (kA)	HW 17 (kA)	HW 18 (kA)
Specimen 1	12.642279	-13.513573	12.7531253	-13.5610973	12.8481733	-13.703669
Specimen 2	12.689803	-13.545234	12.8006493	-13.6244841	12.8640361	-13.656145
Specimen 3	12.5630294	-13.466049	12.7531253	-13.6244841	12.8956972	-13.798717
Specimen 4	12.784851	-13.640346	12.8481733	-13.7036692	12.9749468	-13.798717
Specimen 5	12.6580774	-13.576960	12.8165121	-13.6720081	12.9274229	-13.798717
Specimen 6	12.737327	-13.656145	12.8640361	-13.7036692	12.9274229	-13.767056
Specimen 7	12.6264162	-13.497710	12.737327	-13.592823	12.8798989	-13.735394
Specimen 8	12.7056014	-13.529436	12.7689881	-13.6086213	12.8640361	-13.656145

Average:	12.6759231	-13.55318	12.7927421	-13.636357	12.8977043	-13.739320
Standard Deviation	0.0646	0.0629	0.0441	0.0487	0.0400	0.0575
step-4 (Continue)	HW 19 (kA)	HW 20 (kA)				
Specimen 1	13.006608	-13.81458				
Specimen 2	12.9908097	-13.767056				
Specimen 3	13.054132	-13.909627				
Specimen 4	13.0699948	-13.862104				
Specimen 5	13.054132	-13.893829				
Specimen 6	13.054132	-13.877966				
Specimen 7	12.9749468	-13.893829				
Specimen 8	12.959084	-13.735394				
Average:	13.0204799	-13.844298				
Standard Deviation	0.0399	0.0606				

Table A11: Step-5 (HW 1-20): Halfwave Current Values for C-Gun Machine at Applied Force of 2.2kN

Current values step-5	HW 1 (kA)	HW 2 (kA)	HW 3 (kA)	HW 4 (kA)	HW 5 (kA)	HW 6 (kA)
Specimen 1	12.7214642	-14.210634	13.1016559	-13.7511932	12.9432857	-13.687870
Specimen 2	12.7214642	-14.147247	13.006608	-13.6403469	12.8481733	-13.672008
Specimen 3	12.7056014	-14.131449	12.959084	-13.6720081	12.8956972	-13.751193
Specimen 4	12.7214642	-14.194771	12.9749468	-13.6561453	12.7689881	-13.640346
Specimen 5	12.7214642	-14.226497	12.9432857	-13.5769601	12.8481733	-13.687870
Specimen 6	12.7214642	-14.194771	12.9908097	-13.6244841	12.8323749	-13.672008
Specimen 7	12.737327	-14.131449	12.9432857	-13.592823	12.8640361	-13.608621
Specimen 8	12.689803	-14.147247	13.0224708	-13.7036692	12.8323749	-13.735394
Average:	12.7175065	-14.173008	12.9927683	-13.6522037	12.8541379	-13.681914
Standard Deviation	0.0131	0.0354	0.0491	0.0536	0.0475	0.0433

step-5 (Continue)	HW 7 (kA)	HW 8 (kA)	HW 9 (kA)	HW 10 (kA)	HW 11 (kA)	HW 12 (kA)
Specimen 1	12.8481733	-13.719532	12.8798989	-13.7511932	12.9274229	-13.877966
Specimen 2	12.8798989	-13.767056	13.054132	-13.8779668	13.0858576	-13.973014
Specimen 3	12.8956972	-13.81458	12.9908097	-13.9096279	13.7987172	-14.876034
Specimen 4	12.8006493	-13.767056	12.9432857	-13.7829188	12.9432857	-13.798717
Specimen 5	12.8165121	-13.81458	12.959084	-13.8779668	13.0699948	-14.004675
Specimen 6	12.8006493	-13.719532	12.8481733	-13.7511932	13.006608	-13.941353
Specimen 7	12.7689881	-13.719532	12.8481733	-13.719532	12.9115601	-13.767056
Specimen 8	12.784851	-13.719532	12.8798989	-13.7987172	12.9432857	-13.893829
Average:	12.8244274	-13.755175	12.925432	-13.8086395	13.0858415	-14.016581
Standard Deviation	0.0427	0.0394	0.0693	0.0662	0.2763	0.3336
step-5 (Continue)	HW 13 (kA)	HW 14 (kA)	HW 15 (kA)	HW 16 (kA)	HW 17 (kA)	HW 18 (kA)
Specimen 1	13.1491799	-14.068062	13.3234775	-14.1789734	13.4185254	-14.242360
Specimen 2	13.2600907	-14.115586	13.3393403	-14.2264974	13.5294362	-14.321545
Specimen 3	14.0364015	-14.923558	14.0363796	-14.8918975	14.1314495	-15.018606
Specimen 4	13.0858576	-13.941353	13.1809055	-14.0997238	13.3234775	-14.210634
Specimen 5	13.2442279	-14.083925	13.2918163	-14.1789734	13.4501866	-14.337408
Specimen 6	13.1175188	-14.020538	13.3868642	-14.1789734	13.4343882	-14.321545
Specimen 7	12.9749468	-13.941353	13.2125667	-14.1155866	13.3710014	-14.226497
Specimen 8	13.1016559	-14.083925	13.3551386	-14.1947718	13.5135733	-14.369069
Average:	13.2462349	-14.147288	13.3908111	-14.2581747	13.5215048	-14.380958
Standard Deviation	0.3104	0.2997	0.2527	0.2426	0.2391	0.2469
step-5 (Continue)	HW 19 (kA)	HW 20 (kA)				
Specimen 1	13.5769601	-14.305682				
Specimen 2	13.5769601	-14.416593				
Specimen 3	14.2264974	-15.050267				
Specimen 4	13.4501866	-14.226497				
Specimen 5	13.6244841	-14.416593				
Specimen 6	13.6244841	-14.416593				
Specimen 7	13.4977105	-14.305682				
Specimen 8	13.5769601	-14.384932				
Average:	13.6442804	-14.440355				
Standard Deviation	0.2271	0.2395				

Table A12: Step-6 (HW 1-20): Halfwave Current Values for C-Gun Machine at Applied Force of 2.2kN

Current values step-6	HW 1 (kA)	HW 2 (kA)	HW 3 (kA)	HW 4 (kA)	HW 5 (kA)	HW 6 (kA)
Specimen 1	13.2759535	-14.590890	13.4185254	-14.0839255	13.3393403	-14.147247
Specimen 2	13.1809055	-14.511641	13.4343882	-14.0205387	13.3393403	-14.163110
Specimen 3	13.2284295	-14.479980	13.3710014	-13.9413536	13.3710014	-14.115586
Specimen 4	12.9746244	-14.416593	13.2284295	-13.9096279	13.1967039	-14.036401
Specimen 5	12.959084	-14.305682	13.1808862	-13.8779668	13.1809055	-13.973014
Specimen 6	12.8640361	-14.305682	13.1016559	-13.81458	13.1491799	-13.973014
Specimen 7	12.9908097	-14.353206	13.3393403	-13.9096279	13.3076146	-14.131449
Specimen 8	12.8956972	-14.305682	13.1809055	-13.7829188	13.1967039	-13.973014
Average:	13.0461925	-14.408669	13.2818916	-13.9175674	13.2600987	-14.06410
Standard Deviation	0.1482	0.1024	0.1167	0.0931	0.0820	0.0787
step-6 (Continue)	HW 7 (kA)	HW 8 (kA)	HW 9 (kA)	HW 10 (kA)	HW 11 (kA)	HW 12 (kA)
Specimen 1	13.4185254	-14.337408	13.6244841	-14.5116412	13.7511932	-14.701737
Specimen 2	13.4026626	-14.305682	13.5452345	-14.4641172	13.7036692	-14.622552
Specimen 3	13.3076146	-14.210634	13.4977105	-14.3690693	13.6720081	-14.606689
Specimen 4	13.2125667	-14.163110	13.3710014	-14.3056825	13.5294362	-14.479980
Specimen 5	13.2125667	-14.083925	13.3393403	-14.2106346	13.4660494	-14.353206
Specimen 6	13.1967039	-14.178973	13.4026626	-14.3532065	13.5294362	-14.495778
Specimen 7	13.3868642	-14.305682	13.592823	-14.5116412	13.7987172	-14.733462
Specimen 8	13.1175188	-14.004675	13.3076146	-14.1155866	13.3868642	-14.305682
Average:	13.2818779	-14.198761	13.4601089	-14.3551974	13.6046717	-14.537386
Standard Deviation	0.1054	0.1088	0.1131	0.1331	0.1376	0.1458
step-6 (Continue)	HW 13 (kA)	HW 14 (kA)	HW 15 (kA)	HW 16 (kA)	HW 17 (kA)	HW 18 (kA)
Specimen 1	13.9413536	-14.876034	14.1314495	-14.9869454	14.3215453	-15.113654
Specimen 2	13.8462411	-14.796785	14.0680627	-14.9076958	14.1947718	-15.081993
Specimen 3	13.8462411	-14.812647	14.1155866	-14.8918975	14.2423602	-15.050267
Specimen 4	13.7353949	-14.701737	13.9730147	-14.7809867	14.0839255	-14.923558
Specimen 5	13.6403469	-14.543366	13.8462411	-14.7017371	13.9730147	-14.828510
Specimen 6	13.767056	-14.670075	13.8938296	-14.7492611	14.0839255	-14.907695
Specimen 7	13.9413536	-14.860171	14.1314495	-14.9710826	14.3056825	-15.161178
Specimen 8	13.6720081	-14.575028	13.9096279	-14.7492611	14.0364015	-14.812647
Average:	13.7987494	-14.729480	14.0086577	-14.8423584	14.1552034	-14.984938
Standard Deviation	0.1069	0.1187	0.1094	0.1031	0.1209	0.1251

step-6 (Continue)	HW 19 (kA)	HW 20 (kA)
Specimen 1	14.4165933	-15.192904
Specimen 2	14.2898842	-15.113525
Specimen 3	14.3849321	-15.113654
Specimen 4	14.2423602	-15.034469
Specimen 5	14.1314495	-14.923558
Specimen 6	14.1947718	-14.971082
Specimen 7	14.3532065	-15.145380
Specimen 8	14.1314495	-14.907695
Average:	14.2680809	-15.050283
Standard Deviation	0.1042	0.1002

APPENDIX B

CALCULATED SAMPLE DYNAMIC RESISTANCE PLOTS

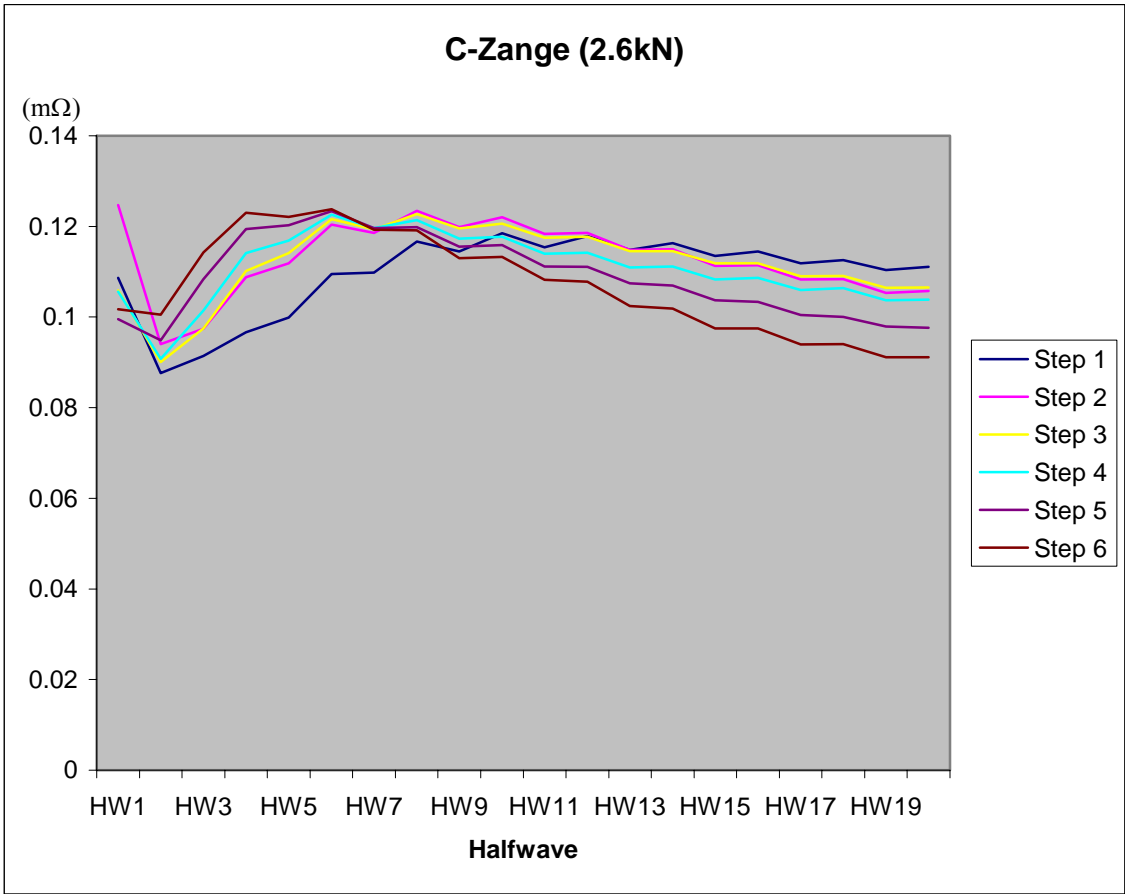


Figure B1: C-Gun (2.6 kN) steps 1-6, Dynamic Resistance plot

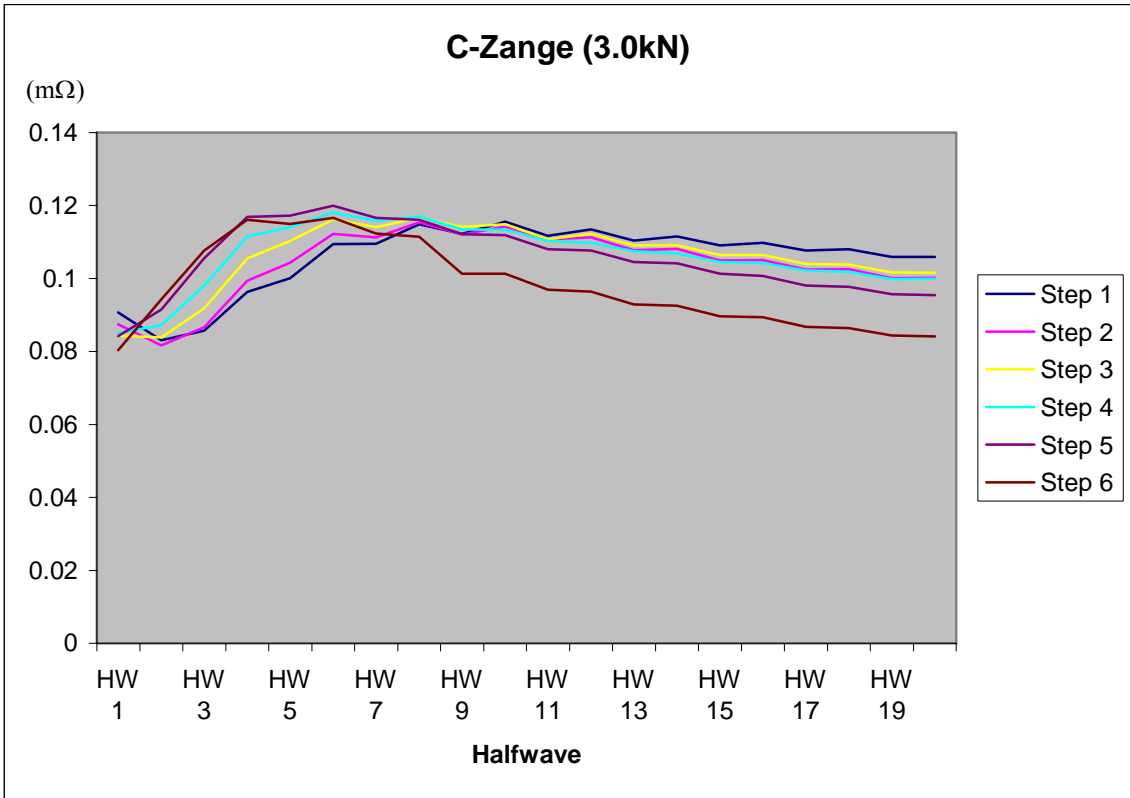


Figure B2: C-Gun (3.0 kN) steps 1-6, Dynamic Resistance plot

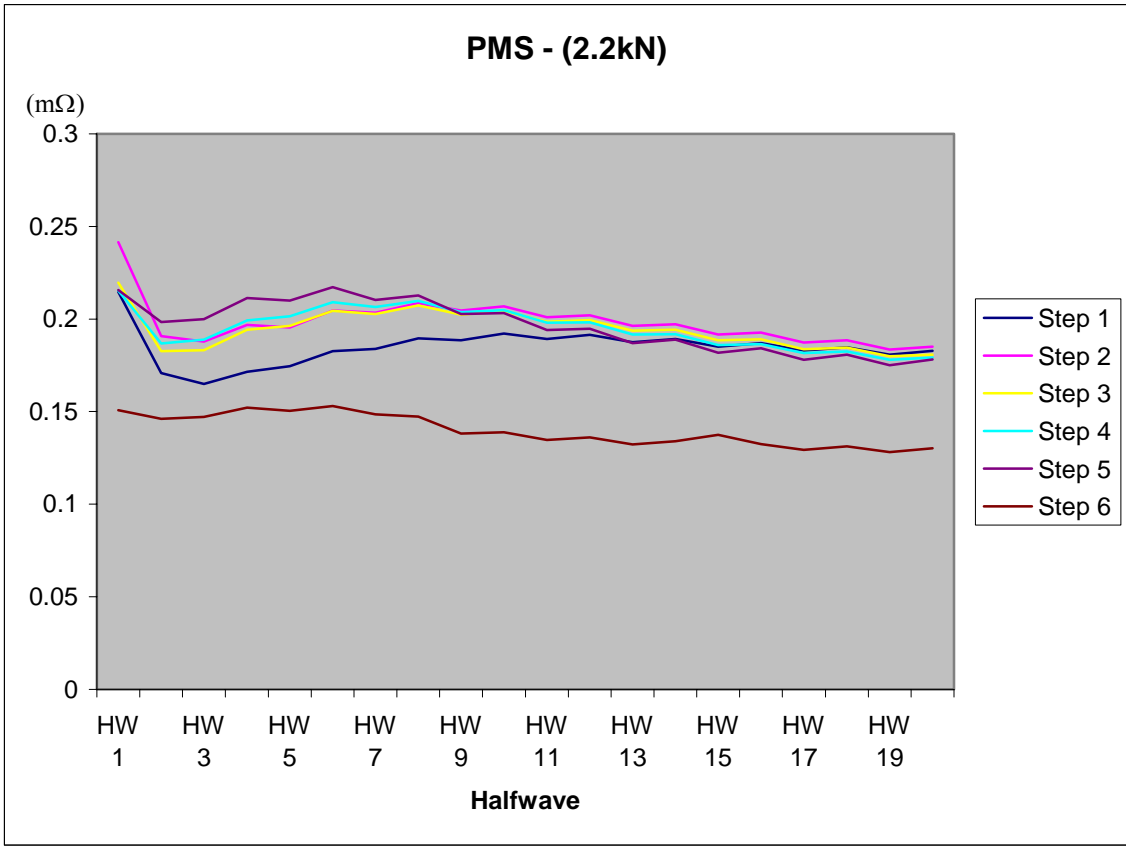


Figure B3: PMS (2.2 kN) steps 1-6, Dynamic Resistance plot

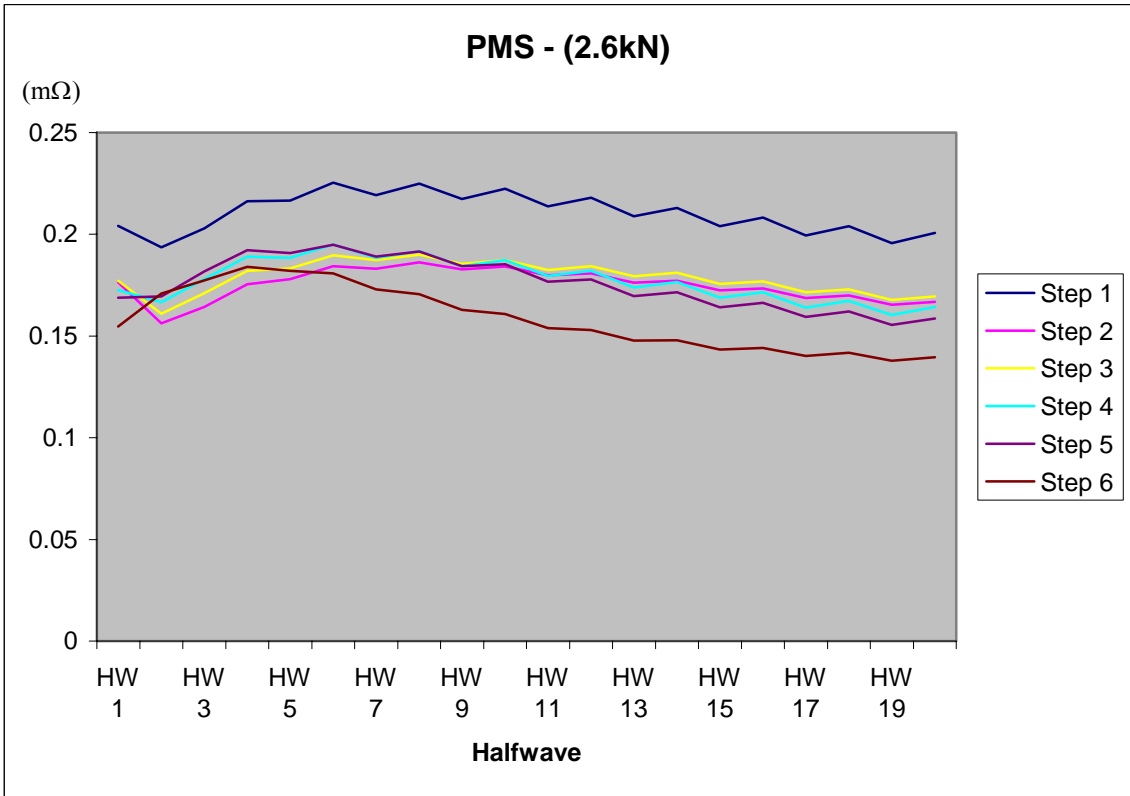


Figure B4: PMS (2.6 kN) steps 1-6, Dynamic Resistance plot

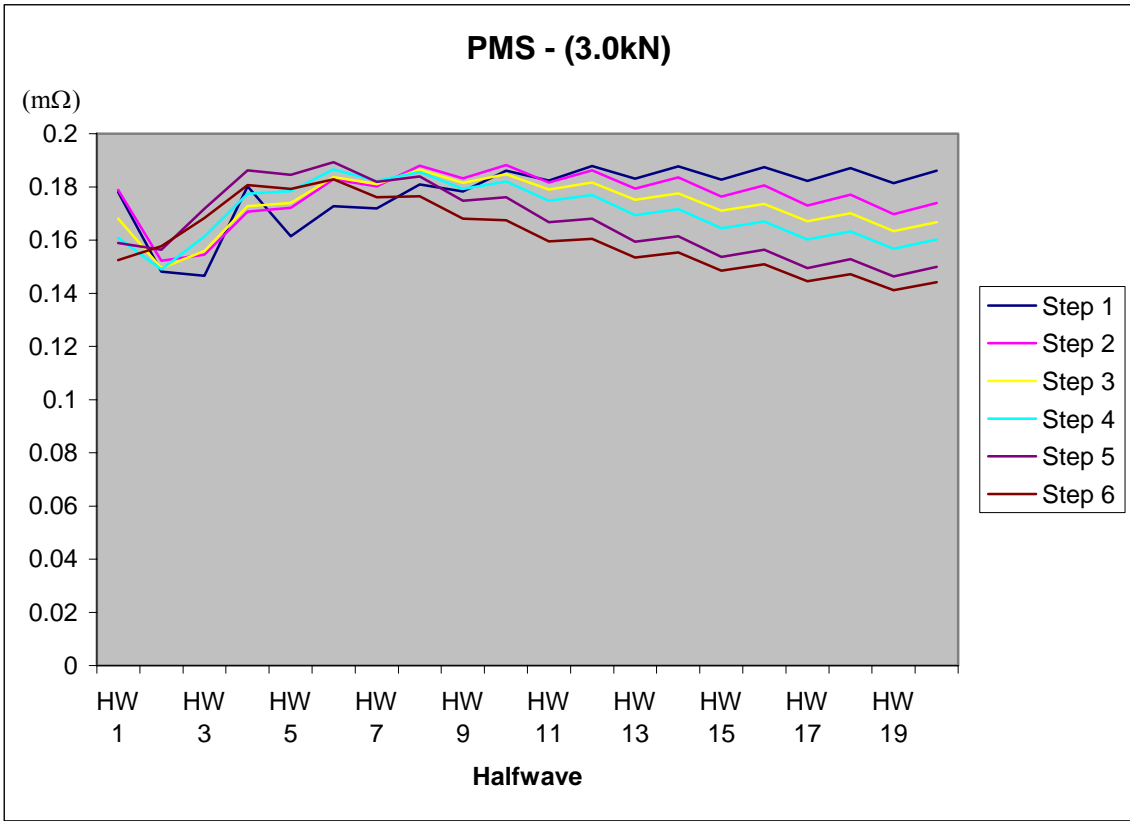


Figure B5: PMS (3.0 kN) steps 1-6, Dynamic Resistance plot

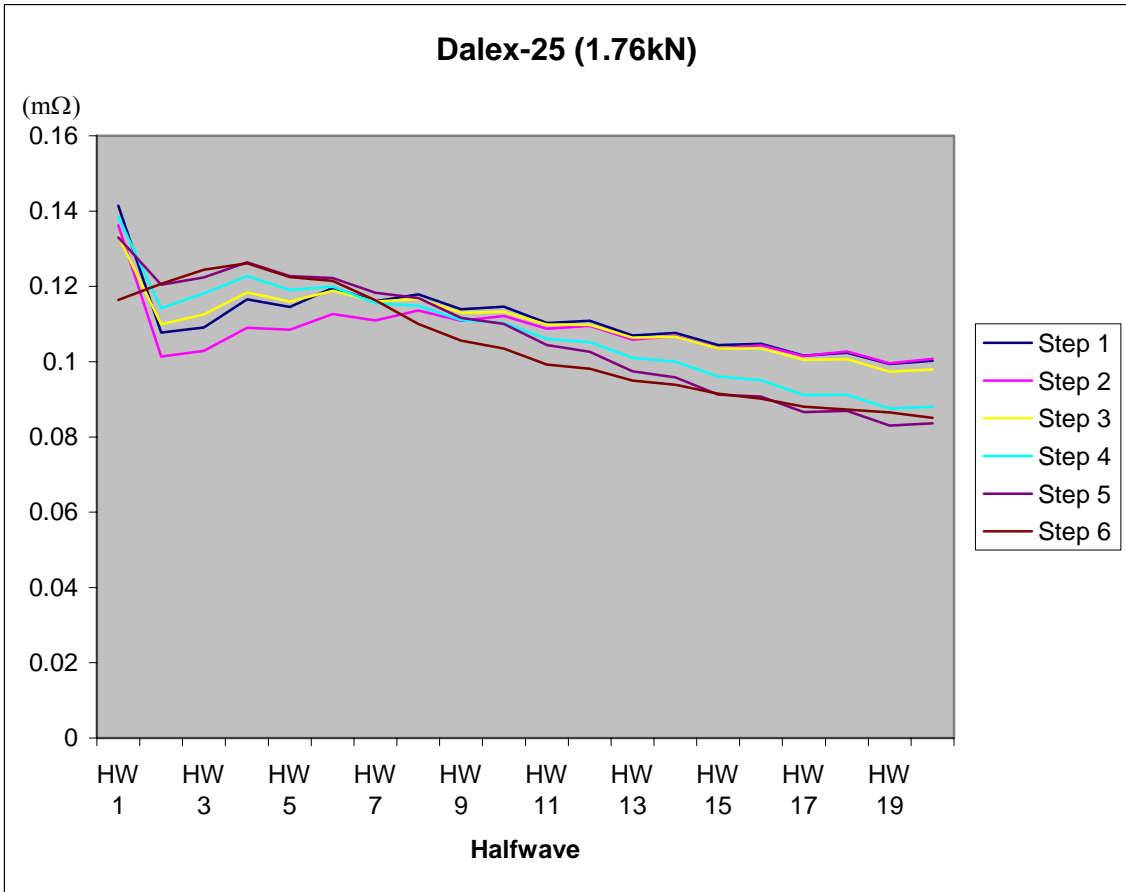


Figure B6: Dalex-25 (1.76 kN) steps 1-6, Dynamic Resistance plot

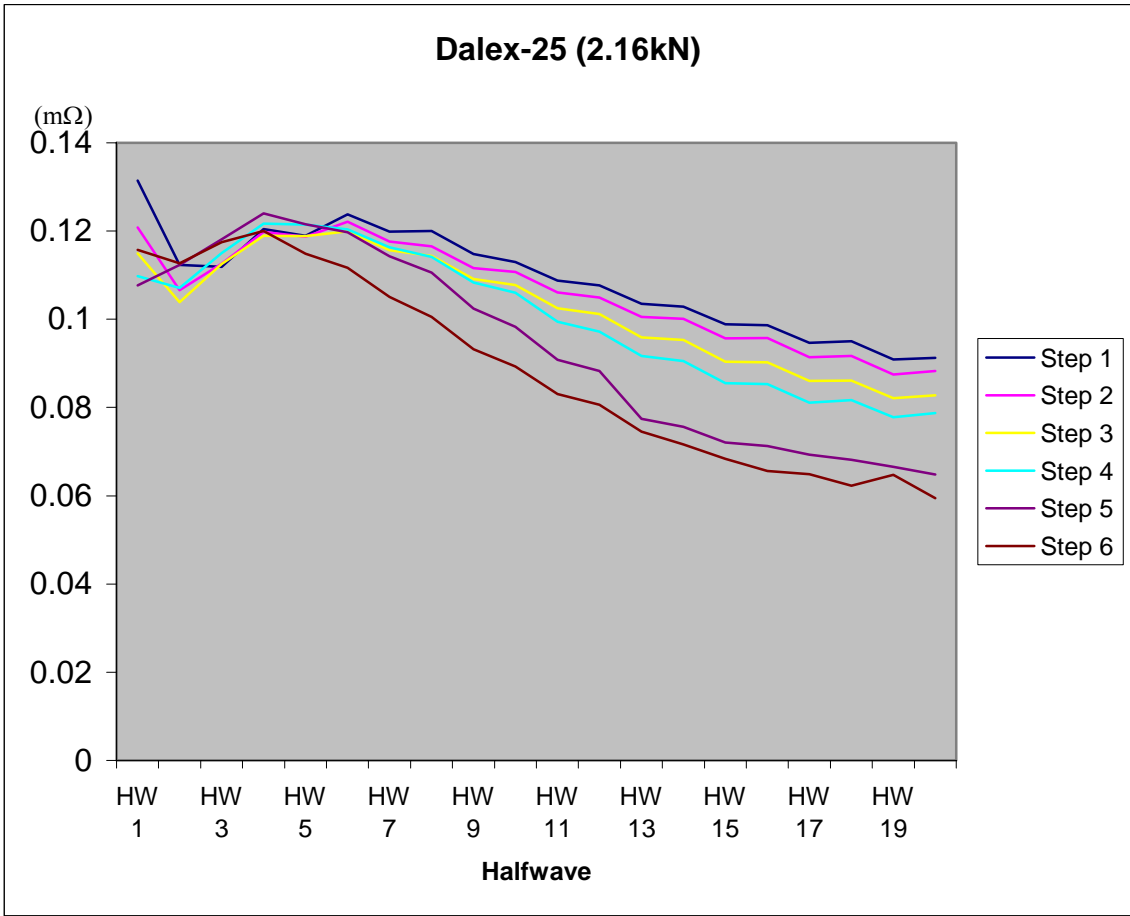


Figure B7: Dalex-25 (2.16 kN) steps 1-6, Dynamic Resistance plot

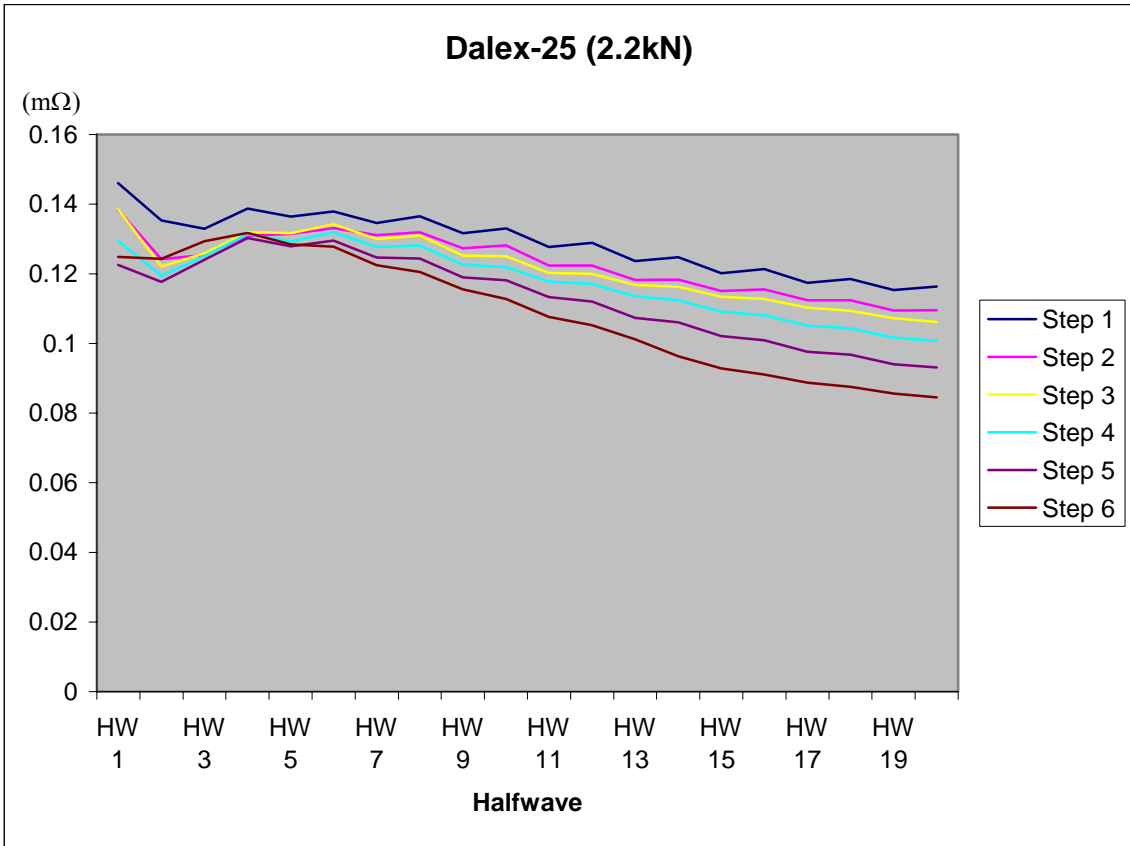


Figure B8: Dalex-25 (2.2 kN) steps 1-6, Dynamic Resistance plot

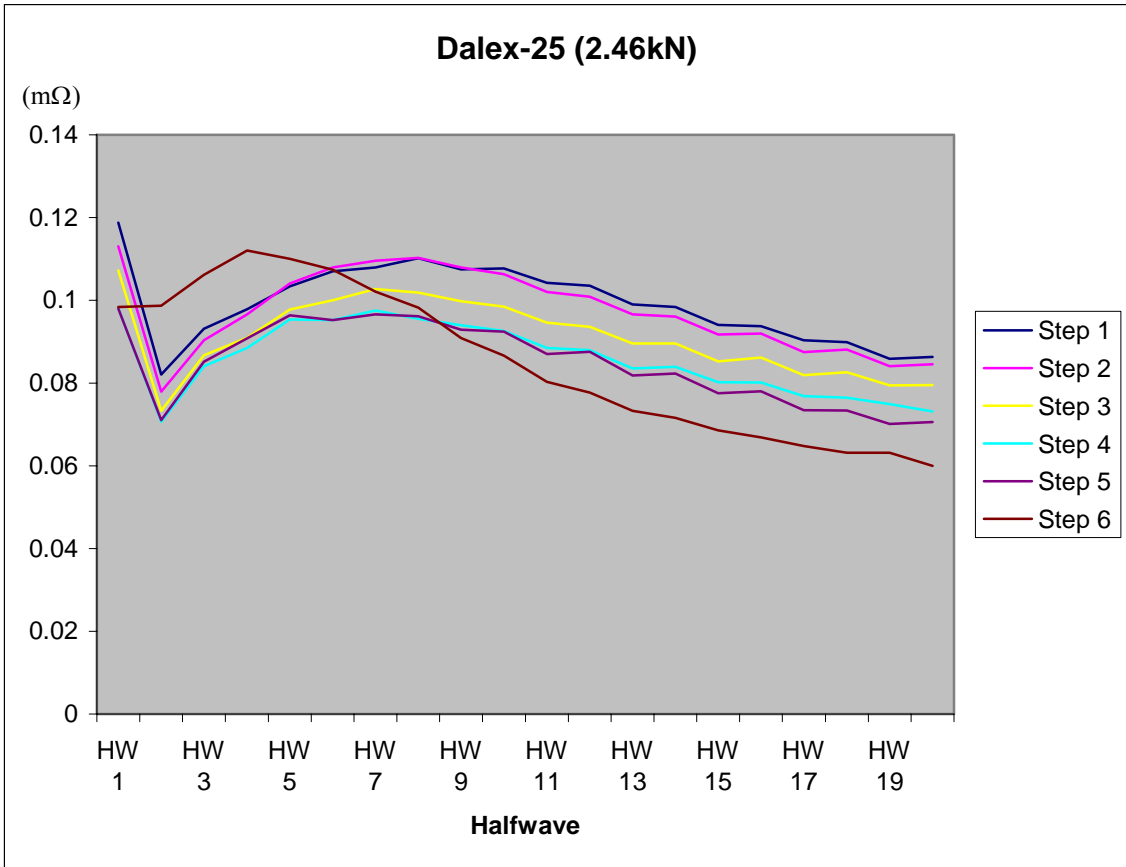


Figure B9: Dalex-25 (2.46 kN) steps 1-6, Dynamic Resistance plot

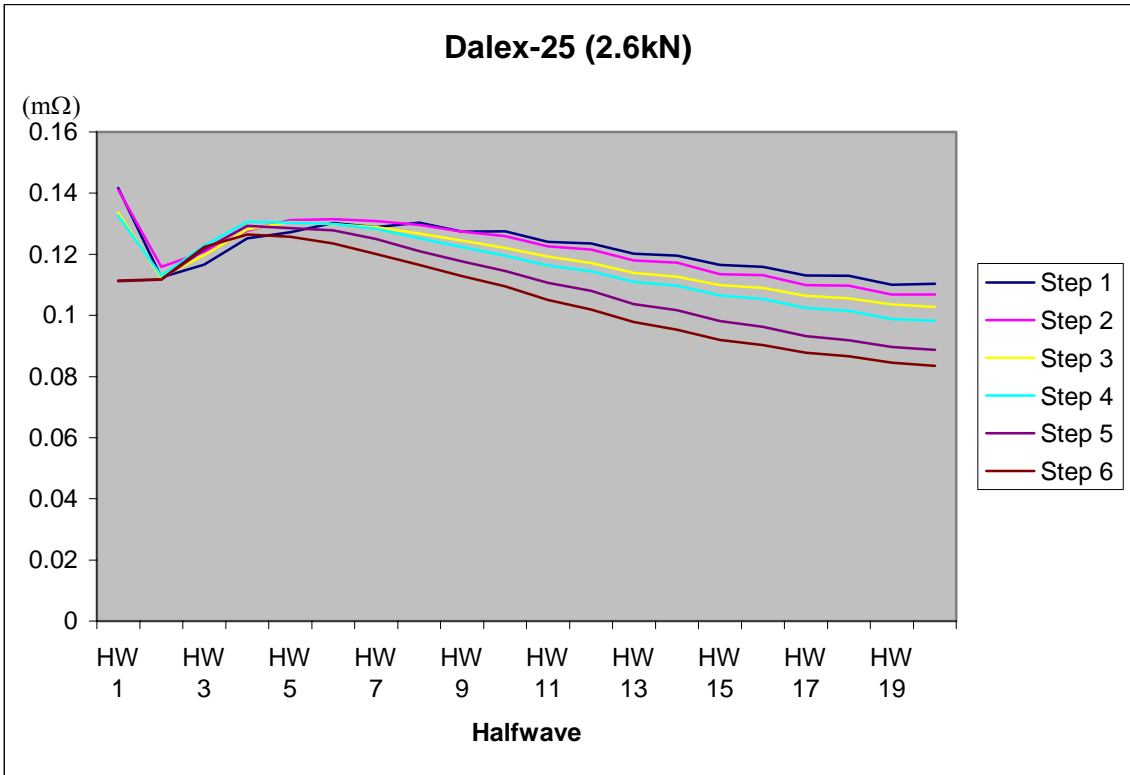


Figure B10: Dalex-25 (2.6 kN) steps 1-6, Dynamic Resistance plot

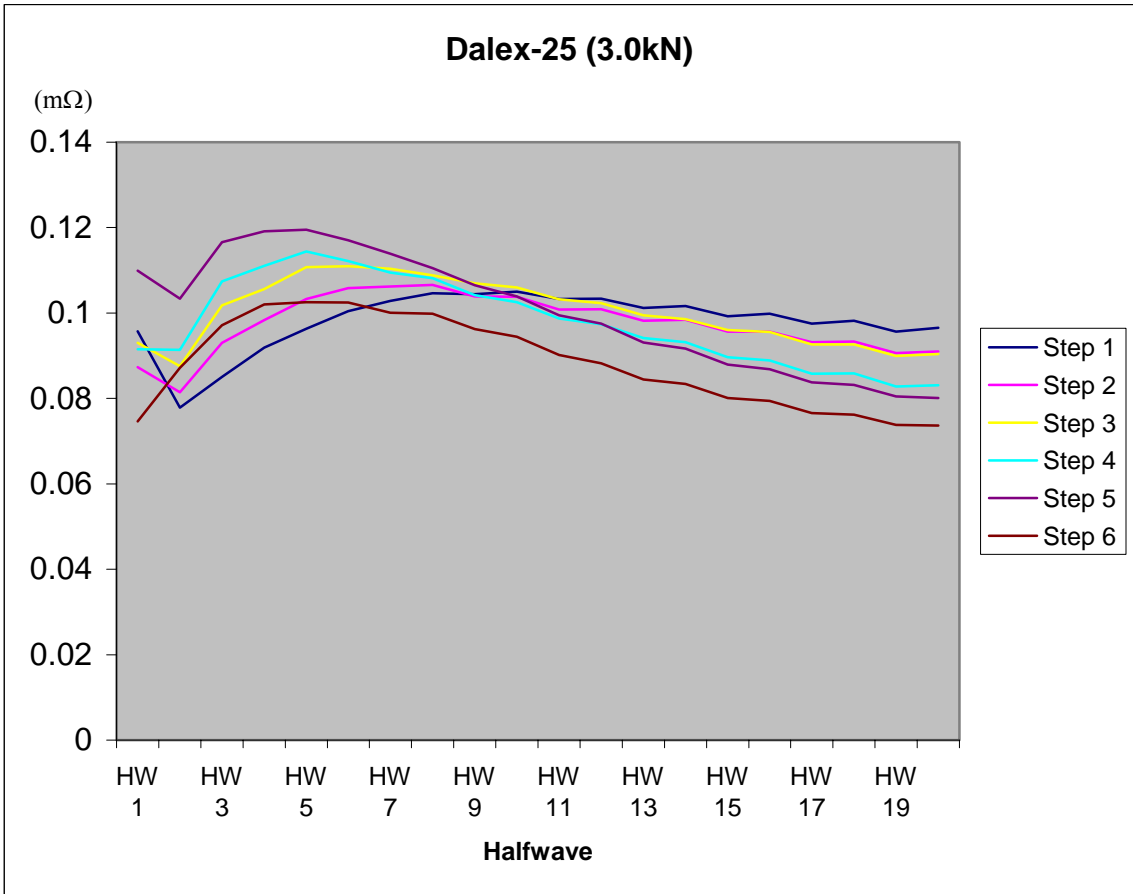


Figure B11: Dalex-25 (3.0 kN) steps 1-6, Dynamic Resistance plot

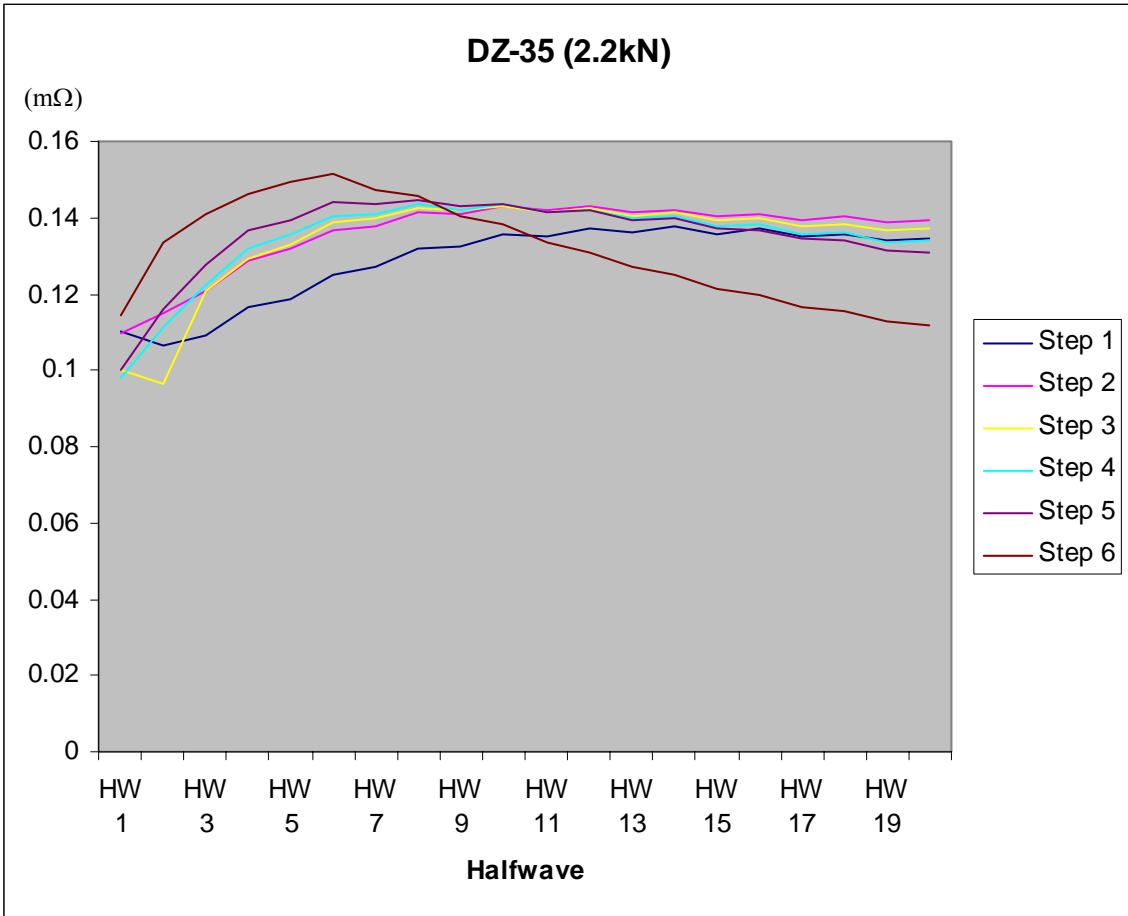


Figure B12: DZ-35 (2.2 kN) steps 1-6, Dynamic Resistance plot

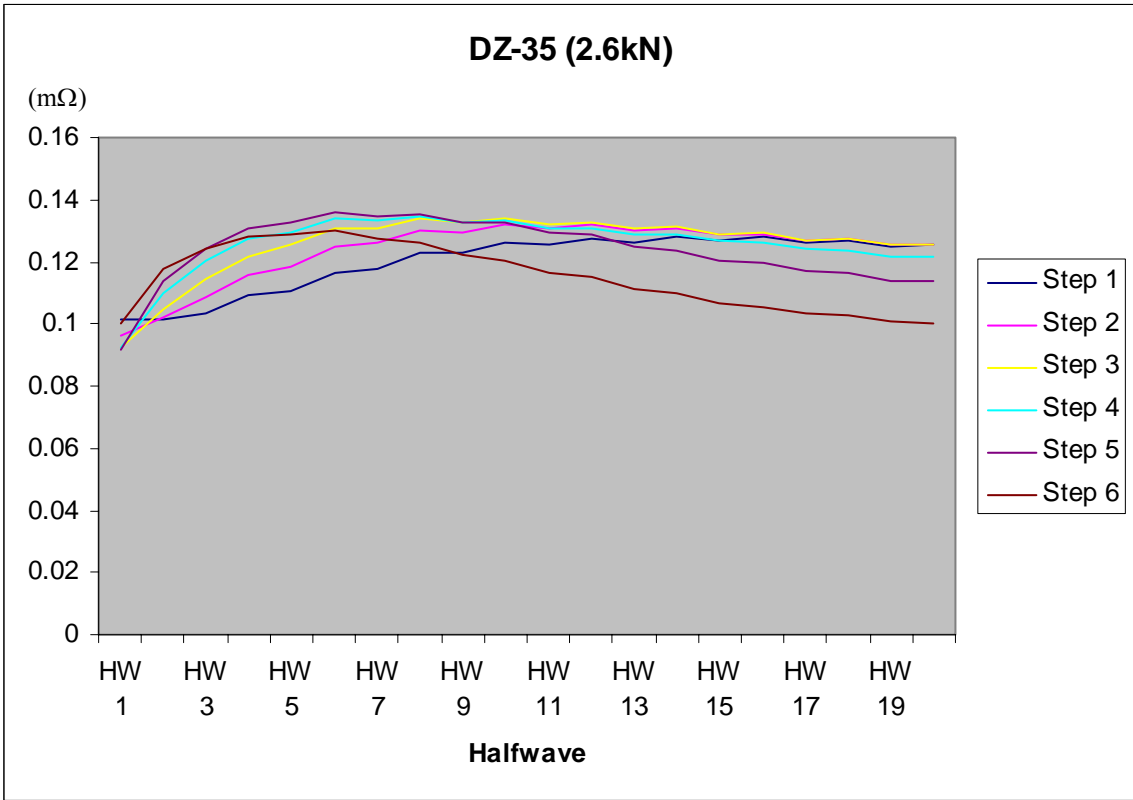


Figure B13: DZ-35 (2.6 kN) steps 1-6, Dynamic Resistance plot

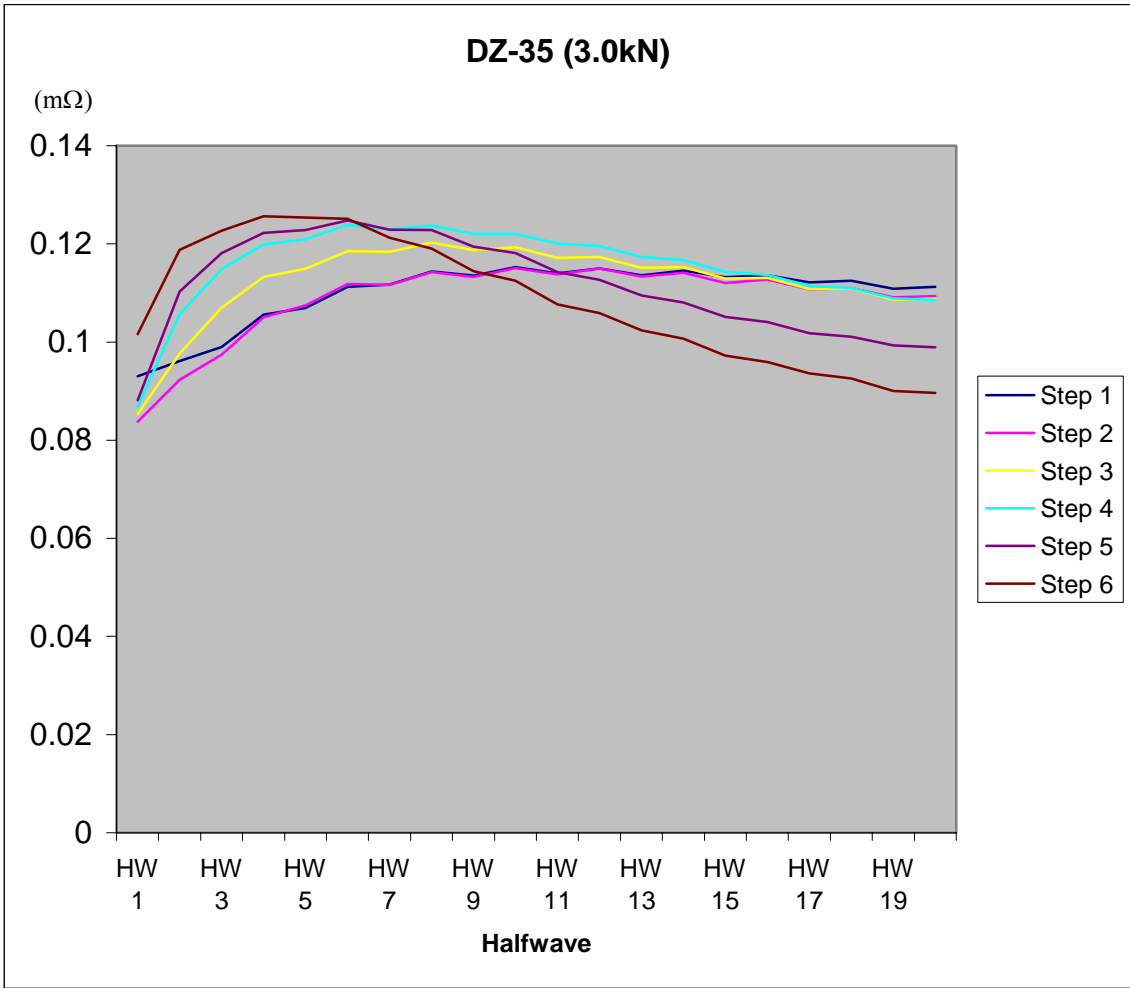


Figure B14: DZ-35 (3.0 kN) steps 1-6, Dynamic Resistance plot

APPENDIX C

FITTED DYNAMIC RESISTANCE CURVES

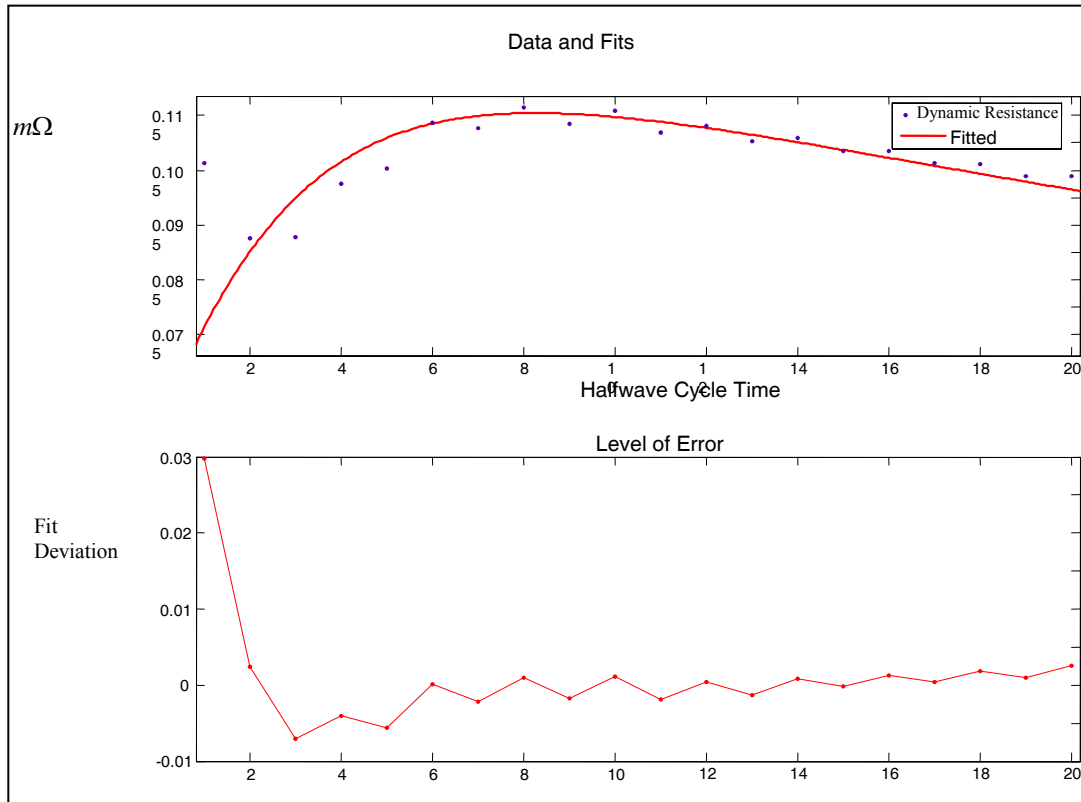


Figure C1: Fitted Dynamic Resistance Curve: C-Gun machine at 2.2kN applied Force.

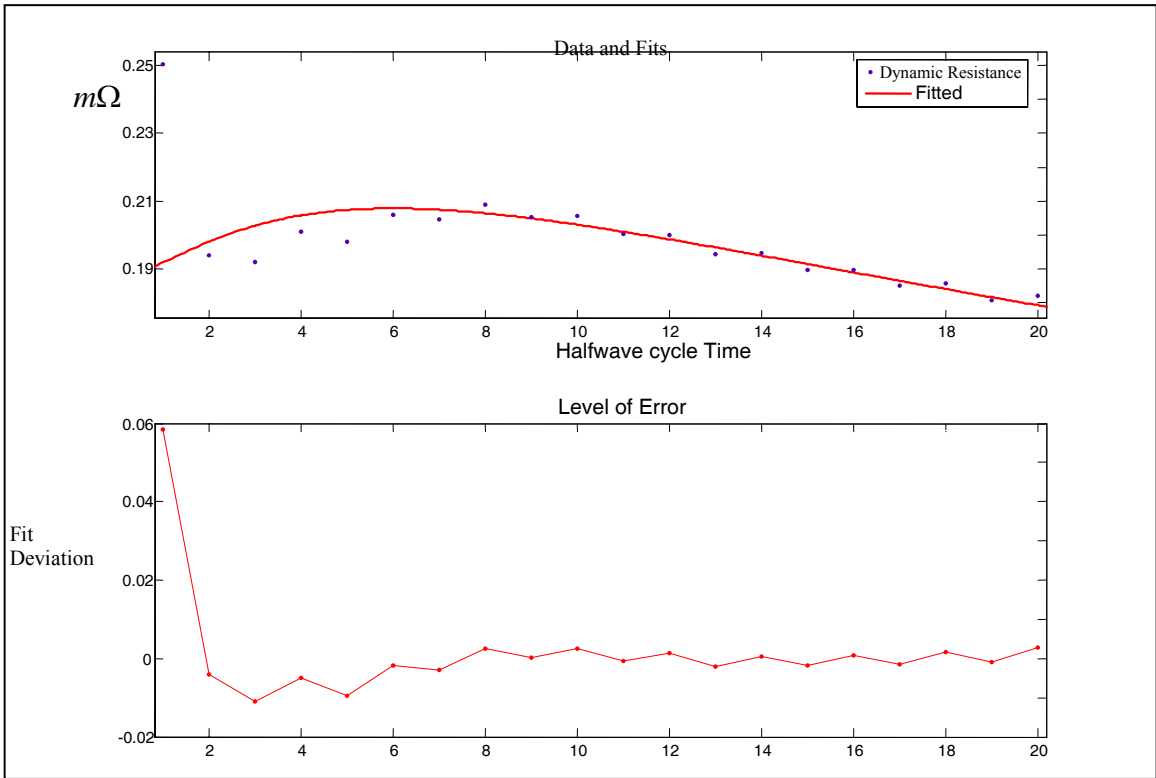


Figure C2: Fitted Dynamic Resistance Curve: PMS machine at 2.2 kN Force.

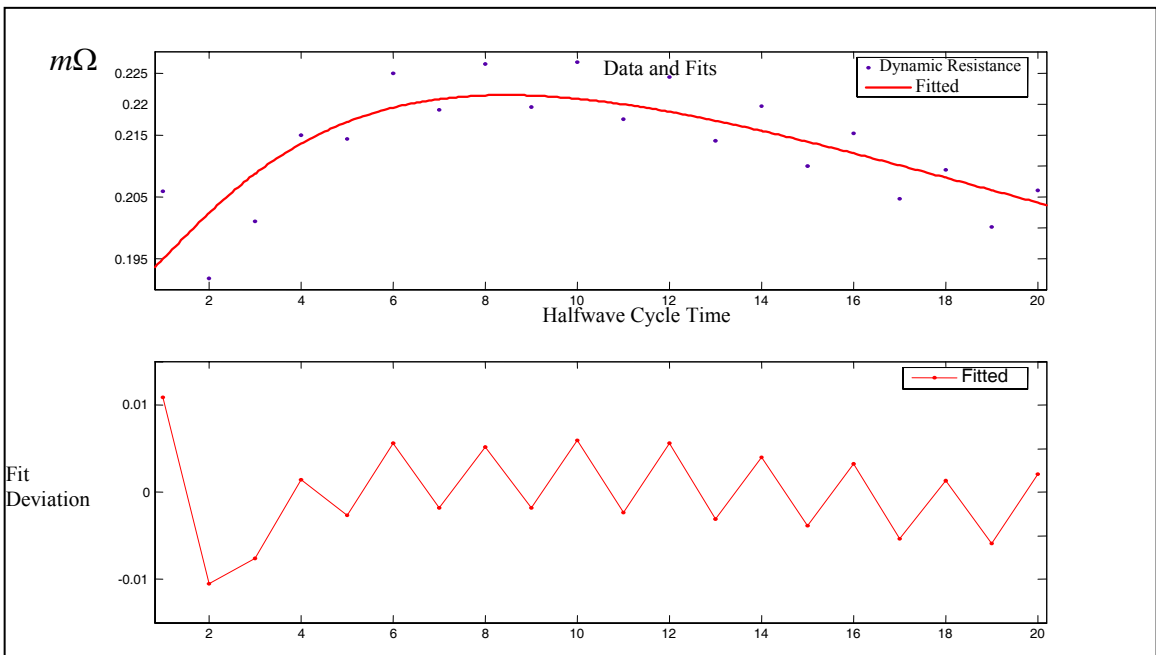


Figure C3: Fitted Dynamic Resistance Curve: PMS machine at 2.6kN Force.

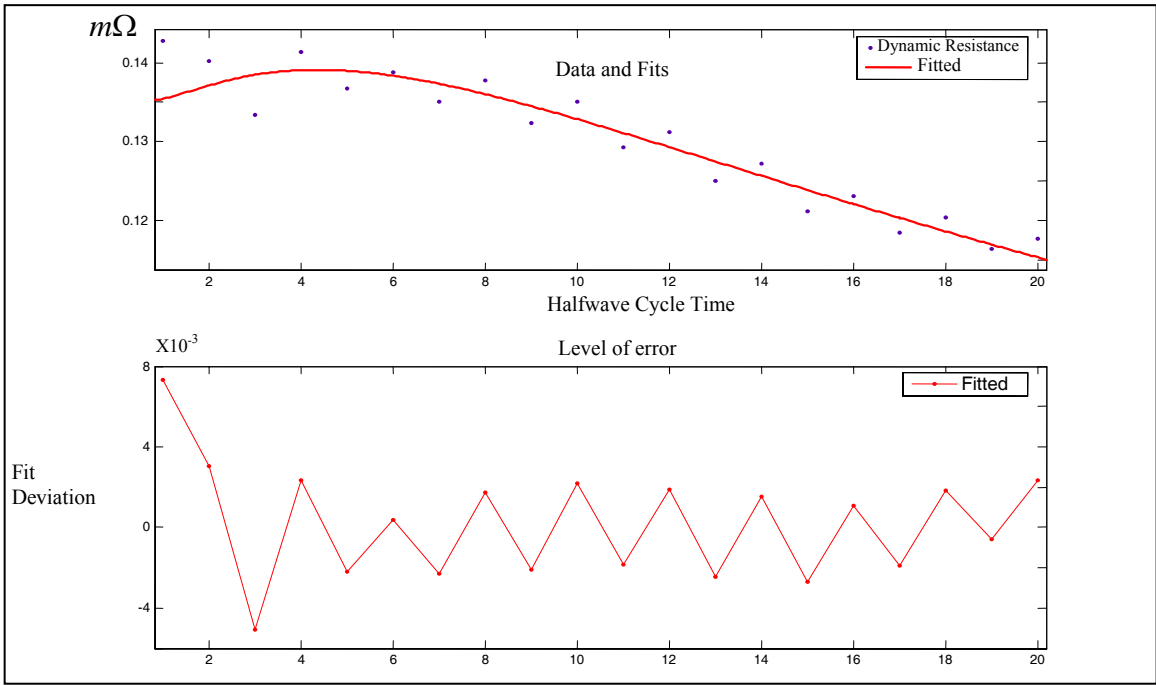


Figure C4: Fitted Dynamic Resistance Curve: Dalex-35 machine at 2.2kN Force.

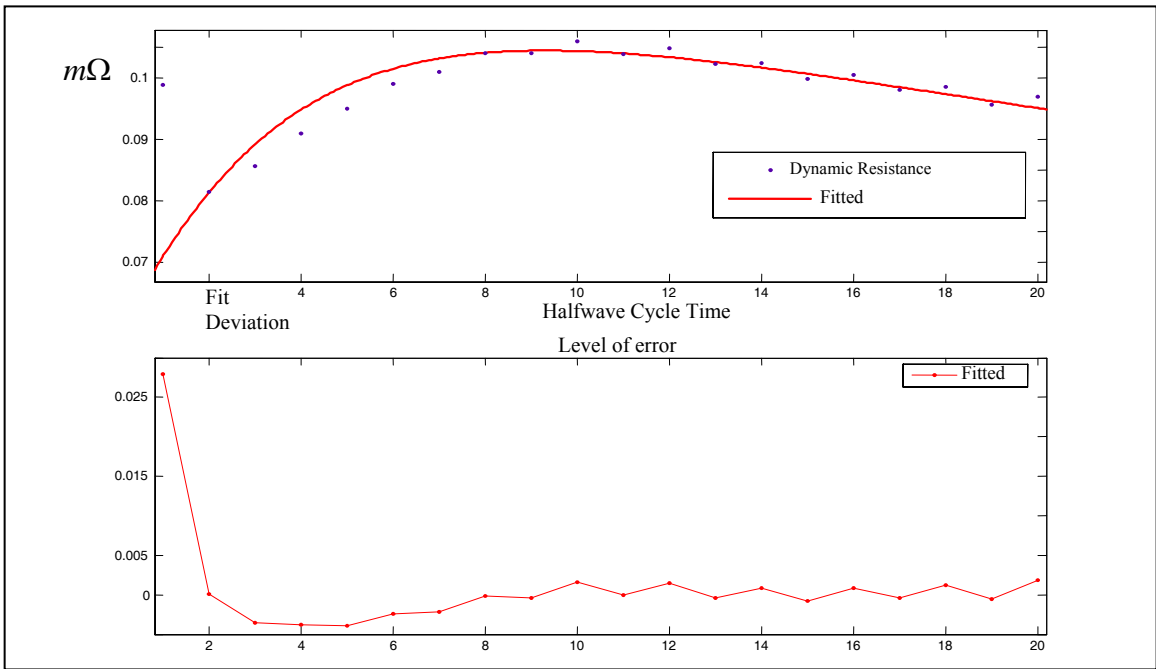


Figure C5: Fitted Dynamic Resistance Curve: Dalex-25 machine at 3.0kN Force.

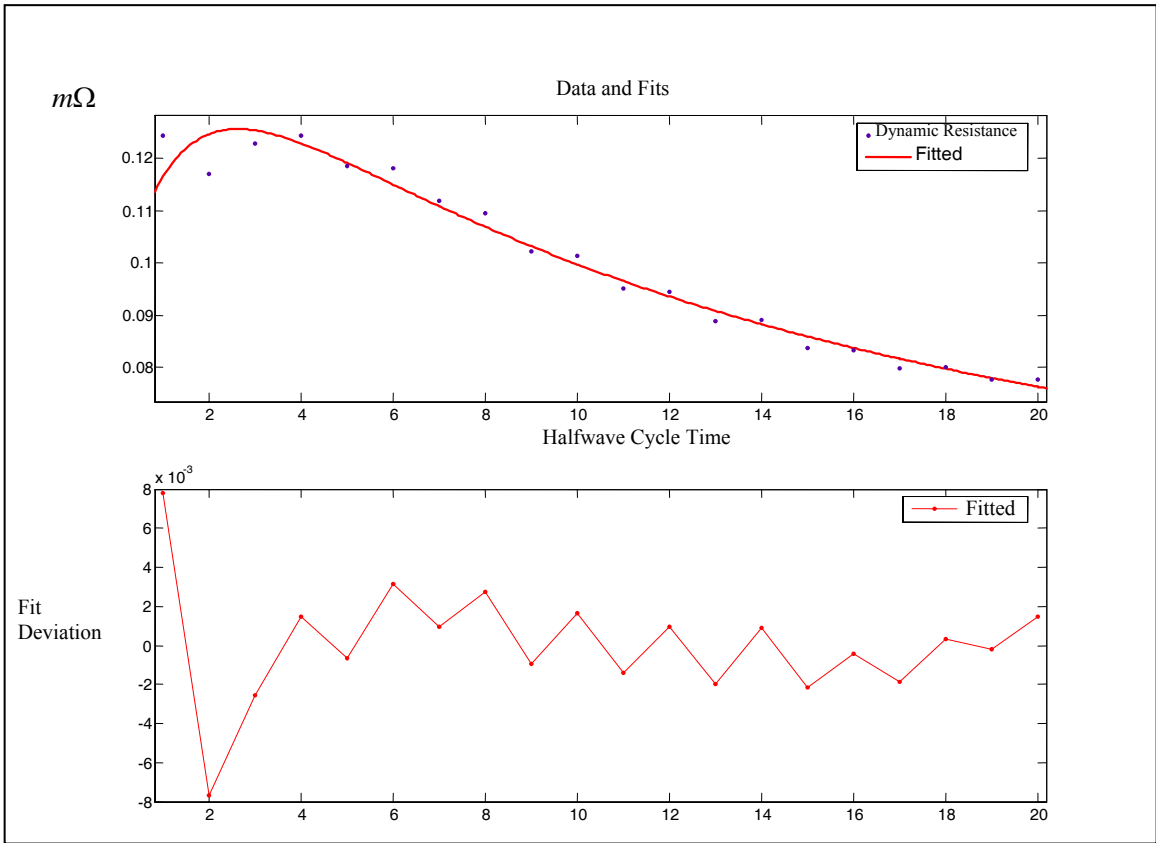


Figure C6: Fitted Dynamic Resistance Curve: Dalex-25 machine at 1.76 kN Force.

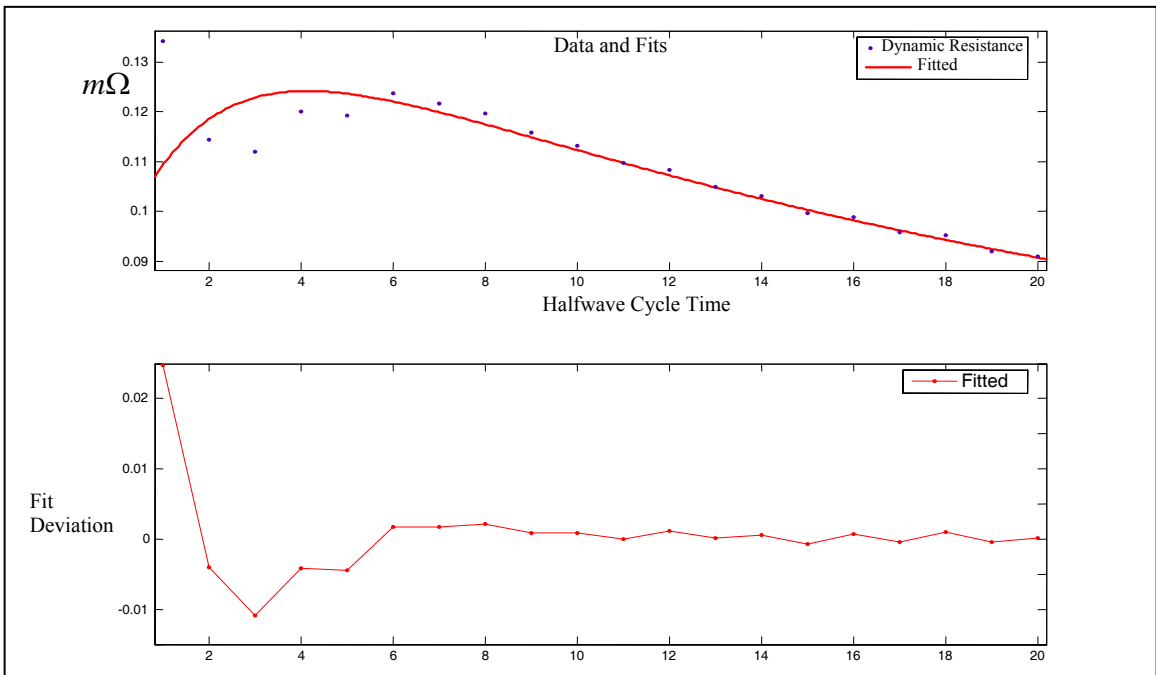


Figure C7: Fitted Dynamic Resistance Curve: Dalex-25 machine at 2.16 kN Force.

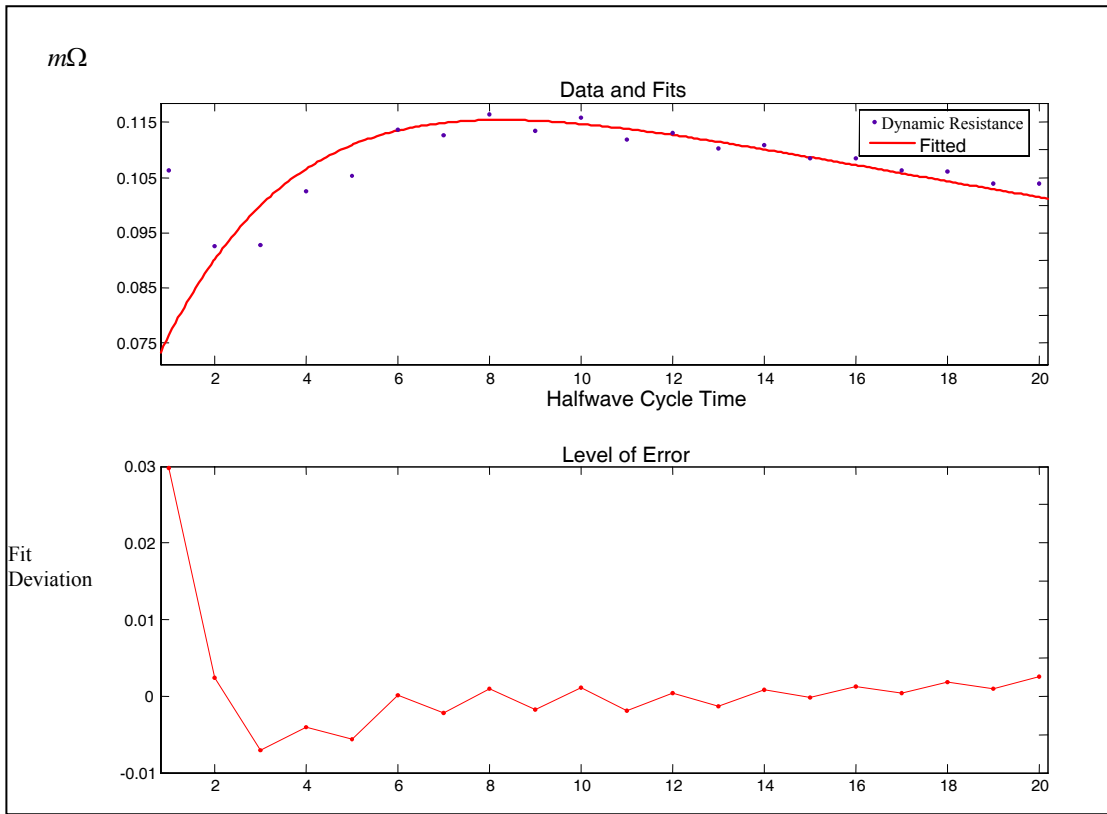


Figure C8: Fitted Dynamic Resistance Model Sample: C-Zange machine (3.0kN).

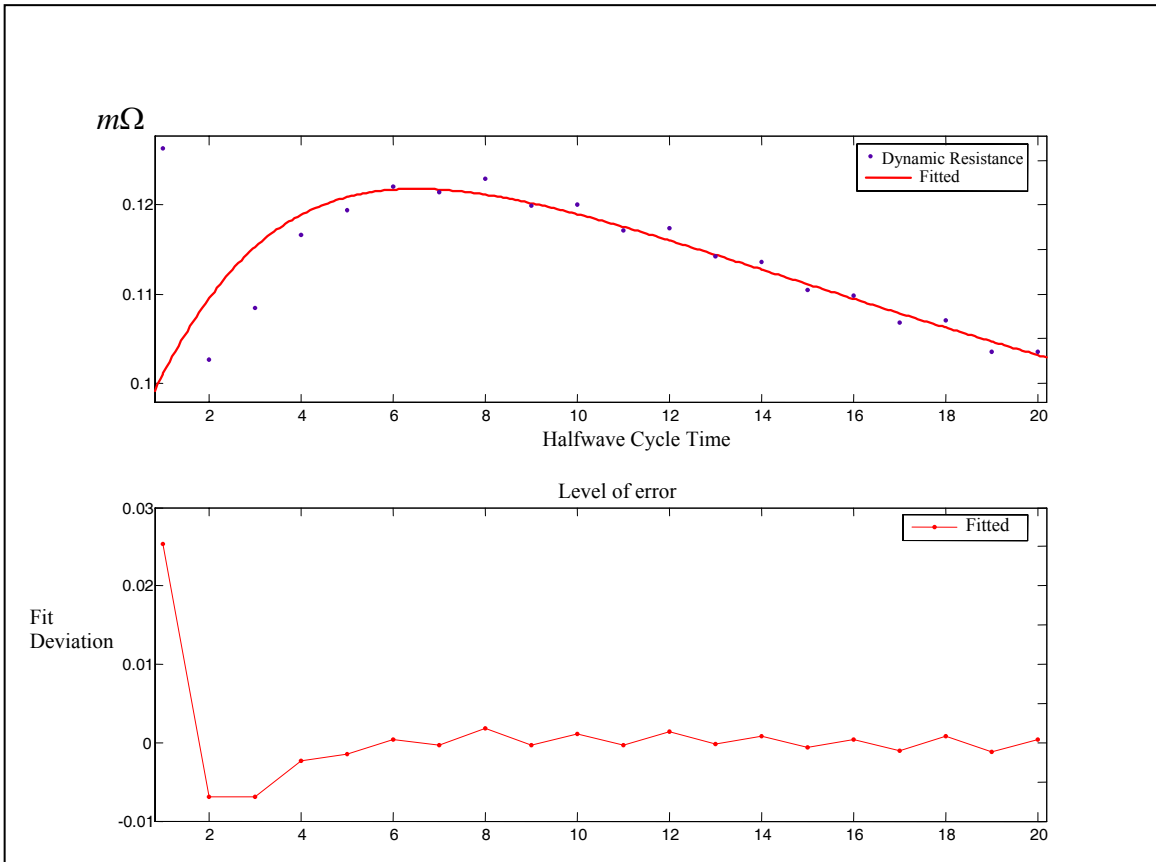


Figure C9: Fitted Dynamic Resistance Curve: Dalex-25 machine at 2.6kN Force.

APPENDIX D

CODE FOR RUNNING EMBEDDED NEURAL NETWORK MODEL: PREDICTING SAMPLE RESISTANCE

Private Sub CommandButton1_Click()

Step by step instructions are given on how to use the 'generated DLL for this purpose.

This function returns the network 'response'.

'Step 1: Create a new neural network object of the NSRecallNetwork type.

'-----

'Step 2: Set the pathName of the generated network DLL.

'-----

The DLL_PATH_NAME below is defined in the Globals module as the 'path to the newly generated DLL.

nn.dllPathName = DLL_PATH_NAME

'Step 3: Load the saved network weights.

'-----

'The initial best weights file is an exact copy of the weights file that was saved 'when the DLL was generated. However, the best weights file will change with each 'run of the TrainNetwork function if the network is reset before training.

nn.loadWeights BEST_WEIGHTS_PATH_NAME

'Step 4: Define the input data.

'-----

'The original breadboard's training input data has been added to this 'workbook in the 'Input' worksheet. This step retrieves the data from this worksheet

into an array then 'transposes this array to get it in the right format for input into the generated DLL.

'The number of inputs in the input data must match the number of inputs expected by the generated DLL.

```
' Dim inputDataTransposed As Variant, inputData As Variant
' inputData = Array(ForceText.Value, DiamterText.Value, KText.Value,
' MText.Value, RoText.Value)
```

```
Dim inputData(0 To 4, 0 To 0) As Variant
inputData(0, 0) = CSng(ForceText.Value)
inputData(1, 0) = CSng(DiamterText.Value)
inputData(2, 0) = CSng(KText.Value)
inputData(3, 0) = CSng(MText.Value)
inputData(4, 0) = CSng(RoText.Value)
```

```
' With ThisWorkbook.Sheets("Input")
'   If .Cells(2, 1).CurrentRegion.Columns.Count = 1 Then
'     inputDataTransposed = .Range(.Cells(2, 1), .Cells(2, 1).End(xlDown)).Value
'   Else
'     inputDataTransposed = .Range(.Cells(2, 1), .Cells(2,
1).End(xlToRight).End(xlDown)).Value
'   End If
' End With
' inputData = TransposeArray(inputDataTransposed)
```

'Step 5: Send the input data to the network DLL.

```
'-----
nn.inputData = inputData
```

'Step 6: Get the network response (output).

```
'-----
```

'The network response is assigned to the return value of GetNetworkResponse
'function.

```
Dim netout As Variant  
netout = nn.getResponse
```

```
outputText.Value = netout(0, 0)
```

'Step 7: Release the neural network object.

```
'-----
```

```
Set nn = Nothing
```

```
End Sub
```

APPENDIX E

CODE FOR RUNNING EMBEDDED NEURAL NETWORK MODEL: PREDICTING OVERALL PROCESS PARAMETER

Private Sub CommandButton1_Click()

Step by step instructions are given on how to use the 'generated DLL for this purpose.
This function returns the network 'response'.

'Step 1: Create a new neural network object of the NSRecallNetwork type.

'-----

'Step 2: Set the pathName of the generated network DLL.

'-----

The DLL_PATH_NAME below is defined in the Globals module as the 'path to the
newly generated DLL.

nn.dllPathName = DLL_PATH_NAME

'Step 3: Load the saved network weights.

'-----

'The initial best weights file is an exact copy of the weights file that was saved
'when the DLL was generated. However, the best weights file will change with each
'run of the TrainNetwork function if the network is reset before training.

nn.loadWeights BEST_WEIGHTS_PATH_NAME

'Step 4: Define the input data.

'-----

'The original breadboard's training input data has been added to this
'workbook in the 'Input' worksheet. This step retrieves the data from this worksheet

into an array then 'transposes this array to get it in the right format for input into the generated DLL.

'The number of inputs in the input data must match the number of inputs
'expected by the generated DLL.

```
' Dim inputDataTransposed As Variant, inputData As Variant  
' inputData = Array(ForceText.Value, ResistanceText.Value, DiameterText.Value)
```

```
Dim inputData(0 To 2, 0 To 0) As Variant  
inputData(0, 0) = CSng(ForceText.Value)  
inputData(1, 0) = CSng(ResistanceText.Value)  
inputData(2, 0) = CSng(DiameterText.Value)
```

```
' With ThisWorkbook.Sheets("Input")  
'   If .Cells(2, 1).CurrentRegion.Columns.Count = 1 Then  
'       inputDataTransposed = .Range(.Cells(2, 1), .Cells(2, 1).End(xlDown)).Value  
'   Else  
'       inputDataTransposed = .Range(.Cells(2, 1), .Cells(2,  
1).End(xlToRight).End(xlDown)).Value  
'   End If  
' End With  
' inputData = TransposeArray(inputDataTransposed)
```

'Step 5: Send the input data to the network DLL.

```
'-----  
nn.inputData = inputData
```

'Step 6: Get the network response (output).

```
'-----
```

'The network response is assigned to the return value of GetNetworkResponse
'function.

```
Dim netout As Variant
```



```
netout = nn.getResponse  
CurrentText.Value = netout(0, 0)
```

'Step 7: Release the neural network object.

'-----

```
Set nn = Nothing
```

```
End Sub
```

APPENDIX F

PREDICTION OF EFFECTIVE CURRENT FOR DESIRED WELD DIAMETER USING CONTROLLER FORM

C-gun Machine with an applied force of 3.0 kN

The screenshot shows a software interface window titled "UserForm1". It contains three input fields: "Force" with the value 3.0, "Resistance" with the value 0.10148, and "Diameter" with the value 3.7. Below these fields is a "CommandButton" and an output field labeled "Current" with the value 6.703784.

Predicted = 6.703784

Actual = 6.48

Prediction accuracy = 96.55%

F1: Effective Current Predicted for C-Gun Machine 3.0kN Applied Force

C-gun Machine with an applied force of 2.6 kN

UserForm1

Force: 2.6

Resistance: 0.08983

Diameter: 6.0

CommandButton

Current: 7.98468

Predicted = 7.98468
 Actual = 8.29
 Prediction accuracy = 95.29%

Figures F2: Effective Current Predicted for C-Gun Machine 2.6 kN Applied Force

C-gun Machine with applied force of 2.2 kN

UserForm1

Force: 2.2

Resistance: 0.1159

Diameter: 5.3

CommandButton

Current: 7.121756

Predicted = 7.121756
 Actual = 7.1
 Prediction accuracy = 99.66%

F3: Effective Current Predicted for C-Gun Machine 2.2 kN Applied Force

Dalex Machine with an applied force of 1.76 kN

UserForm1

Force: 1.76

Resistance: 0.094029

Diameter: 3.5

CommandButton

Current: 5.383359

Predicted = 5.383359
Actual = 5.18
Prediction accuracy = 96.86%

F4: Effective Current Predicted for Dalex Machine 1.76 kN Applied Force

Dalex Machine with an applied force of 2.46 kN

UserForm1

Force: 2.46

Resistance: 0.0816243

Diameter: 3.9

CommandButton

Current: 6.38831

Predicted = 6.38831
Actual = 6.58
Prediction accuracy = 97.04%

F5: Effective Current Predicted for Dalex Machine 2.46 kN Applied Force

Dalex Machine with an applied force of 3.0 kN

UserForm1

Force: 3.0

Resistance: 0.0728734

Diameter: 6.1

CommandButton

Current: 8.358552

Predicted = 8.358552
 Actual = 8.49
 Prediction accuracy = 97.97%

F6: Effective Current Predicted for Dalex Machine 3.0 kN Applied Force

PMS Machine with an applied force of 2.2 kN

UserForm1

Force: 2.2

Resistance: 0.1868678

Diameter: 3.8

CommandButton

Current: 6.474659

Predicted = 6.474659
 Actual = 6.35
 Prediction accuracy = 98.08%

F7: Effective Current Predicted for PMS Machine 2.2 kN Applied Force

PMS Machine with an applied force of 2.6 kN

The screenshot shows a software interface titled 'UserForm1'. It contains four input fields: 'Force' with the value 2.6, 'Resistance' with the value 0.162920004, and 'Diameter' with the value 5.85. Below these fields is a 'CommandButton' and a 'Current' field displaying the predicted value of 7.986079.

Predicted = 7.986079
 Actual = 7.68
 Prediction accuracy = 95.28%

F8: Effective Current Predicted for PMS Machine 2.6 kN Applied Force

PMS Machine with an applied force of 3.0 kN

The screenshot shows a software interface titled 'UserForm1'. It contains four input fields: 'Force' with the value 3.0, 'Resistance' with the value 0.1331025, and 'Diameter' with the value 6.2. Below these fields is a 'CommandButton' and a 'Current' field displaying the predicted value of 8.963214.

Predicted = 8.963214
 Actual = 9.36
 Prediction accuracy = 93.88%

F9: Effective Current Predicted for PMS Machine 3.0 kN Applied Force

DZ Machine with an applied force of 3.0 kN

UserForm1

Force: 3.0

Resistance: 0.10806

Diameter: 4.4

CommandButton

Current: 7.325683

Predicted = 7.325683
 Actual = 7.61
 Prediction accuracy = 95.61%

F10: Effective Current Predicted for DZ Machine 3.0 kN Applied Force

DZ Machine with an applied force of 2.6 kN

UserForm1

Force: 2.6

Resistance: 0.09992

Diameter: 6.0

CommandButton

Current: 8.088946

Predicted = 8.088946
 Actual = 8.32
 Prediction accuracy = 96.43%

F11: Effective Current Predicted for DZ Machine 2.6 kN Applied Force

DZ Machine with an applied force of 2.2 kN

The image shows a VBA UserForm titled "UserForm1" with a blue title bar and a close button. The form has a light beige background and contains the following elements:

- Force: 2.2
- Resistance: 0.13469
- Diameter: 3.7
- CommandButton: A button with a dotted border and the text "CommandButton".
- Current: 6.073895

Predicted = 6.073895
Actual = 6.49
Prediction accuracy = 93.58%

F12: Effective Current Predicted for DZ Machine 2.2 kN Applied Force

APPENDIX G

PAPER SUBMISSION 1

MODELLING DYNAMIC RESISTANCE VARIABLE IN RESISTANCE SPOT WELDING

Pius Nwachukwu Oba, Professor D. Chandler and Dr. S. Oerder
(University of the Witwatersrand, Johannesburg, South Africa)

Prof. Dr.-Ing. Dr. h.c.L. Dorn and Dr. Ing. Kevin Momeni
(Technical University Berlin, Germany)

Abstract

The non linear and complex nature of dynamic resistance variables makes it difficult to predict weld quality. Presented in this paper is the method used to obtain appropriate models for predicting weld resistance from dynamic resistance halfwaves.

An empirical three parameter approximate mathematical function model with dependent and independent variables was developed for curve fitting the nonlinear halfwave dynamic resistance curve. The values of the parameters were used for determining overall resistance for any desired weld diameter. The prediction capability of the empirical model for predicting resistance in any welding machine was improved by passing the outputs from the empirical model through neural network learning. By using the multilayer perceptron (MLP) neural network architecture, resistance of each sample was predicted with an accuracy of about 99.9% to 97%. This estimated resistance can be used for predicting weld quality with good reproducibility.

APPENDIX H

PAPER SUBMISSION 2

MODELLING RESISTANCE SPOT WELDING PARAMETERS FOR PREDICTING EFFECTIVE WELD CURRENT

Pius Nwachukwu Oba, Professor D. Chandler and Dr. S. Oerder
(University of the Witwatersrand, Johannesburg, South Africa)

Prof. Dr.-Ing. Dr. h.c.L. Dorn and Dr. Ing. Kevin Momeni
(Technical University Berlin, Germany)

Abstract

Presented in this paper is a model used for predicting effective weld current (RMS) for desired weld diameter (weld quality) in the resistance spot welding process. Electrical parameters namely effective weld current and dynamic resistance with applied electrode force, are identified as the strongest input signals necessary to predict the output weld diameter. These input parameters are used for developing a neural network process model for predicting effective weld current.

An initial empirical model developed by the authors as was used for predicting sample resistance which was integrated with this model for predicting required effective weld current for any desired weld diameter. The prediction accuracy of this model was in the range of 94% to 99%. This neural network process model was designed by optimising the squared error between the neural network output and the desired output. The neural network process model delivers effective current for any desired weld diameter. The model is observed to predict the desired output accurately.

APPENDIX I

PAPER 3 DEVELOPED FOR PUBLICATION

CASE STUDY ON IMPROVING NEURAL NETWORK PREDICTIVE CAPABILITY APPLICATION IN RESISTANCE SPOT WELDING QUALITY MODELLING

Pius Nwachukwu Oba, Professor D. Chandler and Dr. S. Oorder
(University of the Witwatersrand, Johannesburg, South Africa)

Prof. Dr.-Ing. Dr. h.c.L. Dorn and Dr. Ing. Kevin Momeni
(Technical University Berlin, Germany)

Abstract

A three parameter approximate mathematical function model with dependent and independent variables was used for curve fitting nonlinear halfwave dynamic resistance curve generated from the resistance spot welding process. The value estimates of the parameters were used to develop charts for determining overall resistance of samples for any desired weld diameter. The prediction error in estimating sample resistance using the charts was 16% to 167%.

The empirical model prediction accuracy was improved using neural network artificial intelligency to learn the pattern in the dataset. The two inputs used were applied electrode force and weld diameter while calculated sample resistance from the empirical model was the output. These dataset were used to train four neural network types. These were the Generalised feed forward neural network, Multilayer perceptron network, Radial basis function and Recurrent network. Of all the four network types, the multilayer perceptron had the least mean square error for training and cross validation with prediction error of 65%. Prediction improvement from previous 167%.

The number of input parameters in the multilayer perceptron architecture was increased from the initial two inputs to five inputs by including all the estimation parameters from the mathematical model. This Multilayer perceptron neural network architecture yielded a mean square error in training and cross validation of 0.00037 and 0.000390 with linear correlation coefficient in testing of 0.999 and maximum estimation error of about 0.1% to 3%. An accuracy of 99.9% to 97%.

APPENDIX J

PAPER 4 DEVELOPED FOR PUBLICATION

DESIGN AND IMPLEMENTATION OF PREDICTIVE CONTROLLER FOR THE RESISTANCE SPOT WELDING PROCESS.

Pius Nwachukwu Oba, Professor D. Chandler and Dr. S. Oorder
(University of the Witwatersrand, Johannesburg, South Africa)

Prof. Dr.-Ing. Dr. h.c.L. Dorn and Dr. Ing. Kevin Momeni
(Technical University Berlin, Germany)

Abstract

Presented in this paper is the method used for the design of a predictive controller for predicting effective weld current in the resistance spot welding process using a developed process model. A suitable process model forms an important step in the development and design of process controller for achieving good weld quality with good reproducibility.

The process model developed by the Authors consists of three parameter empirical model with dependent and independent variables used for curve fitting the nonlinear halfwave dynamic resistance curve. To improve the prediction accuracy of this empirical model, the data generated from the model were used to train four different neural network types. Of the four network types trained, the MLP had the least mean square error for training and cross validation of 0.00037 and 0.000390 respectively with linear correlation coefficient in testing of 0.999 and maximum estimation error range from 0.1% to 3%. This model was selected for the design and implementation of the controller for predicting overall sample resistance. Using this predicted overall sample resistance, and applied electrode force, a similar model was developed for predicting required effective weld current for any desired weld diameter. The prediction accuracy of this model was in

the range of about 94% to 99%. The controller outputs effective current for any desired weld diameter. This controller is observed to track the desired output accurately with same prediction accuracy of the model used which was about 94% to 99%. The controller works by utilizing the neural network output embedded in Microsoft Excel as a digital link library.